Shear Wave Elastography in the Assessment of Healthy and Diseased Skeletal Muscle.

Abdulrahman Mohamad I Alfuraih

Submitted in accordance with the requirements for the degree of Doctor of Philosophy

The University of Leeds

School of Medicine
Leeds Institute of Rheumatic and Musculoskeletal Medicine

March, 2019

Intellectual Property and Publication Statements

The candidate confirms that the work submitted is his own, except where work which has formed part of jointly-authored publications has been included. The contribution of the candidate and the other authors to this work has been explicitly indicated below. The candidate confirms that appropriate credit has been given within the thesis where reference has been made to the work of others.

Acknowledgements

First and foremost, praise be to Allah Almighty for the gracious mercy and bountiful blessings that have enabled me to complete my doctorate.

This PhD has been an eye-opening experience, and it would not have been possible without the support of multiple people. I gratefully acknowledge the guidance and support received from my supervisors: Dr Richard J Wakefield (primary), Dr Ai Lyn Tan and Dr Philip O'Connor. I would like to sincerely thank our departmental data analyst, Dr Elizabeth M Hensor, for her statistical advice and support. Many thanks also go to the MUSCLE research team and the staff at the Leeds Institute of Rheumatic and Musculoskeletal Medicine, including Professor Paul Emery, Matthew Farrow, Brian Chaka, Bilkis Begum, Kate Smith, Dominic Bertham, and the rest of the Leeds Biomedical Research Centre staff for the wonderful time I spent there. I am indebted to the referring physicians and participants who volunteered their time to make this work possible. I greatly appreciate the support received from the proficient academic and administrative staff at the University of Leeds. I am grateful to the university for giving me the opportunity to train and supervise their medical and master's degree students. Special gratitude goes to Prince Sattam bin Abdulaziz University and the Saudi Ministry of Education for sponsoring me to undertake my master's degree and doctorate.

I would like to say a heartfelt thank you to my parents, Mohamad and Samiah, for the unwavering words of encouragement and prayers. I would have never achieved this PhD without the sacrifices you made and a myriad of teaching hours. You made me who I am today. I dedicate this thesis to you.

Finally, my deepest appreciation goes to my beloved wife, Alanoud, who has been by my side throughout this beautiful journey, living its ups and downs. You made it joyful and less agonising. Thank you for your unfailing support, encouragement, belief, and patience throughout these years. The priceless memories we had together in the UK will never be forgotten.

Co-author contributions

Chapter 3 - Reliability of shear wave elastography in healthy skeletal muscles.

Abdulrahman M Alfuraih (AMA), Philip O'Connor (POC), Ai Lyn Tan (ALT) and Richard J Wakefield (RJW) conceptualised and designed the study. AMA collected, analysed and interpreted the data and wrote the manuscript. Elizabeth M Hensor (EMH) revised the data and assisted in the statistical analysis. AMA, ALT, POC, EMH, RJW and Paul Emery (PE) revised the manuscript critically for important intellectual content and approved the final manuscript.

Chapter 4 - The effect of ageing on shear wave elastography muscle stiffness in adults.

AMA, POC, ALT and RJW conceptualised and designed the study. AMA collected, analysed and interpreted the data and wrote the manuscript. EMH provided statistical advice. AMA, ALT, POC, RJW and PE revised the manuscript critically for important intellectual content and approved the final manuscript.

Chapter 5 - Muscle shear wave elastography in idiopathic inflammatory myopathies.

AMA, POC, ALT and RJW conceptualised and designed the study. POC and Dr Andreas Ladas scored the MRI images. AMA collected, analysed and interpreted the SWE data and wrote the manuscript. EMH revised the data and statistical analysis. AMA, ALT, POC, PE, EMH, AL and RJW revised the manuscript critically for important intellectual content and approved the final manuscript.

Chapter 6 - Corticosteroids effect on muscle stiffness.

AMA, POC, ALT and RJW conceptualised and designed the study. AMA collected, analysed and interpreted the data and wrote the manuscript. EMH provided statistical advice on multilevel modelling. AMA, ALT, POC and RJW revised the manuscript critically for important intellectual content and approved the final version.

Chapter 7 - Muscle Stiffness in Rheumatoid Arthritis.

AMA, POC, ALT and RJW conceptualised and designed the study. AMA collected, analysed and interpreted the data and wrote the manuscript. EMH provided statistical advice. AMA, ALT, POC and RJW revised the manuscript critically for important intellectual content and approved the final version.

List of publications / presentations arising from the thesis

Original articles

- **Alfuraih, A.M.**, O'Connor, P., Tan, A.L., Hensor, E., Emery, P. and Wakefield, R.J., 2017. An investigation into the variability between different shear wave elastography systems in muscle. Medical Ultrasonography, 19(4), pp.392-400.
- **Alfuraih, A.M.**, O'Connor, P., Hensor, E., Tan, A.L., Emery, P. and Wakefield, R.J., 2018. The effect of unit, depth, and probe load on the reliability of muscle shear wave elastography: Variables affecting reliability of SWE. Journal of Clinical Ultrasound, 46(2), pp.108-115.
- **Alfuraih, A.M.**, Tan, A.L., O'Connor, P., Emery, P. and Wakefield, R.J. (2019). The effect of ageing on shear wave elastography muscle stiffness in adults. Aging Clinical and Experimental Research, (in press).
- **Alfuraih, A.M.**, O'Connor, P., Tan, A.L., Hensor, E.M. Ladas, A., Emery, P. and Wakefield, R.J. (2019). Muscle Shear Wave Elastography in idiopathic inflammatory myopathies: a case-control study with MRI correlation. Skeletal Radiology, (in press).

Conference abstracts

- **Alfuraih, A.M.**, O'Connor, P., Tan, A.L., Hensor, E., Emery, P. and Wakefield, R.J. An investigation into the reliability of shear wave elastography acquisition methods in muscle. *British Medical Ultrasound Society Conference 2016.* (oral presentation)
- **Alfuraih, A.M.**, O'Connor, P., Tan, A.L., Hensor, E., Emery, P. and Wakefield, R., 2017. An investigation into the reliability of shear wave elastography acquisition methods in muscle. Clinical Radiology 2017, 72, p.S11-S12. *Royal College of Radiologists Conference 2017.* (poster presentation)
- **Alfuraih, A.M.**, O'Connor, P., Tan, A.L., Hensor, E., Emery, P. and Wakefield, R., 2017. Does unit of reporting, depth and probe load influence the reliability of muscle shear wave elastography?. Clinical

Radiology 2017, 72, p.S12. *Royal College of Radiologists Conference 2017.* (poster presentation)

- **Alfuraih, A.M.**, Tan, A.L., O'Connor, P., Emery, P. and Wakefield, R.J., 2018. Muscle elastography as a potential novel imaging biomarker in myositis. Annals of the Rheumatic Diseases 2018, 77, p.802-803. *European League Against Rheumatism meeting 2018.* (poster presentation)
- **Alfuraih, A.M.**, Tan, A.L., O'Connor, P., Emery, P. and Wakefield, R.J. The potential role of shear wave elastography for diagnosing idiopathic inflammatory myopathies. *Annual Northern & Yorkshire Rheumatology Meeting 2018.* (oral presentation)
- **Alfuraih, A.M.**, Tan, A.L., O'Connor, P., Emery, P. and Wakefield, R.J., 2019. Muscle stiffness may diminish after corticosteroid treatment. *European League Against Rheumatism meeting 2019.* (poster presentation)
- **Alfuraih, A.M.**, Tan, A.L., O'Connor, P., Emery, P. and Wakefield, R.J., 2019. Muscle stiffness and weakness in rheumatoid arthritis – a shear wave elastography study. *European League Against Rheumatism meeting 2019.* (poster presentation)

Abstract

Skeletal muscle is a complex biomechanical structure that changes in morphology and energy consumption based on the applied load. Available routine assessment methods are limited by invasiveness, subjectivity, cost, or poor sensitivity and specificity. Shear wave elastography (SWE) is a relatively new ultrasound technology that has transformed the management of various diseases by providing a quantitative and real-time assessment of soft tissue stiffness. However, little research has been carried out on muscles.

The narrative literature review demonstrated the variability in muscle SWE acquisition methods and the lack of data on system reliability, as well as the need for objective methods to assess suspected and established muscle diseases. First, two studies on healthy muscles identified various SWE acquisition aspects that could affect the measurement's variability using two SWE systems and recommended the best techniques to improve muscle SWE reliability. Later, a cross-sectional analysis of several age groups demonstrated that ageing was associated with a gradual decline in muscle stiffness with significant reductions appearing in subjects >75 years old. A case-control study showed that idiopathic inflammatory myopathy patients have significantly lower muscle stiffness, which correlates with muscle weakness and MRI scores of oedema and atrophy. A cohort study revealed a decline in muscle stiffness after three and six months of corticosteroid treatment and the patients that exhibited weaker muscle strength at follow-up visits had a greater reduction in muscle stiffness. Lastly, a case-control study on rheumatoid arthritis patients of various disease activities did not substantiate the hypothesis of suspected muscle stiffness alteration.

Overall, SWE demonstrated evidence of face, construct, and responsiveness validity in skeletal muscles. With further adequately powered validating studies, SWE may be used to evaluate the effects of ageing, monitor myositis disease activity, and detect early myopathic side effects of corticosteroids.

Table of Contents

List of Tables

List of Figures

List of Abbreviations

2D	Two-dimensional
3D	Three-dimensional
ACR	American College of Rheumatology
ADM	Abductor digiti minimi
AIX	Aixplorer elastography system
ANCOVA	Analysis of covariance
ANOVA	Analysis of variance
APO	Adductor pollicis obliquus
ARFI	Acoustic radiation force impulse
AUROC	Area under the receiver operating curve
BB	Biceps brachii
BF	Biceps femoris
BMI	Body mass index
BR	Brachioradialis
CARE 75+	Community ageing research 75+
CEUS	Contrast-enhanced ultrasound
CI	Confidence interval
CIM	Corticosteroid-induced myopathy
CK	Creatine kinase
CRP	C-reactive protein
CST	Chair stand test
CT	Computed tomography
DMARD	Disease-modifying antirheumatic drug
DOMS	Delayed onset muscular soreness
DXA	Dual-energy X-ray absorptiometry
EDL	Extensor digitorum longus
EFSUMB	European federation of societies for ultrasound in medicine and biology
ELSA	English Longitudinal Study of Aging
EMG	Electromyography
ES	Erector spinae
ESR	Erythrocyte sedimentation rate
ETGUG	Expanded timed get-up-and-go
EULAR	European league against rheumatology
EWGSOP	European working group on sarcopenia in older people
FDL	Flexor digitorum longus
FHL	Flexor hallucis longus
GCA	Giant cell arteritis
GRA	Gracilis
HAQ	Health assessment questionnaire
ICC	Intra-class correlation coefficient
IIM	Idiopathic inflammatory myositis

IQR	Interquartile range
IS	Infraspinatus
kPa	Kilopascal
LE9	LOGIQ E9
LG	Lateral gastrocnemius
LOA	Limits of agreement
MAS	Modified Ashworth scale
MQI	Muscle quality index
MRE	Magnetic resonance elastography
MRI	Magnetic resonance imaging
MTSS	Medial tibial stress syndrome
MVC	Maximum voluntary contraction
N.m	Newton-meters
NPV	Negative predictive value
NR	Not reported
OMERACT	Outcome measures in rheumatoid arthritis clinical trials
Pa	Pascal
PB	Peroneus brevis
PL	Peroneus longus
RA	Rheumatoid arthritis
RF	Rectus femoris
ROC	Receiver operating characteristic
SAR	Sartorius
SCM	Sternocleidomastoid
SD	Standard deviation
SE	Strain elastography
SM	Semimembranosus
SOL	Soleus
SS	Supraspinatus
SSI	Supersonic imagine
ST	Semitendinosus
STIR	Short tau inversion recovery
SWE	Shear wave elastography
SWV	Shear wave velocity
TA	Tibialis anterior
TB	Triceps brachii
TE	Transient elastography
TP	Tibialis posterior
VI	Vastus intermedius
VL	Vastus lateralis
VM	Vastus medialis
WFUMB	World federation of ultrasound in medicine and biology
WSCV	Within-subject coefficient of variance
WSSD	Within-subject standard deviation

Chapter 1 Introduction

1.1 Background

Skeletal muscle makes up approximately 40% of the human body mass. Over 600 individual skeletal muscles are responsible for voluntary locomotion, posture and positional change as well as being an essential nutrient reservoir. Research has shown that healthy muscles are associated with improved functionality, independence and longer healthy lifespan [1].

Muscle-related disorders have a significant economic impact on the health services with costs exceeding common rheumatological diseases like rheumatoid arthritis [2]. It is known that muscle mass and decreased strength in the elderly contributes to risks of falls, which are estimated to cost the UK approximately £1.7 billion a year [3].

Skeletal muscle is a complex biomechanical structure that varies in size, shape and energy consumption depending on the load applied to it. Currently available routine assessment methods are limited by various factors such as invasiveness (e.g. biopsy), subjectivity (e.g. manual muscle testing), high costs [e.g. magnetic resonance imaging (MRI)] or poor specificity (e.g. electromyography) and sensitivity (e.g. blood tests of muscle enzymes) [4]. A growing body of scientific literature highlights the need for standardised assessment methods of muscle quality in myopathies and ageing-related muscle dysfunctions [5]. There is a paucity of easy to use and rapid tests for objectively quantifying aspects of muscle quality with minimal patient burden in a clinical setting.

To date, B-mode ultrasonography has not played a central role in the diagnosis and management of myopathies, which could be related to its perceived inferior contrast resolution and operator dependency in comparison to other modalities like MRI [6]. However, recent interest has been centred around shear wave elastography (SWE), a novel objective ultrasound technology that can quantify tissues' stiffness. It adds a new parametric dimension of tissue characterisation beyond morphology, echogenicity and vascularity assessments using

conventional ultrasonography. Over the past decade, it has transformed the practice of diagnosing and managing several organ diseases including those of the liver [7], breast [8] and thyroid [8]. Based on its established usefulness in these other organs, SWE has the potential to be developed as a novel imaging biomarker for muscle assessment, which this thesis aims to contribute towards.

There has been increased academic interest in ultrasound elastography over the past decade. Based on PubMed statistics, publications on ultrasound elastography were limited to only 5 scientific papers in 1992 before rising exponentially to more than 1000 in 2014 (Figure 1-1). This increasing prominence in the literature provides an indication of the equipment technical developments and recognition as an imaging tool. Moreover, it has led to investigation into less explored potential applications such as muscle. Figure 1-1 demonstrates the relative lower research activity in the field of muscle elastography.

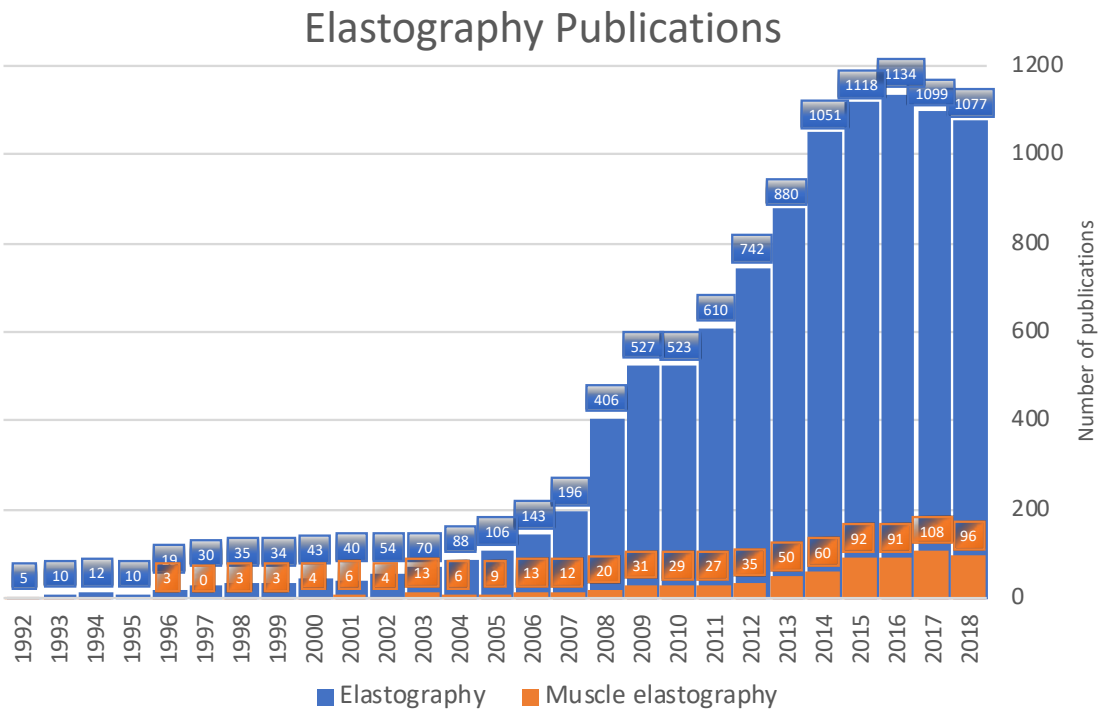

Figure 1-1 Trend of research activity on elastography.

The data represent the number of publications in the major journals indexed by PubMed.

Elasticity can be defined as the property of a material to return to its original shape after being deformed by stretching or compression forces. A brief background on muscle anatomy and physiology will explain the rationale behind measuring muscle elasticity. Skeletal muscle is made up of multiple fascicles separated by the perimysium that group bundles of muscle fibres (myofibres) separated by the endomysium. The multinucleated cell myofibres are packed with myofibrils (muscle fibre units) that extend the length of the cell (Figure 1-2). Within each myofibril are thousands of units called sarcomeres. A sarcomere, the functional unit of the muscle, consists of a thin inelastic actin filament and a thick myosin filament that is connected to an elastic third protein called titin (Figure 1-3). An additional protein named nebulin is also known to have an elastic function by supporting the thin filament stiffness in the sarcomere [9].

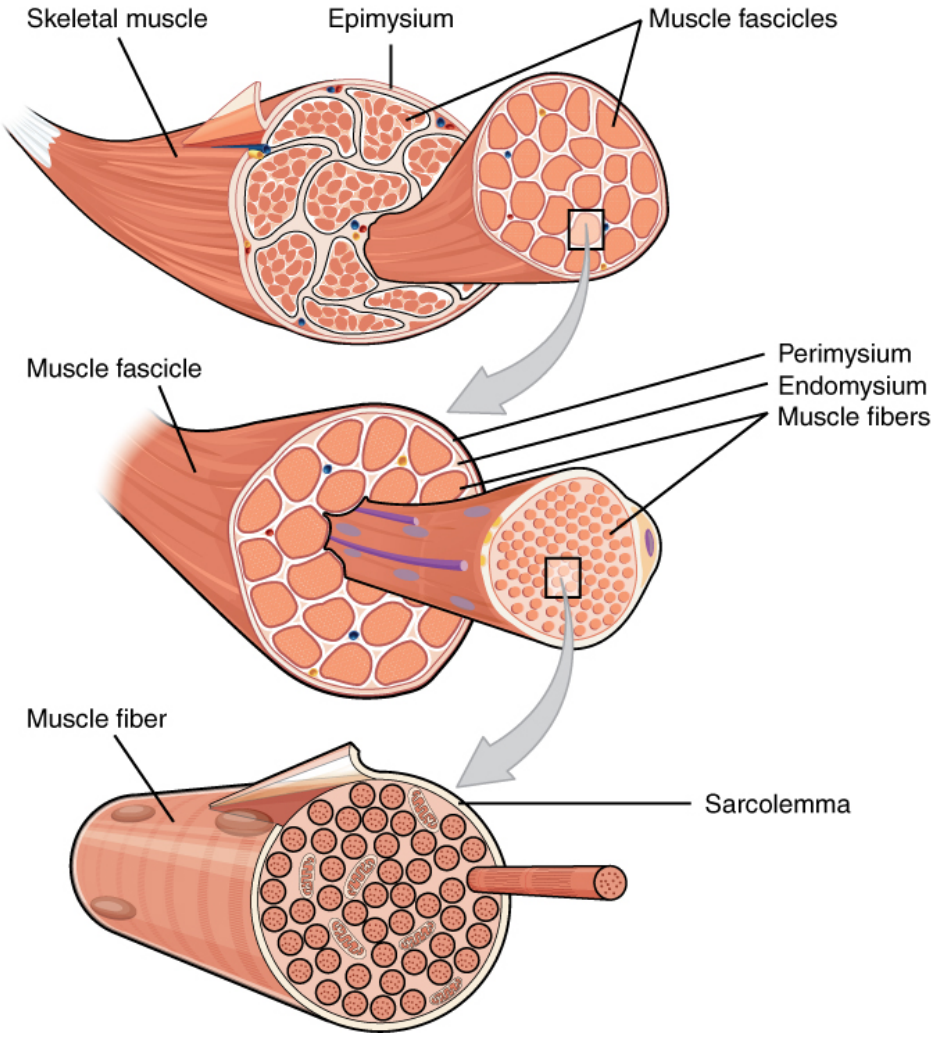

Figure 1-2 The anatomy of skeletal muscle.

(Reprinted with permission from OpenStax, Anatomy & Physiology [10].)

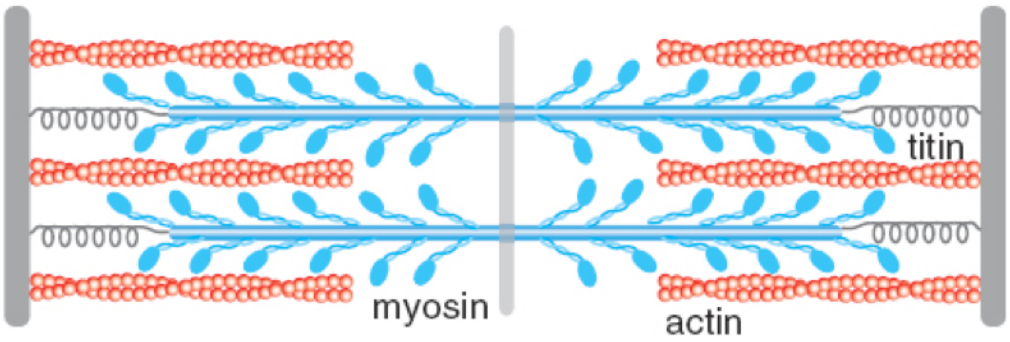

Figure 1-3 A simplified schematic of the sarcomere unit.

The figure shows the sarcomere assembly encompassing the thin and thick contractile filaments (actin and myosin) as well as the elastic, spring-like, titin protein filament. (Adapted with permission from IOP Publishing, New Journal of Physics [11].)

The titin protein (known as connectin) chiefly controls the passive elastic property of myofibrils by acting like a recoil spring for the myosin filaments in the sarcomeres when the muscle length increases to prevent it from overstretching as well as controlling its shortening movement velocity. The biomechanical function of sarcomeres can be clarified by the sliding filament theory [12]. It is based on a myosin filament 'pulling' an actin filament to slide past it (also known as cross-bridge cycling) to shorten a sarcomere. A muscle contraction is generated when the cross-bridge cycling process occurs on millions of sarcomeres in the skeletal muscle.

Skeletal muscle is a biologically elastic organ having the ability to return to its passive length when a shortening active contraction force is ceased. This can be easily demonstrated by making a fist then relaxing. The sliding filament theory and the titin protein elastic function explain the biomechanical property of skeletal muscle. The aforementioned mechanisms become impaired when pathological processes attack the sarcomere [13]. This is most evident with specific genetic mutations causing dysfunction in the myofibrils resulting in numerous forms of myopathies ranging in severity from mild conditions to paralysis at birth [14]. Furthermore, histopathological analyses show that thick filaments are disrupted in cases of autoimmune idiopathic inflammatory myopathies, suggesting that it is not only limited to myofibrillar myopathies [15]. In addition, myosin filament loss was observed in rodents treated with corticosteroids [16]. On the macroscopic scale, a diseased muscle can experience increased intramuscular oedema, fatty infiltration and loss of

muscle fibre (atrophy). Such pathological processes suggest further mechanisms by which the elastic qualities can be disrupted in myopathies.

With significant technological advances in modern imaging, the quest to develop new imaging biomarkers and surrogate outcome measures in diseases is increasing. This helps our understanding of the diseases processes and ultimately improve diagnosis, management and patient care. Currently there is clinical interest in research exploring non-invasive methods for assessing how diseases could influence biomechanical properties of muscle. SWE can help fill this gap in the literature and has potential to be effective in supporting diagnostic and therapeutic decisions. The next two sections will explain how this thesis proposes to contribute to the literature.

1.2 Aims and objectives

The unifying hypothesis of this thesis is:

Shear wave elastography is reliable and able to detect altered skeletal muscle elasticity in various established and suspected muscle conditions.

The primary aim is to explore the applications of SWE as a novel diagnostic and monitoring imaging biomarker in several established and suspected muscle pathologies. To achieve this aim, these objectives were identified:

- To determine the reliability of SWE systems in muscle and develop a reliable scanning technique.
- To explore how ageing influences muscle elasticity.
- To investigate the diagnostic performance of SWE in idiopathic inflammatory myopathies.
- To explore the effect of high-dose steroid treatment on muscle elasticity.
- To explore the nature of muscle elasticity in various rheumatoid arthritis cohorts of different disease activity.

1.3 Thesis structure and overview

The structure of the thesis is outlined below providing an overview of each chapter.

- **Chapter 2:** Narrative literature review

This is a narrative literature review that starts with reviewing the principle, types and established clinical applications of elastography. The literature published thus far on muscle SWE is then extensively evaluated and focused on. This is followed by an overview of the diseases this thesis aims to investigate to demonstrate the need for novel imaging biomarkers, providing context to this thesis. This chapter finally reviews the main currently established muscle assessment methods.

- **Chapter 3:** Reliability of shear wave elastography in healthy skeletal muscles.

This chapter constitutes two reliability studies undertaken to establish the best muscle elastography acquisition techniques in healthy skeletal muscles. It includes a comparative analysis of the reliability between two SWE systems. This chapter substantiates the technical methodology that will be carried across the later studies undertaken in this thesis.

- **Chapter 4:** Muscle elastography across ages.

This chapter aims to explore the influence of ageing on muscle elasticity. This is done in a cross-sectional design by comparing young, middle-aged and elderly participants. The elderly group was recruited from a community cohort of subjects aged above 75 years. Correlations between SWE and measures of frailty are specifically investigated in this elderly cohort. Overall, this chapter focuses on the associations between the properties of muscle elasticity, mass and strength in an ageing population.

- **Chapter 5:** Shear wave elastography in myositis.

This is a case-control study investigating hypothesised altered muscle elasticity in patients with idiopathic inflammatory myopathies. The patients are age and gender-matched to healthy controls then compared to establish the face validity

of SWE as an imaging biomarker. Additionally, this chapter's study compares the diagnostic performance of SWE to magnetic resonance imaging reported features of muscle oedema, atrophy and fatty infiltration.

- **Chapter 6:** Corticosteroids effect on muscle elasticity.

This is a longitudinal cohort study exploring the effects of high-dose corticosteroid treatment. This is performed by following-up patients with giant cell arteritis after three and six months of commencing treatment. Relevant clinical and muscle characteristics are analysed to provide further context in addition to the inclusion of healthy controls. This chapter aims to identify the potential role of SWE for detecting subclinical corticosteroid-induced myopathy.

- **Chapter 7:** Muscle elasticity in rheumatoid arthritis.

This is a case-control study exploring and defining muscle elasticity in RA patients. It investigates the muscle condition in 3 cohorts of RA patients: newly diagnosed untreated, those in disease remission, and those who have a persistent active disease, by correlating muscle strength and functional capacities with muscle elasticity amongst the RA subgroups and healthy controls. The work undertaken in this chapter aims to detect any underlying subclinical muscle involvement in RA using SWE to ultimately help in developing strategies for prevention and treatment in rheumatic diseases.

- **Chapter 8:** Discussion, future directions and conclusions.

This final chapter discusses the main findings and addresses the limitations of this thesis. It also suggests the future directions in the field of muscle elastography research and outlines the important conclusions that can be drawn from this work.

Chapter 2 Literature Review

This chapter is aimed to review literature related to muscle elastography after describing the basic principle of elastography and its types. It also reviews the main pathologies this thesis is focusing on in addition to the available methods of assessment.

2.1 Introduction

The term ‘sound’, according to the Oxford dictionary, is defined as “vibrations that travel through the air or another medium and can be heard when they reach a person's or animal's ear.” In the scientific context, however, sound is defined as the mechanical waves travelling through a compressible medium by means of oscillation periods of compression and rarefaction [17]. Sound and ultrasound share the same physical properties except that ultrasound waves have frequencies higher than humans’ audible limits (20 to 20000 Hz). Ultrasound is also one of the properties animals such as whales, dolphins and bats use to communicate, echolocate and hunt for preys. These animals used ultrasound for centuries or probably millenniums before humans discovered its clinical applications. Nevertheless, long before discovering the usefulness of ultrasound in the medical field, engineers had developed numerous non-medical applications.

2.1.1 History of ultrasound

The Titanic incident in 1912 was one of the sparks that ignited the interest to utilise ultrasound for echo-ranging to help ships avoiding icebergs [18]. Shortly, the first world war spurred the interest of governments to fund research into this field, as scientists were encouraged to develop the science of acoustics in a quest for naval superiority. With the help of a French scientist called Langevin, the French army had the first operational device to help submarines navigate the sea. His contributions to understanding the generation and detection of ultrasound waves helped immensely in the development of the pulse-echo principle used in modern ultrasonography. Despite the devastating effects the two world wars had on our planet, the scientific discoveries during that gloomy

period resulted in significant advancements that helped in the evolution of modern medical ultrasound. Other applications were later discovered, for example, detecting schools of fish underwater [19], non-destructive materials testing as metal flaw detectors [20] and cleaning objects via ‘supersonic jets’ using frequencies up to 400 kHz [21]. The British Medical Ultrasound Society historical collection for ultrasound in Glasgow is a momentous source of artefacts for education and research.

2.1.2 The evolution of ultrasound in medicine

Numerous attempts had failed to introduce ultrasound in the medical field. It was not until the fifties of the last century when Jaffe had discovered the piezoelectric property of the lead zirconate titanate material. This important finding led scientists to the first application of ultrasound in medicine performing ‘midline encephalography’ to detect epidural hematomas in traumatic brain injuries [22]. Soon, other applications in obstetrics and echocardiography started to develop. Though, ultrasound was not commercially available until the mid-sixties; systems were extremely basic and limited to A-mode imaging through the propagation of continuous soundwaves.

Indeed, it was the development of two-dimensional (2D) B-mode ultrasound systems that lead to the widespread use of this speciality and adaptability in radiology departments and throughout hospitals during the seventies. This was the result of significant advancements in electrical circuits and the development of analogue-to-digital converters. Early systems included massive transducers mounted on a large gantry that is manually swept over the patient’s body. Later, microchips were invented leading to an exponential rise in processing speeds, which enabled digital beamforming. The fusing of colour Doppler to B-mode in Duplex imaging was another milestone helping in the assessment of blood flow to organs and tumours. Afterwards, the 1990s witnessed tremendous enhancement in image quality when 2D phased array transducers and harmonic imaging were first introduced. The beginning of the millennium saw a great competition between manufacturers developing a broad spectrum of ultrasound probes tailored for specific scans as well as marketing new technologies like three-dimensional (3D) imaging.

2.1.3 Current status of ultrasound in medicine

Multiple synonymous terms are used interchangeably to describe the utilisation of ultrasound waves for medical imaging such as sonography, ultrasonography and ultrasonic imaging. Nowadays, it shares 22% of the total radiological examinations performed in England (Figure 2-1) with more than 9 million scans performed each year [23]. It plays a vital role in clinical practice; this includes the diagnostic applications for general, small parts, vascular, obstetrics and point-of-care ultrasonography as well as therapeutic applications.

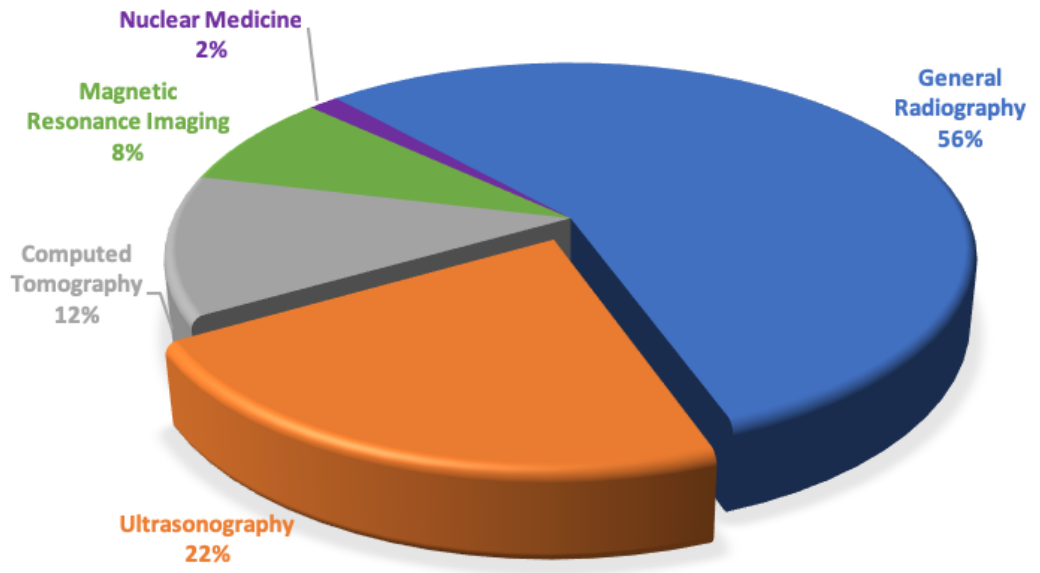

Figure 2-1 Imaging activity in England between April 2017–2018.

This pie graph illustrates how ultrasound accounts for almost one-quarter of the total medical imaging examinations coming as the second most commonly requested modality after general radiography.

Ultrasonography is often viewed prejudicially as inferior to other imaging modalities. Scholars encourage practitioners to embellish the capabilities of ultrasound and educate other medical professionals of its evolving ability for accurate diagnosis and management [24]. In fact, ultrasound can be described as a ‘multiparametric’ imaging technology similar to magnetic resonance imaging (MRI). It encompasses multiple imaging modes ranging from the conventional B-mode, colour and spectral Doppler to the more advanced dynamic imaging such as contrast-enhanced ultrasound and multi-dimensional imaging.

One of the major advantages of ultrasound imaging is its cost-effectiveness with the machine's capital, running and maintenance costs relatively inexpensive compared to other modalities considering the diagnostic value it provides. Accessibility, portability and being readily available at the bedside are additional advantages. Moreover, ultrasound imaging offers unravelled superior spatial resolution that is higher than other imaging modalities [6]. The temporal resolution of ultrasonography is also superior, offering real-time imaging with framerates exceeding 2000 frames/second [25].

To date, there has been no evidence of harmful effects of ultrasonography to humans. This is due to the safe nature of ultrasound as a radiation-free modality based on mechanical waves, not ionising radiation. Despite the lack of any reported incidents, ultrasound involves energy deposition in the body and should always be medically practised according to the safe usage guidelines. Another advantage is the ability to perform dynamic scans to assess the functionality, which is a key technique in musculoskeletal ultrasonography. It is also considered patient-friendly; operators can talk and describe the images whilst performing the examination.

Despite all the positive traits, it has a number of fundamental drawbacks. Image interpretation and acquisition are subjective for the majority of ultrasound modes, including conventional B-mode and Doppler imaging. Therefore, this thesis shares the continual quest in the literature to develop quantitative diagnostic ultrasound techniques. Ultrasound is known for its versatility; however, any strong acoustic impedance mismatch between surfaces limits its functionality. Air and bone are good examples. Ultrasound can assess the bone's cortical surface, but it cannot visualise the endosteum or marrow. Air, on the other hand, produces strong 'dirty' posterior acoustic shadowing that obstructs the visibility of underlying structures. Moreover, ultrasound is notorious for its poor contrast resolution in comparison to MRI [6].

The operation of an ultrasound machine requires a deep understanding of its knobology. A good level of neuromuscular compatibility is an essential skill that ultrasound users should have to operate the probe. This makes ultrasound an extremely operator-dependant modality. Therefore, training courses and certificates have been implemented by numerous institutes and universities for operators to practice the fundamental skills required. Novice operators are

required to perform a large number of scans under close supervision to establish a basic level of competency. This limits the use of ultrasound to experienced and knowledgeable individuals with skilful hands.

2.1.4 Ultrasound in musculoskeletal imaging and rheumatology

Ultrasound has a major role in the diagnosis and management of traumatic and pathologic conditions related to the musculoskeletal system with performance comparable to magnetic resonance imaging (MRI) [26]. In the last decades, ultrasonography had major implications on the practice of rheumatology, and its use increased dramatically. It became an essential bed-side tool within the rheumatology clinical setting. A survey has reported that musculoskeletal ultrasound training is obligatory or recommended in the rheumatology training curriculum of more than half of the surveyed European countries, including the UK [27]. The role of ultrasound in inflammatory arthritis was driven by the need to develop new disease outcome measures, particularly concerning diagnosis and disease activity. It is important to highlight the role and driving forces the European league against rheumatology (EULAR) and the outcome measures in rheumatology (OMERACT) groups have contributed and continue to contribute towards the advancement of ultrasound in rheumatology.

In rheumatoid arthritis (RA), where most research has been conducted, it was found that ultrasound can reliably detect bone erosions more accurately than radiography [28]. Additionally, it helped in the early detection of preclinical inflammation by detecting the presence of synovitis using B-mode and power Doppler imaging. This important finding aids in accurate disease classification and disease activity estimation [29]. Regarding the latter, the composite clinical assessment measurements to determine disease remission have been found inaccurate, as ultrasound showed signs of significant active synovial inflammation using Doppler imaging in patients deemed clinically in remission [30].

In spondyloarthropathies, ultrasound is mainly being used to detect enthesitis to overcome its challenging clinical assessment. Early studies have shown that B-mode ultrasound has better sensitivity over clinical examination in the lower limbs [31]. Later, D'Agostino et al. reported that at least one vascularised enthesis detected on power Doppler offers a high specificity of 81.3% [32].

Despite the good evidence for detecting entheseal abnormalities, consensus on an objective ultrasound scoring system for enthesitis is lacking.

As for crystalline arthropathies, ultrasound can detect important diagnostic features. In gout, for example, the “double contour” sign has been coined as a specific feature of deposited crystals appearing as hyperechoic lines on the hyaline cartilage surface [33]. In pseudogout, however, the deposits are usually seen within the cartilage. Studies have shown that ultrasound may also have a role in monitoring treatment as the double contour sign can diminish or disappear with urate-lowering therapies [34].

In giant cell arteritis (GCA), ultrasound can aid in establishing the diagnosis by detecting the ‘halo’ sign (vessel-wall oedema), stenosis and occlusion. These typical ultrasound features had a superior sensitivity when compared to temporal artery biopsy (54% vs 39%) but inferior specificity (81% vs 100%) [35].

Ultrasound has additional applications in other connective tissue diseases. In Sjogren’s syndrome, it has the potential for replacing invasive procedures for diagnosing salivary gland abnormalities. Additionally, in systemic lupus erythematosus, ultrasound can detect subclinical inflammatory changes such as synovitis and bone erosions in the hands and feet [36]. Measuring skin thickness is another application in scleroderma. Moreover, elastography is now being investigated to explore the quality of skin elasticity in this disease.

With ultrasound becoming more available in rheumatology departments, new applications are being developed in areas such as spondyloarthropathies, crystal diseases, osteoarthritis, vasculitis and connective tissue diseases [37]. Nowadays, the American College of Rheumatology (ACR) and EULAR guidelines endorse the use of ultrasound in the assessment of RA [38].

New emerging ultrasound technologies are also being investigated for musculoskeletal applications such as Contrast-enhanced ultrasound (CEUS) and three-dimensional imaging (3D). CEUS helps in the characterisation of suspicious focal soft tissue lesions [39]. A recent study found that it can detect muscle injuries with a similar performance to MRI [40]. One-third of the lesions detected were not visible on conventional ultrasound. In RA, it can help differentiate active and inactive synovial inflammation [41], detect tenosynovitis

[42] and evaluate response to treatment [43]. Despite the numerous papers published in this field, it is still in its infancy as clinical applications are not well established.

After briefly exploring the history, merits and applications of ultrasound in medicine, the next section will focus on ultrasound elastography– the technology this thesis is centred around. The next section will describe and review its principle, types and main applications.

2.2 Elastography

In ancient medicine, palpation was an important diagnostic technique. It has been mentioned in ancient Egyptian papyrus as a method for detecting abdominal tumours by sensing any abnormal “resistance in the cardia” (i.e. the viscera) [44]. Hippocrates reportedly used it to determine cranial stiffness for head injuries in battles [45].

Nowadays, manual palpation is still an essential method in modern medicine. It provides medical practitioners useful information on tissues elasticity differences as a result of the strain produced (i.e. tissue displacement) from the stress applied (i.e. hand pressure). It is part of the clinical breast examination techniques to palpate the breast’s surface with variable hand pressures in a systematic manner. For males, scrotal palpation elucidates changes that might indicate the presence of a cancerous tumour or varicocele [46]. Although palpation is an indispensable tool in few clinical examinations, it has a number of critical disadvantages. First, it is limited to superficial structures and can only asses abnormally large deep masses that have a different stiffness to neighbouring tissues. Secondly, the interpretation is variable due to the subjective nature of palpation.

Elastography, the imaging of the elastic properties in soft tissues, can overcome these limitations and has rapidly evolved technologically and clinically since its development. Multiple lesions may not demonstrate ultrasonic contrast differences relative to surrounding tissues [47]. Therefore, elastography provides a new parameter that may reveal discernible elastic properties of sonographically invisible lesions.

Several historical publications studied soft tissue displacement using ultrasound as a biomarker for pathology. They utilised numerous techniques such as Doppler velocity measurements [48] and M-mode waveform changes [49]. As they relied on internal sources of stress such as cardiac motion and arterial pulsation, they all could not to define the magnitude and direction of the source of stress causing tissue displacements.

The first scientific article on ‘elastography’ was published in 1991 by Ophir et al. [50]. It explained the principle of what will later be described in this section as ‘strain elastography’. They validated their experiment results on foam block phantoms made of polyester and a slap of bacon by demonstrating changes in elasticity between the different layers that are not visible on B-mode (Figure 2-2). The system Ophir et al. utilised in their first paper was slow and based on a single element transducer; it was not suitable for in vivo clinical experiments. Two years later in 1993, the same research group demonstrated the feasibility and potential application of elastography in muscle and breast in vivo [51]. Their first paper has close to 4000 citations; it generated the interest in this field and led to a dramatic increase in research.

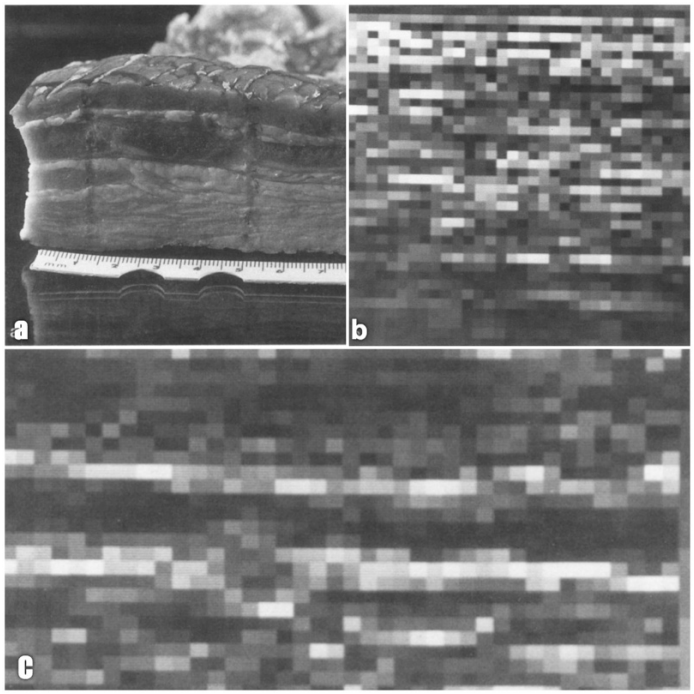

Figure 2-2 Elastography experiment validation by Ophir et al.

Image (a) shows the bacon slap with its distinct layers; (b) B-mode image; (c) elastographic image showing a clear definition of elasticity differences between the layers. (Reprinted by permission from SAGE publishing: Ultrasonic Imaging [50])

2.2.1 Principles of elastography

Elasticity describes the tendency of a material to return to its original shape after being deformed by a straining force of stress. In other words, it is the strain generated by stress applied on its surface. There are two factors contributing to the strain made. The first is the magnitude of applied stress force. The second is the cross-sectional area upon which that force is applied on. The equations defining stress and strain are explained below.

$$\boldsymbol{\sigma = F/A} \qquad \textbf{Equation 2-1}$$

Where σ is stress, F is the force applied and A is the cross-sectional area upon that force is applied on (Figure 2-3). According to the international system of units, stress is measured in Pascal (Pa), force is measured in Newton and area is measured in m^2. Strain (ε), on the other hand, is the deformations (change in length) caused by the stress in comparison to the original length.

$$\boldsymbol{\varepsilon = \frac{change\ in\ length}{original\ length} = \frac{(l_2) - (l_1)}{(l_1)}} \qquad \textbf{Equation 2-2}$$

By knowing the amount of strain caused and the magnitude of the stress applied, we can calculate a modulus of elasticity known as Young's elastic modulus (E). Its unit is the same as for pressure, Pascal (Pa). This modulus is related to a longitudinal strain produced by longitudinal stress.

$$\mathbf{E = \frac{Stress\ (\sigma)}{Strain\ (\varepsilon)}} \qquad \textbf{Equation 2-3}$$

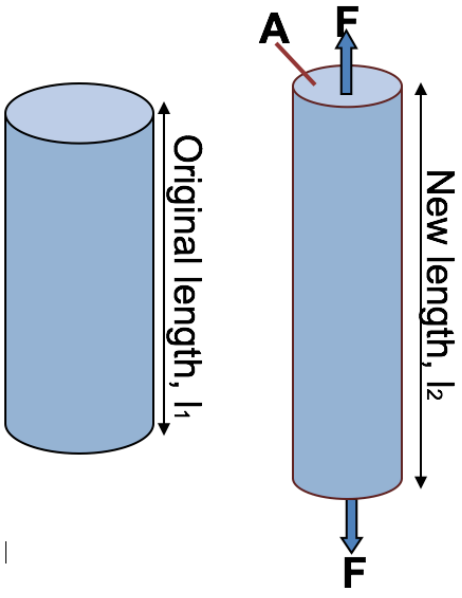

Figure 2-3 Effect of stress and strain on a cylindrical model.

As highlighted in the introduction, conventional B-mode ultrasound images are formed based on the acoustic impedance mismatches, which are the product of tissues density and longitudinal waves velocity. The latter is proportional with the elastic modulus that consequently provides unique and valuable information about the elastic nature of the biological tissues. Some examples of the elastic properties for biologic and non-biologic materials are listed in **Error! Reference source not found.**. There are other derivatives to the elastic moduli such as the shear and bulk modulus. The latter is the three-dimensional version of Young's modulus, meaning that it is the product of a volumetric strain induced by volumetric stress. This modulus is out of the scope of this thesis as it does not apply to ultrasound elastography.

Table 2-1 Young's elastic modulus of various materials.

In biological tissues, elasticity can differ substantially according to the pathological status and acquisition techniques as explained later in chapter 3. Note that there is a factor of a million between soft tissue and hard materials. The values are reported from previous papers [52-57].

Material	Young's modulus (average)
Healthy liver	<7.0 kPa
Cirrhotic liver	50 kPa
Breast	30 kPa
Breast carcinoma	93 kPa
Skeletal muscle (relaxed)	10 kPa
Tendon (relaxed)	150 kPa
Cortical bone	17 GPa
Steel	200 GPa
Diamond	1075 GPa

On the other hand, shear modulus (G) is related to biological tissue's elastic properties. It is defined as the shear strain (deformations in the form of changes in shape) due to a shear force that is not necessarily longitudinal as in Young's modulus (Figure 2-4).

$$G = \frac{Stress\ (\sigma)}{Shear\ strain\ (\varepsilon_s)} \qquad \textbf{Equation 2-4}$$

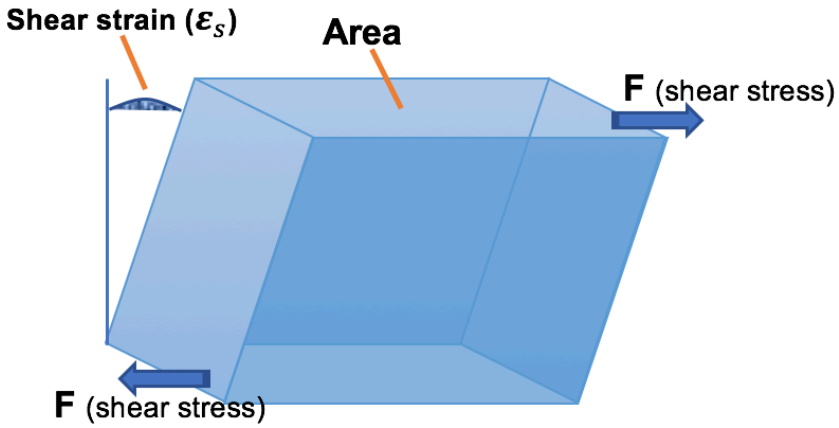

Figure 2-4 Shear modulus represented as the effect of transverse shear stress and strain on a cube model.

These two moduli are related to each other since Young's modulus can be expressed in the equation below

$$\mathbf{E} = \mathbf{2}\,(\boldsymbol{v} + \mathbf{1})\,\boldsymbol{G} \qquad \textbf{Equation 2-5}$$

Where $\boldsymbol{v}$ is the Poisson's ratio, which equals 0.5 for viscoelastic materials like biological tissues. Therefore, Young's modulus (E) can be estimated to be approximately three times the shear modulus (G), and both are expressed in units of kilopascal (kPa). In quantitative elastography methods, such as shear wave elastography, elasticity is commonly provided in Young's modulus. However, it is typical to report the elasticity in the magnetic resonance elastography literature in shear modulus (G=E/3). Therefore, it is important for researchers not to confuse the two moduli when referencing values in the elastography literature.

Although the terms elasticity and stiffness refer to the concept of rigidity, there can be subtle differences in their definitions from the physics perspective [58]. Nevertheless, the terms are used synonymously in clinical literature and this thesis for simplicity. A detailed description of elastography physics can be found in other books and reviews [59-61].

2.2.2 Types of ultrasound elastography

Although this thesis is focused on shear wave elastography (SWE), it is important to review the other types of elastography and discuss the main differences. There are numerous published reviews describing the types of elastography. Classifications and definitions vary considerably amongst them.

Some categorise elastography according to the main concept of the technique, while others focus on the exact technology used for each method. This variability may confuse novice researchers and clinicians interested in elastography. Interested users should understand the classifications, limitations, pros and cons of different types of ultrasound elastography. This knowledge is vital before planning a research project or considering the purchase of an elastography system.

In this thesis, the most common commercially available ultrasound-based elastography technologies will be reviewed based on the main principle of tissue excitation and the displacement detection method. It will mostly focus and elaborate on SWE. A summary of the main types according to this classification are listed in Table 2-2.

Table 2-2 The main types of ultrasound elastography methods

Method	Source of displacement or excitation	Measured property	Commercial systems
Strain elastography (SE)	External manual compression (probe palpation) or Internal physiological motion (cardiovascular or respiratory)	Strain	General Electric Philips Toshiba Samsung Siemens Hitachi Mindray BK Ultrasound Esaote
Shear wave elastography (SWE)	Acoustic radiation force impulse	Shear waves velocity	SuperSonic Imagine General Electric Philips Toshiba Samsung Siemens Hitachi Mindray Esaote
Transient elastography (TE)	External mechanical impulse	Shear waves velocity	Echosens (FibroScan®)

It is important to note that vendors develop their own patent-protected technology. This means that although the main principle is similar, the exact

technical method can be different. These differences and their potential effects on reliability will be discussed in chapter 3.

2.2.2.1 Strain elastography

Strain elastography (SE) is also known in the elastography literature as quasi-static strain imaging or compression elastography. This type of elastography is considered the first generation as it was the one described in Ophir's et al. paper in 1991 [50]. To describe how a strain elastogram is produced, ultrasound waves detection and conversion has to be explained first. When ultrasound echoes return to a transducer, they exert pressure on the piezoelectric elements. This pressure creates radiofrequency (RF) signals that contain intensity information on what the sound waves travelled through in the axial propagation axis. This converted RF signal from a single A-line.

SE is based on tracking tissue displacement by measuring A-line waveform differences before and after compression (Figure 2-5). The machine software defines a short segment for each A-line and cross-correlate it before and after compression. If the A-line signal of the pre-compression corresponds directly (i.e. did not change) to the post-compression, it will be presented as stiff, based on the selected colour look-up table or elastography scale. On the other hand, soft objects will not displace axially as much as stiff objects. Instead, the post-compression A-line waveforms will appear 'squashed' in comparison to pre-compression. All A-lines within the region of interest (ROI) has to be computed to produce an SE image. This is described as the frame-to-frame or pixel-to-pixel method. Operators can choose to have a strain elastogram mapped in greyscale (black is low stiffness and white is high). On modern SE systems, operators can opt for different colour-maps (look-up tables) overlaid on the B-mode image.

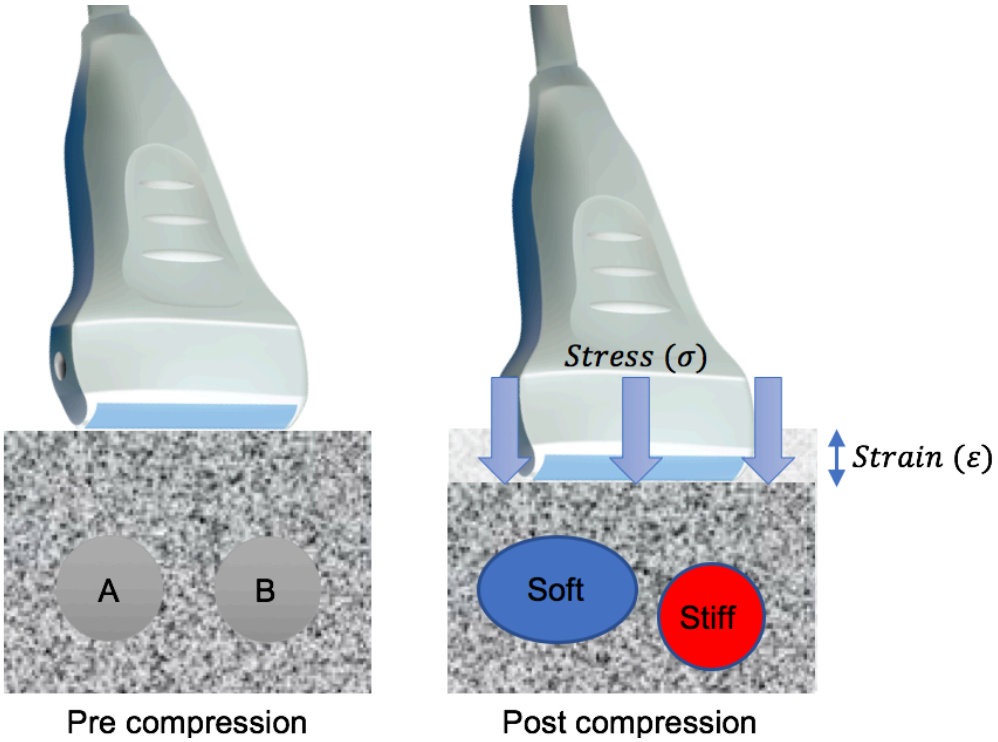

Figure 2-5 The principle of strain elastography.

This simplified model illustrates how similar objects in echogenicity (A and B) have different elastic properties after compression (stress) is applied.

The colours in the SE images represent relative qualitative stiffness. This means that the colours represented are based on the relative stiffness of the lesion being investigated to the surrounding tissue, not a direct objective representation. Nonetheless, because of this feature, it is considered a suitable modality for assessing elasticity variations for focal tissue masses. This explains one of the factors for its limited applicability for investigating diffuse diseases in comparison to SWE based on the published recommendations and guidelines [7, 62, 63].

As the SE principle implies, an operator is required to repeatedly compress and decompress the structure of interest to acquire the axial displacement information needed to create a strain elastogram. The repeated compression cycles applied should be uniformly performed by a skilled operator to acquire good quality images. Barr et al. [64] found that a slight increase of 10% in the compression force by the operator quadruples the elasticity modulus. Gilbertson and Anthony [65] developed a control system in the form of a hand-held actuator fixed to the probe that can quantify and control the compressive force imparted on the skin. Their patented system measure's the force and

controls it within a 4 cm range of motion limit. Hence, maintaining a constant transducer-skin force profile. Despite its promising usefulness for standardising SE, it is not commercially available yet due to the high manufacturing cost and legal concerns. Therefore, compression force variability within and between operators remains as a major limitation in SE. Indeed, the inter- and intra-operator reproducibility, as well as the subjective scoring, has been criticised being poor in SE [66-68].

Because of the qualitative nature of SE, numerous methods were developed to evaluate tissue strain more objectively. Pressure sensors [69], standardised colour scales [70] and strain ratios are the three main methods. The latter is the most common. It is based on using two ROIs; one is placed on the lesion and the other on a normal adjacent structure as a reference. If the ratio is higher than 1, it indicates the lesion is stiffer than the reference and vice versa. This method has been found to provide good results when scanning thyroid [71], breast [72] and prostate [73]. However, the placement of the reference ROI has been found to greatly bias the results [74]. The European Federation of Societies for Ultrasound in Medicine and Biology (EFSUMB) recommended in their published guidelines that although the methods for objectively assessing SE are being developed, they should not be applied in daily clinical practice [7]. Nevertheless, due to SE good value for investigating focal lesions, it has been widely investigated and validated for breast and thyroid lesions characterisation [62, 75, 76].

Limited data is available for SE on muscle. Despite the early invention and availability of SE, most studies were reported on the feasibility of this technique in healthy muscle [77-82]. Two promising and related publications to this thesis investigated the preliminary diagnostic value of SE for myositis [83, 84]. The first investigated SE on a sample of 24 patients with different types of histopathologically confirmed muscular inflammatory disease [83]. The researchers analysed the SE colour images using a special image processing software to extract numerical colour distribution (blue, green, red) intensity data from the images. Their results showed a strong level of proportional concordance between the features of SE and creatine kinase (CK) serum levels. Notably, they reported SE findings of decreased muscle stiffness. However, there was no significant correlation between SE and erythrocyte

sedimentation rate (ESR) or Lactate dehydrogenase (LDH). The results described no information regarding the state of the disease, and the study design was not supported by a control group. The second study [84] assessed the performance of SE in detecting active myositis in children with clinically confirmed juvenile idiopathic inflammatory myopathy (n=18). They classified the colour distribution of SE images as normal or abnormal based on a previously published data of normal children. More specifically, if the dominant colour is green (medium stiffness) it was scored as normal and if the dominant colour is blue (high stiffness) or red (low stiffness) it was scored as abnormal. They found no significant correlation (p=0.63) between the results of SE and MRI features of muscle oedema concluding that it cannot replace MRI for defining disease activity.

Several studies evaluated the value of SE in assessing spastic muscles. Illomei et al. [85] found a strong association (r=0.91; p<0.001) between a custom ordinal score for elasticity and the clinical degree of spasticity (Ashworth scale) in multiple sclerosis patients. They also reported positive results for assessing treatment responses. The value for assessing muscle spasticity was also confirmed in another study for patients with stroke [86]. It reported significantly higher muscle stiffness on the hemiplegic side versus the normal side of the wrist and finger flexor muscles. This suggests a role for SE in diagnosis and follow-up for spastic muscles.

Despite the promising data demonstrating the value of elastography for detecting myopathies, the qualitative data and subjective scoring render the validity of the findings questionable. This is an area where an objective technology that provides qualitative data like SWE can be valuable. The next section will focus on this second generation of elastography.

2.2.2.2 Shear wave elastography

SWE is based on monitoring and measuring the velocity in which shear waves propagate through tissues. It is a dynamic technology, where time-varying acoustic stress forces are applied to induce the propagation of shear waves. Hence, its principle allows objective quantification of tissues stiffness and can be presented as an elasticity map overlaid on a greyscale B-mode image.

Conventional ultrasonography utilises compressional axial waves to produce B-mode images. SWE, on the other hand, utilises shear waves that travel in mediums as a result of shear force. For example, shear waves propagate in the core of the earth as a result of earthquakes seismic energy [87]. The primary difference between these two waves is the displacement motion in relation to the direction of propagation, where compressional (longitudinal) waves displace along the axial line of insonation and shear (transverse) waves displace perpendicular (off-axis) to the angle of insonation (Figure 2-6).

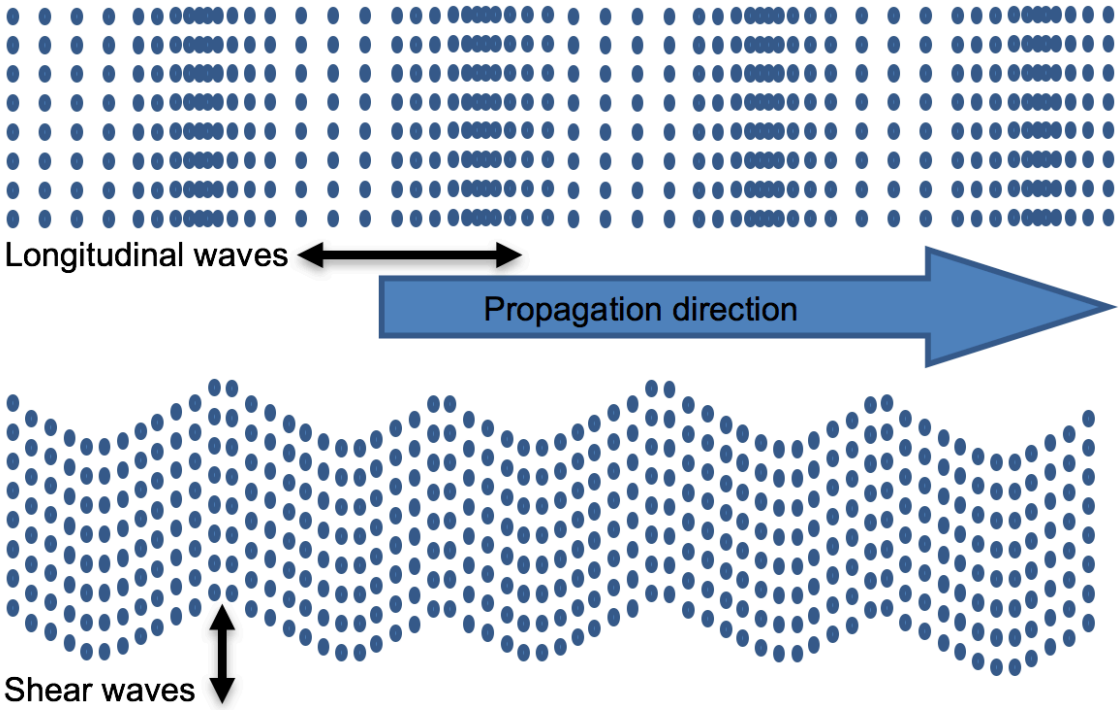

Figure 2-6 Longitudinal and shear waves.

The figure demonstrates the difference between the two waves. Longitudinal (compressional) waves displace the particles making up the material in the form of compressions and rarefactions along the direction of propagation. Shear waves displace the particles making up the material transverse to the direction of propagation.

Normal longitudinal waves travel at high velocities of approximately 1540 m/s through soft tissue. In contrast, shear waves travel at a much slower velocity between 1–10 m/s. This physical phenomenon provides us with the opportunity to track the propagation speeds of the slow shear waves using the much faster longitudinal waves employed in conventional B-mode ultrasonography. This important relationship is particularly valuable for assessing tissues' elasticity as shear waves velocity (SWV) is proportional to elasticity (travel faster in stiff materials and slower in soft materials). It can be converted into Young's elastic

modulus, which is approximately three times the shear modulus using the following equation

$$E = 3\,\rho\,V_S^2 \qquad \textbf{Equation 2-6}$$

where E is Young's modulus of elasticity, 3 is a constant related to Poisson's ratio for strain, ρ is tissue density (assumed to be 1 g/cm^3) and V is the velocity of shear waves. The equation can be rewritten to convert from Young's modulus (kPa) to SWV (m/s).

$$V_S = \sqrt{\frac{E}{3\rho}} \qquad \textbf{Equation 2-7}$$

Most manufacturers offer to present the data as SWV (m/s) or Young's modulus (kPa). However, manual conversion of the measurement between the two units can produce inaccurate estimations, which will be investigated and discussed in chapter 3.

Unlike SE, which requires an external manual physical force in most cases to qualitatively assess the tissues strain, shear wave imaging employs dynamic forms of stress using external mechanical sources or acoustic radiation forces to induce shear waves propagation then measure their velocity. There are currently three main subtypes of shear wave imaging: 1) 1D- transient elastography, 2) point SWE and 3) 2D SWE. The latter is commonly referred to as SWE in the literature, whereas the others are called by their technical or commercial names.

The first, 1-D transient elastography, is the earliest method of shear wave imaging that was first developed in 1995 [88]. It is most commonly known as "FibroScan®", named by the company that commercially introduced it (Echosens, Paris, France) in 2000. It employs a controlled external mechanical vibrator using a piston that produces an impulse on the surface of the skin, which sends a compression wave propagating shear waves in a spherical profile [89]. The external source of excitation explains why it is listed in Table 2-2 as an independent type of elastography, unlike the other SWE methods. This method of elastography is specifically designed and well validated for assessing liver stiffness [7]. It provides a single quantitative elasticity measure for a small area in Young's modulus (kPa) without displaying a B-mode image

for guidance. Due to its limited applicability, it will not be further reviewed in this chapter.

The other two subtypes, point and 2D SWE, utilise acoustic radiation force impulses (ARFI) to induce tissue perturbation. These ARFI pulses are sometimes called ‘push’ pulses for short in the literature. Its principle is based on transferring the mechanical energy from the acoustic radiation force of the pulse into the tissue due to the effect of absorption and attenuation. The acoustic energy is converted into mechanical stress deforming the tissues to generate shear waves travelling laterally perpendicular to the axis of the push pulse. Figure 2-7-a highlights this first step of forming a 2D SWE image. This phenomenon may occur in grayscale B-mode ultrasonography; however, the forces are not strong enough to induce tissue vibrations.

There are several differences between point SWE and 2D SWE. The former focuses ARFI pulses at a specific depth in one location, whereas 2D SWE utilises ARFI pulses at various depths and locations. Currently, there are two commercially available SWE systems equipped with point SWE, the Elast-PQ™ by Philips (first available in 2013) and the Virtual Touch Quantification™ which was the first SWE system that Siemens introduced in 2008.

Due to the ARFI excitation principle in point SWE, it is only possible to acquire a reading for a small ROI ($\approx$ 5mm $\times$ 6mm), hence the name ‘point’. This elastography technique does not produce an elastography image since it only takes a static snapshot of a small ROI. This technique is commonly applied for assessing liver pathology as it can reach great depths up to 8cm [90] and is not markedly affected by ascites like transient elastography. The fixed ROI could be a major problem when evaluating small thyroid nodules since the measurement may inadvertently include normal surrounding tissue [91]. As a result, its small predetermined fixed ROI and the lack elastography image are two major limitations that hinder its applicability.

Since the introduction of point SWE, several medical imaging companies developed the 2D SWE, which is one of the newest types of elastography. It provides an ROI covering a larger field of view to project a 2D elasticity map. This is achieved by sending multiple ARFI pulses in quick succession at various depths and locations (Figure 2-7-a). The propagated shear waves are

then monitored using tracking ultrasound pulses to determine the velocity by calculating the arrival time between lateral points of known distances (Figure 2-7-c). A good analogy for this process is the water ripples observed when dropping a rock into the water. The rock resembles the ARFI that caused the propagation of shear waves which are the ripples in the example. The process of sending successive push pulses and monitoring them enables the acquisition of real-time quantitative elasticity data.

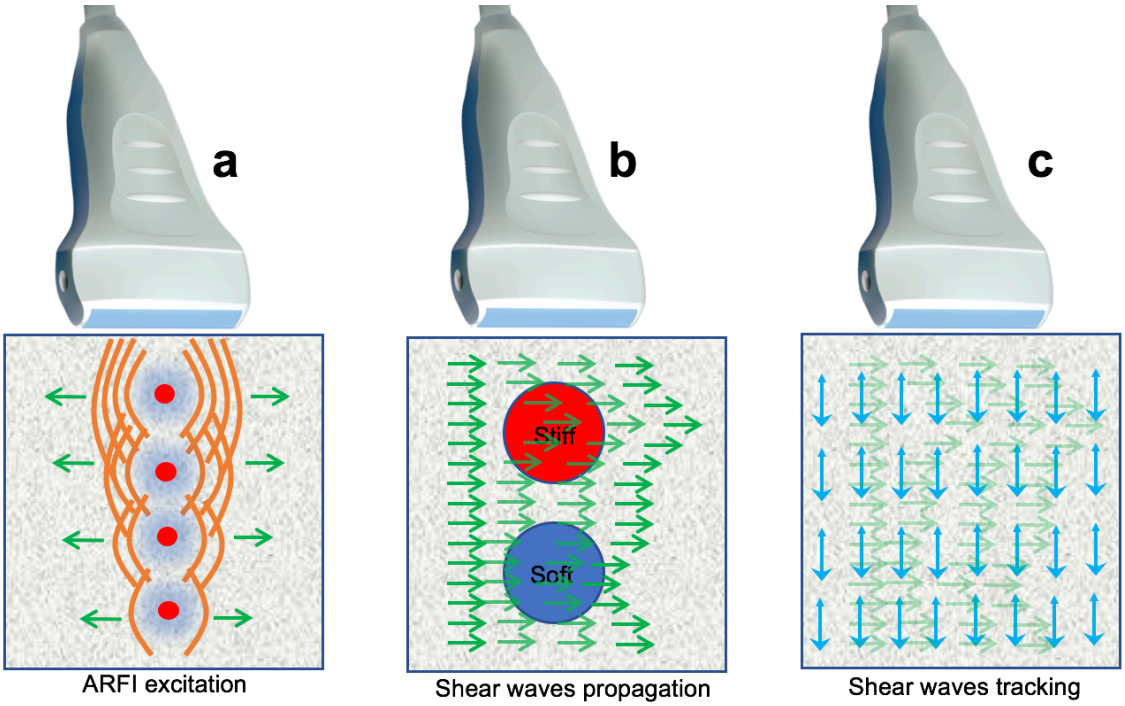

Figure 2-7 The principle of two-dimensional shear wave elastography.

The graph demonstrates a simplified shear wave production and detection model. In image-a, axial ARFI push pulses (red dots) will deform tissues (orange curves) and cause a perpendicular propagation of shear waves bilaterally (green arrows). In image-b, shear waves propagating in one of the directions travel faster in a stiff object and slower in a soft object. In image-c, multiple tracking waves are sent to detect the arrival times of shear waves between objects to measure the velocity. The excitation and tracking methods vary between SWE systems.

The techniques of applying push pulses and tracking shear waves vary tremendously amongst SWE systems. One of the most sophisticated and popular 2D SWE systems is the one developed by the French company SuperSonic Imagine® (SSI) (Aix-en-Provence, France). The method in which the ARFI is sent is similar to the one demonstrated in image-a of Figure 2-7 via focusing them, almost simultaneously, at various axial depths. This amplifies the strength of the ARFI by creating a “mach cone” profile, which may increase

the generation efficiency of shear waves by eight folds in comparison to other SWE systems [92]. Hence, it allows the coverage of up to 4 cm × 9 cm ROI using the convex probe. Moreover, this system employs an ultrafast imaging technology capable of acquiring images with frame rates up to 5000 images per second using its novel 'plane wave' B-mode technology. Their excitation and tracking technology allows the acquisition of real-time data in high temporal resolution. This SSI system was one of the first 2D SWE methods commercialised in 2009, which is why it is one of the most investigated systems in the SWE literature. It should be noted that in the elastography nomenclature, 2D SWE (including SSI) is usually referred to as SWE. This acronym will also be used in this thesis as a reference for 2D SWE.

Multiple studies investigated diagnostic and reliability performance differences between the different shear wave imaging techniques, mostly in the liver [93-109] with few others in breast [110, 111], testes [112] and phantoms [113-117]. Some of these studies investigated SSI and found that it compares favourably to other SWE methods. In a study of 349 patients with chronic liver disease, Cassinotto et al. [108] compared SSI to two other shear wave imaging systems and found that SSI had a significantly better area under the receiver operating curve (AUROC) and accuracy. This finding was also confirmed in several additional studies with a cumulative sample of more than two thousand chronic hepatitis patients [99, 104, 118, 119]. Elkrief et al. [100] reported a significantly better diagnostic accuracy for SSI (87%) in comparison to TE (57%). In breast cancer characterisation, SSI performed slightly better than the Toshiba SWE system (Aplio500, Toshiba Medical System, Tochigi, Japan) [111]. AUROC was 0.892 for the Toshiba SWE compared to 0.930 for the SSI system. However, this better performance was not statistically significant. One study compared various elastography systems on a phantom and showed that SSI provides more accurate and less biased shear wave readings [114]. Despite the mostly positive outcomes in favour of SSI, Sporea et al. [108] reported similar diagnostic accuracy for liver fibrosis and cirrhosis in comparison to two other SWE system. Nevertheless, the evidence presented thus far favours the investigation of this SSI system in muscle due to its accurate elasticity measurements.

2.2.3 Comparison between strain and shear wave elastography

Researchers reviewing the elastography literature will notice a remarkable overlap in the nomenclature. Specifically, using the term “real-time elastography” to refer to both SE and SWE. This inaccurate term may cause potential confusion for novice investigators who are unaware of the principal differences between the two methods. Therefore, it is recommended to refrain from using this generic term to describe their technique as both methods may provide real-time elastograms. Despite the confusion in terminology, there are major differences in the principle and qualities between SE and SWE summarised below in Table 2-3.

Table 2-3 Main differences between strain and shear wave elastography.

	Strain elastography (SE)	Shear wave elastography (SWE)
Physical compression	Required	Not required
Output data	Qualitative	Quantitative
Elasticity information	Relative	Absolute
Depth	Superficial and medium (~<4cm) Depends on the force applied	Superficial, medium and deep (~<8cm) Limited by acoustic power regulations
Operator dependency	Substantial	Moderate
Reproducibility	Moderate-excellent	Excellent
Spatial resolution	Excellent	Good
Frame-rates	30 frames/sec	<1–3 frames/sec
Availability	Widely available	Less available
Applicability	More suitable for focal disease	More suitable for diffuse disease

The major pitfall in SE is its qualitative nature, which may limit the interpretation. Another main weakness of this method is that the relative data presented could show inaccurate strain information. A diffuse stiff disease may show the same degree of elasticity information as a diffuse soft disease when the surrounding reference structures are softer. Indeed, Yang et al. [120]

reported that strain ratios in SE failed to detect various types of diffuse thyroid disease. However, when investigating focal nodular thyroid disease, a recent meta-analysis indicated that SE has a superior specificity but roughly similar sensitivity to SWE [121]. They reported that the sensitivity and specificity of SE were 0.84 and 0.90 respectively, and those of SWE were 0.79 and 0.87 respectively.

Studies comparing the two methods are scarce. Few have shown that SE performs better than SWE [121-123], while others reported similar performances [124-127]. However, numerous studies are showing strong evidence that SWE has a superior performance compared to SE [101, 114, 115, 117, 128, 129]. For example, Franchi-Abella et al. [114] conducted a comparative in vitro phantom study on several SE and SWE systems. They found that SWE systems had a superior quality with more accurate stiffness estimations and less bias. The qualitative SE estimations exhibited biases that were confounded by the position of ROI and target stiffness. Another cohort study investigated the accuracy of SWE versus SE for diagnosing liver fibrosis using biopsy as a reference [101]. The AUROC for SWE and SE were 0.807 and 0.767 (p=0.027) respectively, demonstrating superior diagnostic performance in liver fibrosis.

Nowadays, SWE can perform comparatively to SE for assessing focal tissue lesions with the help of novel quality indicators of the acquired elasticity data. Barr and Zhang [124] compared the diagnostic performance of SWE and SE in breast cancer. They reported that SWE had a sensitivity of 93% and a specificity of 89% in comparison to a sensitivity of 98% and specificity of 87% for SE.

There is still considerable uncertainty with regard to the best applications for each method. The main shortfall of the cited comparison studies is that they generally have a small sample size with some lacking clinical evidence. There is a compelling need for more research into this area on different organs and techniques. This will optimise elastography methods for suitable organs and diseases.

Having an objective quantitative measure is a major advantage in SWE, favouring its utility compared to SE. There is also consensus amongst experts

that SWE provides a better reproducibility since it does not require the operator's input via compression [130-132]. This understanding has been supported by evidence [117]. It is also the experts' consensus that SWE has a shorter learning curve [133]. To produce a semi-quantitative image in SE, a reference ROI need to be located usually on the subcutaneous fat since it is assumed to have a standard stiffness. However, this is not usually feasible and sometimes impossible in muscle elastography for anatomical limitations in lean subjects with a thin subcutaneous adipose layer [134]. In view of what has been reviewed so far, SWE seems to be the best elastography techniques for assessing skeletal muscle because of its several advantages and suitability for assessing diffuse muscle diseases. Therefore, this thesis will only focus on this type of elastography.

2.2.4 Limitations of shear wave elastography

One of the limitations in SWE is the fact that shear waves do not propagate in fluids, limiting its application for characterising cystic lesions (Figure 2-8). This is also because the tracking pulses will have extremely low signals in anechoic objects (e.g. cysts), preventing successful shear waves tracking. Therefore, SWE images will appear void without any colour-coding due to the lack of signals. This also applies to areas with extremely low echogenicity or artefacts such as lesions with marked shadowing or microcalcifications [135].

SWE is susceptible to a number of confounders that could influence the validity of the readings such as internal stress by the cardiac or breathing motion. This is thought to affect liver measurements and should be accounted for through breath-hold techniques for example [7]. In addition, elastography-specific artefacts may arise when acquiring SWE images. For example, Figure 2-8 (A) demonstrates a band-like artefact that has been described recently [136]. It is thought to occur when imaging stiff superficial structures. SWE operators should be aware of this artefact and ensure valid elasticity readings. Other limitations such as the depth, probe load and operator influence should be further investigated and accounted for.

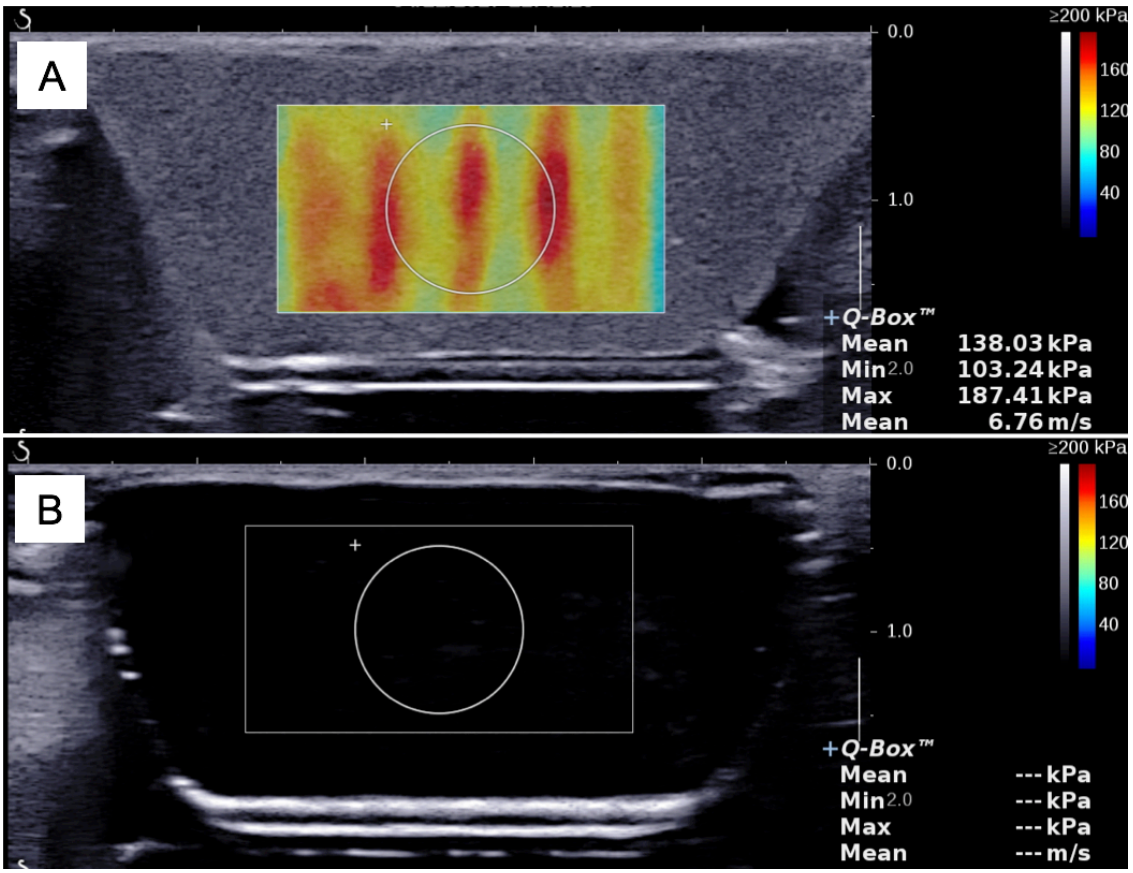

Figure 2-8 Shear wave propagation in solids and fluids.

The figure shows two images for different ultrasound gel pads. Image A is a synthetic solid gelatine pad where shear waves are travelling at 6.76 m/s. Image B is a transparent water-based gel pad where shear waves fail to propagate, and the SWE system detects no elasticity information.

Still, the most critical limitation by far is the variability in the tissue excitation and tracking technologies amongst the elastography systems. The heterogeneity in the commercial systems' design and settings could postulate a discrepancy in reliability and actual elasticity estimations, which will be studied in chapter 3. However, there is still hope with initiatives like the Quantitative Imaging Biomarkers Alliance® that aim to standardise the practice of shear wave elastography [137].

Besides the limitations, there are several assumptions current elastography systems hold when imaging biological tissues such as isotropy, incompressibility and homogeneity. Additionally, the most important assumption is that soft tissue elasticity is linear, when in fact most biological tissues have a viscoelastic property making the strain and deformation more complex than non-biological materials. These assumptions may hold in specific pathological cases (i.e. liver fibrosis) but are violated in numerous other applications. For

instance, skeletal muscle is anisotropic, inhomogeneous and viscoelastic [138, 139]. There is a demand for the development of more complex modelling to account for these violated assumptions [140].

Overall, sonoelastography is an advancing and promising technology. Despite the several limitations and assumptions elucidated above, it has proven to be a valuable imaging biomarker with substantial diagnostic performance in various pathologies. Now after understanding the principle and limitations of elastography, the next section will review the main applications in various organs.

2.2.5 Clinical applications

2.2.5.1 Liver

The first established clinical application of sonoelastography was for diffuse liver diseases. Clinical guidelines were introduced by several international societies [7, 63, 141, 142]. The established role of elastography in the assessment of liver diseases could be one of the primary reasons behind the expansive interest in the medical imaging research community to investigate its potential applications in other organs. Liver elastography introduced the 'proof of concept' to utilise ultrasound-derived elasticity information as a biomarker for characterising pathologies. It has proven to be an indispensable non-invasive tool for evaluating diffuse liver disease by transforming the current hepatology practice.

The World Federation of Ultrasound in Medicine and Biology (WFUMB) recommends avoiding liver biopsy when elastography results are consistent with other clinical findings [63]. A recent systematic review and meta-analysis reported a high SWE pooled sensitivity of 81% and specificity of 91% for evaluating the severity of liver fibrosis in children and adolescents [119]. Another meta-analysis appraised the value of SWE in 13 studies of 2303 adult patients and showed excellent diagnostic performance for staging liver disease across all stages of fibrosis [143]. It reported AUROC for ≥F1, ≥F2, ≥F3 and ≥F4 of 0.85, 0.87, 0.93 and 0.94 respectively. Additionally, more than ten other systematic reviews and meta-analyses confirm these excellent findings for evaluating liver fibrosis [144-153]. Nowadays, the national institute for health and care excellence (NICE) endorses the use of elastography for diagnosing

cirrhosis in patients with hepatitis C virus and people with alcohol-induced liver disease [154]. Moreover, they had previously published a special recommendation for the diagnosis and monitoring of liver fibrosis using elastography [155].

Besides diffuse liver disease, a couple of meta-analyses demonstrated elastography's value for differentiating benign from malignant liver lesions, with a summary receiver operating characteristic (ROC) close to 0.95 in both studies [156, 157]. An additional recent meta-analysis involving 1046 liver lesions also reported similarly positive results (AUROC=87%) [158]. However, its use for this purpose remains under research as none of the international ultrasound societies recognises this application despite the strong evidence. Their consensus is commonly derived from two relatively old studies, which found an overlap between the SWV of malignant an benign tumours [159, 160]. Therefore, the guidelines regarding the role of elastography for diagnosing focal liver are expected to change in future updates.

2.2.5.2 Breast

Mammography and ultrasound are the two invaluable tools for breast cancer screening. However, the false negative rates in mammography and poor specificity, as well as difficulty imaging dense breast in conventional ultrasound, are two major shortcomings [161]. With the realisation of the significance of early diagnosis, elastography had a momentous potential to offer a non-invasive complementary diagnostic tool. Initial breast elastography in vitro research found that cancerous breast tissues are significantly stiffer than benign [52]. Further, early validation studies using SWE reported that there could be up to a threefold increase in the stiffness of infiltrating ductal carcinomas (45.3 kPa ± 41.1) compared to benign lesions (146.6 kPa ± 40.05) [162].

Nowadays, the Breast Imaging Reporting and Data System (BI-RADS) have incorporated the elastography lexicon (soft, intermediate, or hard) to their standardised reporting system. A multicentre study of 939 patients, using the SSI system showed that the addition of SWE to ultrasound-based BIRADS improved the specificity from 61.1% to 78.5% without a significant compromise on sensitivity [163]. Additionally, the latest BIRADS edition (version 5) recommends that a normal elastography result downgrades a category 3 lesion

to category 2 while abnormal elastography upgrades the lesion to category 4A (suggestive of malignancy).

A large meta-analysis of 2424 patients assessed the diagnostic performance of SWE in comparison to histopathology (core biopsy and fine-needle aspirations) and reported a summarised sensitivity and specificity of 0.93 and 0.81, respectively [164]. Besides the high diagnostic value, Cosgrove et al. [165] reported an almost perfect breast SWE intra-operator reliability (ICC=0.87). However, inter-operator reliability was moderate (kappa=0.66). Unlike other organs where the mean elasticity is commonly measured, most common breast elasticity classification schemes use the maximum stiffness as it was found to be the best performing measure [164, 165].

With the growing number of promising studies, international societies have indeed published practice guidelines on breast elastography [62, 133]. NICE had also published an innovation briefing highlighting how the SSI SWE system could have a role for cancer screening in breast assessment clinics [166].

Breast elastography, however, has some limitations. The most important one is that the scoring systems are not standardised. Secondly, breast tissue might undergo non-cancerous structural changes such as fat fibrosis and necrosis and present stiff on elastography leading to false positive results [167]. Additional factors such as breast thickness and lesion depth might increase the rates of false negative results [167]. Nevertheless, SWE limitations can sometimes be useful for characterising lesions. For example in identifying predominantly cystic lesions, where SWE coloured maps will only fill the solid surrounding tissues [168].

Richard Barr, an authority on breast elastography, comments that “the addition of elastography to a standard breast ultrasound will decrease the number of benign biopsies” [169]. Most breast elastography publications were conducted using SE. Additional large and prospective randomised controlled trials are warranted for SWE to assess its impact on clinical management pathways.

2.2.5.3 Thyroid

The thyroid gland is another prominent application for elastography. Thyroid nodules are common across the world, especially in populations with poor iodine supply. Ultrasonography has a high sensitivity for detecting nodules but

falls short for differentiating a number of malignant nodules [170]. The same classical elasticity features of breast lesions also apply to thyroid, where malignant nodules are commonly stiff.

So far, six meta-analyses were published eliciting the diagnostic performance of SWE against histological evidence, each analysing approximately 2000 nodules [171-176]. All reported excellent AUROC ranging from 0.91 to 0.94, except the most recent one by Nattabi et al. was marginally lower at 0.85 [176]. The pooled diagnostic odds ratio were also high ranging from 12.7 to 46.7. Other diagnostic performance metrics like sensitivity, specificity, positive predictive value (PPV) and negative predictive value (NPV) were over 0.90 on average. The similarities in the findings are expected due to the expected overlap in the included studies. Nevertheless, the strong evidence highlights SWE's value and potential for reducing unnecessary biopsies. This can have positive impacts both economically and clinically by reducing the financial costs of biopsies and saving patients undergoing interventional procedures.

Despite the strong favourable evidence, the reality is that SWE is still not adept enough to replace fine needle aspiration for diagnosing thyroid disease. It is so far recommended as complementary method alongside conventional ultrasonography and for following up benign-looking thyroid nodules. WFUMB had recently published specific guidelines on the clinical use of thyroid elastography [76]. It importantly included recommendations on the optimum examination techniques and interpretation methods.

Similar to other elastography applications, various limitations might be of some detriment to thyroid SWE quality. For example, calcified shell nodules are particularly difficult to assess since the central region is essentially non-visible. Similarly, cystic nodules do not produce enough echoes to create an elastogram. Moreover, the effect of nodule size on the reliability of the SWE acquisitions is not explicitly examined yet. There is also relatively little work done on diffuse thyroid disease, which could be due to the effective alternative available markers. However, the results of SWE for the diagnosis of nodular thyroid disease are auspicious. The similar recommendation to breast elastography applies again to the thyroid, where there is a need for prospective large randomised studies.

2.2.5.4 Prostate

Prostate cancer is the most common cancer in men with an incidence of approximately 130 cases diagnosed every day in the UK, based on the latest statistics from Prostate Cancer UK. Considerable advances have been made in the diagnosis and management. However, multiple needs remain unmet such as the validation of new biomarkers for screening, diagnosis and management.

Similar to the breast and thyroid, cancerous prostate masses are stiffer than normal tissue due to increased collagen deposition in the peripheral zone and numerous other pathological processes [177]. The SSI is the only commercial system equipped with an endocavity SWE-capable transducer thus far. Therefore, all transrectal prostate SWE studies were performed using this system. A recent meta-analysis appraised the overall accuracy of 9 research studies that investigated the diagnostic performance of prostate SWE for detecting cancer with histopathological reference [178]. The pooled sensitivity and specificity were 0.84 and 0.86, respectively with an AUROC of 0.91. One drawback to these promising performance indicators is the high variability in the cut-off value adapted amongst the studies, which ranged from 28.5 kPa to 52.0 kPa. The guidelines published by WFUMB recommend using a cut-off value above 35 kPa for malignancy [133]. However, this matter is still dubious, as an adequate distinction between benign and cancerous prostate tissue using SWE remains equivocal.

The fact that prostate SWE is performed trans-rectally adds more steepness to the SWE learning curve. Nonetheless, trans-abdominal prostate elastography was attempted by Bircan et al. [179] to investigate SWE usefulness for determining the severity of BPH and found a significant SWV difference (p=0.02) between the severe BPH cases and the moderates (2.62±0.58 m/s and 2.25±0.55 m/s, respectively). Notably, there was also a substantial difference of more than 1m/s between BPH patients and healthy controls.

So far, the evidence shows that prostate elastography can help in triaging cases for biopsy as well as helping for localisation in targeted biopsies. This could potentially reduce the costs of unnecessary procedures as well as decrease the number of unsuccessful blind biopsies. Additionally, prostate elastography could be indicated for detecting specific lesions that are otherwise not visible on other imaging modalities [180]. Although multiple studies

investigated diagnostic performance, few aimed to test the reliability within and between operators. It is imperative that future studies aim to investigate this aspect.

2.2.5.5 Tendon

Tendon elastography is not as established as the previously described areas of practice. However, it will be reviewed considering the relevance to muscle elastography and the relatively large number of publications. This area was one of the first explored applications of elastography in the musculoskeletal system. Tendons are significantly stiffer than other structures and are inherently isotropic. Their stiffness is not constant in normal cases as they can vary on resting state or tension. Such biomechanical complexity could explain the delayed research activity in comparison to other organs.

While pathologies tend to stiffen tissue due to cancerous or fibrotic changes in other organs, tendons tend to soften in most tendinopathies. The high stiffness in normal tendons can be problematic as shear waves travel at high velocities (>10.0 m/s) and the tracking waves speed could be limited. Most systems had an SWE scale limited to 10.0 m/s. Estimating this was not feasible until the SSI system was validated and increased the scale to more than 16.0 m/s in 2015. Several other systems are still limited to 10.0 m/s.

Several validation studies were published to verify the concept of SWE in tendons. Zhang et al. [181] performed an in-vitro experiment on 8 patellar swine tendons correlating SWE to the tangent traction modulus using a materials testing system. They reported significant correlations ranging from 0.82 to 1.0 (p<0.01). Optimum techniques for scanning human tendons are still being developed.

The Achilles tendon is the most investigated tendon due to its high clinical relevance in sports medicine and rheumatology. Measurements for the Achilles tendon are usually performed in neutral or plantarflexion positions, but infrequently in dorsiflexion as the readings could exceed the upper limit of the SWE scale (≈16.0 m/s) [182]. Normal Achilles tendon SWV was reported to be approximately between 4.8 – 9.8 m/s in the neutral position and between 5.8 – 7.0 in passive plantar flexion [182-188]. The substantial variability in the results could be due to the different types of machines utilised and how each study

defines ankle joint angles for the different positions. Secondary factors such as physical fitness could also be of influence as a recent conference abstract revealed a difference ratio of 1.8 between professional athletes and non-athletic general population Achilles tendon stiffness [189]. A recent study found that ageing could also induce spatial stiffness variations, which is a promising finding as SWE could have the potential for predicting the likelihood of injury [190]. Further evidence is required to validate the findings.

Tendinopathy can distort the tendon's mechanical properties by disorganising the collagenous structures [191]. Although grey-scale ultrasound and Doppler imaging can detect tendinopathy, they do not inform on the mechanical aspect that is more related to the physical function [192]. A study showed that elastography had the strongest correlation to the Victorian Institute of Sport Assessment-Achilles score [(VISA) validated clinical rating for tendon symptoms and dysfunction] when compared against B-mode and Doppler imaging [193].

Dirrichs et al. [185] published one of the largest studies with a sample size of 112 participants. They reported a strong correlation between the VISA scores and tendon elasticity (r=0.81). Adding SWE outcomes to the B-mode and PD scores increased sensitivity from 67.1% to 94.3% but dropped specificity from 81.7% to 69.1%. They also presented a case study of a patient with severe tendon pain over the left side (Figure 2-9). They examined the symptomatic (VISA=54) and asymptomatic (VISA=100) sides and found normal B-mode and PD appearance. However, SWE depicted an abnormally decreased stiffness over the symptomatic side.

With regard to tendon tear, a small pilot study found a significant stiffness difference between torn (56 kPa) and normal (291 kPa) Achilles tendon [183]. However, such findings offer little clinical information as the established clinical methods for assessing tendon tears are valid, reliable and feasible. Nevertheless, SWE could be useful for differentiating complete from partial tendon tears using dynamic SWE scanning. It is hypothesised that stiffness fails to increase upon stretching for full-thickness tendon tears unlike partial tears, which might be difficult to appreciate on B-mode imaging.

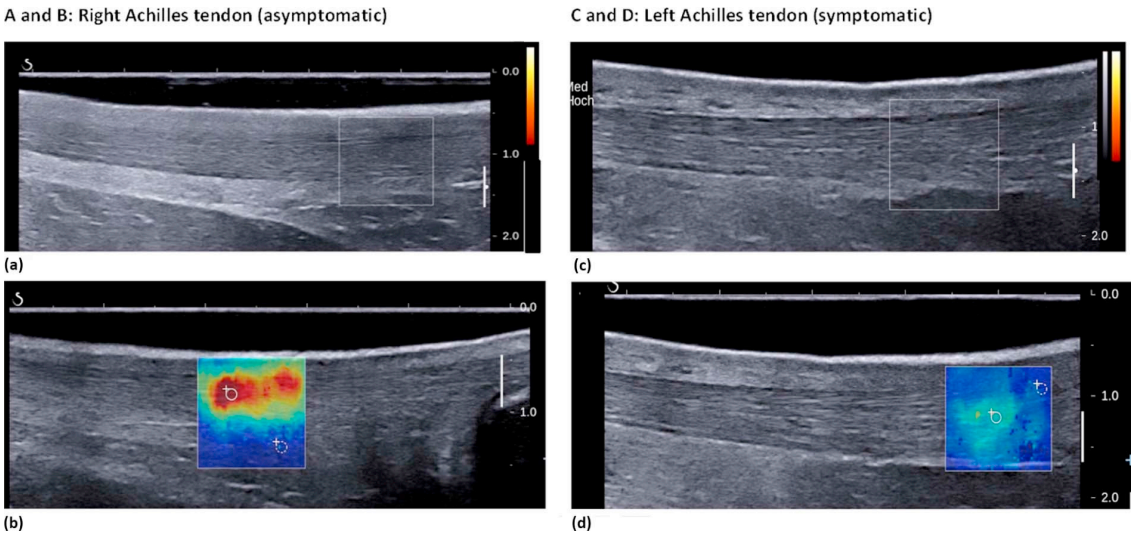

Figure 2-9 Intraindividual SWE comparison for a patient with a unilateral symptomatic Achilles tendon.

B-mode, PD and SWE images for the asymptomatic (a and b) and symptomatic sides (c and d). SWE was the only parameter to detect an abnormality of decreased stiffness for the symptomatic side. (Reprinted by permission from Elsevier publishing: Academic radiology [185])

In contrast, another study suggested that SWE could be used to monitor tendon healing postoperatively [194]. The study longitudinally followed-up twenty-six patients at 12, 24 and 48 weeks after a surgical repair of a tendon rupture. It reported that stiffness increased gradually at each time point (187.7±23.8 kPa, 238.3±25.3 kPa and 289.6±23.4 kPa respectively) and correlated strongly with functional assessments.

The most useful application for tendon elastography could be for tailoring rehabilitative exercises for patients with tendon injuries. More specifically, if SWE shows that the tendon is stiffer than normative readings, eccentric (lengthening) exercises should be performed to loosen the tendon. In contrast, when the tendon is soft, concentric (shortening) exercises will harden the tendon. This type of research has not been performed yet. Besides clinical performance, SWE demonstrated excellent inter- and intra-operator reproducibility results [181, 188], which are superior to the results on SE [195].

Although it is evident that tendon stiffness is lost in tendinopathy, there is so far no validated cut-off values for the diagnosis of any tendon abnormality. There is also no official guidelines or recommendations for tendon elastography. The increasing number of promising publications should stir more interest into this field to establish its clinical role.

2.3 Muscle elastography

After reviewing the important applications of elastography, it is now the time to focus on the central theme of this review, muscle elastography. This section will present a structured narrative review of the published studies on normal and abnormal muscle SWE. The studies were identified after searching the literature using the search terms [(shear wave elastography OR acoustic radiation force impulse OR elastography OR sonoelastography) AND (muscle*)] on PubMed and Embase databases. Moreover, weekly email alerts were set up on Google Scholar and PubMed for new publications containing the relevant search terms.

Before reviewing the literature, the rationale behind measuring muscle elasticity should be briefly explained again. The biomechanical properties of muscles are more apparent in comparison to other biological tissues given that muscles contract and relax to activate motion. In skeletal muscles, moto neurons are responsible for this task by sending electrical impulses to stimulate the action of muscle proteins (actin and myosin) to activate contractions. These contractions are a result of myofibrils (skeletal muscle fibre units) shortening. Myofibrils are composed of chains of contractile units called sarcomeres that are responsible for the shortening action. Each level of contraction changes the elasticity of the muscle, which is experienced when flexing the arm for example.

Pathological processes may alter these biomechanical properties resulting in elasticity changes. Such processes may not induce morphological changes at early disease stages, which will not be depicted on conventional ultrasound imaging. This is concerning considering that muscle's function relies on its contractile properties. SWE could, therefore, be able to diagnose diseased or injured muscle tissue and elucidate the underlying mechanisms of muscular disorders. There is also the potential for monitoring treatment response and disease progression.

It is worth noting that conventional and alternative methods have been utilised to provide indirect inferences on the biomechanical properties of muscle. For example, a couple of old studies estimated Young's modulus by measuring Doppler shifts [196, 197]. More recently, sophisticated muscle hardness meters (myotonemeters) were introduced. They measure superficial mechanical

deformation by producing short compression pulses (15 ms) on the surface via a small probe. The induced superficial deformations are then assessed to quantify muscle's stiffness in units of Newton/meter for surface tension. Akagi and Kusama [198] found no correlation between SWE and myotonometry measures of muscle stiffness. A pilot study compared a commercial myotonometry system (MyotonPRO) versus SWE and reported favourable reliability results for the former [199]. However, myotonemeters are limited to superficial muscles. For example, it does not differentiate between the stiffness of the rectus femoris and vastus intermedius since they are situated axially to each other. In addition, thick subcutaneous fat layers could significantly influence their readings. Indeed, other studies have reported inferior accuracy in deep muscles for myotonometry [200, 201]. Nevertheless, there is potential for myotonometry because of its portability, cost and ease of use.

2.3.1 Shear wave elastography in normal muscle

2.3.1.1 Resting muscle elasticity

Normal muscles have their lowest stiffness in the resting position when the muscle is at its slack length (no passive stretching or active contraction forces applied). Electromyography (EMG) is commonly used in research to confirm this position by checking neuromuscular activity. This position can be considered the easiest to reproduce since it does not involve patient instructions to perform specific contractions. This explains why it is commonly utilised in muscle SWE studies. Kelly et al. [199] found the resting muscle position produced consistently higher ICC reliability results when compared to muscles under load.

Table 2-4 represents a list of normal stiffness values for various muscles. The table demonstrates significant differences amongst muscle groups. This is expected since skeletal muscles have various shapes and fascicle architecture. A more interesting note is the remarkable difference amongst the studies investigating the same muscle. The gastrocnemius medialis is one of most commonly investigated muscles and one where a large range of stiffness can be observed ranging from 8.9 kPa – 33.0 kPa. Although the table only lists normal resting muscles acquired using the longitudinal orientation, several factors and confounders that could be hypothesised to have induced such

discrepancies. For example, variability in body habitus, subject position, operators, SWE system and ultrasound frequency. Variability in the SWE acquisition methods can also be postulated as a probable cause. This will be explored further in one of the following subsections. These disagreements are concerning and limit comparability between studies.

Table 2-4 Normal resting muscle elasticity values using a longitudinal view.

Muscle	Stiffness*	SWE system	Reference
Upper limb			
Biceps brachii	9.3 kPa	SSI	[202] Lacourpaille/2012
	5.1 ± 0.6 kPa	SSI	[203] Yoshitake/2014
Brachialis	5.9 ± 0.2 kPa	SSI	[138] Gennison/2010
Adductor digiti minimi	13.5 kPa	SSI	[202] Lacourpaille/2012
Adductor pollicis	11.4 kPa	SSI	[202] Lacourpaille/2012
Brachoradialis	10.4 kPa	SSI	[202] Lacourpaille/2012
Triceps brachii	9.1 kPa	SSI	[202] Lacourpaille/2012
Lower limb			
Vastus lateralis	9.8 kPa	SSI	[204] Lacourpaille/2012
	14.9 ± 5.2 kPa	SSI	[205] Bontanlioglu/2013
	13.5 kPa	SSI	[206] Dubois/2015
Vastus medialis	13.4 ± 3.7 kPa	SSI	[205] Bontanlioglu/2013
	11.7 kPa	SSI	[206] Dubois/2015
Vastus intermedius	14.5 ± 6.3 kPa	SSI	[207] Wang/2017
Rectus femoris	12.8 ± 3.5 kPa	SSI	[204] Kot et al/2013
	9.7 kPa	SSI	[202] Lacourpaille/2012
	12.3 kPa	SSI	[206] Dubois/2015
	10.3 ± 2.0 kPa	Siemens	[208] Akagi/2015
	2.0 ± 0.4 m/s	Siemens	[209] Tas/2017
Biceps femoris	16.8 kPa	SSI	[206] Dubois/2015
	24.7 ± 4.9 kPa	SSI	[210] Morales/2017
Semitendinosus	12.6 kPa	SSI	[206] Dubois/2015
	15 ± 3.1 kPa	SSI	[210] Morales/2017
Semimembranosus	15.9 kPa	SSI	[206] Dubois/2015
	26.7 ± 6.5 kPa	SSI	[210] Morales/2017
Gastrocnemius medialis	8.9 kPa	SSI	[202] Lacourpaille/2012
	11.1 ± 4.1 kPa	SSI	[186] Arda/2011
	33.0 ± 9.3	SSI	[211] Eriksson/2015
	1.9 ± 0.3 m/s	SSI	[212] Cortez/2016
	14.1 kPa	SSI	[206] Dubois/2015
	16.9 ± 3.8 kPa	SSI	[213] Leung 2017
	18.9 ± 10.2 kPa	SSI	[214] Nakamura/2017
	19.3 ± 3.6 kPa	SSI	[215] Chino/2017
	18.2 kPa	SSI	[199] Kelly/2018

	2.2 ± 0.4 m/s	Siemens	[216] Yoshida/2017
	27.0 ± 18.0 kPa	Toshiba	[217] Ohya/2017
Gastrocnemius lateralis	13.5 kPa	SSI	[206] Dubois/2015
	16.0 ± 4.0 kPa	SSI	[213] Leung/2017
	24.9 ± 11.1 kPa	SSI	[214] Nakamura/2017
	9.4 ± 3.2 kPa	Siemens	[208] Akagi/2015
	18.6 ± 11.4 kPa	Toshiba	[217] Ohya/2017
Soleus	19.2 kPa	SSI	[206] Dubois/2015
	10.7 ± 2.6 kPa	Siemens	[208] Akagi/2015
Peroneus longus	21.0 ± 28.8 kPa	Toshiba	[217] Ohya/2017
Peroneus brevis	12.6 ± 15.3 kPa	Toshiba	[217] Ohya/2017
Flexor digitorum longus	12.0 ± 11.4 kPa	Toshiba	[217] Ohya/2017
Tibialis anterior	13.5 kPa	SSI	[202] Lacourpaille/2012
	3.49 ± 0.58 m/s	SSI	[212] Cortez/2016
Tibialis posterior	10.5 ± 4.8 kPa	Toshiba	[217] Ohya/2017
Gracilis	18.0 kPa	SSI	[206] Dubois/2015
Sartorius	15.9 kPa	SSI	[206] Dubois/2015
Miscellaneous			
Infraspinatus	9.0 ± 3.2 kPa	SSI	[218] Kusano/2017
	27.7 kPa	SSI	[199] Kelly/2018
Supraspinatus	34.0 ± 9.9 kPa	SSI	[186] Arda/2011
	31.2 ± 13.0 kPa	Siemens	[219] Itoigawa/2015
Masseter	1.8 ± 0.5 m/s	Siemens	[220] Badea/2014
	10.4 ± 3.7 kPa	SSI	[186] Arda/2011
Multifidus	16.2 ± 4.8 kPa	SSI	[221] Creze/2017
Longissimus	20.7 ± 8.1 kPa	SSI	[221] Creze/2017
Iliocostalis	14.4 ± 4.2 kPa	SSI	[221] Creze/2017
Trapezius	2.8 ± 0.4 m/s	Siemens	[222] Heizelmann/2017
	17.8 ± 4.8 kPa	Siemens	[198] Akagi/2015
Levator scapulae	15.3 ± 3.3 kPa	Siemens	[198] Akagi/2015
Splenius capitis	13.7 ± 3.9 kPa	Siemens	[198] Akagi/2015
Erector Spinae	16.5 kPa	SSI	[199] Kelly/2018
Transversus abdominis	2.1 ± 0.6 m/s	SSI	[223] Hirayama /2016
	14.1 ± 6.5 kPa	SSI	[224] Hirayama/2017
Lumbar Multifidus	8.5 ± 1.9 kPa	SSI	[225] Moreau/2017

*SWE values presented as means ± standard deviation in kPa for Young's modulus or m/s for SWV . SSI= Supersonic Imagine®

2.3.1.2 Passive muscle elasticity

There is an important relationship between muscle elasticity and length/tension. In other words, stiffness is proportional to the degree of fascicle stretching and contraction. Muscles become passively stretched when its length increases without any active force or load applied. Coombes et al. [226] recently investigated passive muscle elasticity differences for the quadriceps over a range of knee flexion angles. Nineteen participants were positioned on a

dynamometer to calibrate the angles and acquire SWE readings. Muscle activity was monitored using EMG to ensure there is no involuntary contraction and all muscles are relaxed. They found a significant interaction between muscle elasticity and flexion angle (p<0.001) highlighted by a proportional increase in SWV with each incremental rise in knee flexion angle. Additionally, Chino et al. [215] reported a gradual increase in the stiffness of the medial gastrocnemius from 20° plantar flexion (considered the most relaxed position for this muscle) to 20° dorsal flexion.

Dubois et al. [206] investigated quadriceps elasticity in resting (knee extended) and passive stretching (knee passively flexed at 90°) in a small sample of 10 healthy participants. They reported a significant increase and difference between the two positions as elasticity values increased during passive stretching. For example, the rectus femoris increased from 4.1 kPa in resting to 13.9 kPa in passive stretching. Numerous other articles confirm the positive relationship between muscle stretching and elasticity [225, 227-231]. All previous studies highlight the usefulness of SWE for evaluating the passive stiffness patterns in healthy muscles.

It is important to note that it is not uncommon in some research articles and reviews to inaccurately label passive stretching positions as “relaxed or resting”. Although the muscle is relaxed in terms of active contraction, there is an element of passive stretching that significantly contributes to muscle elasticity as highlighted previously. These definitions are critical when comparing normative muscle elasticity values between studies. Therefore, researchers should verify the actual muscle positioning status as defined in the methodology regardless of what the title or abstract states.

2.3.1.3 Active muscle elasticity and force

Active muscle elasticity can be defined as the acquired stiffness measurement upon muscle contraction. It has been found that muscle elasticity is linearly related to active muscle force [203, 232-235]. It is extremely challenging to isolate a single muscle for measurement since joint movements can be controlled by a combination of muscles. Having the ability to quantify individual muscle’s force can offer an insight into how the central nervous system controls force sharing in joints controlled by groups of muscles (e.g. knee). This is

fundamental in the field of biomechanics as well as in pathophysiology to understand why specific muscles are affected/spared and others not in certain diseases. Although EMG can be utilised to measure individual muscle activation, it has a major drawback since muscles may produce various forces for the same activation level due to the complex force-length relationship [236]. Nevertheless, most SWE studies on this topic utilised surface EMG as a reference to monitor muscle's maximum voluntary contraction (MVC) exerted during the elasticity measurement.

Bouillard et al.'s study [234] was one of the first that demonstrated the linear relationship between active muscle elasticity and force level. In their study, they investigated the first dorsal interosseous during isometric index finger abduction in addition to the abductor digiti minimi during isometric little finger abduction. Muscle stiffness was measured consecutively across different contraction levels of increasing torque ramps. They reported an almost perfect coefficient of determination (R^2 = 0.98) between active muscle elasticity and muscle contraction (graph A in Figure 2-10), which was marginally higher than the R^2 between EMG and torque (R^2 = 0.95).

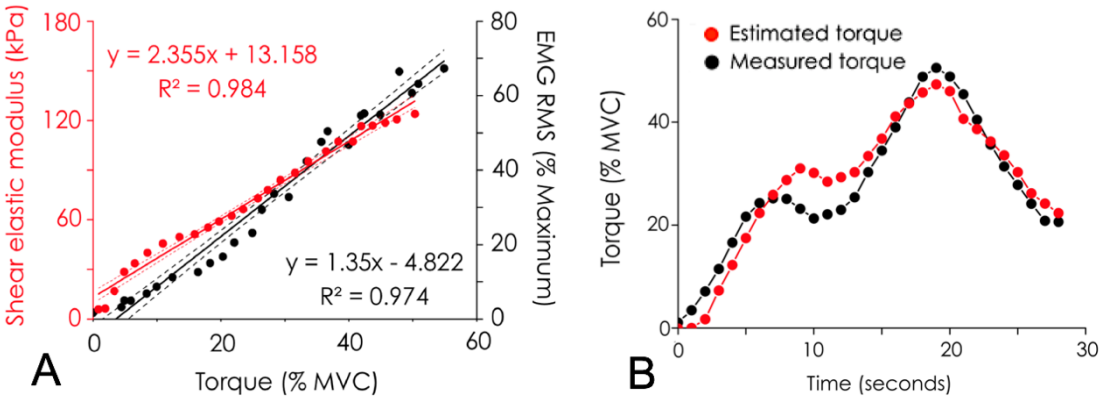

Figure 2-10 Relationship between active muscle elasticity and muscle force during contraction

Graph-A shows a significant correlation between muscle force (%MVC) and muscle elasticity across a linearly increasing ramp of torques (red), which better estimates the regression line in comparison to the EMG estimations (black). Graph-B shows good agreement for muscle elasticity and torque during 30 seconds of random contraction levels. The estimated line was based on the linear regression equation from graph-A. Both figures are for the first dorsal interosseous muscle. (Reprinted by permission from the Public Library of Science: PLOS one [234])

A second experiment where participants were asked to randomly contract their muscles during a 30-seconds contraction period showed a good agreement between muscle elasticity and torque (graph B in Figure 2-10). Although their study had a small sample size (n=10), it sheds light on a promising new biomarker for quantifying individual muscle force.

Later, Sasaki et al. [233] also reported a significant association between muscle force and active muscle elasticity for the anterior tibialis muscle at different ankle joint angles ranging from -15° of ankle dorsiflexion to +25° of ankle plantarflexion. In contrast to the previous study, the coefficient of determination was weak ($R^2 = 0.52$), albeit statistically significant ($p<0.001$). In addition to muscle force, they examined the association between active muscle contraction with muscle fascicle length, which was also significant but weak ($R^2 = 0.42$; $p<0.001$). However, the results presented for muscle contraction were studied upon electrically elicited tetanic contractions rather than voluntary contractions. The small sample size (n=9) and artificially induced contraction are two major limitations of their results.

More recently, Kelly et al. [199] reported a significant gradual increase in erector spinae muscle elasticity from resting to 40% MVC and 80% MVC conditions (15.5 kPa, 25.9 kPa and 29.7 kPa respectively). They also investigated the infraspinatus and medial gastrocnemius muscles, which also showed an increase in stiffness. Yoshitake et al. [203] demonstrated an almost perfect linear proportional relationship (r=0.99) between active biceps brachii stiffness values and different contraction torque levels in a small sample of ten young healthy participants.

The previous evidence highlights the feasibility and validity of estimating individual muscle force by measuring active muscle elasticity using SWE. However, SWE results in active muscle elasticity can be inhomogeneous and notoriously variable [220, 235]. In the Kelly et al. study [199], SWE reproducibility during active contraction was found to be inferior to resting measurements. The intra-operator reliability for the infraspinatus muscle was significantly higher in resting position (ICC= 0.89) in comparison to 80% MVC (ICC= 0.72). Between subjects variability was also higher as the coefficient of variation increased from 7% to 22%. The researchers also found this decreased reliability and increased variability consistent with the other muscles

they examined (erector spinae and medial gastrocnemius). This could be due to the high SWV values contracted muscles can reach which can be beyond the maximum SWE detection limit in old systems resulting in an underestimation of actual stiffness [232]. Another important explanation is the intricacy in controlling the optimum joint angle and level of contraction across patients. Therefore, application in clinical trials or practice can be time–consuming and less feasible without the availability of apt equipment such as dynamometers to check the joint angle and surface electromyography to verify the contraction intensity under investigation.

2.3.1.4 Reliability

With the advent of commercial SWE systems, numerous researchers investigated various aspects of reliability within (intra) and between (inter) operators as well as between sessions and days. Table 2-5 lists reliability results, presented as ICC, from various studies conducted on healthy subjects. Overall, muscle SWE appears to have an excellent inter- and intra-operator reproducibility (ICC >0.80). Notably, ICC of resting positions are marginally higher when compared to passive or active elasticity measurements [199, 225, 229]. Few studies performed inter-day reliability analysis, where the muscle elasticity is re-measured post 24 hours or more. For this type of analysis, SWE reliability was found to be substantial (ICC >0.70) apart from the study by Baumer et al. which reported poor (ICC= 0.33) inter-day reliability for passive muscle elasticity [237].

Reviewing Table 2-4 and Table 2-5 highlights a distinguished prevalence of the SSI system, when approximately 80% of the studies published on muscle SWE utilised it. In addition, the tables demonstrate a remarkable scarcity for data on other SWE systems. This could be because systems, like the LOGIQ E9 by General Electric, had commercialised the SWE package in 2015. Differences in reliability and mean values between systems are expected since each operates a unique SWE technology. Besides, the agreement between SWE systems in muscles is unknown. This warrants research to investigate the reliability of different SWE models and compare their performances on healthy and diseased cases before establishing any guidelines for muscle SWE.

Table 2-5 Summary of multiple studies reporting the reliability of SWE on healthy subjects.

Study	n	Muscle(s)	Machine	Condition	Reliability results*
[202] Lacourpaille/2012	30	MG, TA, VL, RF, TB, BB, BR, APO, ADM	SSI	Resting	Intra-operator= 0.87±0.04 Inter-operator= 0.70±0.14 Inter-day= 0.81±0.06
[238] Koo/2014	20	TA	SSI	Passive stretching	Inter-session= 0.85 – 0.97
[203] Yoshitake/2014	10	BB	SSI	Active contraction	Intra-operator= 0.98 (0.96–0.99) Inter-day=0.95 (0.91–0.97)
[239] Miyamoto/2015	11	MG, BB	SSI	BB-resting MG-passive stretching	Intra-operator= 1.00 Inter-day= 1.00
[211] Eriksson/2015	18	MG	SSI	Resting	Intra-operator= 0.98
[229] Brandenburg/2015	20	MG	SSI	Resting and passive stretching	Intra-operator= 0.75 (resting), 0.67 (passive)
[206] Dubois/2015	10	VM, LG	SSI	Resting and passive stretching	Resting: Intra-operator= 0.91 (VM), 0.92 (LG) Inter-operator= 0.88 (VM), 0.91 (LG) Passive stretching: Intra-operator= 0.92 (VM), 0.94 (LG) Inter-operator= 0.90 (VM), 0.87 (LG)
[240] Rosskopf/2015	22	Supraspinatus	Siemens	Resting	Inter-session= 0.70 (operator 1), 0.80 (operator 2) Inter-operator= 0.89
[223] Hirayama/2015	10	Transversus abdominis	SSI	Resting	Inter-operator=0.57 Inter-day= 0.86 (skilled), 0.59 (unskilled)
[212] Cortez/2016	16	TA, MG	SSI	Resting	Intra-operator= 0.69–0.70 Inter-operator= 0.69–0.73
[225] Moreau/2016	10	Multifidus	SSI	Resting and passive stretching	Resting Intra-operator= 0.92

					Inter-operator= NR Passive stretching Intra-operator= 0.72 Inter-operator= 0.95
[241] Akagi/2016	23	TB	SSI	Resting	Intra-operator= 0.95–0.94
[209] Tas/2017	12	RF	Siemens	Resting	Intra-operator= 0.93–0.94 Inter-operator= 0.95 Inter-day= 0.81–0.91
[237] Baumer/2017	10	Supraspinatus	Siemens	Passive stretching and active contraction	Intra-operator= 0.87 Inter-operator= 0.73 Inter-day= 0.33 (passive), 0.65 (active)
[227] Le Sant/2017	20	GM, GL, SOL, PL, FDL, FHL, TP, TA, EDL	SSI	Passive stretching	Inter-day= 0.79–0.97
[242] Chen/2017	10	BB	Siemens	Passive stretching	Intra-operator= 0.96, 0.93 Inter-operator= 0.87
[213] Leung/2017	5	MG, LG	SSI	Resting	Intra-operator= 0.80–0.98 Inter-operator= 0.94–0.99
[224] Hirayama/2017	10	Transversus abdominis	SSI	Resting	Intra-operator= 0.97
[217] Ohya/2017	9	LG, MG, FDL, TP, PL, PB	Toshiba	Resting	Inter-session= 0.70–0.98
[226] Coombes/2018	19	VL, RF, VM	SSI	Passive stretching	Intra-operator= 0.88–0.95
[199] Kelly/2018	30	IS, ES, MG	SSI	Resting and active contraction	Intra-operator= 0.89–0.95 (resting), 0.72–0.87 (active)

* Reliability results presented as intra-class correlation coefficients (ICC). ADM: Abductor Digiti Minimi, APO: Adductor Pollicis Obliquus, BB: Biceps Brachii, BR: Brachioradialis, IS: Infraspinatus, EDL: Extensor Digitorum Longus, ES: Erector Spinae, FDL: Flexor Digitorum Longus, FHL: Flexor Hallucis longus, GRA: Gracilis, LG: Lateral Gastrocnemius, PB: Peroneus Brevis, PL: Peroneus longus, RF: Rectus Femoris. SAR: Sartorius, SCM: Sternocleidomastoid, SM: Semimembranosus, SOL: Soleus, ST: Semitendinosus, SS: Supraspinatus, TA: Tibialis Anterior, TP: Tibialis Posterior, TB: Triceps Brachii, VL: Vastus Lateralis, VM: Vastus Medialis. n: sample size. NR: not reported.

It should be noted that a number of muscle SWE studies had employed an external image processing software (e.g. MATLAB or OsiriX) to quantify elasticity from the exported elasticity maps which may effect the reliability results [208-211, 217, 226, 227, 229].

It could, however, be beneficial for extracting elasticity information from thin and small structures, such as lung pleura, since ROI cannot be manipulated to such anatomy. In similar cases, an image analysis software with accurate selection tools might be useful. However, this technique is not recommended in any guidelines and should not be employed without plausible justification.

Although it is now clear that muscle SWE reliability results are generally high, a meta-analysis of the published data will provide a deeper systematic insight. However, the technical acquisition methods amongst the results could be variable, which can complicate the analysis. Technical variability could also convolute acquisition methods recommendations and complicate results' reproducibility between studies. Notwithstanding techniques, the experience of the operators could be different and is seldom reported. This is an important and significant factor for acquiring reliable elasticity results [223, 243, 244]. The next section reviews the acquisition methods and technical factors amongst muscle SWE publications.

2.3.1.5 Technical and acquisition methods

Medical imaging technologies must be operated with precise techniques to produce valid and reliable readings that are free from artefacts with optimum quality [245]; SWE is no exception. Numerous studies may adopt a certain acquisition method with no solid reliability basis. Worryingly, such acquisition techniques can become referenced in future publications as a standard by the same or different authors. Validation through in vitro and in vivo experiments in addition to reliability testing is necessary before establishing an optimum technique. Table 2-6 lists a sample of publications detailing the various acquisition methods and technical parameters multiple SWE studies had adapted. It highlights a large variation amongst them.

2.3.1.5.1 Probe orientation

In Table 2-6, eight studies oriented the probe transversely (across fibres), while the other majority oriented it longitudinally (along fibres). Eby et al. [246]

attempted to validate probe orientation in an in vitro experiment. They monitored stiffness changes using SWE in three planes relative to fibre orientation while increasing the tensile load using traditional material testing techniques. Regression coefficients for the association between tensile load and stiffness were only significant using the longitudinal orientation (R^2=0.94; p<0.001). The regression parameters for the other two planes were close to zero and insignificant. However, their study had several limitations. For instance, they did not perform any reliability analysis between the planes and their SWE system was a custom built device. Nevertheless, their results provided the first step for further in vivo human experiments using commercial systems. Cortez et al. [244], using the SSI system, performed a reproducibility analysis and found an apparent superiority in ICC coefficients in favour of the longitudinal plane. Intra- and inter-operator reproducibility were 0.70 and 0.73 respectively; compared to 0.57 and 0.33 in the transverse plane.

Most papers adapting the transverse orientation did not provide a justification for selecting it in their methodology. Though, Ewerson et al. [247] wrote: “muscles were examined with the transducer perpendicular to the muscle fibres to minimize anisotropy”. This justification is implausible as the more reasonable approach would be to examine the muscle in its isotropic (longitudinal) orientation to control for the effect of anisotropy. Notwithstanding evidence presented above, the discrepancy in probe orientation noted in Table 2-6 warrants further investigation. This will elucidate the importance of muscle anisotropy and underline the significance of its effect on elasticity readings reliability.

Table 2-6 Acquisition method examples from muscle SWE studies.

Reference	n	Machine	Probe orientation	ROI	Sites	Acquisition / site	Probe pressure	Unit
1. [138]	5	SSI Aixplorer	Longitudinal Transverse	10mm x 10mm	1	1	NR	kPa
2. [204]	20	SSI Aixplorer	Longitudinal	8mm, 10mm, 12mm	1	4	Light, Moderate, Hard	kPa
3. [202]	30	SSI Aixplorer	Longitudinal	NR	1	2	NR	kPa
4. [248]	20	SSI Aixplorer	Transverse	5mm	1	5	"Minimal"	kPa
5. [249]	20	Siemens S2000	Transverse	15mm × 15mm	1	10	"Minimal"	m/s
6. [238]	20	SSI Aixplorer	Longitudinal	NR	1	3	Stand-off gel	kPa
7. [203]	10	SSI Aixplorer	Longitudinal	30mm	1	3	NR	kPa
8. [220]	25	Siemens S2000	Longitudinal	15mm × 15mm	2	10	NR	m/s
9. [239]	11	SSI Aixplorer	Longitudinal Oblique20^{o}	NR	1	3	Stand-off gel	kPa
10. [244]	16	SSI Aixplorer	Longitudinal Transverse	NR	5	3	"Minimal"	m/s
11. [206]	10	SSI Aixplorer	Longitudinal	15mm × 20mm	1	3	"Minimal"	kPa
12. [240]	22	Siemens S3000	Transverse	15mm × 15mm	1	8	NR	m/s
13. [250]	10	SSI Aixplorer	Longitudinal	NR	1	2	"Minimal"	kPa
14. [223]	10	SSI Aixplorer	Longitudinal	3mm	1	6	NR	m/s
15. [251]	52	SSI Aixplorer	Longitudinal	5mm	1	5	"Minimal"	kPa
16. [247]	10	Siemens S3000	Transverse	15mm × 15mm	1	10	NR	kPa
17. [225]	10	SSI Aixplorer	Longitudinal	NR	2	6	NR	kPa
18. [252]	54	SSI Aixplorer	Transverse	2mm, 4mm	1	NR	NR	kPa
19. [226]	19	SSI Aixplorer	Longitudinal	1.18 cm^2	1	NR	NR	NR
20. [241]	23	SSI Aixplorer	Transverse	5mm	1	3	"No compression"	kPa
21. [199]	30	SSI Aixplorer	Longitudinal	10mm	1	3	"Light"	kPa

2.3.1.5.2 Region of interest size

Besides probe orientation, there was an apparent lack of standardisation for the size of ROI in Table 2-6 except systems with fixed ROI such as the Siemens. Kot et al. [204] evaluated the variation in muscle stiffness readings for three ROI size categories [small (8mm), medium (10mm), and large (12mm)]. They found no significant differences amongst the various size for predicting the mean SWE value (p=0.92). The sizes investigated can be criticised for not being substantially different from each other to highlight potential underlying effects. Likewise, Bortolotto et al. [252] found no difference in passive muscle elasticity between 2mm and 4mm ROI sizes over the majority of the muscles they investigated. These inferential approaches adopted by the previous two studies, of testing for a difference, provides no information on the reliability or readings variability between the different sizes.

On the other hand, another study found that the coefficient of determination for the relationship between active muscle elasticity and torque decreases marginally when reducing the ROI size [250]. The researchers also noted an increase in the ratio of absolute error when decreasing the ROI size. The absolute error quadrupled when ROI size was 1/16 of the original SWE box size, which is considered an extremely small ROI. Similar to the two studies above, it lacked a reliability analysis.

It is not clear whether ROI size has no effect [204, 252] or whether variability is greater with smaller ROI [250]. In breast elastography, ROI size is one of the most important factors influencing the diagnostic performance [253]. Therefore, a reproducible ROI size is essential for elucidating myopathies using SWE.

2.3.1.5.3 Number of acquisitions

The number of acquisitions required to get an average reading as highlighted in Table 2-6 ranged from 1-10 acquisitions. Previous evidence has shown that a single measurement is generally not sufficient as SWV values vary considerably [254]. In contrast, others suggest that a single valid SWE measurement is sufficient to assess liver stiffness in patients with chronic hepatitis B [255]. The standard protocol for performing TE is to calculate the median of 10 repeated readings [256], which has later been anecdotally adapted by in the SWE research community as well. Researchers investigated

if SWE has a high intra-system reliability and whether acquiring less repeated reading is sufficient to yield the same value. Choi et al. [257], evaluated the use of 5-repeated readings vs 10-repeated reading. They concluded that 5-measurements suffice and can replace the conventional protocol. In addition, a relatively large study of 449 participants compared 3 versus 5-repeated SWE readings and found that there is no significant difference in the mean measurements between them [62]. They demonstrated that it is enough to perform 3 repeated acquisitions and yield the same mean value of 5. Indeed, the EFSUMB guidelines, in recommendation number 13, state that for SWE a minimum of 3-repeated readings suffices to obtain consistent results [7].

2.3.1.5.4 Probe pressure

Theoretically, any applied stress will contribute to the resultant strain (page 16). Thus, the transducer load or any compression applied by the operator may affect the SWE measurements. In muscle SWE, Kot et al. [204] investigated the differences amongst three compression levels [light (probe placed on top), moderate (gentle force on the skin) and hard (great force)]. As expected, there was a significant difference when different probe compression levels were applied. Again, the sole testing for difference provides little information on the best technique to adapt, as it merely informs that the mean values are statistically different. The authors recommended the use of the lightest transducer's pressure even though their statistical analysis does not support this inference. Another study reached the same conclusion after testing five subjects only [258].

In thyroid elastography, Lam et al. [259] reported that increasing probe load on the skin surface results in a significant rise in thyroid stiffness and may also influence the diagnostic performance. Barr and Zhang [64] were the first to investigate the effect probe pressure on elastography. Despite the small sample size of ten patients, they showed that fatty tissue could have the same stiffness as an adjacent cancerous mass when a 'significant' precompression is applied. The superficiality of breast tissue can amplify the effect of probe pressure. This effect is likely to be important for muscle SWE.

Testing the effect of hard probe compression can be considered unreasonable since it should result in an invalid high stiffness reading. In contrast, testing

justifiable and feasible techniques should be attempted. For example, comparing the reliability between minimal probe load and the use of a standoff gel layer between the probe and skin surface. Indeed, Table 2-6 shows variability between the studies for the type of probe pressure applied as some had used “light” or “minimal” pressure, while others used a standoff gel layer.

2.3.1.5.5 Unit

Unit of reporting is another aspect with an apparent lack of consensus (Table 2-6) and represents a major problem. Studies cannot compare their results with another if units are different. Several papers [202, 212, 247, 250] used equation 6 on page 25 to manually convert their findings from m/s to kPa or vice versa. Such manual conversion is not scientifically accurate. The resultant ROI estimation in kPa is the mean of all the pixels after converting each pixel using the same formula. If the result value is manually converted to kPa from the mean value of all pixels in m/s, the square root of the sum will be calculated instead of the sum of the square root from each pixel, generating a calculation error. The margin of this error is hypothesised to increase when the assessed area is heterogeneous with varying degrees of stiffness.

The SWV (m/s) and Young’s modulus (kPa) are considered synonymous units to represent tissue elasticity. However, the original unit acquired in ultrasound in the SWV in m/s. It is not clear if the SWE software mathematical calculation of kPa from the original SWV has any influence on the reliability of muscle SWE.

As systems’ performance varies from one to another, standardisation of the parameters mentioned previously is important. Developing and optimising a robust technical and acquisition methodology is essential for acquiring reliable results to detect true abnormal muscle stiffness. The technical factors reviewed above in addition to others such as depth and leg dominance will be investigated and further discussed in the next chapter.

2.3.1.6 Sex and age factors

It is widely accepted that sex-based differences exist on multiple muscle characteristics such as strength and mass [260, 261]. However, it is not well-understood if sex is a significant factor in the muscle elasticity of healthy and pathological cases or not. Chino and Takashi [251] analysed the passive

gastrocnemius medialis stiffness in 52 young participants (half females) and found no significant differences by sex at any ankle position. Similarly, another study evaluated its effect in a sample of 40 healthy participants and found no sex-based differences in passively stretched vastus intermedius muscles [207]. However, the sex difference was significant when they measured active muscle elasticity upon isometric MVC (p<0.001). For the vastus lateralis, males and females had an active muscle elasticity of 173.8 ± 43.7 and 122.6 ± 58.1 respectively (p<0.001). Similar findings were also reported in a previous pilot study [205]. These differences are expected since it is known that active muscle elasticity correlates with strength.

Chen et al. [242] demonstrated in a small study that biceps brachii passive elasticity is significantly influenced by sex; females had a significantly higher SWV than males (2.34 m/s and 2.17 m/s respectively). They discussed that this could be related to the decreased oestrogen levels in their female cohort considering their perimenopausal/menopausal status. This explanation was criticised by another researcher who equitably commented that male subjects could have even lower levels of oestrogen rendering their extrapolation inaccurate [262]. In contrast, males were found to have approximately 8% greater SWV when compared to females [222]. The researchers linked this finding to the influence of muscle thickness, which was also higher in males. These detected sex differences were negated in several other publications of active [207, 263] and resting muscle elasticity [186, 252]. The exact effect is still unclear based on the observed discrepancies above.

As for age, it is accepted that human skeletal muscle undergoes structural changes due to ageing [260, 261, 264]. Such changes may alter the biomechanical properties and postulate a change in muscle elasticity. Wang et al. [207] reported the same muscle elasticity between young (mean age=27.6) and middle-aged (mean age=56.7) when muscles are relaxed; but, upon contraction, young were significantly higher than middle-aged (p<0.001). On the other hand, Heizelmann et al. [222] used the same age group definitions but reported that muscle stiffness is marginally higher in elderly (3.07 ± 0.49 m/s) in comparison to young (2.84 ± 0.58). They hypothesised that the demonstrated changes could be due to the increase in collagen fibre deposition that muscle fibres undergo with ageing. With that in mind, muscle stiffness did

not differ over the left trapezius (p=0.346). Although their study had a good sample size of 278 participants (110 males and 168 females), the age range was only up to 73 years and did not include old cohorts >75 years. Moreover, their elderly group (>60) consisted of only 24 participants.

A study on 30 female Japanese participants found no passive muscle elasticity difference between 15 young (mean=23 years) and 15 old (mean=75 years) over the medial and lateral gastrocnemius muscles [214]. Similarly, another study with a good sample size (n=127) found no positive or negative correlation between the variables of age and muscle elasticity (p=0.50) [186] In contrast, it was found that ageing may decrease resting muscle elasticity by approximately 20% [208]. More specifically, the rectus femoris decreased from 10.3 kPa in young to 8.5 kPa in elderly. The observed age-related differences, however, were only significant for the rectus femoris and lateral gastrocnemius but not for the soleus.

The studies above had a drawback of dichotomising the age variable (young vs elderly), which is inadvisable for several reasons [265]. For instance, it assumes that two persons aged 59.5 and 60.0 are significantly different when the actual difference is only half a year. Alternatively, considering age as a continuous variable or categorising it into multiple ordinal groups with gaps in-between the groups is preferable and could reduce the amount of lost statistical power [265].

It is common in SWE studies to add the effect of demographics on muscle stiffness readings. However, most of the articles have a small sample size that does not permit deeper analyses of factors like sex and age. To this point, it is not clear if ageing decreases [207, 208, 216], increases [222] or causes no change [186, 214] in muscle elasticity. Furthermore, it is not yet clear if the lost muscle elasticity is the reason behind reduced explosive power in elderly or not.

The few studies reviewed above are insufficient to draw conclusions on the influence of sex and age on muscle elasticity. Investigating the effect of ageing on muscle elasticity, while accounting for the functional and strength capacities, could provide additional value to the body of available evidence. Moreover,

individuals above 75 years old should be incorporated in future studies to understand the magnitude of changes in these extreme ages.

2.3.1.7 Exercise

The previous subsections demonstrate how muscle stiffness correlates with torque during exercise. Prior to exercise, static stretching, as a warm-up technique, was found to significantly drop muscle stiffness by approximately 18% after a minimum of 20-second stretching session [218]. A 7-minute massage session had the same effect, inducing an immediate, albeit short-term, drop in stiffness [211]. However, the muscles regenerated their original stiffness after 3 minutes. SWE is able to detect the best exercise programme for targeting a specific individual muscle [224]. It is done by comparing the highest stiffness the muscle is experiencing during the exerted force between the different exercises. This could become an important application especially for deep muscles like the transversus abdominis, since assessing its activation is difficult using other techniques like EMG.

Several studies investigated muscle stiffness changes pre and post-exercise programmes. The posterior lower leg muscles were assessed in 20 young male volunteers before and immediately after a 30-minute running task [217]. It was found that stiffness was only significantly higher in the tibialis posterior and flexor digitorum longus muscles, which increased from 3.5 kPa to 4.6 kPa (p=0.035) and from 4.0 kPa to 5.5 kPa (p=0.019) respectively. The authors explained that this finding confirms their hypothesis that these two muscles are the major contributors to medial tibial stress syndrome (MTSS). They concluded that SWE could be a valuable technique for detecting abnormal stiffness in these muscles as a risk factor for developing MTSS in running sports.

Leung et al. [213] reported a 75% increase in the stiffness of the medial and lateral gastrocnemius as well as a 42% increase in Achilles tendon as a result of the eccentric heel-drop exercise. The observed difference ratio indicates that muscles bear larger mechanical loads than tendons during some exercises. Assessing muscle stiffness before and after a six-week resistance training revealed no significant increase [241]. This may suggest that muscles are resilient in terms of adapting their elasticity after long-term training programmes to prevent subsequent damage. Indeed, skeletal muscle has a fascinating

adaptive property called muscle plasticity where it can change in structure and function as a response mechanism for increased muscle load or activity. Leung et al.'s paper could lay the foundation for building knowledge on the association between muscle plasticity and stiffness.

Lacourpaille et al. [266] aimed to investigate if the amount of immediate exercise-induced rise in stiffness reflects the magnitude of force deficit measured two days after. They split their 53 participants into two groups; group1 performed eccentric (more damaging) exercises, and group 2 performed concentric (less damaging) exercises. Both groups experienced increased muscle stiffness 30-minute post-exercises ranging from 26% to 159%. They observed a substantial negative correlation (r= -0.82; p<0.001) between the relative increase in muscle stiffness at 30 minutes and the relative decrease in peak torque after 48 hours for group 1 only that performed the more damaging eccentric exercise. The researchers did not, unfortunately, record muscle stiffness at the 48-hour time point, which could have elucidated the effect of delayed muscle soreness on muscle elasticity and highlighted how strongly it correlates with their observations. Early detection of exercise-induced muscle damage via SWE may be utilised to prevent re-injury by predicting the optimum magnitude of exercise loads athletes should undergo in rehabilitation.

2.3.2 Shear wave elastography in muscle pathologies

Histology proves that there is variability within and between muscles in terms of fibres type and arrangement, fat content and vascularity based on the function [267]. Although the agreement between histology and muscle SWE is yet to be established, evidence from the previous sections confirms the variation in elasticity amongst muscles. Following the same logic, SWE could be able to quantify abnormal elasticity in muscles that had undergone pronounced structural changes due to pathological mechanisms like inflammation and denervation.

There is a considerable scarcity in the literature for articles investigating the role of SWE in muscle diseases. Table 2-7 is a summary of published studies investigating the role of SWE in various muscle pathologies. Muscle spasticity is one of the commonly investigated disorders using SWE in post-stroke

patients [268-270] and in children with cerebral palsy [271-274]. This is due to the predominantly subjective and qualitative methods for assessing spastic muscles like the Modified Ashworth Scale (MAS) which assesses muscle tone based on the resistance sustained during passive stretching. SWE showed strong evidence that spastic muscles exhibit an increased stiffness when compared to a non-paretic limb as well as healthy controls. Further, Wu et al. [270] and Bilgici et al. [271] reported a positive linear correlation between MAS and muscle stiffness (r= 0.66; *p*=0.001). The former also reported an excellent intra- and inter-operator reliability of 0.85 and 0.77 respectively. In a recent study, Bilgici et al.'s [273] group evaluated the usefulness of SWE for detecting response to botulinum toxin A injection. It identified a decreased muscle stiffness after the treatment in agreement with the established clinical measures, opening the door for a feasible application in clinical practice. Indeed, this may improve treatment delivery by identifying the best injection location. Additionally, combining this objective measure to MAS can yield more accurate and useful results. Two of the previous studies tested their subjects' muscles in a resting relaxed muscle state and during passive stretching [269, 270]. Both suggested measuring muscle elasticity during the resting state since it was the position that detected the abnormality and yielded significant results.

One study examined how myosteatosis (fatty infiltration in skeletal muscle) can alter muscle elasticity using SWE [275]. It investigated the effect of fatty degeneration in the supraspinatus muscle after tendon rupture on a sample of forty-two patients that underwent rotator cuff repair. The researchers utilised MRI spectroscopy using the SPLASH-technique as a gold standard for quantifying the degree of fatty infiltration. They found that SWE correlated strongly with MRI spectroscopy (r=0.82), but correlated weakly with the Goutallier scale (r=0.40), which is another MRI-based classification for fatty infiltration based on T1 images. This indicates that SWV increased in muscles with high fatty depositions, which do not conform to what is expected theoretically since adipose tissue has a lower elastic modulus than muscle [59]. Myosteatosis should theoretically result in decreased rather than increased stiffness. The addition of a healthy group in their study design would have provided valuable results. Nevertheless, the mechanism on how myosteatosis influences elasticity needs to be elucidated further in future studies.

SWE seems to be a promising tool for identifying the specific muscles associated with low back pain [276]. A multiple logistic regression analysis showed that SWE was a significant and independent variable for determining low back pain with an odds ratio (95% CI) of 4.13 (1.17, 14.63), while muscle mass and spinal alignment were not. Lacourpaille et al. published two papers on the potential role for SWE in Duchenne muscular dystrophy. The first established the difference in elasticity associated with this genetic disorder [277]. While the second indicated that stiffness progressively increased with disease duration after 12 months [278].

Moreover, SWE can quantify muscular rigidity in neurological disorders as patients with Parkinson's disease exhibited higher Young's modulus readings when compared to healthy controls [279]. Increased stiffness in the triceps surae was reported in cases with medial tibial stress syndrome (MTTS) [280]. Though, a similar later study tested numerous calf muscle including the triceps surae but only found a significant difference in the flexor digitorum longus and tibialis posterior [281]. Differences in the technical factors between the machines or in the acquisition techniques could explain these disagreements. Such inconsistency, rather a discrepancy in some situations, in the results between studies is a great challenge facing muscle SWE and can possibly hinder usefulness in research and clinical practice.

In contrast, several studies demonstrated that myopathic processes lead to a loss in normal muscle stiffness. A pilot study of eight GNE-related myopathy patients demonstrated decreased SWV of 2.63 m/s in comparison to healthy controls with SWV of 3.83 m/s (p=0.011) [258]. Active muscle stiffness was degraded in patients with patellofemoral pain syndrome [205].

It is not clear how skeletal muscle elasticity react to impaired muscle performance due to delayed onset muscle soreness (DOMS). One study showed that resting biceps brachii stiffness increased by 46% (p=0.005) when examined 1-hour post an unaccustomed maximal eccentric exercise, but returned to normal stiffness after 48 hours and 21 days [282]. The change at 1-hour did not conform with changes on MRI, which after 48 hours detected an increased signal indicating oedema. Later, another study assessed their participants before and 60 hours of eccentric heel drop exercise. On the contrary, they reported that muscle stiffness decreased by 19% from 2.2 ± 0.26

m/s before the exercise to 1.78 ± 0.24 m/s (p=0.008) 60 hours post exercise [283]. This change was associated with increased MRI T2 signal intensity and a remarkable rise in creatine kinase from 141.3 u/l to 3629.1 u/l. It is not clear if the change in muscle stiffness only occurs as an acute (1-hour) or delayed (60 hours) response as a sign of DOMS. The disagreement could be due to the different plasticity properties between the biceps and gastrocnemius muscles.

The reviewed literature above and listed below in Table 2-7 demonstrate how the published SWE studies on muscle diseases are generally heterogeneous. Amid this sparsity, the application for assessing muscle spasticity seems the closest to be established in clinical practice. To date, there are no studies using SWE to study the elastic properties in muscle inflammation or elasticity changes related to corticosteroids treatment. Nevertheless, the limited evidence above shows promise for the future of muscle SWE. It has the potential to be developed as an effective evaluation technique for skeletal muscles to improve the diagnosis and management of myopathies.

Table 2-7 Summary of SWE studies on muscle pathologies.

Study	Pathology	Correlation with	No of cases	Control	Muscles	Results
[205] Botanlioglu/2013	Patellofemoral pain syndrome (PFPS)	SWE only	11	22 healthy	VL, VM	Active muscle stiffness was **lower** in patients with PFPS in VM only.
[282] Lacourpaille/2014	Delayed onset muscular soreness (DOMS)	MRI	16	No	BB, Brachialis	Muscle stiffness **increased** 1-hour post exercise but **did not change** at 24 hours and 21 days and did not correlate with MRI T2 relaxation times.
[283] Hotfel/2018	Delayed onset muscular soreness (DOMS)	MRI	15	No	GM, SOL	Muscle stiffness **decreased** 60 hours post exercise in GM only and correlated to increased T2 signal intensity on MRI.
[198] Akagi/2015	Neck and shoulder stiffness symptoms	Myotonemeter	24	No	Trapezius	**No correlation** between muscle stiffness and clinical symptoms or myotonometry readings.
[258] Carpenter/2015	GNE-related myopathy	SWE only	8	5 healthy	GM, GL	SWV was **lower** in patients with GNE-related myopathy than healthy.
[280] Akiyama/2016	Medial tibial stress syndrome (MTSS)	SWE only	24	20 healthy	GM, SOL, PL, TA	The resting muscle stiffness across all muscles was **higher** in patients with MTSS.
[281] Saeki/2018	Medial tibial stress syndrome (MTSS)	SWE only	14	10 healthy	GM, GL, SOL, PL, PB, TP	The stiffness of the FDL and TP only were **higher** in subjects with a history of MTSS than in those with no history of MTSS.
[279] Du/2016	Parkinson’s disease	Parkinson's disease rating scale (UPDRS)	46	31 healthy	BB	Stiffness was **higher** in patients and correlated with UPDRS.

[284] Leong/2016	Tendinopathy	SWE only	26	17 healthy	Upper trapezius	Muscle stiffness was **higher** in athletes with rotator cuff tendinopathies during both active and passive arm positions.
[285] Zhang/2017	Tendinopathy	Patellar tendon stiffness	36	No	VL, RF	Patients had significantly **higher** passive stiffness in VL only and associated with higher patellar tendon stiffness.
[275] Gilbert/2017	Fatty infiltration	MR spectroscopy	42	No	SS	SWV strongly correlated with MR spectroscopy **increasing** with higher fat water ratio.
[277] Lacourpaille/2015	Duchenne muscle dystrophy	SWE only	13	13 healthy	GM, TA, VL, BB, TB,	Stiffness was significantly **higher** for all the muscles.
[278] Lacourpaille/2017	Duchenne muscle dystrophy	Muscle force and electrical simulation	10	9 healthy	GM, TA, VL, BB, TB, ADM	SWE detected **increased** muscle stiffness in patients over a 12-month period in all muscles except BB and ADM.
[276] Masaki/2017	Low back pain	SWE only	9	23 healthy	ES, multifidus	The multifidus stiffness was **higher** in patients with low back pain.
[286] Burke/2017	Fracture fixation	SWE only	17	Normal side	Pronator quadratus	Muscle SWV **decreased** after fixation surgery for distal radial fractures.
[268] Jakubowski/2017	Post-stroke muscle spasticity	Joint stiffness	14	Non-paretic side	GM, TA	Muscle stiffness was significantly **higher** in the paretic side in GM only and did not correlate with joint stiffness.
[270] Wu/2017	Post-stroke muscle spasticity	Modified Ashworth scale (MAS)	31	Non-paretic side	BB	Muscle stiffness was significantly **higher** in the paretic side and correlated with MAS.

[269] Mathevon/2018	Post-stroke muscle spasticity	SWE only	14	Non-paretic side	GM, TA	Muscle stiffness was significantly **higher** in the paretic side.
[274] Lee/2016	Muscle spasticity	Fascicle strain and ankle torque.	8	Less affected side	GM, TA	Muscle stiffness was significantly **higher** in adults with cerebral palsy and correlated with fascicle strain and ankle torque.
[272] Brandenburg/2016	Muscle spasticity	SWE only	13	13 healthy	GL	Muscle stiffness was significantly **higher** in children with cerebral palsy.
[271] Bilgici/2017	Muscle spasticity	Modified Ashworth scale (MAS)	17	25 healthy	GM	Muscle stiffness was significantly **higher** and correlated with MAS.
[273] Bilgici/2018	Muscle spasticity	Modified Ashworth scale (MAS)	12	No	GM	SWE detected **decreased** muscle stiffness after botulinum toxin A injection in children with cerebral palsy and correlated with MAS.

BB: Biceps Brachii, IS: Infraspinatus, ES: Erector Spinae, LG: Lateral Gastrocnemius, PB: Peroneus Brevis, PL: Peroneus longus, RF: Rectus Femoris. SOL: Soleus, ST: Semitendinosus, SS: Supraspinatus TA:Tibialis Anterior, TP: Tibialis Posterior, VL: Vastus Lateralis;VM: Vasus Medialis

2.4 Muscle diseases

2.4.1 Ageing

The complex natural phenomenon of ageing comes with several structural, biochemical, cellular and functional pathogeneses affecting skeletal muscle health [260, 261, 264, 287]. With increasing age, muscles undergo a reduction in fibre number and size, more prominently in fast-twitch type II fibres [288]. Additional quantitative properties like function and strength are diminished. Other qualitative changes also occur in terms of muscle architecture and fibre morphology as well as biochemistry. The elastic fibre system in the muscle extracellular matrix starts to lose its resistance property and becomes softer with ageing [289].

The process of muscle ageing starts roughly from the fourth decade of human life [260]. Longitudinal research shows that after the age of 75, muscle mass and strength are lost at a rate of 1% and 3% per year respectively, with some variations by sex [290]. Figure 2-11 reveals the subtle downward trend in muscle mass across ages in a large cohort of 1280 females, measured using dual-energy X-ray absorptiometry (DXA). The World Health Organisation (WHO) published a world report on ageing and health that contain valuable information on this topic with recommendations for maintaining muscle health via physical activity [291].

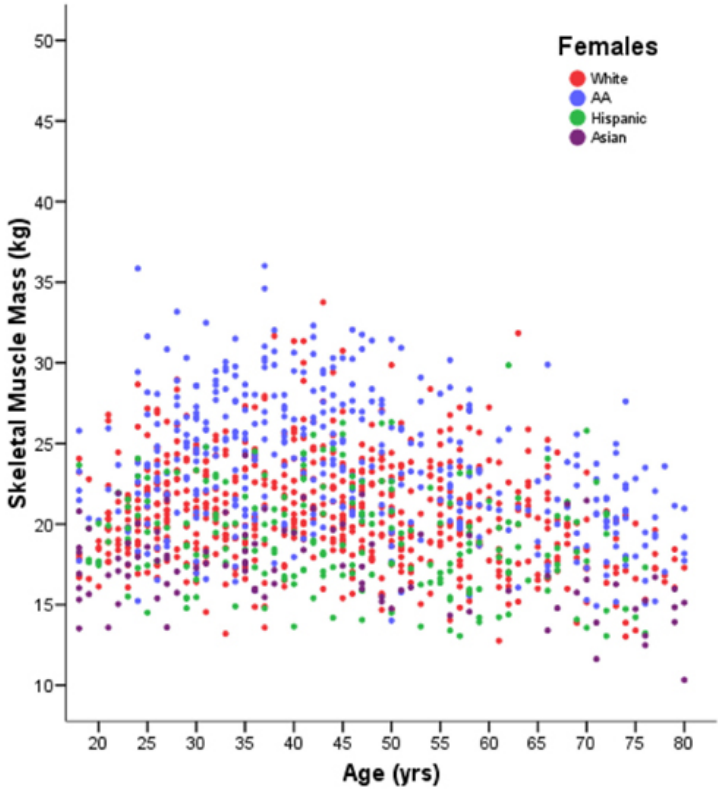

Figure 2-11 Skeletal muscle mass decline in a large sample of females between 18 and 80 years from various ethnicities.

Reprinted by permission from Wiley online Library: American Journal of Human Biology [292].

The progressive loss of muscle mass due to ageing was first described as 'sarcopenia' in 1989 [293]. Sarcopenia has been a hot topic in research during the last decade, and its definition is evolving. Recent studies added the reduction of muscle function or physical performance to the definition [294, 295]. The term sarcopenia can sometimes be confused with cachexia and frailty. The former is defined as the combined involuntary loss of muscle and fat masses, which is usually induced by an underlying pathology like cancer [296] whereas frailty is the combined reduction in both physiological reserves and mental capabilities that result in an increased vulnerability in older adults [297]. Sarcopenia is recognised as a major factor of frailty, though its prevalence is twice that of frailty [298]. It is a serious condition that has a significant impact on the patient's lifestyle and health. It is associated with a higher risk of falls [299], disability [300] and increased mortality rate [301]. Moreover, it has a great financial burden on health care systems, costing the United States approximately £15 billion a year [302]. It is a multi-factorial disease, but ageing

is accepted as a primary factor. Secondary factors related to activity, disease or nutrition are also recognised.

One study reported that the prevalence of sarcopenia could reach up to 13% in people aged 60–70 [298]. By 2050, the prevalence is expected to quadruple, affecting more than 200 million patients worldwide [295]. With its high prevalence rate and acknowledged risks, experts highlight the need for new biomarkers for objectively monitoring sarcopenia and evaluating therapeutic interventions [5, 303].

On the other hand, several researchers play down the importance of sarcopenia by introducing a relatively new condition called dynapenia, which recently attracted substantial attention. It is simply defined as the age-related loss of strength; first described in 2008 by Clark and Manini [304]. They argue the inaccuracy of the notion that loss of strength is directly related to the decline in muscle mass. Alternatively, they propose that ‘neural’ and ‘muscular’ factors defined by alterations in muscle contractile properties and neurological functions are the mechanisms behind the loss of normal muscle function due to ageing. According to them, the term sarcopenia should be limited to its original definition relating solely to the loss of muscle mass due to ageing.

Later publications supported the clinical relevance of dynapenia [305-307]. They stress the importance that dynapenia is the chief contributor to physical dependence that ultimately leads to disability in the elderly. Delmonico et al.’s [290] cohort study on 1678 elderly subjects above 70 years demonstrated that the loss of strength is faster than the loss of mass by approximately 5-folds. In fact, they reported that gaining muscle mass did not prevent the loss of strength (isokinetic leg muscle torque).

The average relative risk of poor physical performance and disability in the elderly population was 1.37 and 2.20 for sarcopenia and dynapenia respectively [307]. It is apparent that the volume of contractile proteins present in a muscle is not the sole variable responsible for the magnitude of force production. Additional factors such as muscle architectural differences and the fast to slow muscle fibre type transition are observed and strongly linked with muscle strength deficit in ageing populations [308].

The principle of sarcopenia is centred around muscle mass. As it will be clarified in the next subsection, a sole reduction in muscle function and strength does not characterise an elderly individual as sarcopenic, even if the person completely lacks muscle force capacity. In other words, if an elderly person aged 85 and have severe muscle weakness not being able to stand or walk but has normal muscle mass– he/she will be categorised as healthy according to the sarcopenia definition [295]. This basic example supports the depreciation of the prime importance of muscle mass alone as the direct and fully responsible factor for disability.

Despite the supporting evidence and convincing principle of dynapenia, it is still in its infancy. Nevertheless, it is generally agreed that skeletal muscle undergoes numerous changes due to ageing including myosteatosis and myofibrosis. These are two muscle impairing processes that occur in relationship with ageing [309]. Myosteatosis, as explained previously, results in increased fat deposition in muscle tissues, whereas, in myofibrosis, the normal muscle fibres are replaced with fibrous connective tissue. Accurate characterisation and the development of new muscle biomarkers is essential for better health outcomes.

The nature of muscle elasticity in ageing muscles is currently unclear. The few papers reviewed in section 2.3.1.6 are inconclusive. A study correlating muscle elasticity with measures of strength and function on multiple age groups can provide more informative evidence. The promising evidence that the detrimental effects of ageing are reversible encourages more research into identifying new diagnostic and monitoring imaging biomarkers such as muscle elasticity using SWE [310].

2.4.1.1 Diagnosis

Several groups have tried to identify diagnostic criteria and establish screening methods such as the Special Interest Group of The European Society for Clinical Nutrition and Metabolism [296], the International Working Group on Sarcopenia [294], the European Working Group on Sarcopenia in Older People (EWGSOP) [295] and the Society of Sarcopenia, Cachexia and Wasting Disorders [311]. There is a large level of heterogeneity amongst the diagnostic methods and abnormal cut-off points each group suggests. It is apparent that a universal agreement on the definition and diagnostic criteria is lacking.

Nevertheless, EWGSOP is considered the most prominent and established group. They developed an algorithm for the diagnosis of sarcopenia that includes three outcome domains: muscle mass, strength and physical performance [295]. Reduction in muscle mass in addition to strength or physical performance is the criteria they used to identify sarcopenia (Figure 2-12). They have also specified cut-off points to follow in each aspect adopted from previous studies. Numerous research articles have criticised the performance of the algorithm and endorsed the need for developing new diagnostic tools and biomarkers [312]. This indeed is necessary along with the continuous evolvement of sarcopenia's definition and genetic discoveries [313]. A validity reassessment of the proposed cut-off points was also suggested [314].

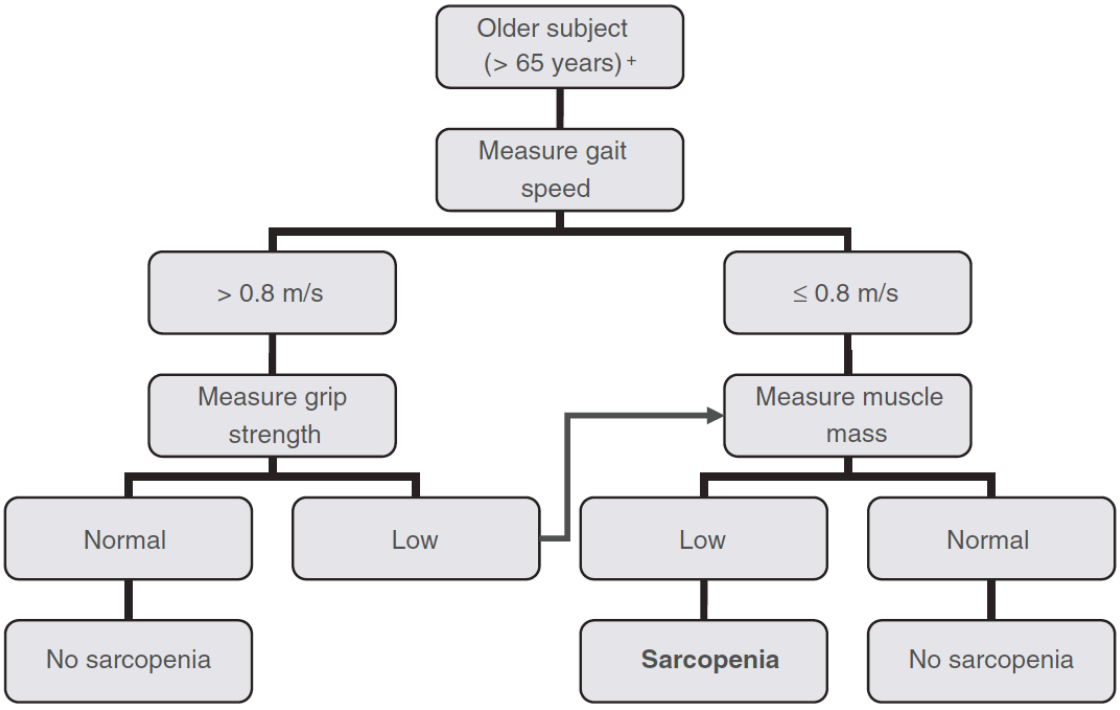

Figure 2-12 Proposed working decision algorithm for sarcopenia.

Reprinted by permission from Oxford University Press: Age and Ageing [295].

In contrast, the limited acknowledgement of the dynapenia concept in medical research hindered the development of specific diagnostic criteria. Nevertheless, the original authors who suggested this concept proposed a working decision algorithm to define it (Figure 2-13). It suggests that older people above 60 years be screened initially for risk factors then worked on accordingly. A limited series of defined risk factors has not been defined yet, albeit multiple potential

factors have been suggested in the same paper. Although it seems feasible, there is so far no data to support its validity.

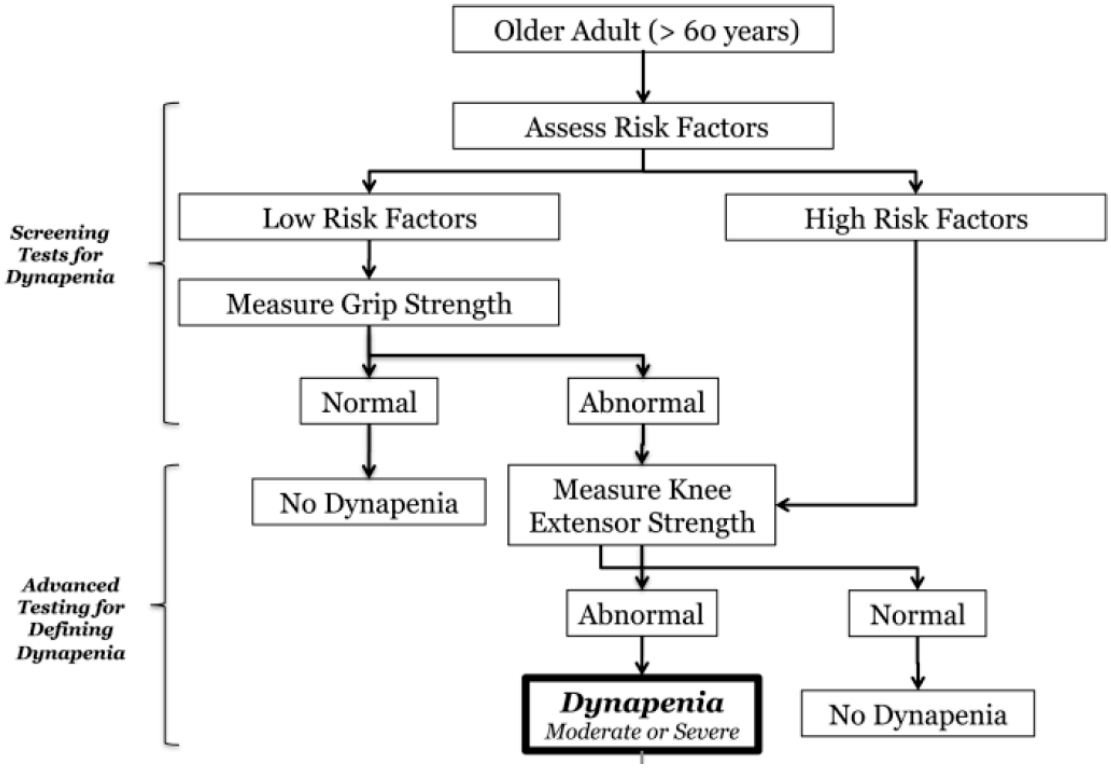

Figure 2-13 Proposed working decision algorithm for dynapenia.

Reprinted by permission from Oxford Press: Journals of Gerontology [307]

Exploring the nature of muscle elasticity in elderly cohorts could provide valuable insight for developing novel biomarkers for the diagnosis of age-associated muscle pathologies. Accurate definition and diagnostic methods are imperative for establishing effective treatment plans as well as prevention programmes. Novel imaging technologies, such as SWE, has the potential to serve as a new imaging biomarker and become a key tool in disease detection and management in ageing muscles. It can improve our general understanding of ageing to promote a healthy life course. The ageing-related structural changes to skeletal muscle explained at the beginning of this section suggests that age could have a significant impact on muscle elasticity. This supports the rationale behind investigating muscle elasticity using SWE on several age groups, including elderly above 75 years old, in chapter 4.

2.4.2 Idiopathic inflammatory myopathies

Idiopathic inflammatory myositis (IIM), commonly called myositis, is a family of rare autoimmune inflammatory myopathies which have multiple types but are

mainly classified into the three most common: polymyositis, dermatomyositis, and inclusion body myositis [315]. Patients with IIM are characterised as having proximal muscle weakness, elevated muscle enzymes and presenting myositis-specific and associated autoantibodies in addition to a proliferation of inflammatory infiltrative cells [315]. IIM is known to be associated with high mortality and morbidity rates [316]. When left unmanaged at an early stage, it can result in poor prognosis and quality of life [317]. So far, researchers have not reached unanimous consensus in terms of a clear definition for histological and pathogenic aspects of this debilitating pathology.

2.4.2.1 Diagnosis

Almost all studies relied on the pathological changes observed using muscle tissue biopsies. Little research was dedicated to elucidating the mechanisms of involvement or to introduce new methods of assessment. Nevertheless, several diagnostic criteria have been proposed over the years for inflammatory myopathies [318-323]. There are a lot of similarities amongst them, whereby suspected patients must present certain clinical and laboratory findings in addition to a positive muscle biopsy.

The criteria by the European Neuromuscular Centre Criteria (ENMC) elaborated on the importance of biopsy and included a detailed definition of the histological features for each disease type [321]. Muscle biopsy is a fundamental and indispensable diagnostic tool that is described in all published diagnostic criteria including the one by the international myositis assessment and clinical study groups [322]. Despite its importance, muscle biopsy is an invasive procedure, which is known to be associated with risks and complications such as bleeding and infection [324]. Most studies reported previously mentioned the need for an open biopsy, which requires a larger skin incision that scars the skin and occasionally requires general anaesthesia as well as general surgeon assistance. It also requires equipped labs with sophisticated devices to test the samples. Additionally, it is contraindicated for patients taking anticoagulant therapy. After open biopsies, patients do not often resume their normal daily activities and are advised to rest [325]. Besides, MRI is usually necessary to locate the biopsy sample site. This introduces an additional problem for claustrophobic patients as well as being an expensive

and often inaccessible imaging modality. Therefore, muscle biopsies have multiple medical as well as economical drawbacks.

2.4.2.1.1 Medical Imaging in myositis

None of the myositis groups endorses imaging techniques as a criterion for diagnosis or follow-up, despite numerous studies demonstrating its useful role. Nevertheless, some myositis centres in Europe include medical imaging in their criterion. For example, the German Cancer Research Centre employs both MRI and Ultrasound for diagnosis [326]. Whole-body MRI is first used to detect oedematous muscle changes that manifest in polymyositis and dermatomyositis. If this is positive, a contrast-enhanced ultrasound is then performed to detect active increased perfusion regions, which will accordingly be targeted for biopsy. If the MRI is negative, they consider other differential diagnoses. However, if the MRI is positive but ultrasound is negative, they consider other types of myopathies. With the aid of imaging localisation and guidance, biopsy sampling error can be decreased; hence, minimising false-negative rates [327].

On the other hand, SWE is a non-invasive imaging technology that can evaluate the elasticity of tissues with no known associated complications. Inflammatory myopathies may alter the internal composition of muscles, as a group of enzymes called matrix metalloproteinases are involved in the genesis of inflammatory myopathies [328]. By analysing biopsies from acutely inflamed patients, a study found these enzymes attacking phagocyte cells and causing muscle fibre loss [329]. Multiple other studies also found muscle fibre size variability [330, 331], atrophy [330-340] and necrosis [332, 334, 337, 341, 342]. These pathological changes postulate that muscle's biomechanical properties might be altered, which supports the rationale for investigating SWE diagnostic performance in inflammatory myopathies. It could, ultimately, provide a useful, readily available and relatively cheap non-invasive assessment tool. This will be investigated in chapter 5.

2.4.3 Corticosteroid-induced myopathy

Corticosteroids are naturally occurring hormones produced by the adrenal glands. Analogous of these hormones can be synthetically produced for medical use as well. It is one of the most important anti-inflammatory

medications for immunological and neoplastic diseases. Corticosteroids are mainly classified into glucocorticoids and mineralocorticoids. Common corticosteroid medications, such as prednisolone constitute predominantly of glucocorticoids and low concentration of mineralocorticoids.

Several serious side-effects are known to be associated with the administration of corticosteroids; myopathy is one of the most common. This induced myopathy was first noted by the excess of endogenous corticosteroids in Cushing syndrome patients, occurring in more than half of the cases [343]. Iatrogenic corticosteroid myopathy is less common, occurring in a severe form in approximately 21% of the patients receiving this medication [344]. It is expected to be higher in more milder forms of myopathy. One case-control study demonstrated that myopathy is 6.7 (95% CI 4.8, 9.3) times more prevalent in patients receiving corticosteroids than normal subjects [345].

Patients usually present with proximal muscles weakness prominently in the lower limbs. This becomes clinically clear when patients struggle standing up from a chair due to the proximal thigh and hip girdle muscles weakness. Patients also have difficulties walking upstairs or performing overhead movements in daily life activities. In acute forms of corticosteroid-induced myopathy, serious adverse events can occur such as rhabdomyolysis which could potentially lead to kidney failure [346]. In addition, myopathy may affect the respiratory muscles in intensive care patients and cause severe dyspnoea [347]. Experts in corticosteroid-induced myopathy recommended the introduction of clinical screening programmes to prevent progression consequences [348].

There is no consensus in the literature on the relationship between treatment duration and the onset of myopathy. Previous studies mentioned that steroid myopathy symptoms start after three to six months for doses higher than 15-20 mg per day [349]. Recent studies, however, states that it can be acute and occur after several doses higher than 40 mg [346, 350]. Symptoms onset can also take as long as one year [351]. Therefore, susceptibility varies considerably and is believed to be patient-specific. Risk of myopathy for doses of 60 mg/day is sevenfold higher than doses of 5 mg/day [345].

Giant Cell Arteritis (GCA) is an inflammatory disease of unknown aetiology affecting mainly the scalp temporal artery. It is treated with relatively high doses of corticosteroids over prolonged periods of few months or years. According to published guidelines by the British Society for Rheumatology, treatment starts with 40–60 mg/day for GCA [352]. Several studies and reviews reported the association between GCA and the adverse side-effects induced by corticosteroid therapy [353-355].

2.4.3.1 Diagnosis

The diagnosis of iatrogenic corticosteroid myopathy is difficult and may be overlooked in diseases exacerbated by muscle weakness such as myositis. Discriminating primary inflammatory disease symptom flairs and steroid-induced myopathy is an additional diagnostic dilemma. Limited diagnostic methods are currently available; most have significant drawbacks. Muscle enzymes such as CK and aldolase usually appear within the normal limits [356]. EMG tests also have a poor sensitivity; it may detect abnormal myopathic findings in late chronic stages [357]. Histology can show atrophy characterised by the reduction of type IIB muscle fibres size [358].

Such pathological muscle fibre changes may induce biomechanical alteration were SWE had demonstrated the ability to detect [359, 360]. The stiffness of these myopathic muscles is unknown. Elasticity, measured using SWE, can serve as a new relatively cheap and non-invasive imaging biomarker. Therefore, chapter 6 is dedicated to investigating if high dose steroid treatment induces any muscle elasticity changes or not.

2.4.4 Suspected muscle involvement in rheumatoid arthritis

Patients with RA are known to have decreased muscle mass, strength and performance [361-363]. Yet, muscle involvement in RA has not been fully explored. The association between RA and IIM is still an under-investigated field of research. Nevertheless, several factors such as inflammation, limited range of motion, sedentarism as well as medications have been recognised to induce inflammatory myopathies [330, 364]. Recognition of the muscle involvement in RA was discovered many years ago. However, the literature has overlooked this subject for years. Sixteen accessible in-vivo research articles were found studying this association (Table 2-8).

Table 2-8 Summary of studies investigating muscle involvement in RA.

Study	RA subjects	with muscle symptoms	Healthy controls	Methods	Findings
1. Curtis and Pollard/**1940 [365]**	11	-	-	Muscle biopsy	•Cellular infiltration of lymphocytes. (8/11) •Muscle fibres atrophy. (8/11)
2. Steiner et al/**1946 [366]**	24	-	196	Muscle biopsy	•Nodular infiltration of lymphocytes. •Muscle fibre degenerative changes
3. Steiner and Chason/**1948 [341]**	27	27	126	Muscle biopsy	•Nodular infiltration of lymphocytes. (endomysial and perimysial) (26/27) •Degenerative fibre changes. (27/27)
4. Traut and Campione/**1952 [332]**	16	16	-	Muscle biopsy	•Mononuclear cells infiltration (endomysial and perimysial). (16/16) •Muscle fibre atrophy. (16/16) •Degenerative fibre changes. (16/16) •Mild perivascular infiltration. (15/16)
5. Yates/**1963 [333]**	32	23	28	EMG	•Abnormal short duration. (12/32)
				Muscle biopsy	•Nodular infiltration of lymphocytes. (14/23)
6. Haslock et al/**1970 [342]**	34	8	-	Muscle biopsy	•Nodular infiltration of lymphocytes. (5/8) •Necrosis. (6/8)
7. Edstrom and Nordemar/**1974 [334]**	13	-	-	Muscle Biopsy	•Muscle fibre atrophy (mostly type II). •Necrosis.
8. Wroblewski and Nordemar/**1975 [335]**	12	12	-	Muscle Biopsy	•Muscle fibre atrophy. •Signs of degeneration (lipofuscin granules) and regeneration (satellite cells).
9. Magyar et al/**1977 [336]**	100	-	-	Muscle Biopsy	•Nodular infiltration of lymphocytes. (61/100) •Muscle fibre atrophy of type II.
10. Halla et al/**1984 [337]**	31	-	-	EMG	•Abnormal short duration and low amplitude. (6/31)
				Muscle biopsy	•Mononuclear cell infiltration. (10/31) •Muscle fibre atrophy of type II. (18/31)

					•Necrosis. (16/31)
11. Miro et al/**1996 [338]**	21	21	-	Clinical	•Muscle weakness (16/21) and myalgia (8/21).
				Laboratory	•Elevated CK (1172 U/L). (8/21)
				Muscle biopsy	•Inflammatory cell infiltration (8/21) •Muscle fibre atrophy of type II. (11/21) •Vasculitis. 1(/21)
12. De Palma et al/**2000 [339]**	30	-	12	Muscle biopsy	•Inflammatory cell infiltrates. (7/30) •Muscle fibre atrophy. (7/30) •Myofibrils separation. (7/30)
13. Agrawal et al/**2003 [340]**	23	14	-	Clinical	•Muscle weakness and myalgia.
				EMG	•Abnormal polyphasic short duration and low amplitude. (14/14)
				Laboratory	•Normal CK. (14/14)
				Muscle biopsy	•Muscle fibre atrophy. (Type I 3/11, Type II 9/11) •Fibre size variability. (9/11) •Inflammatory cell infiltration. (8/11)
14. Ancuta et al/**2009 [330]**	120	23	-	Muscle biopsy	•Inflammatory cell infiltration (immunohistochemically).
15. Nakajima et al/**2011 [367]**	142	12	-	Laboratory	•Myositis-specific antibodies. (9/12)
16. Ancuta et al/**2014 [331]**	103	8	-	Clinical,	•Proximal symmetrical myalgia. (7/8)
				Laboratory	•Elevated CK, normal LDH.
				MRI	•High T2 and STIR signals.
				US	•Homogenous hyperechoic focal regions and increased Doppler signals.
				EMG	•Abnormal polyphasic short amplitude and duration.
				Muscle biopsy	•Inflammatory infiltration of B-, T-lymphocytes. (6/8) •Muscle fibre atrophy. (Type I 2/8, Type II 3/8) •Large fibre size variability. (8/8)

All studies performed biopsies to tests muscle involvement, and the most common findings were inflammatory infiltration of mononuclear cells, muscle fibres atrophy and necrosis. Four out of the sixteen studies used electromyography (EMG) and found myopathic abnormal electrical potentials of short duration and low amplitude.

Curtis and Pollard [365] in 1940 were the first to recognise muscle involvement; using a conventional light microscope, they found cellular infiltrates in four of eleven rheumatoid arthritis patients. Following this, other researchers started studying muscle involvement and reported the inflammatory infiltration presenting in a nodular pattern under the microscope and introduced the terms ‘nodular myositis’ and ‘nodular polymyositis’ [366, 368, 369]. These studies claimed this manifestation to be unique for secondary myositis complicated by RA. However, this was later challenged and refuted in several studies, which found these nodules to be non-specific and presented in other connective tissue diseases [370, 371].

The mechanism of involvement was not understood even until the mid-70s. Wroblewski and Nordemar [335] indefinably thought that the inflammatory muscle reactions could be caused by viral infections! It can be argued that muscle involvement in RA is still not fully understood yet. Some researchers introduced the term ‘rheumatoid myositis’, a muscular disease that occurs in RA patients due to an immune inflammatory infiltrate processes [337]. Others looked at this from a clinicopathological perspective, whereby the diagnostic classification criteria for this connective tissue disease can coincide with those from idiopathic inflammatory myopathies; thus patients can be diagnosed with an ‘overlap syndrome’ [372]. Some studies suggest that long use of drugs such as corticosteroids and chloroquine might explain the association between rheumatoid arthritis and myositis [367, 373]. One of them [367] investigated the prevalence of RA in a cohort of 142 myositis patients. They identified twelve patients who had RA before the onset of myositis. Having collected serum samples every six months before developing muscle symptoms in three of their subjects, they identified pre-existing myositis-specific antibodies. The onset of myositis ranged from 2–5 years after establishing the diagnosis of RA. Their study results indicate a high frequency of preclinical myositis in RA patients.

The question of whether RA or the medications used was the underlying cause to develop myositis is yet to be answered.

The evidence reviewed above postulates a myopathic involvement in RA. There is a paucity of research supporting this postulation. It is not clear if the degree of joint inflammation has an influence on the adjacent muscles. Therefore, novel biomarkers such as muscle elasticity could highlight subclinical abnormal myopathic mechanisms. The study conducted later in chapter 7 explores the hypothesised altered muscle elasticity in several RA cohorts using SWE.

2.5 Methods of muscle assessment

Muscle assessment methods are designed to test one or more aspects of muscle quality. The dilemma is that there is so far no consensus on the outcome measures defining ‘muscle quality’ as it has been described in numerous ways in the literature. Multiple factors were described underpinning skeletal muscle quality; these include muscle mass, myosteatosis, myofibrosis, metabolism, force production, aerobic capacity, neural activation and thermoregulation [305, 374].

The term ‘muscle quality’ had initially emerged in the muscle ageing literature to elucidate intricate intramuscular characteristics. However, it is being used more frequently in the context of myopathic conditions. Few researchers tried to simplify the term by limiting it to the functional status. They introduced the term muscle quality index (MQI) as the ratio between muscle strength and muscle mass. Initially, Takai et al. [375] developed a simple muscle power index based on calculating the time to perform ten repeated chair rises whilst accounting for anthropometric factors such as leg length and body mass. Later, Barbat-Artigas et al. [376] incorporated the previous index into a new MQI criterion that assesses muscle strength and power. Figure 2-14 illustrates the criteria workflow; it starts by measuring the ratio of muscle strength per unit of muscle mass using a handgrip dynamometer and a bioelectrical impedance analysis machine followed by measuring the ratio of the muscle power index per unit of muscle mass. It then categorises muscle quality as normal, low or

poor based on the scores being higher or lower than the standard deviation (SD) values of a healthy young population.

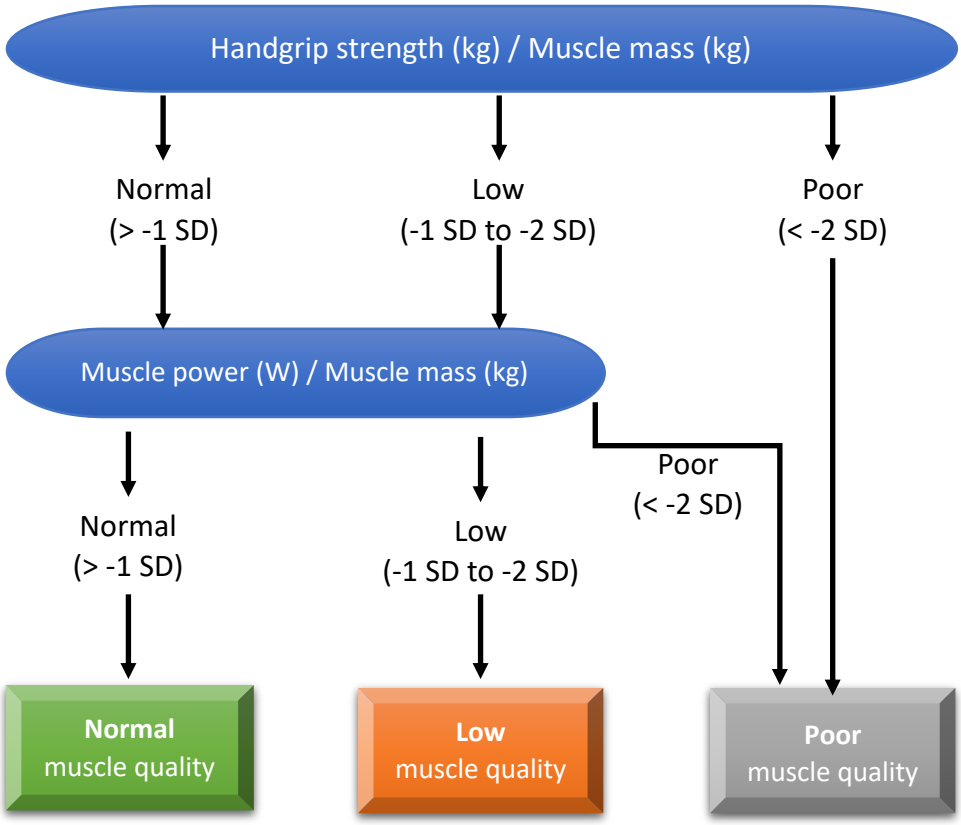

Figure 2-14 Muscle quality index criteria

Handgrip strength is measured using a handgrip dynamometer and muscle power is measured using the index developed by Takai et al. [375]. Muscle mass is assessed using a bioelectric impedance analyser. Adapted from Barbat-Artigas et al. (2012) [376].

Both studies' proposed muscle quality indices are feasible but rather crude assessments, limited only to the functional status. They do not incorporate other crucial factors of muscle quality mentioned earlier. It is critical to note the multifaceted and complex aspects of muscle quality. Experts highlight the need to develop a comprehensive framework for assessing muscle quality using quantitative objective measures [5].

To date, muscle elasticity, assessed using SWE, is not considered one of the characteristics of muscle quality since there is insufficient data to confirm or refute its merit. This thesis can help in building a foundation for future work to substantiate the role of SWE in multiple established and suspected muscle diseases. Therefore, the scope of this thesis is limited to assessing the

biomechanical muscle construct via SWE and testing how it correlates with other muscle quality factors. The assessment methods used to detect some of the muscle quality factors are reviewed in the next subsections below as a number of them will be utilised in chapters 4, 5, 6 and 7.

2.5.1 Muscle enzyme blood tests

Diseases causing extensive damage to the myofibrils lead to the leak of intracellular muscle enzymes into the bloodstream. These include creatine kinase (CK), alanine aminotransferase (ALT), lactate dehydrogenase (LDH), aspartate aminotransferase (AST) and aldolase. CK is the most preferred muscle enzyme to evaluate in myopathic conditions due to its specificity and high concentration in skeletal muscle [377]. Its appearance in the blood in abnormal quantities is considered an indirect marker of muscle damage. Extremely high concentrations of CK (>1000 units/l) aids in distinguishing a muscle disease condition from neurogenic causes of myopathy.

Elevated serum levels of CK, LDH, AST or ALT are one of the variables included in the recent EULAR/ACR classification criteria for adult and juvenile idiopathic inflammatory myopathies, with a score weight of 1.4 points [323]. It is one of the core set measures indicating the degree of activity in this group of myopathies [378]. Furthermore, serial CK evaluations after an elevated result at the baseline is an effective method for monitoring disease progression and response to treatment. However, elevated CK levels alone is a poor predictor of muscle biopsy results due to the common normal levels in cases of dermatomyositis and inclusion body myositis (sensitivity= 48%) [4]. Serum aldolase can be elevated when CK is normal in these cases but is rarely tested due to its poor specificity and sensitivity.

Despite its value, muscle enzyme tests can have poor sensitivity. Testing muscle enzymes do not seem to have an established role in diagnosing steroid-induced myopathy since they are usually within the normal range. Nevertheless, an old study reported a profound CK increase up to 410 folds normal values in approximately 60% of patients treated with high doses of steroid [379]. The patients were, however, of various severe non-muscular illnesses and treated with different types of corticosteroids. On the contrary, it was reported that the CK levels decreased below the normal range in 20

healthy volunteers receiving 8 mg/day dose of dexamethasone (mineral glucocorticoid) for one week [380].

Best practice guidelines recommend the evaluation of muscle enzymes as the first investigation to order for screening. However, vigorous exercise such as running a marathon or performing eccentric movements in unaccustomed muscles can trigger a rise in CK levels. It can also be persistently elevated in normal subjects (known as hyperCKemia) especially from African-American descent as well as in cases of hypothyroidism and nephropathy. Overall, serum CK blood test is an essential indicator of muscle injury but can be of low sensitivity in several myopathic conditions.

2.5.2 Strength and functional tests

Muscle strength is defined as the peak torque [Newton-meters (N.m)] or force [Newton(N)] produced during maximal voluntary skeletal muscle contraction. It is accepted that physical functional abilities are partially explained by muscle strength. Certain levels of muscular strength are required to perform daily life activities, which will define an individual's physical independence.

2.5.2.1 Handgrip strength.

Isometric handgrip test is a simple, established and reliable method for skeletal muscle strength assessment [381]. It is measured using a handheld dynamometer that produces objective strength (squeeze) readings in units of kilogram-force (kg_F). It has been used clinically to diagnose muscle weakness, follow-up rehabilitation progress and predict bone mass [382]. It can also be used as a good predictor of total body muscle strength (R^2=0.80; p<0.001) [383]. This conformability with global muscle strength and ease of use expedited its adaptability in clinical settings. Systematic reviews recommended utilising handgrip tests as a screening tool for mortality and disability in middle-aged and older adults [384, 385].

There are numerous test protocols, but the one by the American Society of Hand Therapists is the most widely established [386]. They recommended using the JAMAR handgrip dynamometer (Paterson Medical, Warrenville, IL, USA) which most researchers also consider the golden standard. According to their protocol, subjects must be seated on an armless chair, elbow flexed at 90°

and shoulder abducted. Then, recording the mean of three maximum strength readings while alternating hands with 30-sec rest intervals in between.

2.5.2.2 Knee extension/flexion strength.

Isokinetic dynamometry is the recognised gold standard method for assessing the strength of the quadriceps (extension) and hamstrings (flexion) muscle groups. It is assessed using commercially-available dynamometers, which measure peak and average muscle torque. Most strength dynamometers produce similar strength measurements and negligible inter-manufacturer variability [387]. Dynamometers are more sensitive than manual muscle tests and produce reproducible results [388]. However, these systems are more suitable in research centres due to the high price tag and large space needed. There are alternative cheaper, smaller and portable dynamometers suitable for clinical settings. However, they lack standardised protocols; hence, inconsistent reports can be found in the literature.

Muscle strength testing can be performed using various contraction settings. Isokinetic testing is considered the most widely investigated and advocated strength outcome (versus isometric) by researchers to use and report in clinical research [389]. It has been shown to reflect the common global body strength construct [390]. Isokinetic muscle strength can be performed using modern electromechanical dynamometers such as the Biodex isokinetic system 4 (IRPS Mediquipe, UK). In isokinetic settings, this device applies an operator-selected constant angular velocity, which controls the angular momentum that a participant cannot exceed whilst performing the test. This action can be performed in concentric (muscle shortening) or eccentric (muscle lengthening) motions. The former is usually preferred since eccentric muscle strength seems to be preserved in diseases associated with ageing and weakness [391, 392]. This demonstrates that the loss of isokinetic concentric strength occurs earlier and is more sensitive for detecting a premature loss in functional capacities [392]. The reason behind this phenomenon is unclear but appears to be linked with the sarcomere cross-bridge cycles in the sliding filament theory (explained in chapter 1) becoming impaired in aged muscle.

In RA, decreased muscle knee extension strength is associated with physical disability, especially in women [393]. A small pilot study of female RA patients found that knee flexor peak torque of 31 N.m was significantly lower than age-

matched healthy controls who had a peak torque of 43 N.m [394]. Similarly, Meireles et al. [395] found decreased strength results in knee extension/flexion bilaterally compared to healthy controls. Another study reported a direct relationship between knee extension/flexion strength with disease activity [396]. After following subjects over a year, it was suggested that a 10 points increase in joint pain index is explained by 2.1 N.m decrease in isokinetic extension torque. Additionally, for each 1 point increase in knee joint swelling index, extension torque decreases by 7.5 N.m. Not all studies, however, demonstrated strength deficit in knee extension/flexion in RA patients. For example, a study compared 50 stable RA patient to 500 healthy controls found no significant difference in knee extension strength [361].

In myositis, isokinetic knee strength is used and recommended as one of the extended set measures for disease activity assessment in clinical trials [378]. Unlike manual muscle testing, dynamometers provide an objective measure of muscle strength and are sensitive to detect mild degrees of muscle weakness in myositis. Mosca et al. [397] reported that isokinetic knee extension/flexion strength testing was the most sensitive tool from three other tests for detecting declined muscle strength in 27 myositis patients. In a group of 13 polymyositis and dermatomyositis patients, maximal knee strength results were sensitive to changes in CK levels with a high reliability coefficient of 0.98 for both inter- and intra-observer reproducibility [398].

In the muscle elastography literature, dynamometers are usually used for positioning purposes to confirm the desired muscle stretch/joint angle is achieved. Section 2.3.1.3 reviewed how active muscle stiffness measured using SWE can be used to predict MVC estimated using EMG. No studies have so far aimed to elucidate the resting muscle elasticity relationship with isokinetic strength measurements.

2.5.2.3 Short Physical Performance Battery (SPPB)

SPPB is a group of three test components used to assess physical function [399]. It includes repeated chair stands, standing balance and gait speed tests. The sum result of the three components is expressed as a mean value ranging from 0 (best physical performance) to 12 (worst physical performance). SPPB is increasingly being adopted in physical performance studies especially on

elderlies, due to its simplicity and standardised objective measurements. However, it is not commonly used in younger patient cohorts.

2.5.2.4 Expanded Timed Get-Up-and-Go (ETGUG)

Similar to SPPB, this test measures a series of important functional tasks that mostly focuses on dynamic balance. The test is simple; it records the time it takes the subject to stand up from a chair, walk 10 meters, turn around, walk back and sit down. Bohler et al. [400] found moderate correlations when comparing the shorter test version (TGUG) scores to the health assessment questionnaire (HAQ) (r=0.62), clinical disease activity index (r=0.50) and visual analogue score (r=0.61). A similar association with HAQ was also reported in another study [401].

2.5.2.5 Gait speed

This is the simplest and most adopted test to assess physical function. All sarcopenia groups, including EWGSOP, used this test in identifying subjects at risk of sarcopenia. Large studies looked at this test and found an association with survival in older people [402] in addition to predicting disability [403]. There are variations to this physical performance test, mostly concerning the pace and distance. Gait speed serves as an integral tool for triaging subjects to further assessments before establishing the final diagnosis.

Significant negative correlations with muscle quality were reported for gait parameters in older adults [404]. In general, assessing gait speed provides basic, albeit fundamental, insight into physical function. Hence, it is part of the SPPB and ETGUG tests, which offer more comprehensive physical performance assessment.

2.5.2.6 30-second chair stand test

There are several chair stand test variations. The 30-s chair stand test (CST) version is one of the versions aimed to assess muscle endurance and strength, which was first introduced in 1999 by Jones and Rikli [405]. It involves recording the maximum number of stands a subject can perform in a window of 30s. The major advantages of this test are its validity, reliability and ease of use. However, it is commonly criticised for its floor effect in subjects that cannot stand unassisted.

The CST demonstrates good responsiveness and construct validity in myositis. This was reported in a longitudinal study showing that CST correlates inversely with serum CK level [406]. Stand count declined by >3 in relapsing patients when compared to patients in remission. In elderly, CST had acceptable criterion validity as it correlated with leg press performance (r=0.78, p<0.001) [405]. The scores gradually decreased from 14.0 to 12.9 to 11.9 stands across age groups in decades from the 60s to the 70 to the 80 respectively.

Overall, a combination of muscle tests to assess peak strength in the upper limbs (grip strength) and lower limbs (Isokinetic knee extension/flexion), physical function (ETGUG) and muscle endurance (30-second chair sit to stand) can offer a relatively comprehensive skeletal muscle evaluation of the functional muscle capacity. This battery of tests will form the muscle assessment methodology in chapters 4, 5, 6 and 7.

2.5.3 Electromyography

The skeletal muscle electrical activity can be evaluated using nerve conduction studies and EMG tests. This can be tested in resting or active states via surface electrodes or needle electrodes inserted into the muscle belly. The recorded electrical potential patterns (phases, duration and amplitudes) can indicate certain muscular or neuromuscular disorders. For example, myopathic conditions usually represent short, small and polyphasic electrical impulses compared to normal bi or triphasic impulses found in a healthy muscle upon activation.

EMG is particularly useful when combined with other investigations for diagnosing primary muscle disease. It is important to note that the EMG results should not be overemphasised since abnormal findings are not certainly pathognomonic. In myositis, for example, characteristic EMG abnormalities can support the diagnosis but are not specific, with similar findings occurring on other myopathies [407]. Therefore, EMG is merely employed for differentiating the underlying myopathic cause of weakness from neuropathological conditions. The recent EULAR/ACR myositis criteria highlighted the limited use of EMG in clinical practice [323].

Needle EMG tests are principally invasive. The site where the needle has been inserted is usually traumatised and may negatively influence the accuracy of a

needle biopsy if sampled from the same site [408]. Fortunately, a large number of myopathic conditions occur bilaterally in a symmetrical fashion, so biopsies can be performed on the contralateral side to where the EMG has been performed.

With regard to steroid-induced myopathy, EMG patterns are usually normal in the early stages, and only mild abnormal patterns can appear in chronic stages [357]. In contrast, EMG detected abnormal results in the muscles of RA patients, indicating a level of myopathic involvement. This was reported in Table 2-8 as the majority of studies which utilised EMG have reported polyphasic, short amplitude and duration electrical potentials [331, 333, 337, 340]. As for ageing, mobility-limited elderly have weak EMG signal amplitudes indicating diminished neuromuscular activation capability [409]. This finding, however, is not observed in older adults with no mobility limitations.

There is a proportional relationship between muscle contraction and the sum of recruited motor neurons required to activate a voluntary contraction. One of the drawbacks of EMG is that upon a maximum contraction the number of motor neurons activated can be beyond the EMG detection limit due to the interference from other neighbouring motor neurons. Thus, the actual produced potentials of an individual muscle may no longer be distinguished. On the other hand, SWE can predict the contraction level of an individual muscle with no interference. SWE results demonstrated a strong coefficient of determination when regressed to EMG [234]. Therefore, SWE may have a potential application in electrophysiological studies to indirectly measure the degree of muscle activation via increased muscle stiffness elicited in active contraction. The investigation of this potential application is beyond the scope of this thesis.

2.5.4 Biopsy

Muscle biopsy is an essential tool in establishing the diagnosis and characterisation of suspected myopathies. It is usually the last diagnostic investigation test after a positive screening of strength, serum muscle protein levels and electrodiagnostic tests. The biopsied sample is usually obtained from the vastus lateralis or biceps brachii muscles. Figure 2-15 explained the steps of this procedure and demonstrates its invasiveness. Evaluation

techniques range from basic histopathology to more sophisticated immunocytochemistry.

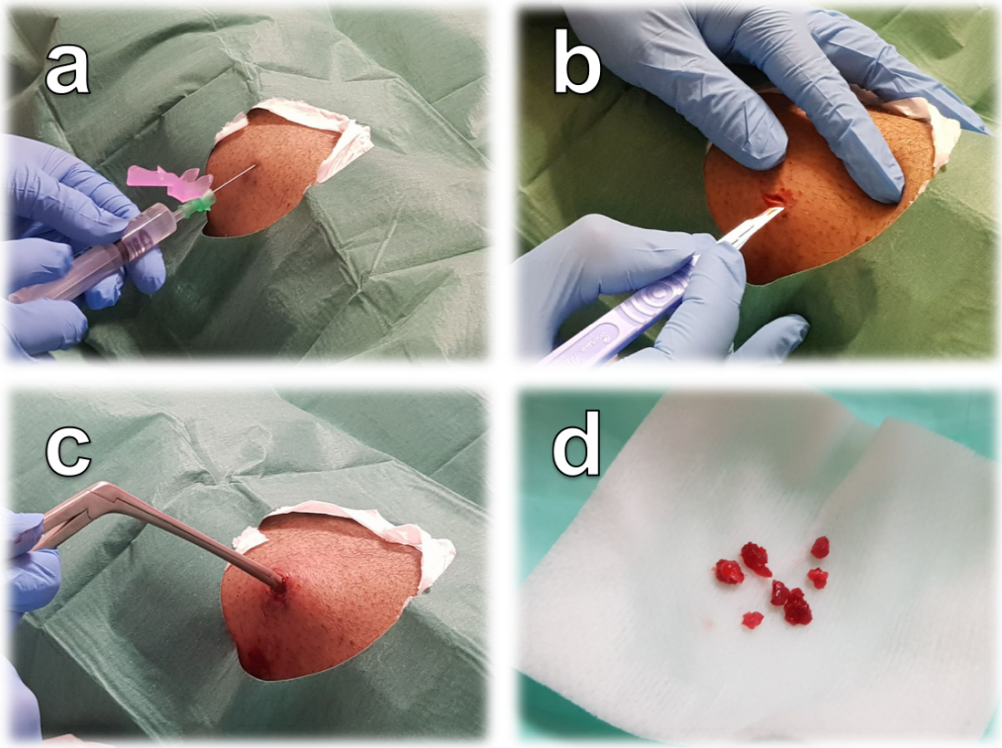

Figure 2-15 Percutaneous muscle punch biopsy from the vastus lateralis.

A- local lidocaine is injected to anesthetise the site. B- a scalpel is used to open an incision of approximately 1cm. C- Tilley Henckel punch is advanced and rotated multiple times into the muscle. D- the obtained specimen of skeletal muscle. The patient's consent was obtained to capture and publish the images.

In idiopathic inflammatory myopathies, muscle biopsy is the primary diagnostic method stated in all diagnostic guidelines. The main histopathological features include endomysial, perimysial and perivascular inflammatory infiltrates in addition to the presence of necrotic and regenerative myofibres. One of the major advantages of muscle biopsy in myositis is the specificity in subclassifying the disease. For example, thickened capillaries and perifascicular atrophy/necrosis are specific for dermatomyositis whereas amyloid deposits and rimmed vascules are specific for inclusion body myositis. Therefore, muscle biopsy is used as gold-standard in medical research.

In steroid-induced myopathy, the diagnosis does not rely on muscle biopsy. Nevertheless, histology shows preferential atrophy of type 2-b muscle fibres with additional features including significant variations in fibre sizes and rarely necrosis [410]. In contrast to myositis, inflammatory infiltrating cells are absent.

The observed findings were sometimes linked to the duration and dosage of the corticosteroid treatment. Many of the detected structural alterations postulate a change in the elastic property in these cases.

Muscle biopsy is not usually utilised in investigating ageing-related muscle conditions. Nonetheless, evidence shows type 2 muscle fibre atrophy and changing fibre type distribution in addition to mitochondrial and neurogenic alterations in subjects over 70 [411]. On the other hand, multiple signs of inflammatory and non-inflammatory muscle biopsy findings are reported in RA subjects in Table 2-8 including atrophy, necrosis and infiltration of lymphocytes [330-342, 365-367, 412].

Despite the fundamental role of muscle biopsy, it has various limitations. It is not uncommon to sample undiagnostic specimens or collect adipose rather than muscle tissue in percutaneous muscle biopsy. The sample may be less satisfactory with poor diagnostic yield than the open, but more invasive, biopsy. Additional limitations include a sampling bias where the targeted area contains unaffected tissue. Moreover, muscle biopsies are not suitable for prognostic and routine assessments. Therefore, there is an ongoing quest in the imaging research field to find alternative non-invasive methods to diagnose muscle disease. Indeed, SWE has come a long way towards decreasing the number of unnecessary liver and breast biopsies as reviewed earlier in this chapter.

2.5.5 Imaging

Medical imaging has a secondary, albeit growing, role in the assessment of skeletal muscle diseases. MRI and ultrasound are the two major technologies used, with the former holding the largest share of muscle applications. Other modalities, such as general x-ray radiography, computed tomography and nuclear medicine have limited to no role due to their relatively inferior soft tissue contrast resolution and radiation risk. The next two subsections will briefly review the roles of ultrasound and MRI in assessing the muscle conditions related to this thesis.

2.5.5.1 MRI

MRI is the most useful imaging modality for evaluating skeletal muscle conditions, which is largely due to its excellent contrast resolution. Its applications include diagnosis, monitoring, directing interventions and

assessing severity. The MRI principle is based on exploiting the behaviour of the hydrogen atom protons after being excited by radiofrequency pulses in a strong magnetic field. Received signals are recorded to form magnetic resonance images based on the distribution and density of fat and water within the muscle. Multiple parameters can be tuned to emphasise specific differences in the muscle tissue composition and structure. T1-weighted image sequences provide good details on muscle morphology and signs of myosteatosis. In contrast, T2-weighted image sequences are sensitive to fluid signals. However, these signals are not specific as muscle oedema and fat are both hyperintense. Therefore, fat-saturated short tau inversion recovery (STIR) sequences are utilised to provide truly fluid-sensitive images to accentuate signs of inflammation by suppressing fat signals (Figure 2-16).

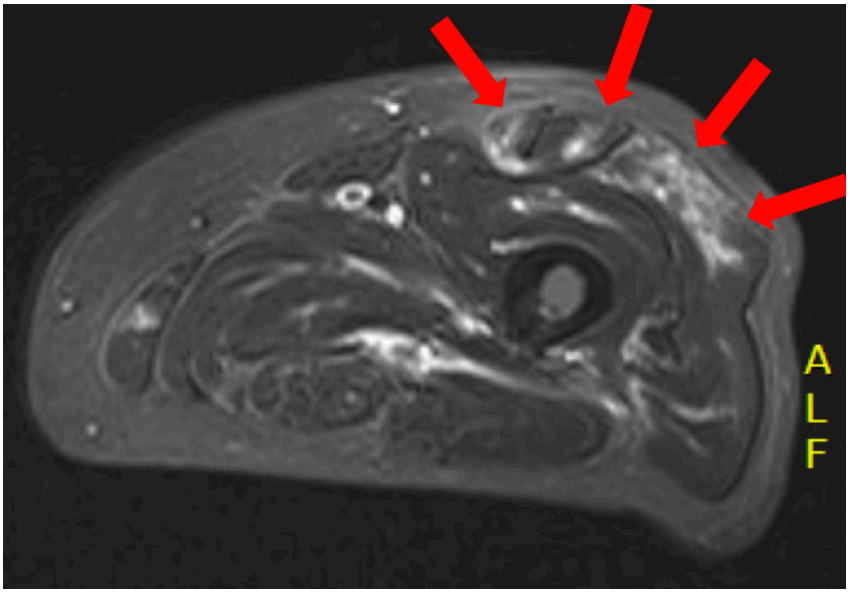

Figure 2-16 Fat-saturated MRI of muscle inflammation.

Fat-saturated STIR image of the left thigh in an active case of dermatomyositis demonstrating intramuscular oedema (red arrows) in the vastus lateralis and rectus femoris muscles.

Despite not being endorsed in any established clinical guidelines so far, MRI's role is growing for diagnosis and management of myositis. Starting with diagnosis, MRI can be of added value in early suspected myositis with normal CK levels as well as for detecting specific muscle involvement patterns in subgroups. A recent retrospective study of 66 newly-diagnosed myositis patients revealed that the whole-body MRI positive rate (86.4%) is not significantly different (p=0.258) to biopsy (92.4%) [413]. A prospective study of

12 inclusion body myositis cases showed that, unlike in dermatomyositis and polymyositis, distal limb segments are typically affected in MRI, which conforms with the clinical representation [414]. MRI can aid in selecting regions of active inflammation to guide biopsy, substantially decreasing rates of false-negative results [327].

As for myositis management, MRI showed that muscle oedema decreased during treatment using conventional disease-modifying anti-rheumatic drugs [415] or biologics [416]. Moreover, MRI can be of value in myositis cases with persistent muscle weakness to differentiate signs of disease activity (high intramuscular signals on STIR images) from damage (atrophy on T1-weighted images) [417]. This is helpful in guiding therapeutic decisions. However, the lack of a validated and standardised scoring system is a major limitation standing in the face of MRI from being routinely adopted as a routine method of myositis assessment. The recently published EULAR/ACR myositis classification criteria omitted MRI due to the lack of sufficient evidence of its validity and reliability [323].

The literature is scarce for data on the role of MRI in diagnosing steroid-induced myopathy. Most of the studies were focused on investigating the effectiveness of the corticosteroid treatment in myopathies using MRI rather than exploring the potential induced myopathy. Lovetti et al. [418] mentioned that it might be “impossible” to distinguish steroid-induced myopathy from a primary underlying myopathy using MRI.

In the ageing literature, MRI is employed to estimate body composition or asses age-related muscle changes like myosteatosis. MRI is regarded as the gold-standard technique for quantifying limb-specific or whole-body muscle mass [419]. It was able to prove that sarcopenia determinately affects the lower limbs at a higher rate than upper limbs [419]. Using multiparametric MRI techniques, a recent study has revealed that age was a significant predictor of increased fat percentages within the thigh muscles [420].

Novel MR technologies such as magnetic resonance elastography (MRE) may offer new insights into the assessment of skeletal muscle. Its principle is based on utilising an external mechanical device strapped to the muscle surface that produces compressional waves to stimulate the propagation of transverse

shear waves. Modified phase-contrast sequences are then utilised to monitor shear waves velocity and convert them into MR elastograms. A study on 9 myositis patients revealed a significantly decreased muscle stiffness compared to healthy controls [421]. Similar to SWE, the value of muscle MRE in clinical and research settings has not been substantiated yet.

2.5.5.2 Ultrasound

Ultrasonography facilitates bedside assessment of echogenicity, vascularity and determination of the nature of lesions (cystic versus solid). Although readily-available and relatively inexpensive, it is limited by several factors such as operator's inexperience, small field of view and steep learning curve. Multiple articles are published on the role of ultrasound for assessing muscle with the majority focusing on sports injuries.

Normal muscle appears hypoechoic with a heterogeneous pattern and speckled echogenic dots arising from the perimysial connective tissue in the transverse plane (Figure 2-17). When scanned parallel to the muscle fibres (i.e. longitudinally), the fascicular pattern of the muscle becomes visible. The overlaying subcutaneous fat appears relatively hypoechoic in the longitudinal plane with multiple bright septa within this adipose layer. Ultrasound allows high-resolution imaging of superficial muscles, but it can be limited when imaging deep pelvic or trunk muscles (e.g. deeper than 5 cm).

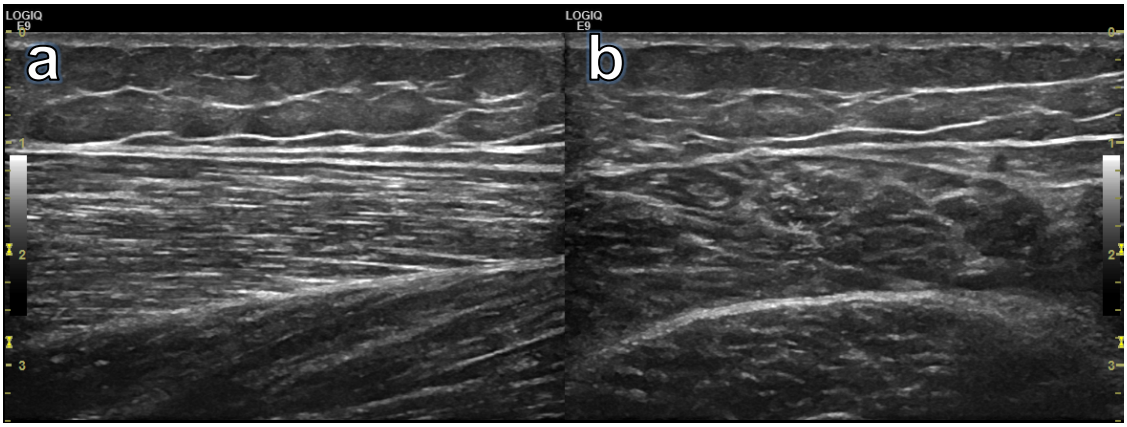

Figure 2-17 Normal B-mode ultrasound appearance of healthy muscle.

a: longitudinal plane (along muscle fibres). b: transverse plane (across muscle fibres).

Several myopathies can alter the normal muscle echogenicity in B-mode images. For instance, quantitative assessment of echo intensity reveals that it is increased in cases of dermatomyositis and polymyositis. A study of 70

myositis patients confirmed this finding and reported that ultrasound's sensitivity (82.9%) is not significantly different from EMG (92.4%) or CK levels (68.7%) [422]. Similar findings were reported in another study of acute juvenile dermatomyositis [423]. However, the basic sign of hyperechogenicity is not specific; it may appear in cases of infectious or traumatic aetiologies [424]. Nevertheless, Noto et al. [425] reported that inclusion-body myositis (n=6) have a predisposition to cause an increased echogenicity in the flexor digitorum profundus in contrast to the flexor carpi ulnaris. This contrasting echogenicity marker was not observed in the cases of polymyositis or dermatomyositis (n=6). Hyperechogenicity can also be prevalent not only oedematous changes but also in muscle atrophy, which is a sign of damage in myositis. Atrophy, however, comes with a marked reduction in muscle size.

Most of the papers cited in the previous section were relatively old (before 2000). Research into the role of conventional ultrasound imaging in myopathies has decreased significantly since then. Novel ultrasound technologies have come forward in the last couple of decades. Technologies like contrast-enhanced ultrasound have shown a promising sensitivity and specificity (73% and 91% respectively) compared to that of MRI (100% and 88% respectively) for detecting active myositis [426].

With regard to ageing, muscle echogenicity appears to negatively correlate with the 30-second chair stand test ($r= -0.505$, $p<0.01$) and isometric peak torque ($r= -0.409$, $p<0.01$) in active elderly women [427]. Furthermore, ultrasound has been investigated as a method for quantifying muscle mass through several parameters like thickness, width, length and cross-sectional area. Using the latter, Young et al. [428], observed a 25% reduction in the quadriceps muscle mass when comparing young (20–30 years) versus elderly (70–80 years). Taking advantage of the excellent spatial resolution, other researchers utilised a sophisticated image analysis software and detected a decline of 10–20% in muscle fascicle length as a result of ageing [429]. When compared to MRI, ultrasound had an almost perfect agreement (ICC=0.999) in a small study of only 6 healthy individuals [430]. Indeed, most studies in this research area were small and conducted on young asymptomatic cohorts. There is so far limited evidence to establish the reliability of B-mode ultrasound for measuring muscle size according to a recent systematic review [431].

The role of ultrasound in rheumatic conditions for investigating joint and entheseal disease has been reviewed at the beginning of the chapter. There is so far little knowledge on the nature of muscle quality in rheumatic conditions using ultrasound. Likewise, there are no papers investigating the role of ultrasonography in steroid-induced myopathy. Despite the feasibility of ultrasonography, it does not seem to have an established clinical application for myopathies to date. This could be because of the inherently lower contrast resolution as well as the subjective nature of image interpretation. Therefore, there is a growing trend for developing new quantitative ultrasound technologies that look beyond conventional greyscale and Doppler imaging to discern muscle pathologies. This thesis will hopefully contribute towards that cause by developing the methodology and investigating the role of muscle SWE in various aspects.

Chapter 3 Reliability of shear wave elastography in healthy skeletal muscles

In this chapter, two cross-sectional studies sought to investigate the reliability of shear wave elastography in healthy skeletal muscles and test the effect of acquisition methods. The results from this chapter have been published as:

1- *Alfuraih, A.M., O'Connor, P., Tan, A.L., Hensor, E., Emery, P. and Wakefield, R.J., (2017). An investigation into the variability between different shear wave elastography systems in muscle. Medical Ultrasonography, 19(4), pp.392-400.*

2- *Alfuraih, A.M., O'Connor, P., Hensor, E., Tan, A.L., Emery, P. and Wakefield, R.J., (2018). The effect of unit, depth, and probe load on the reliability of muscle shear wave elastography: Variables affecting reliability of SWE. Journal of Clinical Ultrasound, 46(2), pp.108-115.*

3.1 Introduction

In medical as well as other sciences, reliable and consistent measurements serve as the foundation for clinical evaluation. Reliability can be defined as the performance of the diagnostic tool in terms of variability between subjects and the consistency of the repeated measurements [432]. As measurements error may inherently exist in new diagnostic methods such as SWE, testing the measurements consistency and precision is vital in research and clinical applications. Moreover, it is essential to validate the techniques to ensure the development and utilisation of the most reliable acquisition method and minimise measurement error.

In chapter 2, the narrative literature review of healthy muscle SWE studies identified a considerable variability in the acquisition methods amongst the studies. The reliability indices varied considerably, which is hypothetically related to the different techniques operated. In-vivo stiffness assessment of a skeletal muscle is complex because of its varying anatomical structures. SWE has to overcome anatomical challenges such as anisotropy, shape and length

changes and heterogeneity with respect to myoaponeurotic structures. These features could influence muscle SWE measurements [206, 212].

The review in chapter 2 demonstrated some variability regarding probe orientation. Most studies used the longitudinal plane while others favoured the transverse [204, 240, 247, 248]. Several studies have investigated the effect of scanning muscles in more than one plane; the majority reported better reliability in the longitudinal orientation [138, 212, 239]. Only one study evaluated potential SWE differences from different locations within a muscle and found differences in elasticity and readings reliability [212]. Several SWE manufacturers offer the option to select an ROI of various sizes and shapes. Two studies have tested the use of variable ROI sizes and reported conflicting results; it is not clear whether ROI size has no effect [204] or whether variability is greater with smaller ROI [250].

SWE machines track the propagation of shear waves to estimate shear wave velocity (SWV) by calculating the difference in the shear wave arrival time between two or more locations of known distances. Several commercially available SWE systems offer the option to report readings in SWV (m/s) and Young's modulus (kPa). When performing muscle SWE, repeated consecutive acquisitions that have the same SWV but slightly different Young's modulus can be frequently encountered. Such occurrences suggest that the original SWV reading could potentially be more reliable than Young's modulus.

The SWE systems also allow placing acquisition sample boxes at different depths extending to approximately 75% of the corresponding maximum depth of B-mode. Several articles have reported on the effect of depth in different tissues [123, 247, 258, 433]. However, none have investigated its effect on reliability. Although shear wave propagation is known to be depth dependent [247], there is no standardised protocol or recommendation regarding measurement depth in muscle.

SWE is less operator-dependent than strain elastography; however, it still depends on the operator's handling of the probe concerning the pressure applied. Different degrees of probe load or precompression force have been shown to result in significantly different SWE readings on breast and thyroid tissues [64, 259]. Previous studies investigating probe load and depth applied

statistical inferences to merely test for difference without testing for reliability to recommend a specific, reliable method.

No previous studies have reported on the elasticity of the dominant versus non-dominant thigh muscles. As muscular development and loading of a dominant limb could postulate a difference in its muscle elasticity. Assessing this could help understand possible between limb differences, which should be taken into account when conducting SWE research studies.

Acquisition method standardisation will help reduce technically-induced variation and improve the ability to evaluate the sensitivity to change of muscle elastography to interventions. Additionally, knowledge of muscle SWE reproducibility between systems is vital for results comparison in future studies. So far, no studies have investigated muscle SWE performance between different manufacturers, which might be attributed to the dominance of older systems over newly introduced ones.

This chapter describes evidence of technical validity and is divided into two main sections that include two related technical reliability studies. Each section comprises the aims, methods, results and discussion for one of the studies. The first study investigated probe orientation, location and ROI size in addition to comparing the performance of two SWE systems to report the inter-system reproducibility. The second study investigated the effect of units, depth and probe load on the readings reliability. The underlying hypothesis for the two studies is that the reliability of muscle SWE is dependent on acquisition methods and altering them produces variable readings.

3.2 Study 1. Probe location, orientation, ROI size and between systems variability

3.2.1 Aims

The aims of this first study were threefold: first, to test the effect of using different probe orientations, locations and ROI size combinations; second, to determine the reliability of a relatively new SWE system in normal human resting muscles; third, to compare the new system performance to another well-validated and established SWE system.

3.2.2 Materials and methods

3.2.2.1 Participants

Twenty asymptomatic healthy volunteers (13 males) of mean (SD) age 38.7 (14.9) years and BMI 25.3 (4.2) kg/m^2 participated. Volunteers with a history of musculoskeletal or rheumatic conditions were excluded. All participants were asked to refrain from any strenuous or sporting activities 24 hours prior to the study to moderate possible confounding exercise effect. The study received the research ethics committee's approval (ref: 14/LO/1785) and was performed under good clinical practice guidelines. All participants gave written consent.

3.2.2.2 Equipment

Two-dimensional SWE measurements were acquired using the recent commercially released SWE package for the General Electric LOGIQ E9 system [(LE9); GE Healthcare, Buckinghamshire, UK] using a linear 9-5 MHz probe. The LE9 utilises the comb-push excitation method that simultaneously transmits multiple comb-like ARFI pulses to produce shear waves. Then, time-interleaved shear wave tracking is used to estimate shear wave velocity [434].

A rectangular shear wave box of 2 $\times$ 2.2 cm was used. The box was centred at a depth of 2.5 cm, although this varied slightly between patients due to varying body habitus. An SWE scale of 7.1 m/s was chosen. Because of the anisotropic nature of muscles, and to the Youngs' Modulus (in kPa) assumptions of isotropy and homogeneity, measurements were recorded in units of shear wave velocity (m/s). To avoid probe-induced stiffness, minimal probe compression was used to ensure good skin contact.

3.2.2.3 Shear Wave Elastography Reliability

To test the effect of aponeurotic structures and angle of muscle fibres on SWE readings, the rectus femoris muscle was chosen because of its bipennate anatomy. The participants were asked to lie supine in a comfortable position. They rested on the bed for five minutes before acquiring measurements to avoid possible locomotion-induced stiffness. Any SWE acquisition containing stripy or marked artefacts were excluded. The following variables were analysed:

Location. Using ultrasound guidance, the proximal and distal myotendinous junctions of the right leg were marked using a surgical marker. The muscle was

then marked at 25% (superior), 50% (mid) and 75% (inferior) to define reference points for the level and location of acquisitions (Figure 3-1.a). Two additional points were marked on either side of the mid-point (medial and lateral). Superior, mid and inferior points were performed to test muscle aponeurosis effect on SWE. Medial and lateral points ensured scanning was performed in the centre of both muscle bellies.

Orientation. To test the effect of anisotropy, the probe was positioned in three different angles according to fibre orientation: transverse (across the fibres; Figure 3-1.b1), longitudinal (along the fibres; Figure 3-1.b.2) and oblique (along the thigh; Figure 3-1.b.3). For the superior, mid and distal locations, where the two rectus femoris bellies merge to the central aponeurosis, the probe was oriented across the thigh for a transverse plane and along the aponeurosis for the oblique fibre orientation. As for the longitudinal plane, the probe was rotated slightly medially or laterally until multiple fibres can be visualised on the B-mode image.

ROI size. Three ROI sizes 15mm^2 (small), 75mm^2 (medium) and 200 mm^2 (large) were selected within each SWE acquisition. The area was displayed to ensure accurate and consistent ROI sizes (Figure 3-2). The circular ROI for the different sizes were always located at the centre of the shear wave box. The readings were repeated three times for each combination of location-orientation-ROI. The probe was removed and replaced each time. As a result, each examination consisted of 135 SWE readings (five sites, three probe orientations, three ROI sizes and three repetitions).

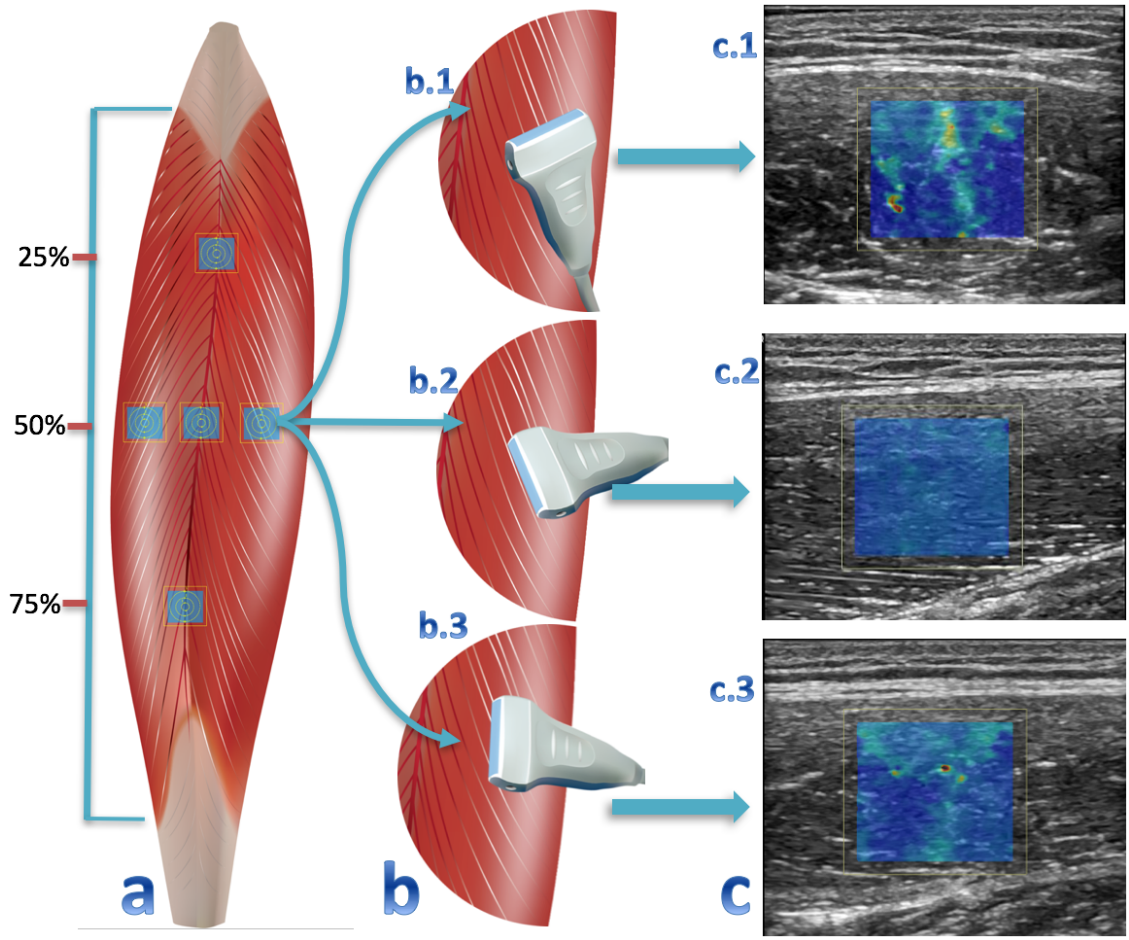

Figure 3-1. An illustration of the scanning protocol.

Image-a shows the rectus femoris muscle with the three points used between the proximal and distal myotendinous junctions in addition to the five locations selected. Image-b demonstrates the three probe orientations from the medial location as an example: b.1 transverse (across the fibres), b.2 longitudinal (along the fibres), and b.3 oblique (along the thigh axis). Image-c shows examples of each orientation's corresponding image.

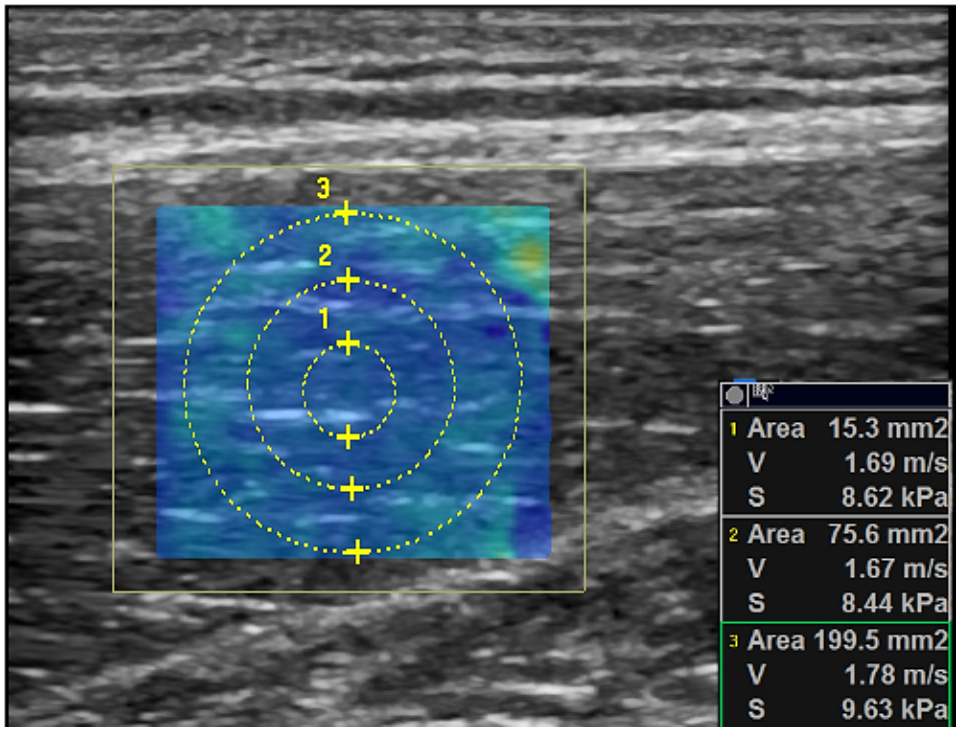

Figure 3-2 shows the three ROI sizes: small (1), medium (2) and large (3) with corresponding SWE readings.

The image was acquired longitudinally from the lateral location.

3.2.2.4 Shear Wave Elastography System Comparison

Upon finishing the LE9 SWE reliability scans, participants were moved to an adjacent room to have the examinations repeated on another SWE system machine [Aixplorer (AIX), Supersonic Imagine, Aix-en-Provence, France] which is widely considered the gold standard [138, 139, 212, 239, 248]. This system was supplied by the vendor as a short term loan to trial and compare its performance. To generate shear waves, the AIX system sends multiple successive ARFI pulses which are focused at different depths in tissue. These pulses generate a “Mach cone” shaped shear wave profile, which increases the efficiency and amplifies the distance of the propagated shear waves [92]. Following this, utilising ultrafast imaging technology, a flat wave insonifies the whole imaging plane to track and quantify shear wave velocity. Thirteen participants were tested for this comparison. Readings were obtained using the SuperLinear™ SL10–2MHz probe. The probe frequency, shear box size and depth, scale, SWE mode and reference points were adjusted to be as close as possible to the LE9 system. Due to time constraints, the full study protocol was shortened with only mid, lateral and medial locations being scanned. Additionally, only the medium ROI size of 10mm in diameter was used, which is

equivalent to 75mm^2 (medium) on LE9. Each comparative examination consisted of 27 SWE readings (three sites, three probe orientations, one ROI sizes and three repetitions).

3.2.2.5 Statistical analysis

Statistical analyses were performed using SPSS V.21 (IBM Corp. Armonk, NY). Measurement error was represented as within-subject coefficient of variation (WSCV). The within-subject standard deviation (WSSD) of log-transformed values was calculated using the method described by Bland and Altman [435]. Reliability and variability of different ROI sizes were assessed in a single, commonly-used plane (longitudinal) and location (lateral), then one ROI size was chosen to simplify the reliability assessments in each combination of different planes and locations.

Intra-class correlation coefficients (ICC) were used to measure the intra-system reliability, and were interpreted as follows: .00–.20 'poor agreement', .21–.40 'fair agreement', .41–.60 'moderate agreement', .61–.80 'substantial agreement' and >.80 'almost perfect agreement' [436].

To compare LE9 with AIX, ICCs for inter-system reproducibility were calculated. Additionally, to assess inter-system agreement, Bland-Altman 95% limits of agreement (LOA) and their 95% confidence intervals were computed. This involved taking an initial mean of the three measurements per condition, then adjusting the variance estimates for the inter-system differences accordingly [437].

3.2.3 Results

3.2.3.1 Location, orientation and ROI effects

SWV did not differ substantively by ROI size; reliability indices indicated the small ROI did not perform quite as well as the larger sizes (Table 3-1). Medium ROI demonstrated the best reliability and lowest WSCV and was chosen for the remaining analyses. Mean velocities were generally lowest in the longitudinal plane and highest in the transverse plane, irrespective of location (Figure 3-3). In the oblique plane, values were higher and more variable than in the longitudinal plane, but showed a similar pattern across locations. Velocities in both planes were highest in the superior location and lowest in lateral/medial. In contrast, the transverse plane showed the opposite trend.

Table 3-1 Shear wave velocities for the three ROI sizes from the lateral location using the longitudinal orientation.

ROI size	Velocity (m/s)		WSCV (%)	ICC (95% CI)
	Mean	95% CI		
Small	1.86	1.78, 1.94	6.8	.61 (.37–.80)
Medium	1.83	1.77, 1.90	4.3	.76 (.57–.89)
Large	1.86	1.79, 1.93	4.3	.74 (.54–.87)

Mean velocity and 95% Confidence Intervals (CI) were calculated using the mean of the three repeated measurements per participants.

Table 3-2 Shear wave velocities means, lower and upper 95% confidence intervals (CI) and within-subjects coefficient of variance (WSCV) for all combinations of orientation and location.

Orientation	Location	Velocity (m/s)		WSCV (%)
		Mean	95% CI	
Transverse	Superior	2.26	2.06, 2.49	15.8
	Mid	2.40	2.24, 2.58	16.9
	Lateral	2.19	2.02, 2.37	13.1
	Medial	2.44	2.27, 2.63	18.0
	Inferior	2.64	2.46, 2.84	15.2
Oblique	Superior	2.36	2.12, 2.62	14.7
	Mid	2.18	2.00, 2.37	15.4
	Lateral	2.10	1.98, 2.23	8.7
	Medial	1.88	1.75, 2.00	12.7
	Inferior	1.92	1.82, 2.03	8.1
Longitudinal	Superior	2.15	1.99, 2.32	9.8
	Mid	2.01	1.86, 2.16	11.9
	Lateral	1.83	1.77, 1.90	4.3
	Medial	1.85	1.78, 1.93	7.2
	Inferior	1.87	1.77, 1.98	5.7

ROI=region of interest; WSCV=within-subject coefficient of variation. Mean velocity and 95% CI were calculated using the mean of the three repeated measurements per patient. The medium ROI size was used in all combinations.

Table 3-3 Reliability of different location and orientation combinations

Results are demonstrated as ICC within each (intra) and between (inter) systems. The mean difference is also listed with associated limits of agreement (LOA).

Orientation	Location	Intra-system ICC (95% CI)		Inter-system ICC (95% CI)*	Mean difference (m/s)	LOA (95% CI)
		LE9	AIX			
Transverse	Superior	.64 (.41, .82)	-	-	-	-
	Mid	.47 (.20, .72)	.81 (.61, .93)	.12 (-.24, 1)	0.18	±1.15 (0.66, 1.65)
	Lateral	.62 (.38, .81)	.87 (.71, .95)	.65 (.41, 1)	0.17	±0.64 (0.40, 0.88)
	Medial	.41 (.14, .68)	.81 (.59, .93)	.27 (-.03, 1)	0.19	±0.95 (0.58, 1.32)
	Inferior	.48 (.21, .72)	-	-	-	-
Oblique	Superior	.72 (.51, .87)	-	-	-	-
	Mid	.61 (.37, .81)	.95 (.88, .98)	.15 (-.21, 1)	-0.10	±1.06 (0.60, 1.51)
	Lateral	.65 (.42, .83)	.70 (.42, .88)	.53 (.26, 1)	0.08	±0.54 (0.34, 0.74)
	Medial	.45 (.18, .70)	.90 (.78, .97)	.60 (.30, 1)	-0.03	±0.45 (0.26, 0.64)
	Inferior	.62 (.38, .81)	-	-	-	-
Longitudinal	Superior	.71 (.50, .86)	-	-	-	-
	Mid	.65 (.41, .82)	.92 (.82, .97)	.43 (.18, 1)	0.12	±0.56 (0.34, 0.78)
	Lateral	.76 (.57, .89)	.98 (.95, .99)	.71 (.48, 1)	0.07	±0.49 (0.31, 0.68)
	Medial	.55 (.29, .77)	.97 (.92, .99)	.54 (.27, 1)	0.05	±0.38 (0.23, 0.53)
	Inferior	.80 (.64, .91)	-	-	-	-

* One-sided lower limit 95% confidence interval (CI). ICC=intraclass correlation coefficient; LOA=limits of agreement.

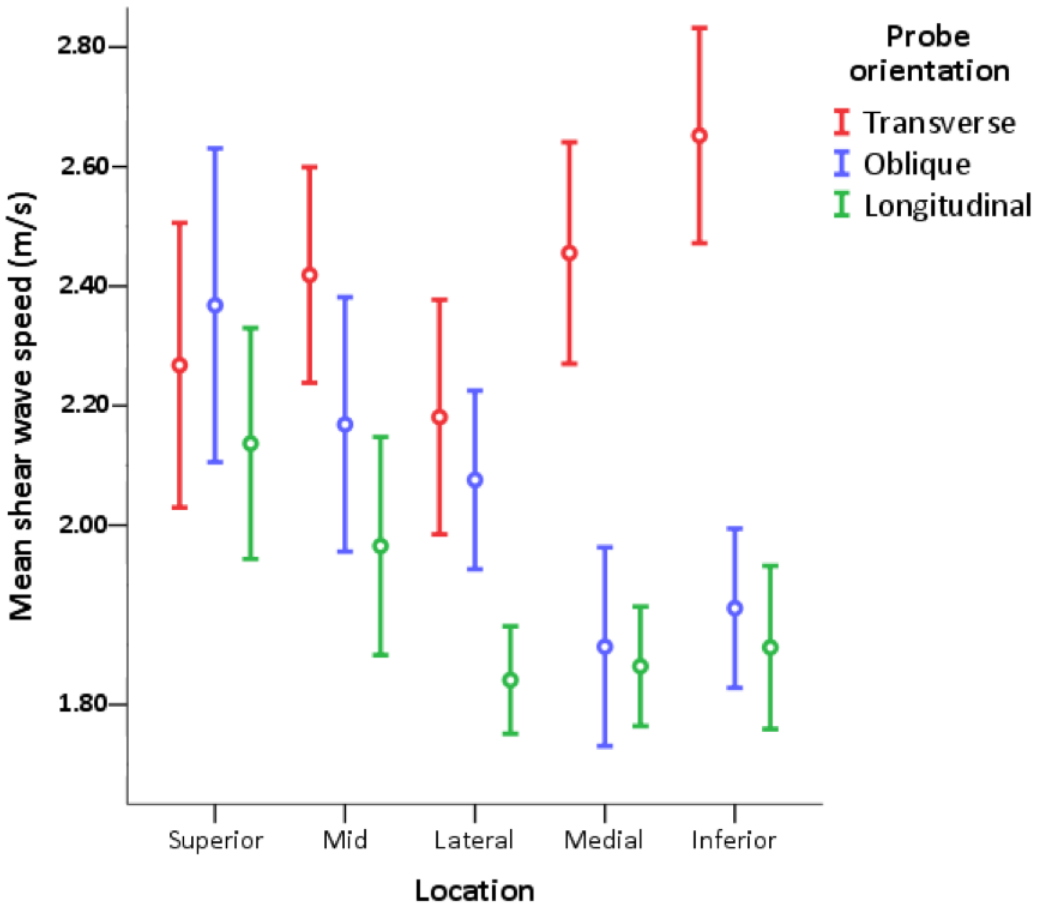

Figure 3-3 Mean (ln-transformed) mean shear wave velocity and 95% CI recorded for each method.

3.2.3.2 Reliability of LE9 measurements

Within-subjects variability (WSCV) decreased gradually from transverse to oblique to longitudinal; it was highest in transverse medial (18.0%) and lowest in longitudinal lateral (4.3%) (Figure 3-4 and Table 3-2). Transverse planes generally resulted in lower ICCs indicating 'fair' agreement, except for the superior and lateral locations (Table 3-3). There was greater reliability across all longitudinal planes. The lateral-longitudinal and inferior-longitudinal combinations resulted in the highest ICCs of 0.76 and 0.80 respectively, which represent substantial agreement. Oblique planes results showed moderate agreement in almost all locations. Overall, the trends with respect to the combinations that yielded the lowest variability were similar, whether they were assessed using the ICC values, or the WSCVs.

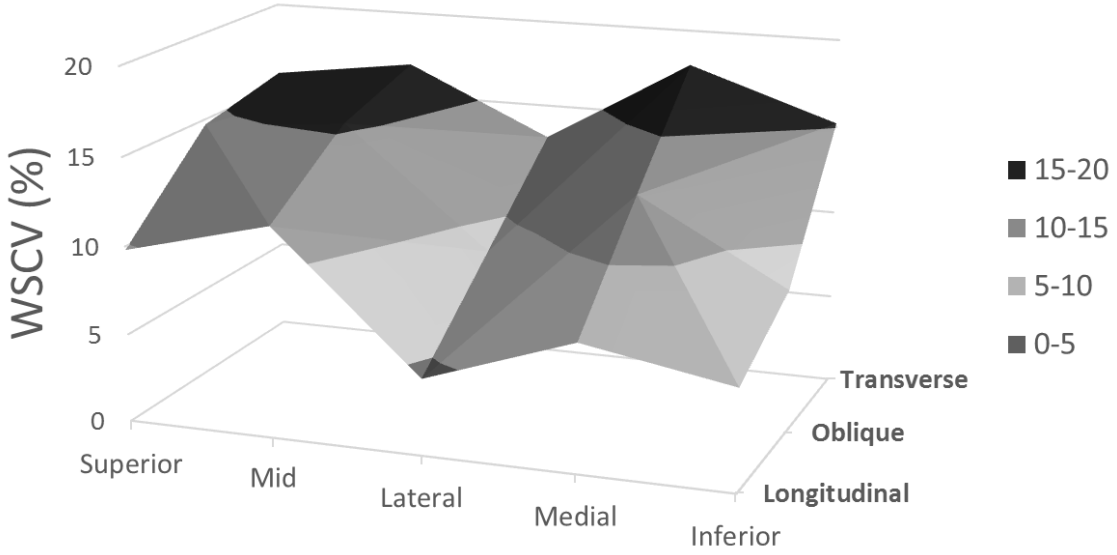

Figure 3-4 Surface plot showing within-subject coefficient of variation (WSCV) for each method.

The longitudinal-lateral combination achieved the lowest variability (4.3%).

3.2.3.3 System comparison

SWE on AIX produced almost perfect intra-system reliability (>.80) in all combinations except lateral-oblique, in comparison to the moderate to substantial internal consistency found for LE9 (Table 3-3). Similar to LE9, the lateral-longitudinal combination produced the most internally consistent SWE readings.

Comparing the two systems, transverse planes and mid locations were associated with poor to fair inter-system ICCs. The longitudinal lateral combination achieved the strongest agreement of ICC (95% CI) = .71 (.48, 1). Figure 3-5 shows that both systems recorded high mean readings in the transverse plane, but with wide CIs. In longitudinal, both recorded lower and more stable readings. As for mean differences, the best results were obtained in the medial and lateral locations in oblique or longitudinal planes; mean differences ranged from -0.03 to 0.08 indicating little bias between the systems for these combinations. However, the 95% LOA and the confidence intervals around them were comparatively wide, ranging from ±0.38 (0.23, 0.53) to ±0.54 (0.34, 0.74), given that mean SWV was approximately 1.80 m/s. Bias was greatest using the transverse plane in the medial and mid locations; SWV from

LE9 exceeded AIX by 0.19 and 0.18 m/s respectively, and the limits of agreement were twice as wide as for lateral-longitudinal. Bland-Altman plots for examples of the best (lateral-longitudinal) and worst (mid-transverse) combinations are presented in Figure 3-6. The scatterplot in Figure 3-7 suggests that although no trend was visible for individual location-orientation combinations, when considered together, disagreement seemed to increase in measurements at higher SWVs. However, this could be because most of the higher SWVs were recorded in the transverse plane.

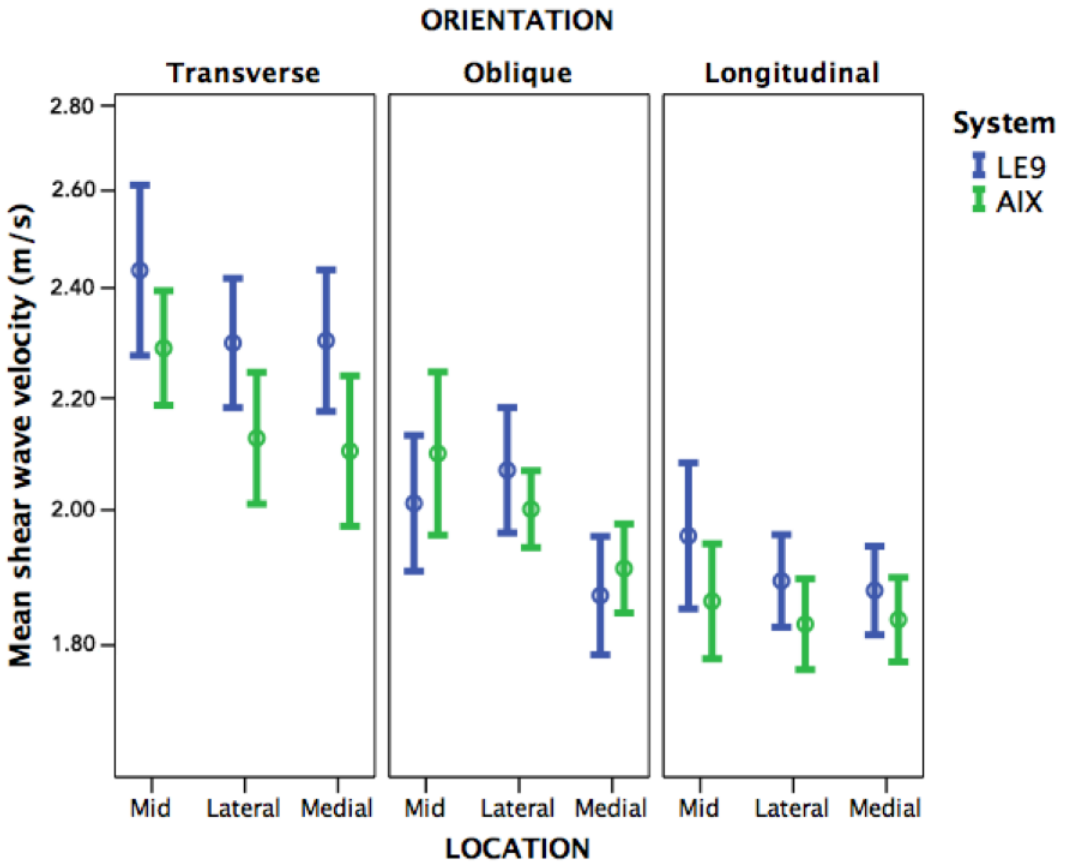

Figure 3-5 Error bars representing mean (ln-transformed) shear wave velocity and 95% CI between the two systems for each method.

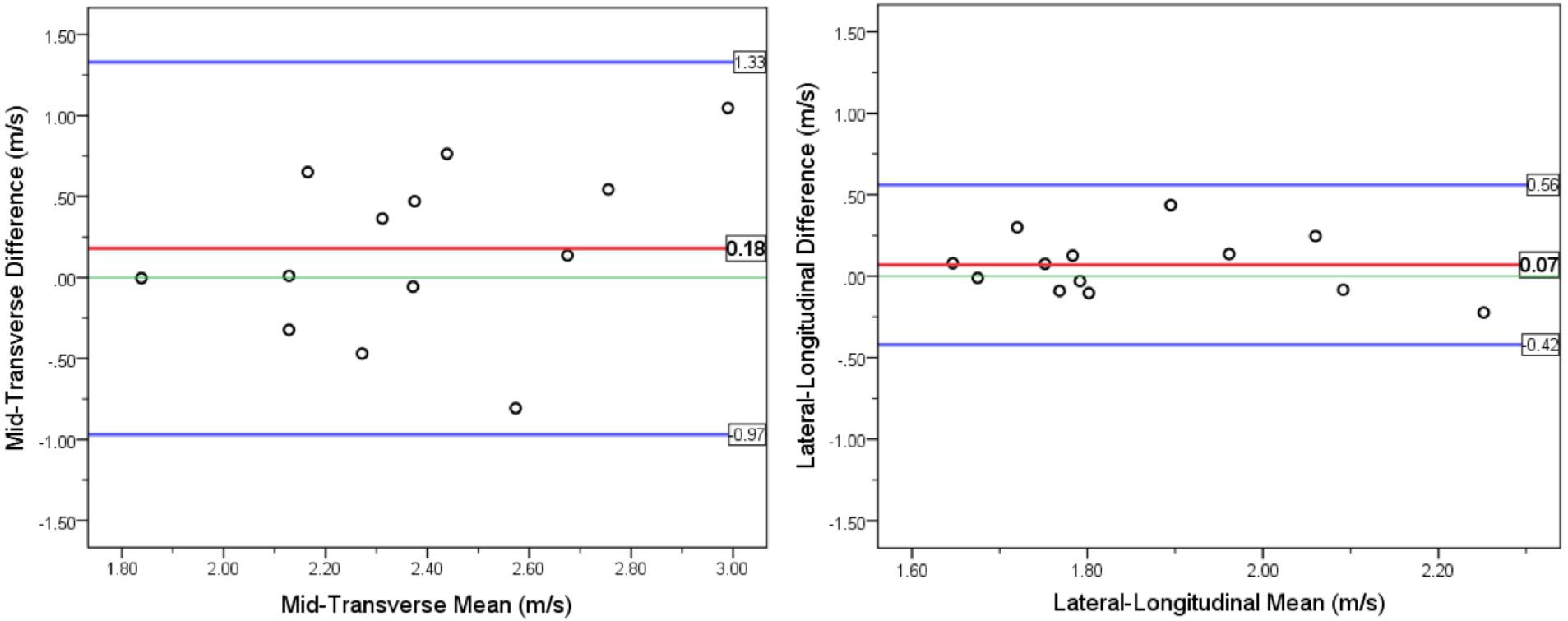

Figure 3-6 Two Bland-Altman plots of LE9 and AIX for the best (right: lateral longitudinal) and worst agreement (left: mid transverse).

The middle green line is the zero-difference line, the red line is the mean difference between the two systems and the two blue lines represent the upper and lower 95% limits of agreement.

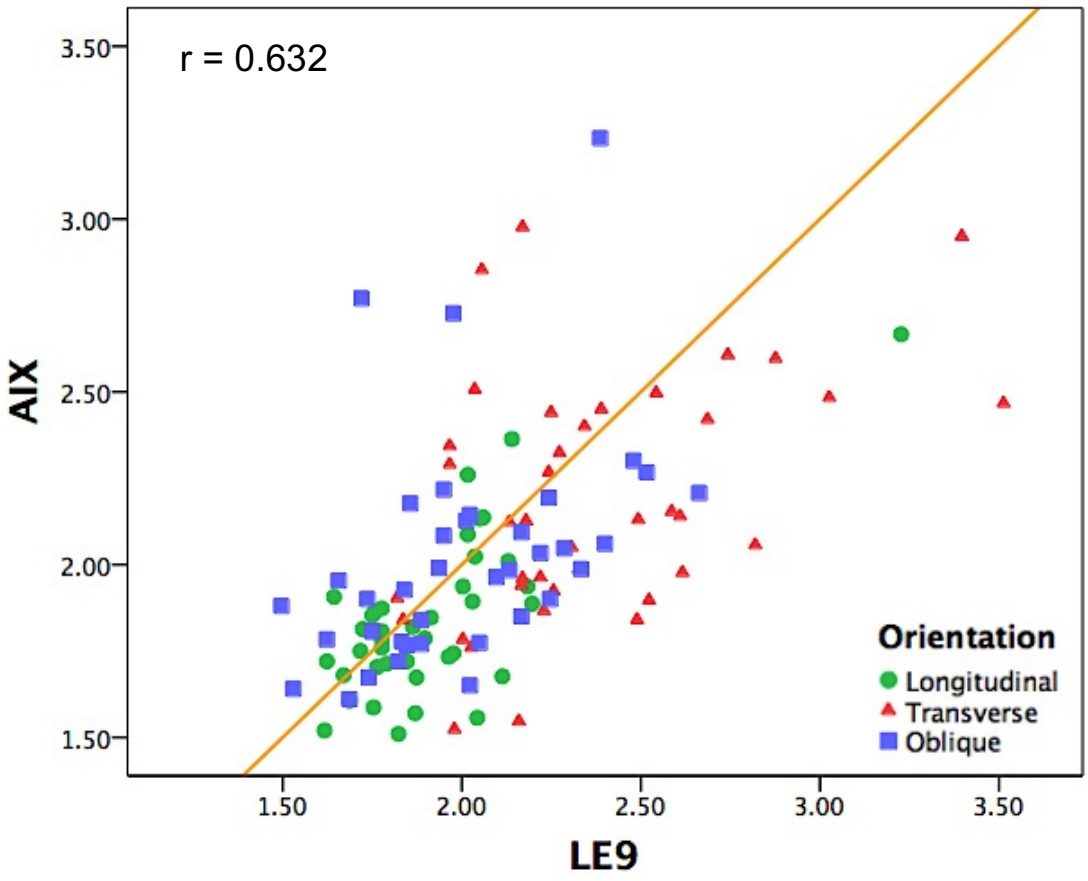

Figure 3-7 Scatterplot of the association between the two systems.

The orange line represents the ideal agreement (y=1*x).

3.2.4 Discussion

SWE is a promising modality that has demonstrated its value in several medical specialities. Currently, relatively little data exists on muscle and specifically how different acquisition methods and machines affect elasticity readings.

The first aim of this study was to evaluate the influence of utilising various ROI sizes, probe orientations and location within the muscle. With respect to the ROI size, results were similar to Ates et al. [250], in that a smaller ROI is associated with less reliable readings. Kot et al. [204] found no significant difference in the mean elasticity values between small, medium and large ROI sizes; however, this inferential approach would not detect differences in variability between the different sizes. The results demonstrate that utilising a small ROI produced greater variability, and hence a lower ICC than medium or large ROI. This finding should be interpreted cautiously because the ROI size might be tailored for the specific purpose of the examination. For example, large ROI for diseases affecting a large muscle area and small ROI for small

focal lesions. This finding may accord some superiority to SWE systems that allow free ROI size selection.

The results suggest that the best probe orientation to use when scanning muscles is the longitudinal (parallel to muscle fibres) (Figure 3-1.b2). When referencing the probe orientation in anisotropic structures, one must refer to the orientation of the fibres and not to the direction of the muscle or body part. This is particularly important in muscles with fibres running obliquely to the long axis of the muscle like the rectus femoris (Figure 3-1.a). Therefore, studies that merely report the probe being oriented ‘longitudinally’ might have been orientated with an oblique plane relative to the muscle fibres [212, 235].

As for mean SWV, the findings in Figure 3-3 and Figure 3-5 are discordant to Gennisson et al. [138] and Cortez et al. [212] whom both found slower velocities in the transverse plane. The disagreement could be related to the different muscle groups investigated. In a relaxed unloaded muscle, the shear wave velocity is slower in longitudinal than transverse, but as the muscle is loaded, velocity in the longitudinal plane increases and exceeds transverse [88]. Nevertheless, the results are in agreement with what Carpenter et al. reported in the rectus femoris muscle [258]. Figure 3-5 demonstrated that both systems were affected by anisotropy in the transverse and oblique planes to the same extent, as SWV increased and became less stable. When qualitatively assessing SWE boxes, longitudinal planes were associated with a homogenous low SWE stiffness map (Figure 3-1.c2). In comparison, the high stiffness and heterogeneous SWE maps observed in the transverse planes (Figure 3-1.c1) may be induced by the poor propagation of shear waves in an anisotropic structure. Oblique plane maps (Figure 3-1.c3) produced a lower level of heterogeneity than transverse plane maps, but it was not as uniform as longitudinal plane maps. This finding was observed on both systems.

With regard to the probe location within the muscle, lateral and medial regions showed the least variable readings. This shows the importance of standardising the site of acquisition within muscles. A previous study has also found differences but the locations selected did not include aponeurotic structures [212]. Based on the evidently increased variability at the superior mid and inferior sites, the avoidance of locations where tendon, myotendinous and myoaponeurotic structures are present is advised. Because ICCs can vary

between homogeneous and heterogeneous populations, even if the within-patient variability remains the same, some authors advocate the reporting of WSCVs instead. Both quantities were provided and found the trends with respect to the location-plane combinations yielding the least variable results to be similar.

The second aim evaluated the reliability of the LE9 in-vivo. So far, this is the first study to test this system's reliability and compare its performance on musculoskeletal imaging. Here, the LE9 reliability on the rectus femoris muscle in a relaxed resting position was assessed. The effect of location and orientation was apparent on the agreement analysis, similar to that found by Cortez et al. [212]. The poor agreement observed in transverse planes might result from the anisotropic nature of muscles that might have disturbed shear wave propagation. On the other hand, scanning parallel to muscle fibres discerned the highest agreement. These results show that LE9 can reproduce longitudinal plane acquisitions better than transverse and oblique planes in all locations. The best reliability was achieved in the lateral location and longitudinal probe angle.

The final aim was to compare the LE9 SWE performance to an established shear wave unit (AIX) that could be considered an industry gold standard. No previous studies have tested the inter-machine reproducibility between different SWE systems in muscle. Each system utilises its patent-protected technology that is fundamentally different regarding shear wave generation and tracking. The comb-push excitation method on LE9 sends multiple smaller laterally-separated push pulses simultaneously. This method may produce shear waves lower in amplitude when compared to the focused Mach cone push method on AIX. This difference may suggest that AIX performs better on focal depths deeper than 2.5 cm because of the superior focusing technique and higher shear wave amplitude.

AIX achieved almost perfect consistency ranging from .81–.97, which is relatively similar to .83 reported by Lacourpaille et al. [202]. Furthermore, testing AIX on different muscles, others found higher ICCs of .98 and 1 [239, 250]. These better results could have been enhanced by not removing and reapplying the probe between acquisitions. When compared with the AIX, LE9 performed comparably in some location/plane combinations. The transverse

plane had a greater effect on intra-system ICCs for LE9 than AIX, resulting in comparatively poor inter-system ICCs. The lower amplitude, less focused comb-push method on LE9 might have been challenged in this anisotropic orientation, as explained by the decreased intra-system reliability on the transverse plane. Only one study was found that compared LE9 and AIX performances. It was done on a phantom experiment as well as single samples of breast and liver in-vivo cases [438]. Similarly, it reported good agreement with an advantage to AIX. In this study, the most feasible and reliable combination (longitudinal-lateral) resulted in a substantial agreement between the two systems according to ICC measures.

Bland-Altman plots reported in Figure 3-4 demonstrate the importance of selecting optimum acquisition techniques to acquire reproducible SWE estimations between different systems. Despite the high ICC obtained, the 95% LOAs were wide even for the best-performing longitudinal-lateral combination (±0.49 m/s), which indicates a potential for discordance between measurements by approximately 26%. A larger study (around n=100) focusing on this single location-orientation combination would be required to obtain more accurate estimates of these limits. This should warrant future studies on muscle SWE wishing to compare results between different systems.

3.3 Study 2. Effect of unit, depth and probe load on reliability

3.3.1 Aims

The aim of this study was to test the effect of using different reporting units, acquisition depth and probe load on the reliability of SWE in healthy skeletal muscle. A secondary aim was to test if leg dominance had an impact on muscle elasticity.

3.3.2 Materials and methods

3.3.2.1 Participants

Twenty healthy participants (12 males) from various ethnicities, volunteered for this cross-sectional study. The mean ± SD age and BMI were 36 ± 11.8 and 23 ± 3.1 respectively. Similar to study 1, all participants were asymptomatic with no history of musculoskeletal disorders. None of the participants was considered athletic or engaged in competitive exercise programs. Participants were instructed to avoid any strenuous activities 24 hours before the test to minimise confounding factors. The study was conducted under the same ethical approval of the last study. Written informed consent was obtained from all participants.

3.3.2.2 Shear wave elastography reliability

The SWE software package on the General Electric LOGIQ-E9 system (GE Healthcare, Buckinghamshire, UK) employing a linear 9-5 MHz probe was utilised for this study. A circular ROI with an area of 75mm^2, equivalent to 1cm in diameter, was chosen for all SWE acquisitions except for the small abductor digiti minimi muscle, for which a smaller ROI was used to cover a 1 cm × 1.2 cm shear wave elastography box. Based on the findings of study 1, all acquisitions were performed with the probe oriented longitudinally to muscle fibres. The probe was placed approximately at midportion between proximal and distal myotendinous junctions of each muscle. Measurements were obtained from the muscle belly away from any myoaponeurotic or myotendinous structures. Three consecutive measurements were recorded for each muscle and acquisition method.

3.3.2.2.1 Muscles and positioning

Four muscles were investigated in a resting state: vastus lateralis, biceps femoris, biceps brachii and abductor digiti mini. Selecting them was based on choosing muscles from various depths, architectures and sizes. All participants were asked to relax their muscles before the examination for five minutes. For vastus lateralis, participants laid supine with knees fully extended and feet slightly everted. For biceps brachii, participants remained in the same previous position and were then asked to bend their elbow (90°), relax their shoulder and rest the supinated forearm on their torso. Next, for abductor digiti minimi, the dominant hand was pronated and rested on a cushion with the fifth finger being maintained in a slight abduction by the operator's hand. Lastly, for biceps femoris (long head), participants laid prone, bent knees (90°) and rested legs against a wall. These positions allowed the investigation of the muscles in a resting state, ensuring no passive stretching or active contraction could affect the readings. The same order was followed when acquiring SWE images.

3.3.2.2.2 Units

After each acquisition, the mean reading of the ROI was displayed and recorded in SWV (m/s) and Young's modulus (kPa). The latter is derived from SWV using equation 2-6 explained in the previous chapter. The system's software calculates the sum of the value of each pixel in m/s squared and multiplies it by 3. Two decimal places were reported by the machine and used in the analyses for each unit. Depth, probe load and leg dominance analyses were performed using SWV.

3.3.2.2.3 Depth

For vastus lateralis only, three SWE acquisitions were recorded, each containing three ROIs (superficial/moderate/deep) positioned serially along the axial beam axis (Figure 3-8). Depth from the skin to the centre of each ROI sample was recorded. The superficial and deep ROIs were placed away from the muscle edges (epimysium) to avoid the potential effect on elasticity. All ROIs had the same area of 75mm^2. Readings were repeated three times to test for reliability.

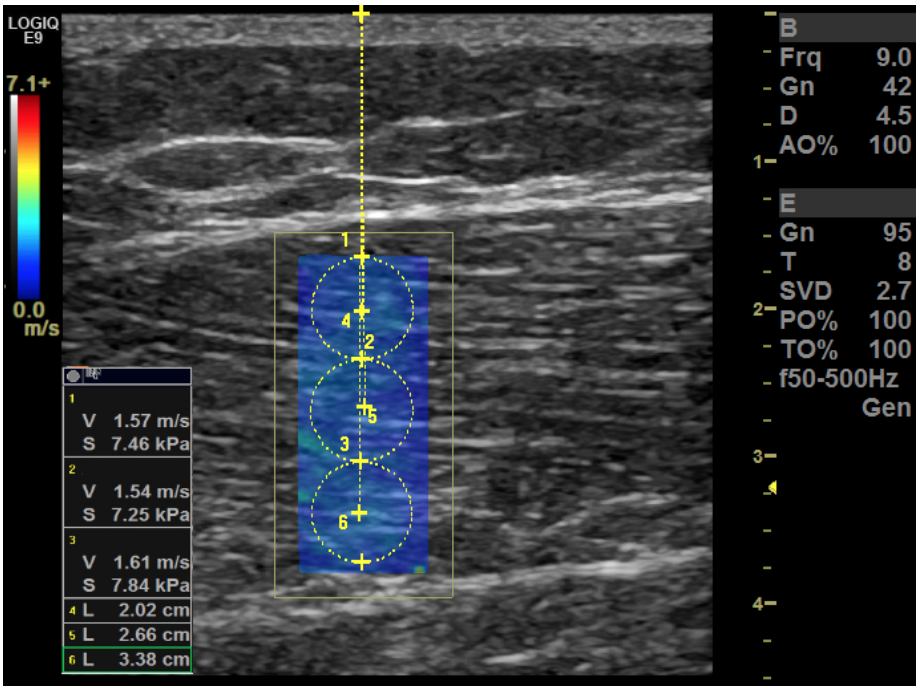

Figure 3-8 SWE of the vastus lateralis muscle demonstrating ROI placement at three different depths.

3.3.2.2.4 Probe load

For vastus lateralis only, readings were acquired using two probe load techniques. Firstly, with the probe in light direct contact with the skin without flattening or deforming the superficial epimysium layer. Secondly, without contacting the skin using a copious amount of 'standoff gel' clearly visible on top of the images. These two acquisition methods were chosen as they might be the easiest to reproduce in clinical situations. They are also the most reasonable to be tested in terms of applying the lightest pressure on the skin. Three measurements were acquired successively for each technique.

3.3.2.2.5 Leg dominance

Patients were asked about their leg dominance at the beginning of each exam. When unsure, they were asked, "Which leg would you kick a ball with?" [439]. The same acquisition methods and location were applied when scanning the non-dominant side. This investigation was performed on the vastus lateralis only.

3.3.2.3 Statistical analysis

Repeated measures ANOVA with post-hoc Bonferroni-corrected pairwise comparisons were used to compare mean SWV between muscles; terms were

included for muscle (4 levels) and repeated measurement (3 levels). The same test was used to compare the vastus lateralis elasticity between dominant and non-dominant leg as well as between using normal probe load and standoff gel. A two-sided p-value of less than 0.05 was considered significant. Reliability was quantified using one-way random (average measure) ICC of the three repeated measures for each muscle and acquisition method. The reliability coefficients were interpreted using the same definition of study 1.

Bland-Altman mean bias and 95% limits of agreement were used to evaluate probe load with and without a standoff gel. WSCV was calculated as a measure of variability by calculating within-subject standard deviation then dividing it by the mean [435]. To investigate whether the depth of assessment affected reliability, a multilevel model was constructed that included random terms for participants (level 3), relative depth of assessment (superficial/moderate/deep; level 2) and repeated measurement (level 1). Measured depth of assessment (cm) was included as an explanatory variable. Log-likelihood values from models with and without an additional term that modelled the variability of level 1 SWE measurements as a function of measured depth of assessment were compared. SPSS version 24 (IBM Corp., Armonk, N.Y., USA) and MLWin 3.00 (Centre for Multilevel Modelling, University of Bristol) [440] were utilised to perform statistical analysis.

3.3.3 Results

Pairwise comparisons revealed that SWV differed between all muscles (p<0.001) with the exception of vastus lateralis and biceps brachii, where the mean SWVs were both 1.76 m/s (p=1.00). The largest difference was between the abductor digiti minimi and biceps femoris [mean difference (95% CI) 1.01 (0.92, 1.10)]. Table 3-4 lists the means for each muscle in addition to variability and reliability results using the two reporting units. Using SWV (m/s), reliability coefficients were almost perfect (ICC >0.80) across all muscles. Although within-subject variability, demonstrated as WSCV, was lowest for the abductor digiti minimi, Figure 3-9 shows relatively large between-subject variability (wide 95% CI) amongst the readings. The difference in reliability between the units was only noticeable for the vastus lateralis muscle with and without standoff gel. Otherwise, ICC coefficients between the units were identical. Association between them for the four muscles is plotted in Figure 3-10.

As for depth, Figure 3-11 illustrates that mean SWV was not affected by depth [SWV per cm (standard error)=0.013 (0.029); likelihood ratio test X^2=0.65, *p*=0.42]. However, there was strong evidence that at greater depths of assessment the repeated SWV measurements were more variable (likelihood ratio test X^2=41.4, *p*<0.001) (Figure 3-12). Approximately 95% of measurements are expected to lie between -2 and +2 SD around the mean; estimated variance (SD^2) of 0.07 at 4 cm depth equated to an interval of ±0.53 m/s, whilst at 6 cm (variance=0.17) this increased to ±0.82 m/s.

Mean SWV (m/s) was not significantly different when using a standoff gel in comparison to normal probe load [mean difference (95% CI) 0.03 (-0.03, 0.09), *p*=0.32]. Reliability decreased from almost perfect agreement (ICC=0.83) to the lower margin of substantial agreement (ICC=0.62) for normal probe load and standoff gel respectively. WSCV doubled when using a standoff gel, increasing from 4.4% to 9.0%. Using the latter technique, mean SWV decreased by 0.03 m/s expressing negligible average bias (Figure 3-13); the 95% limits of agreement were ±0.25 (95% CI 0.15, 0.35).

No significant mean SWV difference was found between the dominant and non-dominant vastus lateralis [-0.04 (-0.09, 0.01), *p*=0.08]. ICC (95% CI) for the non-dominant vastus lateralis was 0.80 (0.59, 0.91), which is similar to ICC for the dominant side reported in Table 3-4.

Table 3-4 Mean, variability and reliability of the different muscles for the two SWE units.

Muscle	Shear wave velocity (m/s)			Young's modulus (kPa)		
	Mean (95% CI)	WSCV	ICC (95% CI)	Mean (95% CI)	WSCV	ICC (95% CI)
Vastus lateralis	1.76 (1.71, 1.81)	4.4%	.83 (.65, 93)	9.61 (9.02, 10. 20)	11.0%	.77 (.52, .90)
Vastus lateralis (standoff gel)	1.73 (1.66, 1.80)	9.0%	.62 (.20, .84)	9.56 (8.75, 10.37)	20.0%	.56 (.08, .82)
Biceps brachii	1.76 (1.71, 1.81)	3.1%	.91 (.82, .96)	9.40 (8.81, 9.98)	6.6%	.91 (.82, .96)
Abductor digiti minimi	2.55 (2.46, 2.65)	2.1%	.97 (.94, .99)	19.90 (18.37, 21.43)	4.6%	.97 (.94, .99)
Biceps femoris	1.54 (1.48, 1.60)	4.6%	.90 (.79, .96)	7.59 (6.99, 8.19)	9.0%	.90 (.79, .96)

WSCV= within-subject coefficient of variation.
ICC= Intraclass correlation coefficient.

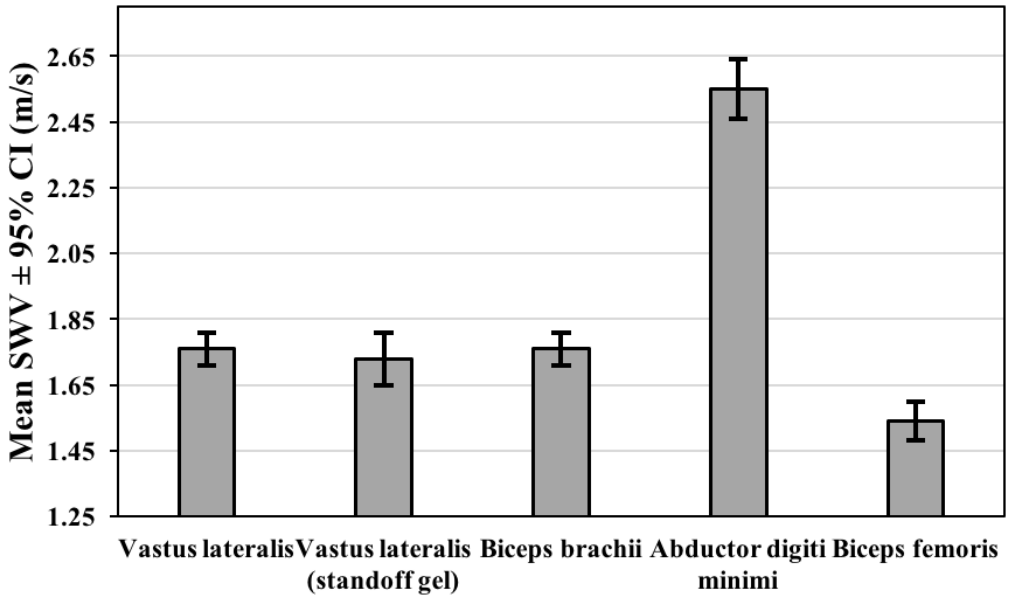

Figure 3-9 Bar chart demonstrating mean SWV for the different muscles.

The standoff gel acquisition method is also included showing larger between-participants variability (wider 95% CI) in comparison to the normal acquisition.

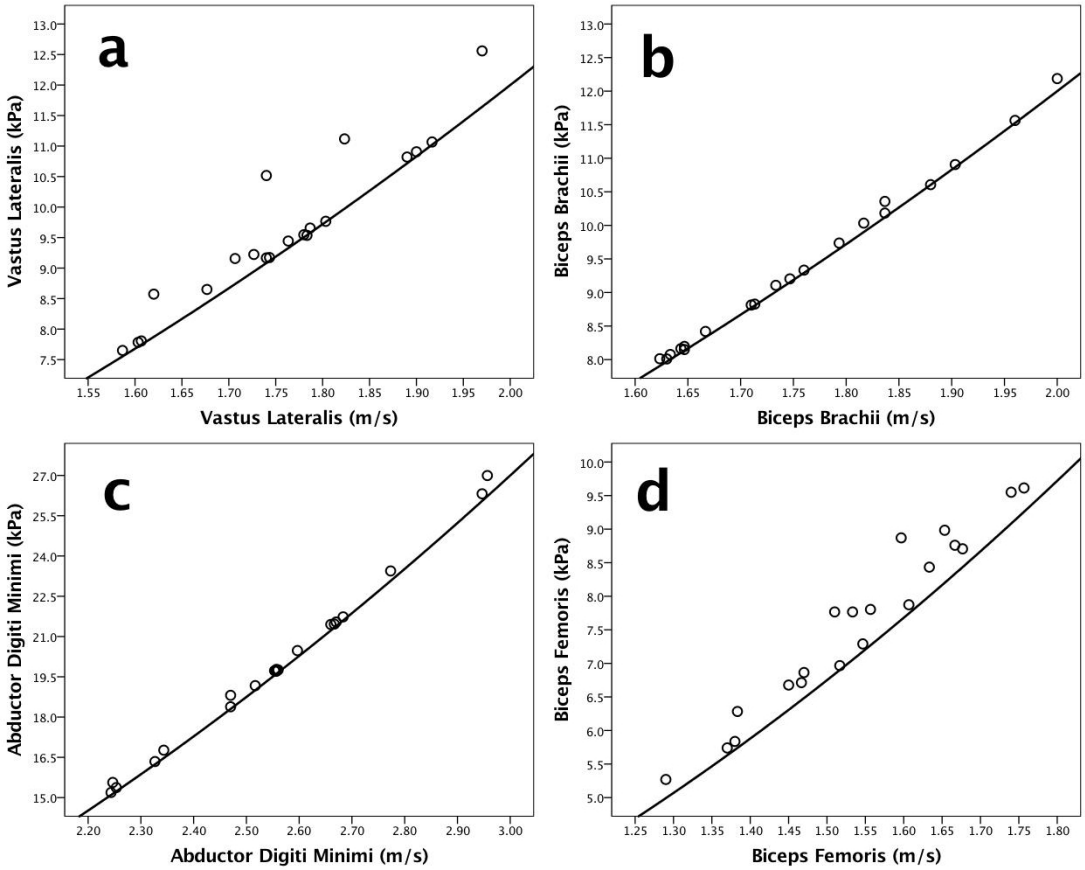

Figure 3-10 Association between kPa and m/s units.

In each case, the plotted line represents the direct transformation $kPa=3(SWV)^2$. The degree of association was lower in vastus lateralis and biceps femoris where, on multiple occurrences, kPa overestimated m/s.

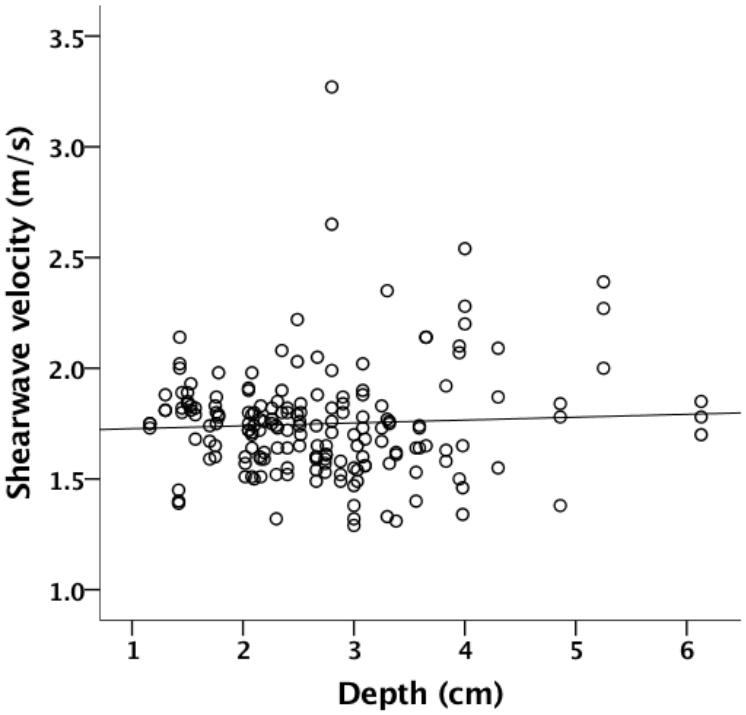

Figure 3-11 Scatterplot showing no substantial influence of depth on mean SWV.

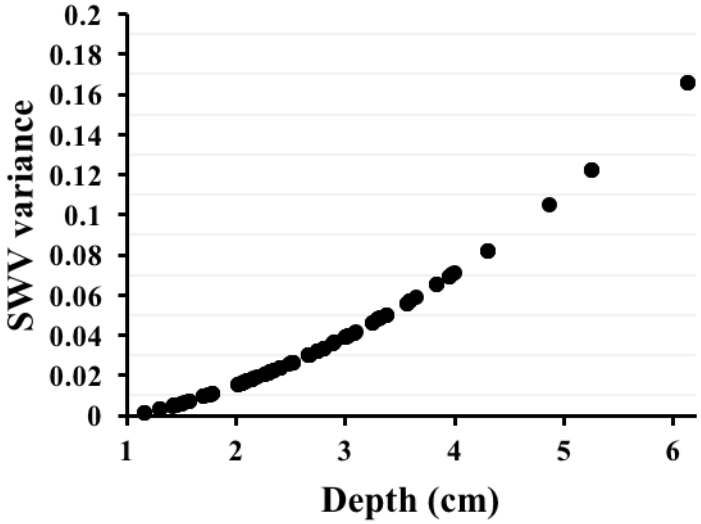

Figure 3-12 Estimated variance of SWV measurements as a function of measurement depth.

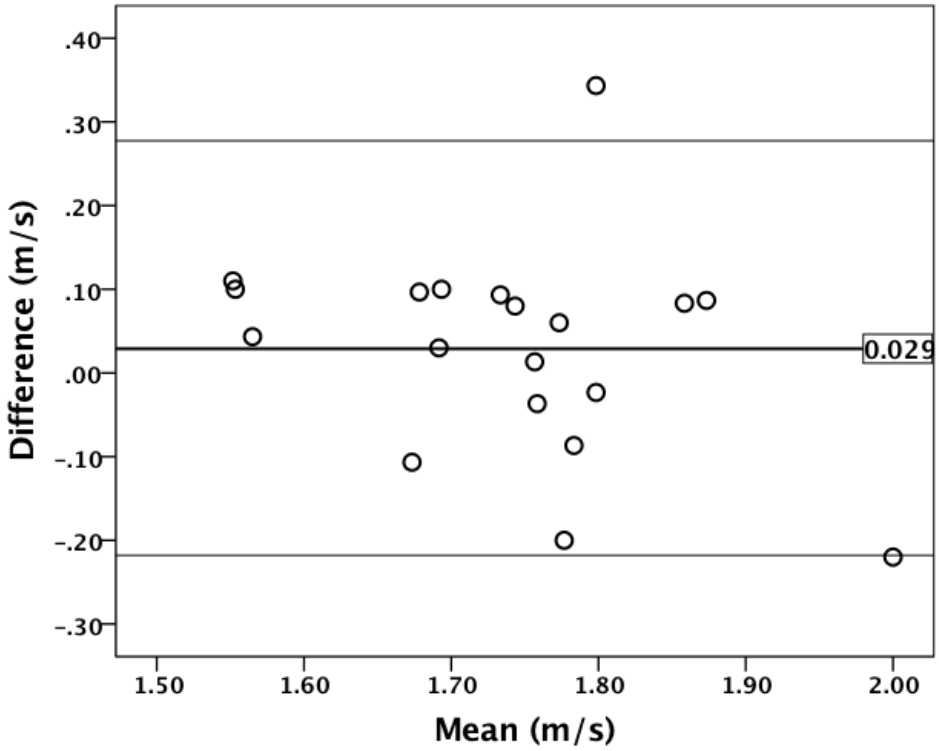

Figure 3-13 Bland-Altman plot demonstrating the difference against the mean between the measurements with and without standoff gel.

The central line is the mean SWV difference between the two methods displaying small, negligible bias (0.03 m/s). The two lines represent the upper and lower 95% limits of agreement at -0.22 m/s and 0.28 m/s. The width of the limits indicates that readings could vary by 14% between the two methods.

3.3.4 Discussion

This second reliability study set out to evaluate factors which may be important in the standardisation of muscle SWE assessment. No previous studies have tested the same variables using the same technical and statistical methodology. There is also limited knowledge on the performance of newly introduced shear wave systems, such as the one utilised in this study (LOGIQ-E9). The majority of previous SWE studies were designed to test diagnostic performance for various pathologies without specifically focussing on possible variations induced by acquisition methods. The results confirmed that the type of unit of measurement, depth of measurement and overlying pressure from the probe might all influence the final SWE reading.

The first part confirmed that SWE readings differed between the muscles. For example, there was a significant difference in mean SWV between the

quadriceps (vastus lateralis) and hamstring (biceps femoris) muscle. Dubios et al. [206] reported stiffness readings of 13.5 kPa and 16.8 kPa for vastus lateralis and biceps femoris respectively. The mean elasticity readings for vastus lateralis and biceps femoris were lower (9.61 kPa and 7.59 kPa respectively) and were in agreement with what Lacourpaille et al. reported [202]. The latter study found a significantly higher stiffness in the abductor digiti minimi (13.5 kPa) although lower than this study reported mean elasticity (19.9 kPa). As these studies by Dubois et al. [206] and Lacourpaille et al. [202] utilised the same SWE system (SuperSonic Imagine, Aix-en-Provence, France), the discrepancy may be due to factors related to acquisition methods. Ewerson et al. [247] investigated the biceps brachii muscle and reported an SWV that is almost the same as the presented reading (1.76 m/s versus 1.77 m/s). Therefore, it should be expected that variations in agreement occur between studies depending on machines and acquisition methods.

The reliability of SWE, as presented by the ICC coefficients in Table 3-4, indicate the LOGIQ E9 can acquire repeated measurements with similar reliability to what others have reported on similar healthy skeletal muscles but different systems [212, 239, 441, 442]. The ICC for the average of several measures were reported instead of single measures considering that the average of at least three acquisitions is necessary to provide reliable readings in clinical practice [62].

Reliability appeared to be higher for the superficial muscles in comparison to the deeper muscles. Although the abductor digiti minimi muscle resulted in the highest ICC and lowest WSCV, the 95% CI in Figure 3-9 were wide indicating large mean SWV variability between the participants. The reason for this feature is unclear and could be related to anatomical factors like muscle size or technical factors like muscle relaxation upon positioning.

Several elastography systems offer the option to report SWE readings in SWV (m/s) and Young's modulus (kPa). The original measurement the machine records is SWV; it mathematically converts it to Young's modulus for each pixel then reports the average of all pixels in kPa. This conversion method produces two problems. Firstly, in consecutive acquisitions, the readings may have the same mean SWV but different standard deviations due to heterogeneity in the ROI pixels. In such instances, the acquisition with the higher standard deviation

will have an artificially larger Young's modulus. This will cause variability in kPa but not in m/s rendering it less reliable. This is evidenced when looking at the ICC in Table 3-4 for vastus lateralis. The remarkably greater WSCV in kPa is expected due to the larger range of the results. Moreover, kPa will overestimate elasticity in heterogenous acquisitions (high standard deviation) due to the effect of squaring in the equation. The difference in reliability between the two units was only noticeable in the vastus lateralis muscle due to the several occurrences of repeated measurements of similar SWV from heterogeneous acquisition samples having different standard deviations. This discrepancy problem and variation in reliability between the units is expected to be larger in pathologies as shear wave maps tend to be even more heterogeneous. Figure 3-10 illustrates that the two units are not theoretically synonymous as they did not fit the line in all observations.

The second problem is when kPa value is manually calculated from mean m/s the square root of the sum will be calculated instead of the sum of the square root of each pixel, generating an error. There will be no error if the acquired shear wave map is completely homogenous with all pixels presenting the same value in m/s. The error will become greater if the shear wave map is heterogeneous. This conversion error is common in the SWE literature when researchers compare their results to others.

There are additional inaccuracies associated with converting the velocity readings to Young's modulus. The variation in soft tissues densities is neglected, as Young's modulus assumes density is constant and equals 1 g/cm^3. This is inaccurate, as the density differs and is higher for muscles (1.06 g/cm^3) than fat (0.90 g/cm^3) for example [443, 444]. Young's modulus assumes that tissues are isotropic and homogeneous; both assumptions are violated when investigating muscles.

Only one previous study by Youk et al. [445] has compared SWE units. They tested the diagnostic performance of the two units on 130 breast masses. Although the diagnostic performance indices were not identical, there was no significant difference between mean m/s and kPa. Nevertheless, they reported a significant difference in specificity and area under the curve when using the standard deviation of the entire lesion as a diagnostic method. This current study is the first to compare the reliability between the two units. Using SWV as

a surrogate for tissue elasticity is recommended instead of Young's modulus. This will help both with study result reliability and allow more accurate comparison between studies.

Investigating depth is of particular importance, as reliability may diminish at greater depths due to the attenuation of the acoustic push pulses and tracking waves. In this study, mean SWV did not appear to be influenced by depth, in disagreement with previous studies which reported conflicting results between each other. Ewerson et al. [247] found SWV decreasing marginally with depth (R^2=.019; *p*-value not reported). In contrast, Carpenter et al. [258] reported substantive increase with depth (r=.54, p<0.001) for the rectus femoris and negligible increase (r=.17 p=.057) for the gastrocnemius. Both studies had a small sample size of ten and five participants respectively. None reported on the reliability of SWV at the different depths. Carpenter et al. [258] attempted to study the effect of depth by testing for difference between two random depths, named 'superficial' and 'deep'. They reported a significant difference between them. Their approach provides limited evidence on the effect of depth on the acquisitions integrity. No previous studies have analysed the effect of depth as a continuous variable on muscle SWE in the same methodology.

Variability of the readings increases quadratically at greater depths as illustrated in Figure 3-12 and equation 2. Therefore, acquiring readings deeper than 4 cm is not recommended as the variability increases substantially reaching variance=0.17 at 6 cm, equating to 95% of readings lying within ±0.82 m/s. This is a wide interval given the mean SWV was 1.76 m/s. Currently, there is no known cut-off point for acceptable variability in SWE. However, considering depth feasibility, the variance of 0.07 at 4 cm depth, equating to ±0.53 m/s, might be considered an acceptable variability. Likewise, recent guidelines on thyroid SWE recommend that acquisitions should not exceed depths of 4–5 cm [8]. The strength of the acoustic radiation force impulse (push pulse) diminishes at higher depths (>5.5 cm) rendering the generated shear waves too weak to be tracked accurately [446]. This point does not apply to other transducers with lower frequencies. The SWE mode on the utilised machine is only available on the linear 9–5 MHz probe. Further research on higher BMI participant groups is necessary to validate the findings. Depth

investigation results from phantoms may not be generalised to muscles because of anisotropy that may influence waves propagation in muscles [441].

Although SWE removes much of the operator dependency in comparison to strain elastography, probe load is one of the remaining operator-dependent factors. Carpenter et al. [258] investigated the effect of probe load on muscle tissues over five healthy participants by testing normal probe contact versus slight axial stress. The same investigation was performed previously by Kot et al. [204], and both found a significant difference between the techniques but did not conduct any reliability analysis. Again, the lone testing of difference is less informative and does not provide a useful evidence on the most suitable method to recommend. Others investigated the effect of hard probe compression, which may be considered unreasonable and will most likely result in false, inconsistent readings due to impracticality and the high degree of stress which will certainly affect stiffness [64, 447].

This study sought to investigate the reliability of probe load using two reasonable, practical and easy to replicate techniques. The results support placing the probe in direct contact with the skin without any compressional force or standoff gel. The microbubbles in the gel layer may have possibly decreased the quality of the push pulse resulting in larger variance and lower reliability. The finding for standoff gel should not be generalised to other organs such as breast where most lesions are superficial, as it could be useful and reliability may be higher. Despite no significant differences between the mean SWV for the two methods, the 95% CI of the limits of agreement indicates that reading variability ranges between 8.5% – 20%. It suggests that results may not be accurately compared between studies utilising different probe load acquisition techniques.

Leg dominance can relate to muscular development and potential bilateral variation. After reviewing the muscle SWE literature in chapter 2, most research studies perform SWE on a single side because of the time limitations. This study is the first to investigate the potential difference between sides. The results show that the similarity assumption between the dominant and non-dominant side is valid for the vastus lateralis muscle. This finding may not be directly generalisable to pathological cases because unilateral disease development is possible. Nevertheless, this finding is helpful to researchers in

verifying that halving scanning time by scanning one side can be acceptable in healthy participants.

3.4 Limitations

Both studies are original from several perspectives and discuss important considerations in SWE research and clinical applications. However, they have several limitations. First, only one sonographer performed all the acquisitions; consequently, inter-operator reproducibility was not tested due to the unavailability of a second operator. Second, only forty participants (twenty per study) were recruited rendering the sample size relatively small; to compensate for this, the acquisition protocol collected a large number of acquisitions. Regarding the first study, the longitudinal probe orientation on the superior, mid and inferior locations was problematic because of the unique rectus femoris pennation anatomy, which might have resulted in a slight deviation towards medial or lateral muscle bellies. As for the second study, probe load, depth and dominance were only tested on vastus lateralis because of time limitations.

3.5 Conclusions

This chapter demonstrates the technical validity of muscle SWE and underpins its potential to investigate myopathies reliably. The results revealed that using different ROI sizes, locations, probe orientations, measurement units, depth and probe loads can individually and collectively produce variable SWE estimations. SWE systems demonstrated strongest internal agreement when the probe was in a longitudinal plane relative to the muscle fibres in a predefined area that does not contain myotendinous or myoaponeurotic structures.

SWE units (m/s and kPa) are not synonymous. Readings in kPa may be affected by tissue heterogeneity and were less reliable in comparison to m/s. In musculoskeletal applications, SWE readings should always be reported and interpreted in SWV (m/s). However, studies on other SWE applications should report the readings in m/s and kPa to allow comparison with other studies using a similar SWE system. SWV proportionally increase in variability as depth increases despite no significant change in the mean value. Placing the probe in

direct contact with the skin using minimal pressure yields more reliable readings in comparison to utilising a standoff gel between the probe and skin surface. Attention to these factors helps in acquiring reliable readings.

Internal consistency for the two SWE systems using the best acquisition method was high; however, the 95% limits of agreement were wide, and results can vary by up to 26%. Studies using different SWE systems should be compared with care, and prospective studies should use the same machine. The superior reliability of the AIX system supported its purchase to be used for the following studies in this thesis.

Chapter 4 The effect of ageing on shear wave elastography muscle stiffness in adults.

This chapter describes a cross-sectional study investigating the effect of ageing on muscle stiffness amongst young, middle-aged and elderly healthy cohorts. The results have been published as: Alfuraih, A.M., Tan, A.L., O'Connor, P., Emery, P. and Wakefield, R.J. (2019). The effect of ageing on shear wave elastography muscle stiffness in adults. Aging Clinical and Experimental Research, (in press).

4.1 Introduction

The world's population is ageing rapidly. The population size of people above 60 years old has approximately doubled to more than 900 million since 1980 and is expected to grow exceeding 2 billion by 2050 [448]. In comparison to 2017, the number of elderly (≥75 years old) is projected to triple by 2050, rising to nearly 425 million [448]. These numbers present a challenge. With ageing, muscle mass and strength decrease at a rate of 1% and 3% per year respectively [290]. This decline is associated with multiple clinical and health consequences.

Loss of mass and strength in elderly individuals is associated with a three-fold greater risk of disability and two-fold greater risk of mortality [449]. Ageing-related muscle health deterioration has been shown to be a primary factor for an increased risk of falls and loss of independence [450, 451]. Fall-related injuries, in turn, place a substantial burden on the health care system and society [452]. Furthermore, the decline in resting metabolic rate is an established consequence of age-related loss of muscle mass [453]. This is linked to further repercussions such as a decline in daily energy expenditure and reduced physical activity, which are risk factors for developing type II diabetes [454].

The literature review in chapter 2 highlighted the association between ageing and muscle stiffness. Histologically, aging is associated with changes in muscle composition including myosteatosis, myofibrosis [260, 261, 264] and changes in the muscle elastic fibres [455]. Such changes may alter the biomechanical properties resulting in changes to stiffness. The novel quantitative ultrasound-

based shear wave elastography (SWE) technology may offer new insights on how the ageing phenomenon affects muscles' biomechanical properties in a healthy population.

Previous evidence has highlighted how tendon stiffness is significantly reduced in older populations [456, 457]. However, there is currently a paucity of evidence in the SWE literature for data on how ageing may influence muscle stiffness and how it correlates with measures of function in elderly populations. Section 2.3.1.6 in chapter 2 highlighted a few muscle SWE studies that analysed the age variable as a secondary factor for changes in muscle stiffness. No research to date been dedicated to assessing muscle stiffness differences amongst various age groups while accounting for other primary variables such as sex, muscle mass, strength and physical function.

There are several, albeit not consistent, theoretical reasons why muscle stiffness change with ageing. It has been reported that an increase in collagen fibres in ageing muscle promotes an increase in muscle stiffness [458, 459]. In contrast, others suggest that the elastic fibre system in the muscle extracellular matrix starts to lose its resistance property and becomes softer with ageing [289]. Additional factors are known to occur in aged muscles like myosteatosis, variability in fibre sizes and numbers and impaired connective tissue support the second hypothesis [287, 309, 392, 460]. It is important to note that these reports were conducted in preclinical settings on rats via invasive and clinically impractical methods, calling for clinical validation using feasible methods such as SWE.

4.2 Aims

The primary aim of this chapter was to investigate to what extent muscle stiffness measured by SWE differed amongst healthy young, middle-aged and elderly cohorts. The secondary aim was to understand how muscle stiffness links to the ageing concepts of primary sarcopenia (loss of muscle mass due to ageing) and dynapenia (loss of muscle strength due to ageing) by evaluating muscle stiffness correlation with muscle strength and mass.

4.3 Methods

4.3.1 Study design

This study was conducted in a cross-sectional design by recruiting healthy participants and testing their muscle stiffness, strength, function and body composition in a single visit. Ethical approval for this study was granted by the UK research ethics committee (Ref: 17/EM/0079) and health research authority prior to commencing recruitment. All participants provided written informed consent before entering the study. Assessments were conducted at the Leeds Biomedical Research Centre based at Chapel Allerton Hospital in Leeds from May 2017 to September 2018.

4.3.1.1 Participants and age groups

To elucidate potential ageing-related muscle stiffness differences, three age groups were chosen, young (20–35 years), middle-aged (40–55 years) and elderly (above 75). In the muscle ageing literature, age classifications vary considerably. The justification for choosing the three groups and age ranges was based on several scientific and feasibility factors. From the muscle strength perspective, muscle strength peaks at ages 20–35 then plateaus or shows signs of decline at ages 40–50 then a rapid decline occurs above 65 years [461-463]. Muscle mass follows the same pattern but declines at a slower rate [292]. The nomenclature conforms with these definitions in several dictionaries.

As for the elderly group, although the threshold for sarcopenia and dynapenia is 65 years [295, 307], previous longitudinal studies reported a significant decline in muscle strength and mass above 75 years [464]. Therefore, the elderly age group was defined as participants aged above 75 years. A second factor was that the available data for recruiting elderly participants was limited to volunteers above the age of 75, as explained further in the next sub-section. Additionally, testing participants above 75 years may yield proportionally higher ratios of abnormal muscle properties than ages between 65–75 with relatively lower risks of sarcopenia and dynapenia.

Stratifying the adult population into groups allows the investigation of potential differences in new biomarkers between extreme cases (e.g. young versus elderly). Additionally, it is recommended to categorise age into multiple ordinal

variables with gaps in-between to avoid assuming significant differences when the actual difference between subjects in two contiguous cases is only half a year for example [265]. In other words, the classification of young=20–35 and middle aged=40–55 is better than young=20–40 and middle aged=40–55.

4.3.1.2 Sample size

The sample size was calculated based on the effect size from a relatively similar previous study investigating the effect of age between young (mean age of 22) and old (mean age of 69) [208]. Despite the different elastography system utilised, the derived mean muscle stiffness and standard deviations were considered acceptable to calculate an optimum sample size for this study. The G*Power statistical power analyses software was utilised to calculate the sample size based on the one-way ANOVA test [465]. At alpha=0.05, power (1-Beta)=0.90, effect size of 0.48 (detect 20% difference), the required sample size is n=60, suggesting at least 20 participants per group. The output from the software is reported in Table 4-1.

Table 4-1 Inputs and outcomes from the sample size calculation

F tests - ANOVA: Fixed effects, omnibus, one-way		
Analysis:	A priori: Compute required sample size	
Input:	Effect size f	0.4841345
	α err probability	0.05
	Power (1-β err probability)	0.90
	Number of groups	3
Output:	Total sample size	**60**
	Actual power	0.9151879

4.3.1.3 Eligibility and recruitment

Participants eligibility for young and middle-aged groups was based on i) aged 18–35 years old or 40–55 years old; ii) being asymptomatic; iii) no previous history of muscle, neurological or joint disorder; iv) not currently taking or been on a corticosteroid treatment for the past three years with doses >5mg/day; v) not currently taking or been on an HMG-CoA reductase inhibitors (statins) for

the past three years. The same criteria apply to the elderly group (aged 75 years or older) except they may have concomitant osteoarthritis due to the high prevalence of this disease in the elderly population, which can be impossible to exclude [466].

The young and middle-aged groups were recruited from the University of Leeds and the Leeds teaching hospitals trust as well as advertisements via social media. A collaborative research group [the Community Ageing Research 75+ (CARE 75+)] [467] provided a database of 103 potential community-dwelling elderly volunteers aged above 75. They were initially recruited from local general practitioner practices, and agreed to be approached to participate in other relevant research studies.

To select a healthy elderly cohort, all potential volunteers in the CARE 75+ database had an Edmonton frailty scale of ≤ 5 (the 'not frail' group). This scale assesses various domains of frailty (cognition, general health status, functional independence, social support, medication usage, nutrition, mood, continence and functional performance) and has demonstrated good validity and reliability [465]. Additionally, they had an English Longitudinal Study of Aging (ELSA) frailty index score of ≤ 14, representing the healthy groups of 'fit' and 'well' that are not 'vulnerable' or 'frail'. The ELSA frailty index assesses more than 50 deficits related to sensory and functional impairments, self-reported co-morbidities and cognitive function test [468]. Moreover, all eligible participants had a Montreal Cognitive Assessment (MoCA) score of ≥ 20, representing normal subjects with no mild signs of dementia. The combination of these frailty and cognitive filters ensured the recruitment of a healthy elderly population. The health status concerning sarcopenia will be investigated later in the chapter.

The elderly database included the demographics, contact details and additional useful variables such as the Edmonton frailty score, the ELSA frailty index, the SF-36 physical function and SF-36 general health. An invitation letter was posted to the eligible potential elderly volunteers then followed up with a phone call. The recruitment process is highlighted in the flowchart in Figure 4-1.

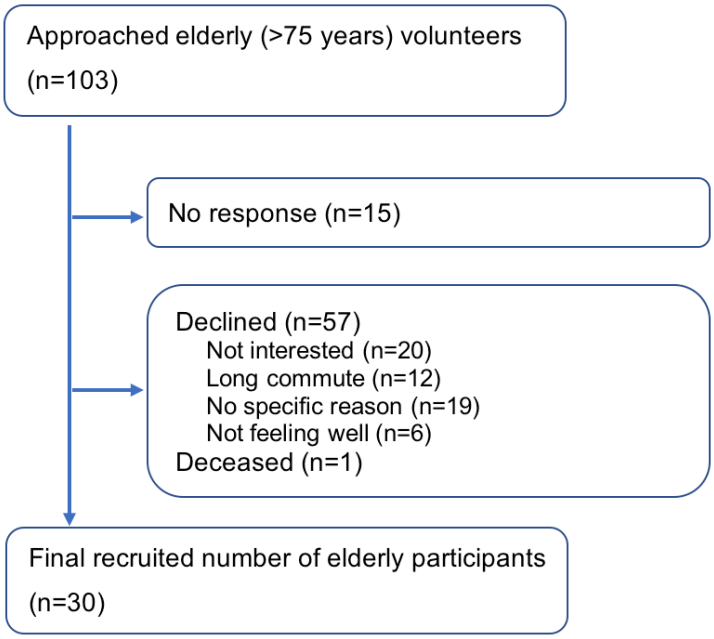

Figure 4-1 Flowchart for recruitment of the elderly participants.

4.3.2 Shear wave elastography

The employed SWE system was the two-dimensional Aixplorer (Supersonic Imagine, Aix-en-Provence, France) system using the SuperLinear™ SL10–-2MHz probe. This system had demonstrated the best reliability in the previous chapter. The muscles investigated were the four quadriceps [vastus lateralis (VL), rectus femoris (RF), vastus medialis (VM) and vastus intermedius (VI)], the three hamstrings [biceps femoris (BF), semitendinosus (ST) and semimembranosus (SM)] and the biceps brachii (BB). The muscles were scanned in the most relaxed muscle positions (Figure 4-2). The quadriceps were also assessed during static passive stretching (90° passive knee flexion position) to investigate the muscle elastic property when the muscle fibres are elongated under passive tension without any active force or load applied. The other muscles were only assessed during the resting position to avoid prolonging the scanning time (30 minutes). This position protocol demonstrated reliable readings in the previous chapter and other published studies [206]. The scan focused on the dominant side for all muscles since the second study in the last chapter showed no significant influence of limb dominance on muscle stiffness.

Before scanning, all participants were placed in a supine position on the scanning bed and were asked to relax for five minutes, which allowed time to

briefly explain the principle of SWE in simple terms in addition to explaining the positions and muscles being scanned. Figure 4-2 was shown as a guide to demonstrate the optimum positioning protocol. A correct participant position was verified and adjusted when needed.

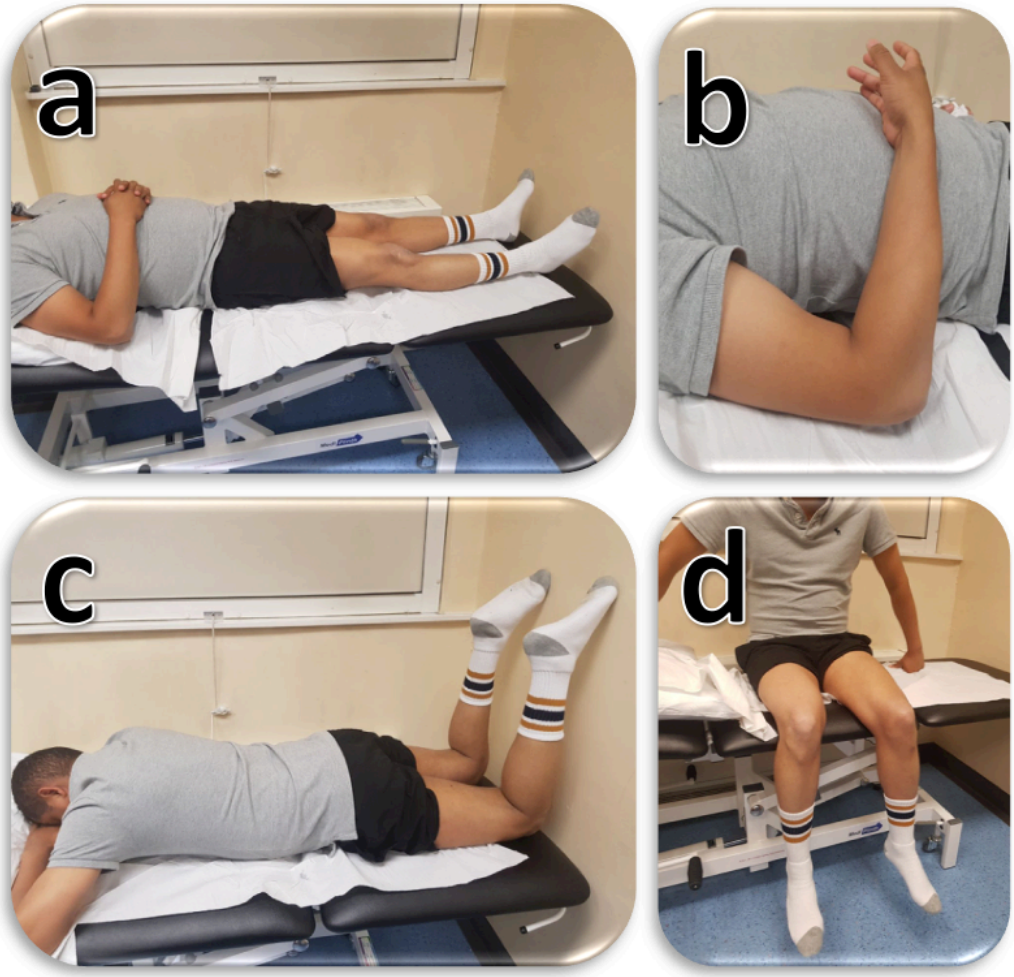

Figure 4-2 Muscle SWE measurement positions.

Image a (quadriceps rested): supine on a flat bed. Image b (biceps brachii rested): elbow flexed at 90° with the forearm rested on the body and hand in supination. Image c (hamstrings rested): prone on a flat bed with the knees flexed at 90° and rested on a wall. Image d (quadriceps stretched); seated with the hips and knees flexed at 90° without touching the floor. The scan followed the same images order in all participants.

4.3.2.1 Technical acquisition method

The technical acquisition methods that demonstrated the best outcomes in the previous chapter were applied again. Namely, the ultrasound probe was oriented along the muscle fibres. The region of interest (ROI) size was set at 10 mm in diameter unless the muscle area was smaller where a smaller ROI was used. No readings were acquired within a myotendinous junction or the

epimysium layer as they may affect the measurements due to their intrinsic higher stiffness. SWE acquisitions were repeated three times per muscle and recorded in units of meters per second (m/s). The probe was placed on top of the skin with a minimal load while ensuring no external pressure could deform the tissues and affect the measurements.

4.3.3 Muscle assessments.

Various muscle tests were performed to assess strength, physical function and muscle mass. These were employed to investigate their relationship with muscle stiffness. The tests protocols are described below and are also reviewed in chapter 2.

4.3.3.1 Handgrip strength.

The isometric handgrip muscle strength test is a simple and easy to perform test, which can be used to predict total body muscle strength [383]. The test was performed using the Jamar Plus+® electronic hand dynamometer (Lafayette Instrument Company, Lafayette, USA). The followed protocol was the established one by the American Society of Hand Therapists [386]. Briefly, participants were seated in a neutral position with the shoulder adducted and neutrally rotated, elbow flexed at 90° and forearm in a neutral position. Participants were instructed to squeeze the handgrip dynamometer as hard as they can per hand. The mean of three measurements was recorded for the dominant hand.

4.3.3.2 Expanded Timed Get-Up-and-Go (ETGUG).

The ETGUG is a sensitive and objective test that assesses multiple functionally essential tasks such as balance, standing and walking [469]. It is performed by measuring the time to complete a series of test components. The expanded form of the test includes timing multiple subtasks and a longer walking distance. It has shown higher reliability than the original short version and an excellent criterion validity [470]. ETGUG is an endorsed test for assessing the physical performance of the elderly [295], and for discriminating functionally impaired elderly subjects from healthy elderly and young controls [469].

The participant were asked to stand from a chair (sit to stand) then walk at their normal pace towards a cone placed 9.5 meters away (gait initiation and walk 1), turn around and walk back towards the chair (turn around and walk 2) then

sit down (slow, stop, turn and sit) (Figure 4-3) [469]. A tape was placed on the floor to mark 2, 8 and 10 meters. Times were recorded when the participant a) stood upright; b) passed the 2 m mark; c) passed the 8 m mark; d) passed the 8 m mark again after turning; e) passed the 2 m mark again after turning and f) after sitting down (Figure 4-3). Times were recorded using a smartphone stopwatch.

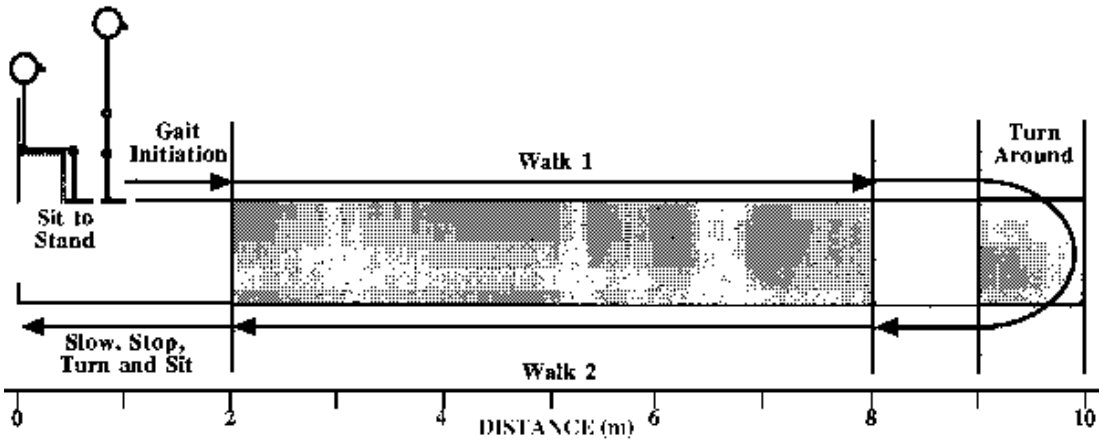

Figure 4-3 A schematic diagram for the expanded timed get-up-and-go test components.

(Reprinted by permission from the Journal of Rehabilitation Research & Development [469].)

4.3.3.3 4 meter gait speed.

There is a non-linear relationship between leg strength and gait speed [471]. The 4-m gait speed test is a straightforward test to perform that objectively assesses the functional walking capacity and provides predictive value for the risks of frailty, disability and hospitalisation rate [472]. It is considered the gold-standard test for functional assessment in elderly populations and is commonly used in research and clinical settings [473]. Moreover, it is the initial test in the European Working Group on Sarcopenia in Older People (EWGSOP) diagnostic algorithm for identifying sarcopenic subjects (check Figure 2-12 in chapter 2) [295]. Therefore, only the elderly participants performed this test as part of their sarcopenia assessment.

Gait speed is included as a subtask in the ETGUG test. However, subjects are timed for walking 6 m instead of 4 m. Although the time can be estimated indirectly from the ETGUG, it was performed independently for better accuracy. Participants were asked to walk at their normal pace in a testing zone of 8 m that starts with an acceleration zone of 2 m and ends with a deceleration zone

of 2 m [473]. The time for walking the middle testing zone of 4 m between the two zones was measured in m/s. Gait speeds below the cut-off of 0.80 m/s are considered slow requiring further strength and muscle mass assessments [295, 474].

4.3.3.4 30-second chair stand test (CST).

The CST is an established method for assessing lower body strength and endurance. It can be used to predict the capacity to perform various daily life tasks such as climbing the stairs and getting out of a chair. It was introduced to overcome the floor effect of the old 5-repetitions sit to stand chair test. The CST was able to detect differences due to ageing amongst elderly subjects of various age groups as well as between physically active and inactive subjects [405]. It had a perfect reproducibility (ICC=1) in elderly subjects with a mean age of 83 years [475].

Participants were asked to sit in the middle of a standard 43 cm high chair placed against a wall with their arms crossed over chest, feet flat on floor and shoulder width apart before being instructed to perform the maximum number of chair sit to stands they can within 30-sec [405]. The proper position and standing form was demonstrated to all participants. They were asked to practice two repetitions before starting. The total number of sit to stands within the 30-sec window was recorded. A stand was counted if a participant finished more than halfway up at the end of the test. Participants that failed to stand without assisting themselves using their hands scored zero.

4.3.3.5 Knee extension/flexion strength.

People with low knee strength are at increased risks of disability and mortality [464]. Isokinetic knee strength testing is considered the gold standard in muscle strength assessment and is a common method used to measure muscle strength in clinical research [389, 476]. Isokinetic dynamometry systems are rotation devices with a fixed axis of rotation that can apply a constant user-selected angular velocity [477]. When a desired angular velocity (e.g. 60°/sec) is selected (preset), the system has a resistive braking mechanism to monitor the preset angular velocity relative to the actual force applied to rotate the arm by the subject. The braking moment is increased if the actual angular velocity is higher than the preset and vice versa. This process is monitored in a closed feedback loop approximately 1000 times per second.

The Biodex system 4 (IRPS Mediquipe, UK) was used. Since lower limb strength is lost more rapidly than upper limb strength [478], only lower limb muscles (quadriceps and hamstrings) were assessed. The chosen protocol tested the concentric isokinetic knee extension and flexion movements set at 60°/sec angular velocity. The concentric motion was preferred over eccentric since the latter is usually preserved in diseases associated with muscle weakness and ageing [392, 479]. Isokinetic angular velocity at 60°/sec can be tolerated by most age groups especially the elderly and is commonly selected in research [480]. Additionally, most daily life activities require power and force generated at low velocities [481].

Participants sat on the Biodex chair and were stabilised by two crossing trunk straps, a pelvis strap and a thigh strap (Figure 4-4). The lateral femoral epicondyle was aligned with the system's rotational axis. The Biodex arm's attachment was strapped distally above the ankle malleoli. Participants started with a warm-up of knee extension and flexion before performing the actual recorded test of three sets of three knee extension and flexion repetitions at 100% effort separated by a 30 sec rest period between the sets. Participants were instructed and encouraged to "push" or "pull" against the ankle pad as hard and fast as possible. The standardised protocol used across all participants was based on a previous study reporting high test-retest reliability (ICC=0.94) and low within-subject variation [482].

The isokinetic strength outcomes of interest were the peak torque [Newton-meters (Nm)] to represent muscle strength (maximum force generated) and average power (Watts) to represent muscle power (work done per unit of time) based on the mean of the three repeated sets. Strength and power measurements were normalised to body weight (Nm/kg for peak torque and Watts/kg for average power). Both outcomes are important for muscle assessment, though power is lost faster than strength with ageing [295].

Figure 4-4 Isokinetic knee strength assessment using the Biodex system

The figure demonstrates an example of the isokinetic knee extension/flexion test.

4.3.3.6 Muscle mass

Muscle mass is an essential component in muscle function. Ageing inevitably results in the loss of muscle mass as explained in chapter 2. Muscle mass was measured in this study to evaluate the sarcopenic status of the elderly in addition to evaluating a potential association with muscle stiffness.

Multiple experts consensus statements, including EWGSOP, accept bioelectrical impedance analysis (BIA) as a valid, reliable and feasible tool for assessing muscle mass [295, 483]. BIA works by measuring electrical impedance caused by tissue upon an alternating low electrical current (e.g. 90μA) travelling through the body. As fat does not conduct electrical charges efficiently, BIA exploits this impedance property to estimate fat mass by calculating the difference between body weight and fat-free mass. The latter is composed of 73.2% water, acting as electrolytes to conduct electrical currents. Further information on BIA fundamentals and technical details can be found in other reviews [484].

Body composition estimates of muscle and fat masses were obtained using the Tanita DC-430 MA (Tanita Europe B.V., Manchester, UK) dual frequency (6.25kHz / 50kHz) 4 electrodes stand-on BIA system. Absolute muscle mass (kg) was recorded from the BIA then normalised by height and represented as the muscle mass index (mass/height^2). This system's results are accurate and repeatable (less than 1% variation within itself) for the intended use in clinical research [485]. The manufacturer guidelines for research were followed, and the default programmed equations for predicting body compositions were used.

4.3.4 Elderly assessment for sarcopenia

For the purpose of assessing the recruited non-frail elderly participants' muscle condition, sarcopenia was defined according to the EWGSOP criteria [295] as low muscle mass with weakness and/or low gait speed. The sarcopenia cut-off values for BIA-measured muscle mass were the widely-adapted values by Jannsen et al. [486] based on statistical analysis from National Health and Nutrition Examination Survey III data on older (≥60 years) men and women (n=4509). Sarcopenic subject defined as having a muscle mass index of ≤10.76 kg/m^2 and ≤6.76 kg/m^2 for males and females respectively. These values are the most stringent and conservative compared to others reported in the literature [487]. The cut-offs for the 4 m gait speed and grip strength tests were adapted from the large conducted study by Laurentani et al. [474]. These were also endorsed in the EWGSOP definition. A 4 m gait speed ≤0.80 m/s was the cut-off for low speed whereas the low grip strength cut-off was <30 kg and <20 kg for males and females respectively.

4.3.5 Statistical analysis

Statistical analyses were undertaken using SPSS version 25 (Armonk, NY: IBM Corp). The data normality distribution was checked using histogram plots and Shapiro–Wilk test. The one-way ANOVA test was used to determine if there is a statistically significant difference in SWV amongst the various age groups. The null hypothesis was that mean SWV for young, middle-aged and elderly are equal. Since the one-way ANOVA is an omnibus test statistic and does not inform which age groups were significantly different from each other, a post-hoc Tukey-corrected multiple comparisons test was employed [488].

The association between SWV and the muscle assessment variables was tested using Pearson's correlation coefficients to understand how muscle stiffness correlates with muscle strength, function and mass. Moreover, the correlations with elderly-specific variables (ELSA frailly index, the SF-36 physical function and SF-36 general health) were evaluated.

To further understand the underlying muscle stiffness process, multiple linear regression analysis was performed to evaluate which independent (explanatory) variables are significantly associated with SWV. To ensure a parsimonious model and avoid over-fitting, recommended methods for selecting the independent variables were followed [489]. Clinically relevant and biologically plausible independent variables were first drafted then screened for linearity with SWV and multicollinearity amongst each other. Only the variables that had a linear relationship with the dependent variable and are not collinear were retained. A variable was omitted if it was a descendant of other variables. Upon inspection of these conditions, the age, sex and BMI variables were retained and incorporated into the multiple regression model. This satisfied the general rule-of-thumb that there should be at least 15 participants for each independent variables incorporated in the model [489].

4.4 Results

4.4.1 Participants information and muscle assessments

A total of 77 participants volunteered in this study, of which 26 young, 21 middle-aged and 30 elderly with a mean age (SD, range) of 28.1 (4.1, 20–35), 48.5 (5.2, 40–55) and 81.7 (4.1, 77–94) respectively. The descriptive statistics of the main characteristics are listed in Table 4-2. It shows that the BMI and fat mass gradually increased with age and were significantly different amongst the groups. In contrast, the gradual reduction in muscle mass and muscle mass index was not substantial enough to result in a significant difference.

The elderly group had a mean (SD) frailty index, SF-36 physical function and SF-36 general health scores of 9.5 (3.3), 71.4 (21.9) and 70.0 (13.4) respectively. Their mean 4-m gait speed was 0.90 (0.14) m/sec. Their sarcopenia assessment flowchart is illustrated in Figure 4-5.

Table 4-2 Main characteristics of the study participants.

Characteristic	Young (n=26)	Middle-aged (n=21)	Elderly (n=30)	p-value‡
Sex	13 Females (50%)	15 Females (71%)	13 Females (56%)	0.32
Age (years)	28.1 (4.1)	48.5 (5.2)	81.7 (4.1)	**<0.001**
Males (years)	28.0 (4.0)	47.1 (5.2)	82.0 (4.2)	**<0.001**
Females (years)	28.3 (4.3)	49.1 (5.3)	81.4 (4.1)	**<0.001**
Height (cm)	169.0 (10.6)	167.2 (10.2)	161.2 (7.3)	**0.007**
Weight (kg)	71.3 (21.9)	71.7 (12.2)	75.5 (12.6)	0.57
BMI	24.5 (5.3)	25.6 (3.6)	28.8 (4.7)	**0.002**
Fat mass (kg)	16.1 (10.6)	18.9 (5.0)	26.7 (8.6)	**<0.001**
Muscle mass (kg)	53.3 (14.8)	51.0 (10.7)	46.3 (8.2)	0.08
Muscle mass index	18.3 (3.1)	17.7 (2.2)	17.7 (2.3)	0.69
Smoking	5 (23%)	7 (33%)	11 (37%)	0.18
pack-years†	1.25 (4.3)	1.8 (1.3)	7.5 (16.5)	0.16
Drinking alcohol	13 (50%)	10 (43%)	21 (70%)	0.12
(units/week) †	5.0 (13)	6.0 (6.5)	5.0 (12)	0.58
VAS score (global health) (mm) †	6.0 (14)	6.5 (17)	10.0 (25)	0.25

* Data in brackets represent standards deviation for means, or percentages for ratio.
† Median and interquartile range.
‡ p-values significant at 95% are highlighted in bold. Continuous variables tested via one-way ANOVA or Kruskal-Wallis test, and categorical data tested using Chi-square test.

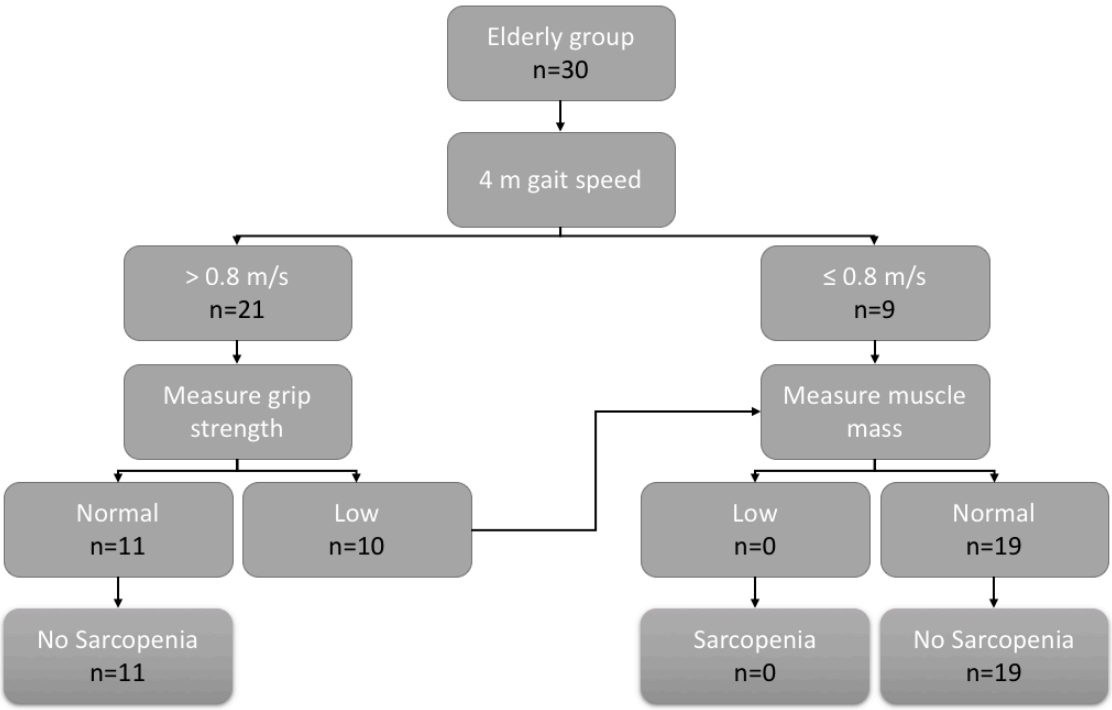

Figure 4-5 Flowchart of sarcopenia assessment in the elderly age group.

The flowchart demonstrates that none of the elderly participants was sarcopenic.

The one-way ANOVA results of the muscle assessments in Table 4-3 showed a significant difference amongst the three age groups (p<0.05). Further post hoc multiple comparisons analysis revealed that the significant differences only existed between the elderly group and the two younger groups. However, the knee extension torque and power were the only tests that showed significant differences between all groups (p<0.001).

The elderly group were approximately 4 sec slower in the ETGUG test. They had a significantly lower grip strength of 26.3 kg compared to 36.7 kg and 35.4 kg for young and middle-aged respectively. On average, the young and middle-aged performed 5–7 more chair stands in 30 sec than the elderly (p<0.001).

Table 4-3 Results of the muscle tests for the three age groups.

Characteristic	Young [(a)]		Middle Aged [(b)]		Elderly [(c)]		p-value*	Post hoc[†]
	Mean (SD)	95% CI	Mean (SD)	95% CI	Mean*	95% CI		
ETGUGT, sit to stand (sec)	1.0 (0.2)	0.9, 1.1	1.1 (0.4)	0.9, 1.3	1.5 (0.4)	1.4, 1.6	**<0.001**	a,b<c
ETGUGT, Gait initiation (sec)	0.9 (0.2)	0.8, 0.9	0.9 (0.3)	0.7, 1.0	1.1 (0.4)	0.9, 1.2	**0.019**	a,b<c
ETGUGT, Walk 1 (sec)	4.3 (0.4)	4.2, 4.5	4.4 (0.7)	4.1, 4.7	5.3 (0.9)	5.0, 5.7	**<0.001**	a,b<c
ETGUGT, Turn around (sec)	2.8 (0.3)	2.7, 3.0	3.0 (0.7)	2.7, 3.3	3.6 (0.8)	3.4, 3.9	**<0.001**	a,b<c
ETGUGT, Walk 2 (sec)	4.4 (0.4)	4.2, 4.6	4.4 (0.7)	4.0, 4.7	5.4 (1.0)	5.1, 5.8	**<0.001**	a,b<c
ETGUGT, Slow, stop (sec)	2.6 (0.4)	2.5, 2.8	2.7 (0.6)	2.5, 3.0	3.6 (0.7)	3.3, 3.9	**<0.001**	a,b<c
ETGUGT, Total time (sec)	16.1 (1.4)	15.6, 16.7	16.4 (3.1)	15.0, 17.8	20.6 (3.6)	19.3, 22.0	**<0.001**	a,b<c
Chair sit-to-stands in 30 sec	20.0 (5.8)	17.7, 22.4	17.9 (3.1)	15.3, 20.6	12.3 (4.4)	10.7, 14.0	**<0.001**	a,b<c
Handgrip strength (kg)	36.7 (10.8)	32.3, 41.2	35.4 (9.0)	31.3, 39.5	26.3 (10.6)	22.4, 30.3	**0.001**	a,b<c
Knee extension torque (Nm/kg)	1.9 (0.6)	1.7, 2.2	1.5 (0.5)	1.2, 1.7	0.8 (0.3)	0.7, 0.9	**<0.001**	a>b>c
Knee flexion torque (Nm/kg)	1.0 (0.3)	0.9, 1.1	0.9 (0.2)	0.7, 1.0	0.5 (0.2)	0.4, 0.5	**<0.001**	a,b>c
Knee extension power (W/kg)	1.2 (0.4)	1.0, 1.4	0.9 (0.3)	0.7, 1.0	0.4 (0.2)	0.4, 0.5	**<0.001**	a>b>c
Knee flexion power (W/kg)	0.6 (0.2)	0.5, 0.7	0.5 (0.1)	0.4, 0.6	0.3 (0.1)	0.2, 0.3	**<0.001**	a,b>c

* Significant one-way ANOVA p-values at 95% are highlighted in bold. [†] Result of the post hoc Tukey-corrected multiple comparisons.

4.4.2 Shear wave elastography

The SWE measurements, listed in Table 4-4, identified significant differences during the resting position for all the tested lower limb muscles and the BB from the upper limb. The SWV was higher in the passively stretched position in the quadriceps. However, it did not result in significant differences amongst the age groups. The results can be better appreciated graphically in the clustered error bars in Figure 4-6 during the resting position and in Figure 4-7 during the passive stretching position.

The mean SWV difference between the middle-aged and young groups over all muscles was -4.1% ranging from 0.5% to -7.3%. As for the elderly and middle-aged, the mean difference was -12.9% and ranged from -6.5% to -18.8%. The highest mean difference of -16.5% was observed between the elderly and young groups with the differences amongst the muscles ranging from -11.0% to -23.3%. The VI and BB exhibited the smallest differences whereas the VM and SM were the highest. Despite the gradual decreasing SWV the muscles, the post hoc analysis revealed that only the VL had a significantly decreasing SWV between all three age groups. The other muscles were only significantly lower in the elderly participants (p<0.001). SWE examples are shown in Figure 4-8.

The correlations between muscle stiffness and the main clinical and muscle assessment variables are listed in Table 4-5. Age, as expected from the one-way ANOVA results, had a significant negative correlation ranging from -0.450 to -0.822 for the BB and SM respectively (p<0.001). Weak to moderate correlations were detected for the BMI. Fat mass had a relatively stronger and more consistent correlation compared to muscle mass.

ETGUG showed that shorter times were significantly associated with higher muscle stiffness. However, this was not significant for the BB (r=-0.19, p=0.084). A higher count of chair stands and stronger grip strength had significant positive correlations with SWV (r=0.522 and 0.436 respectively in SM). Overall, isokinetic knee strength exhibited the strongest correlations especially in the VL and SM. In the elderly group, there was a significant negative correlation between SWV and the ELSA frailty index in the RF, VI and SM with coefficients (p-values) of -0.386 (0.035), -0.470 (0.009) and -0.412 (0.024) respectively. Other elderly variables showed no significant correlations.

Table 4-4 Muscle shear wave velocity in the healthy young, middle-aged and elderly participants.

Muscle	Young [(a)]		Middle Aged [(b)]		Elderly [(c)]		p-value*	Post hoc†
	Mean (SD)	95% CI	Mean (SD)	95% CI	Mean (SD)	95% CI		
Vastus lateralis (VL)	1.77 (0.15)	1.70, 1.83	1.64 (0.12)	1.59, 1.70	1.48 (0.16)	1.42, 1.53	**<0.001**	a>b>c
passively stretched	2.77 (0.24)	2.68, 2.87	2.72 (0.42)	2.53, 2.92	2.68 (0.31)	2.56, 2.80	0.54	-
Rectus femoris (RF)	1.80 (0.14)	1.74, 1.85	1.72 (0.11)	1.67, 1.77	1.58 (0.16)	1.52, 1.64	**<0.001**	a,b>c
passively stretched	2.21 (0.21)	2.13, 2.30	2.07 (0.18)	1.99, 2.16	2.25 (0.41)	2.09, 2.40	0.18	-
Vastus Medialis (VM)	1.71 (0.12)	1.67, 1.76	1.68 (0.14)	1.62, 1.74	1.38 (0.10)	1.34, 1.42	**<0.001**	a,b>c
passively stretched	2.56 (0.20)	2.48, 2.64	2.50 (0.26)	2.38, 2.62	2.45 (0.28)	2.34, 2.55	0.21	-
Vastus Intermedius (VI)	1.91 (0.11)	1.86, 1.96	1.92 (0.19)	1.83, 2.01	1.70 (0.22)	1.61, 1.78	**<0.001**	a,b>c
passively stretched	2.46 (0.28)	2.34, 2.58	2.39 (0.33)	2.24, 2.54	2.44 (0.40)	2.28, 2.59	0.72	-
Biceps Brachii (BB)	1.95 (0.22)	1.87, 2.04	1.85 (0.15)	1.78, 1.92	1.73 (0.18)	1.67, 1.80	**<0.001**	a,b>c
Biceps Femoris (BF)	1.73 (0.12)	1.68, 1.78	1.64 (0.14)	1.58, 1.70	1.40 (0.17)	1.34, 1.47	**<0.001**	a,b>c
Semitendinosus (ST)	1.71 (0.10)	1.67, 1.75	1.64 (0.14)	1.57, 1.70	1.38 (0.16)	1.32, 1.44	**<0.001**	a,b>c
Semimembranosus (SM)	1.80 (0.12)	1.75, 1.85	1.70 (0.12)	1.65, 1.76	1.38 (0.17)	1.32, 1.45	**<0.001**	a,b>c

* Significant one-way ANOVA p-values at 95% are highlighted in bold. † Result of the post hoc Tukey-corrected multiple comparisons.

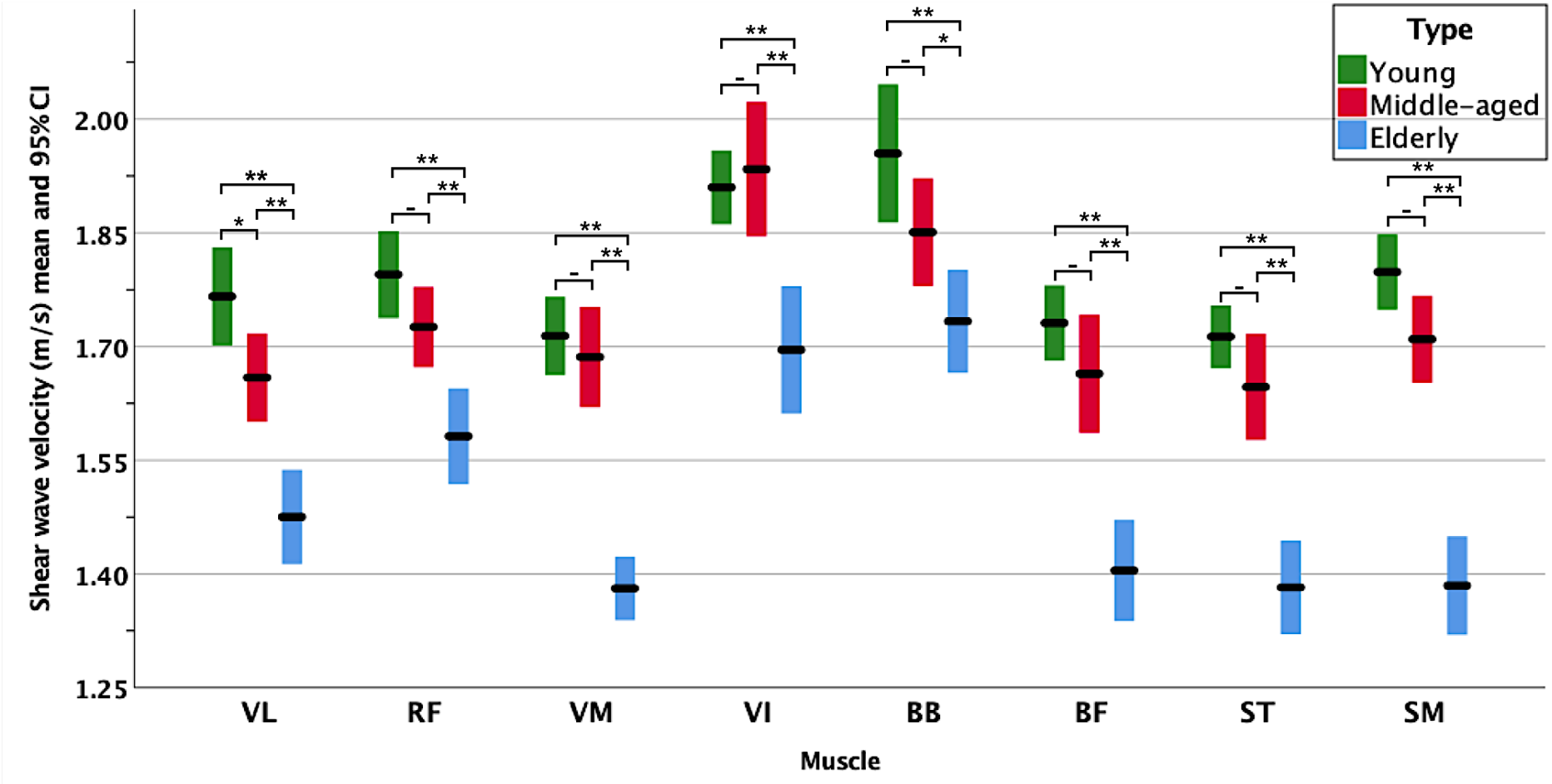

Figure 4-6 Clustered error bars for the mean muscle shear wave velocity in the relaxed resting position.

The asterisks labels above the bars indicate significance at 0.05 level (*) and 0.01 (**) while the hyphen (-) indicate a lack of statistical significance (p >0.05).

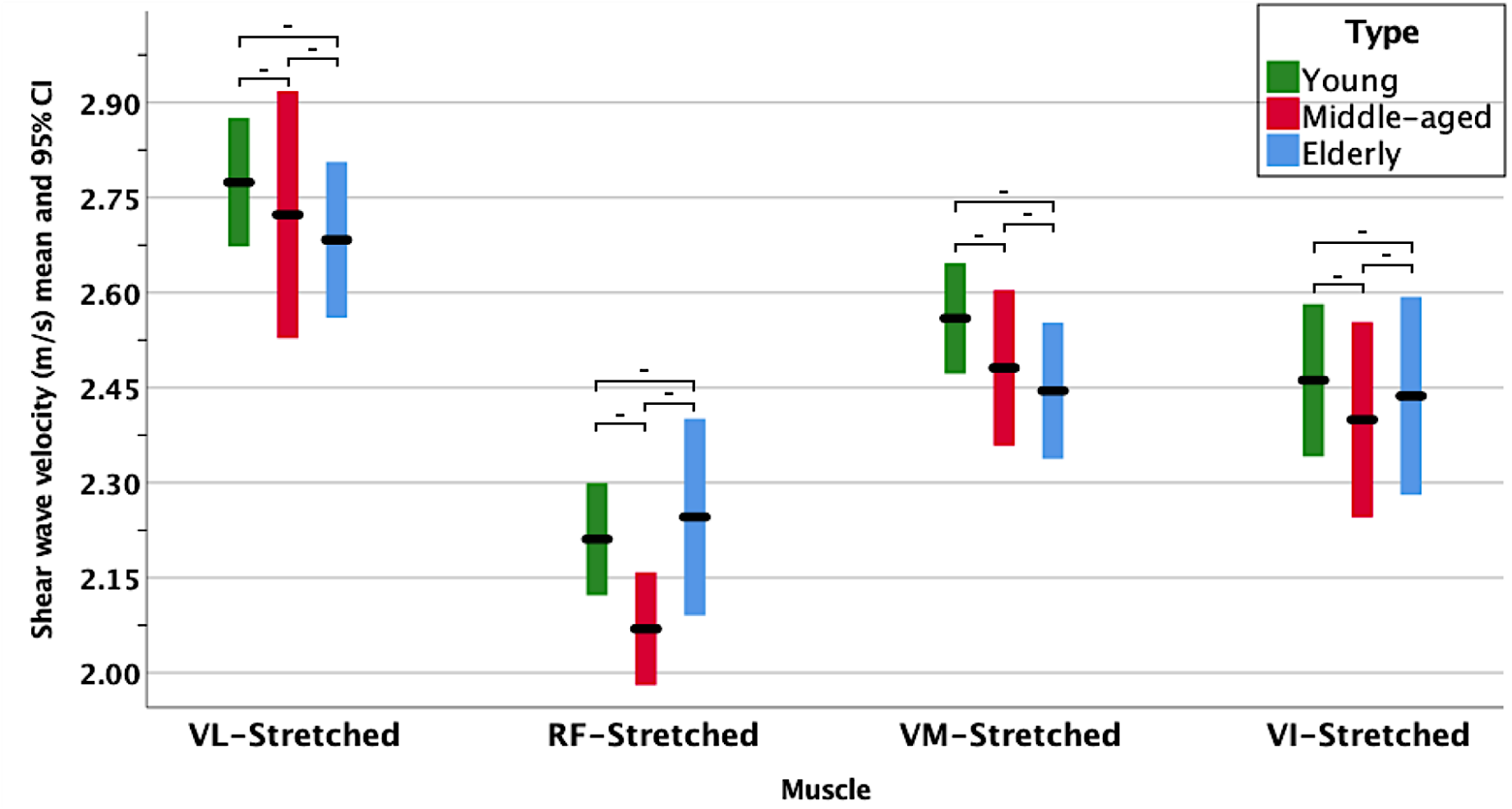

Figure 4-7 Clustered error bars for the mean muscle shear wave velocity during the passively stretched position.

The hyphen (-) above the bars indicate lack of statistical significance ($p > 0.05$).

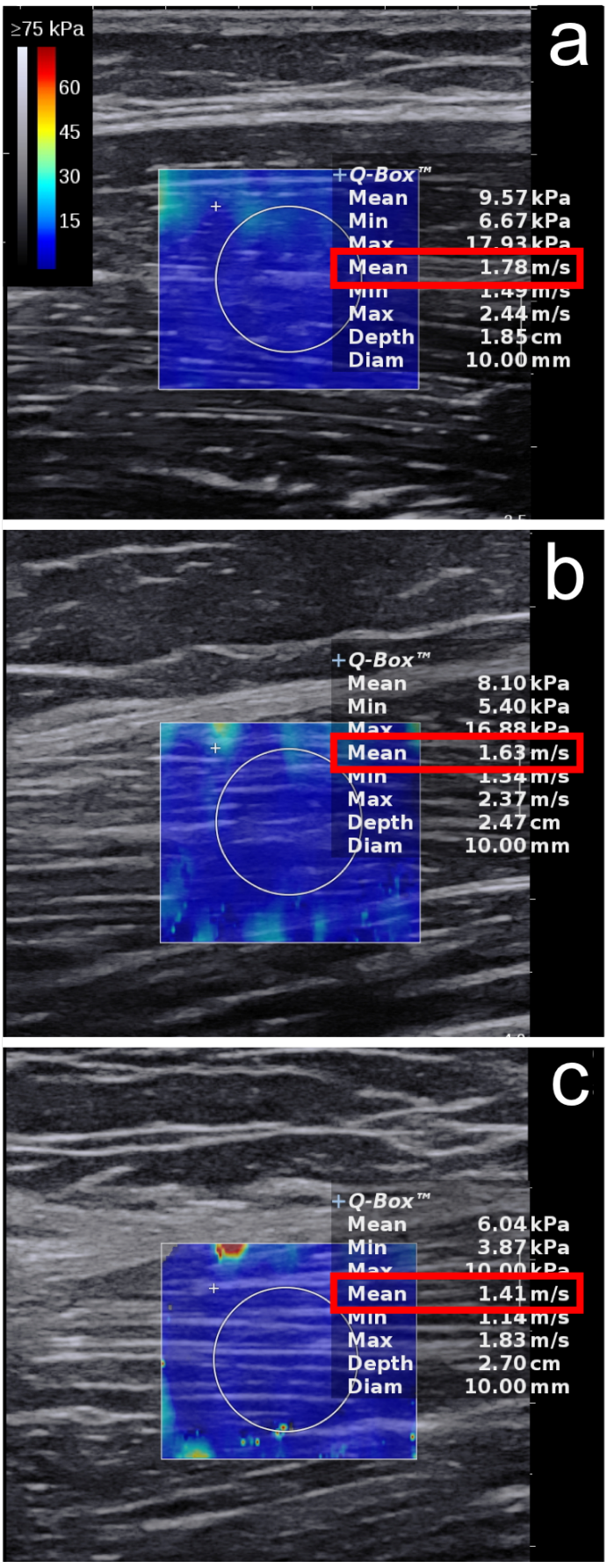

Figure 4-8 Shear wave elastography examples from (a) young (22 years), (b) middle-aged (55 years) and (C) elderly (80 years) participants.

Table 4-5 Muscle shear wave velocity correlations with clinical and muscle test variables for all participants.

	VL	RF	VM	VI	BF	ST	SM	BB
Age	-.680**	-.568**	-.770**	-.464**	-.744**	-.778**	-.822**	-.450**
BMI	-.346**	-.323**	-.210	-.323**	-.315**	-.316**	-.427**	-.250*
Fat mass (kg)	-.453**	-.421**	-.385**	-.392**	-.474**	-.414**	-.542**	-.330**
Muscle mass (kg)	.216	.146	.276*	.226	.266*	.231	.316**	.189
ETGUGT, Total time (sec)	-.386**	-.288*	-.367**	-.380**	-.338**	-.366**	-.560**	-.198
30-sec Chair stand test	.354**	.294**	.482**	.261*	.373**	.365**	.522**	.267*
Handgrip Strength (kg)	.285*	.256*	.343**	.293*	.344**	.297**	.436**	.287*
Knee extension torque (Nm/kg)	.587**	.454**	.636**	.356**	.547**	.542**	.640**	.443**
Knee flexion torque (Nm/kg)	.540**	.405**	.603**	.385**	.497**	.491**	.641**	.422**
Knee flexion power (W/kg)	.579**	.447**	.613**	.350**	.535**	.501**	.623**	.456**
Knee extension power (W/kg)	.540**	.439**	.600**	.333**	.489**	.479**	.640**	.422**

* Correlation is significant at the 0.05 level (2-tailed).
** Correlation is significant at the 0.01 level (2-tailed).

Multiple linear regression was employed to elucidate the influence of age, sex and BMI on muscle stiffness. The obtained results showed that neither sex or BMI explained a significant variation in SWV in all muscles. In contrast, age was consistently a significant predictor of SWV in the regression model. Therefore, the regression analysis was rerun with only age included as an

independent variable in the model. The full results of the two models on the investigated muscles are included in Table 4-6. BMI was a significant independent variable in the SM muscle only. This finding can be considered insignificant due to its inconsistency across the other muscles as well as its insignificant effect on R^2 in the model (p=0.052).

The adjusted R^2 for the VL, RF, VM, VI, BB, BF, ST and SM were 0.455, 0.314, 0.587, 0.205, 0.191, 0.547, 0.600 and 0.671 respectively. In other words, 45.5% of the variance in SWV is explained by age in the VL muscle as an example. Repeating the regression analysis using stepwise regression with the additional variables in Table 4-2 included resulted in the same findings.

Table 4-6 Multiple regression predicting shear wave velocity from age, sex and body mass index.

	Vastus Lateralis					
	Model 1			**Model 2**		
Variable	**B**	**β**	**Sig.**	**B**	**β**	**Sig.**
Constant	.662			.771		
Age	-.003	-.680	**<.001****	-.003	-.628	**<.001****
Sex				-.025	-.106	.219
BMI				-.003	-.131	.160
R^2	.463			.484		
$\triangle R^2$				.021		.160
	Rectus Femoris					
	Model 1			**Model 2**		
Variable	**B**	**β**	**Sig.**	**B**	**β**	**Sig.**
Constant	.653			.732		
Age	-.002	-.568	**<.001****	-.002	-.514	**<.001****
Sex				-.010	-.050	.606
BMI				-.003	-.141	.179
R^2	.323			.340		
$\triangle R^2$				.017		.179
	Vastus Medialis					
	Model 1			**Model 2**		
Variable	**B**	**β**	**Sig.**	**B**	**β**	**Sig.**
Constant	.672			.606		
Age	-.004	-.770	**<.001****	-.004	-.805	**<.001****
Sex				.009	.035	.643
BMI				.002	.092	.261
R^2	.593			.600		
$\triangle R^2$				.007		.261
	Vastus Intermedius					
	Model 1			**Model 2**		
Variable	**B**	**β**	**Sig.**	**B**	**β**	**Sig.**
Constant	.725			.911		
Age	-.002	-.464	**<.001****	-.002	-.378	**<.001****

Sex				-.047	-.196	.056
BMI				-.005	-.214	.053
R^2	.215			.279		
△R^2				.064		.053
	Biceps Brachii					
	Model 1			**Model 2**		
Variable	**B**	**β**	**Sig.**	**B**	**β**	**Sig.**
Constant	.719			.770		
Age	-.002	-.450	**<.001****	-.002	-.413	**<.001****
Sex				-.001	-.005	.965
BMI				-.002	-.099	.387
R^2	.202			.210		
△R^2				.008		.387
	Biceps Femoris					
	Model 1			**Model 2**		
Variable	**B**	**β**	**Sig.**	**B**	**β**	**Sig.**
Constant	.676			.750		
Age	-.004	-.744	**<.001****	-.004	-.717	**<.001****
Sex				-.023	-.087	.275
BMI				-.002	-.064	.455
R^2	.553			.562		
△R^2				.009		.455
	Semitendinosus					
	Model 1			**Model 2**		
Variable	**B**	**β**	**Sig.**	**B**	**β**	**Sig.**
Constant	.672			.682		
Age	-.004	-.778	**<.001****	-.004	-.768	**<.001****
Sex				.005	.019	.803
BMI				-.001	-.031	.707
R^2	.606			.607		
△R^2				.001		.707
	Semimembranosus					
	Model 1			**Model 2**		
Variable	**B**	**β**	**Sig.**	**B**	**β**	**Sig.**
Constant	.749			.844		
Age	-.005	-.822	**<.001****	-.005	-.759	**<.001****
Sex				-.005	.087	.186
BMI				.026	-.161	**.025***
R^2	.675			.701		
△R^2				.026		.052

B= unstandardized coefficient. β=standardised coefficient. R^2= coefficient of determination. *p<0.05, **p<0.01. △=change.

4.5 Discussion

Structural and molecular changes in ageing muscles could impair its mechanical properties [287, 392, 460]. A previous rationale for human tissue to increase in stiffness with ageing has been presented [490]. However, studies have demonstrated a significant reduction in tendon stiffness in older age [456, 457].

This study is one of a few to investigate the effect of ageing on muscle stiffness. To date, it is the first to incorporate strength and functional correlations to substantiate their associations with muscle stiffness throughout an adult age-span. The study systematically scanned all quadriceps and hamstring muscles, recommended in a previous study and not been simultaneously investigated before [208]. Additionally, the majority of prior work have not included elderly subjects above 75, which has previously been recommended [491]. This was accomplished in this study by recruiting healthy elderly participants up to 94 years.

The results determined a gradual reduction in resting muscle stiffness throughout adulthood with a significant decline most notable in the elderly (>75 years) group. This was true on all the tested muscles, which display different fibre arrangements and functions. These findings support the hypothesis that known age-related histological features of muscle such as myosteatosis, variability in myofiber size and corrupted connective tissue may promote the loss of normal muscle stiffness. This was also proposed previously by the work of Rodrigues & Rodrigues Junior [289], consistent with the elastic fibre system in the muscle extracellular matrix starting to lose its resistance property and becoming softer with ageing.

In contrast, this study has not confirmed previous research demonstrating increased muscle stiffness with ageing due to increased collagen concentrations. For example, Ochala et al. [492] reported that ageing induced an increase in ‘instantaneous stiffness’ (ratio between force change during muscle shortening and corresponding sarcomere length change). This was experimented using mechanical testing of single muscle fibres on a small sample (n=12). The discrepancy between their results and the current study might be explained by the principally different techniques utilised to estimate

muscle stiffness. Their method estimated stiffness from a force production perspective whereas SWE uses SWV as a surrogate for tissue stiffness. Nevertheless, their findings were also supported in other research conducted also in-vitro on a microscopic ultrastructural level [493, 494].

In the SWE literature, there is also a lack of consensus to whether muscle stiffness decreases [208, 216], increases [222, 495] or does not change [186, 207, 214] with ageing. Though, the presented results are in agreement with the majority of the literature. For example, Akagi et al. [208] reported a significant reduction of 17% in the RF stiffness, decreasing from 10.2 kPa in the young to 8.4 kPa in the elderly (p<0.001). Similarly, Yoshida et al. [216] found a comparable decline in muscle stiffness of approximately 9% in the gastrocnemius. These percentages are similar to the observed average range of reduction in this study.

On the other hand, opposite trends of increasing muscle stiffness with ageing were reported in two previous studies. The first only observed a significant increasing trend in subjects above 60 years (p=0.03) when the BB muscle was at full extension (passively stretched) [495]. The second study by Heizelmann et al. [222] reported a small, but statistically significant, increase in the stiffness of the trapezius (p=0.005) and erector spinae (p=0.04) muscles in subjects above 60 years. Interestingly, this was only true over the right side for the trapezius but not the left.

It is difficult to pinpoint the factors contributing to the discrepancy between the present study and two studies above. Potentially, it might be explained by the difference in the muscle-joint positioning and muscle groups investigated. Indeed, the first study looked at the BB during full extension while the second tested two back muscles. In this respect, it may be useful to investigate if the back muscles undergo an atypical ageing process to lower limb extremity muscles. Additional factors cannot be excluded such as the different SWE systems employed based on the previous chapter's results of disagreements in SWV between the two systems.

Studies using SWE [207] and magnetic resonance elastography [496] confirm the observed decreasing trend with a lack of statistical significance between young and middle-aged groups. The muscle ageing process does not appear to

start until the sixth decade when declines in muscle strength and mass emerge [292, 461-463]. Significant declines take place above 75 years as risks of fall and frailty increases [464]. This probably explains the overall lack of difference between young and middle-aged, except in VL.

The increased muscle stiffness in the quadriceps during 90° knee flexion was expected due to the passive muscle tension applied. However, it is interesting that muscle stiffness during passive stretching is preserved in older age, which was also observed in a previous study on the VI muscle [207]. The mechanism behind this remains unclear. Considering that all of the recruited participants were healthy, it may be speculated that passive muscle stiffness is preserved to maintain normal muscle contractility and function.

The observed lack of influence of sex on SWE is in agreement with previous studies that also reported no significant differences between males and females in resting muscle stiffness [207, 251]. BMI, in contrast, correlated weakly with SWV and failed to explain variations in SWV in the regression model when age was included as an independent variable. This failure was also reported previously and is not surprising given the inferior specificity of BMI in general [495].

The secondary aim of this study was to elucidate the relationship of muscle stiffness to muscle mass and strength, the principal components of sarcopenia and dynapenia respectively. There was a stronger correlation with fat mass compared to muscle mass, which correlated poorly with just two of the scanned muscles. On the other hand, weaker muscles and worse physical performance were associated with decreased muscle stiffness. Considering that a stiffer muscle may be able to generate force quicker [497], the observed loss in muscle stiffness in the elderly group may explain the positive correlation with low muscle strength.

The implications of this study findings are important. The decreased muscle stiffness in the elderly subject and its correlation with reduced strength could compromise the delivery of tensile muscle power of the muscle fibres to the tendon. This may suggest an increased exposure risk of muscle fibres to rupture or deformation, consequently increasing rates of physical frailty. Hence, SWE could be a useful tool for evaluating and screening elderly subjects at risk

of sarcopenia and frailty. Besides, the higher average reduction between elderly and young in muscle stiffness (16.5%) compared to muscle mass (13.1%) may speculate a better role of SWE in predicting earlier muscle changes associated with ageing. However, further research is required to establish these roles. In terms of future study design, the results highlight the importance of adjusting for age in future muscle SWE studies, especially when the cohort involves a wide age range.

The results hold great promise for SWE in the field of elderly care medicine for highlighting the impact of ageing on muscle stiffness. Future studies should aim to compare muscle stiffness in sarcopenic and non-sarcopenic subjects to elucidate the value of SWE for assessing muscle quality. Currently, abnormal muscle stiffness is not a risk factor for falls in the elderly population; researching this could yield valuable evidence. Future studies are also encouraged to control for physical activity to strengthen the relationship between muscle stiffness and age. As with all ultrasound applications, appropriate training to ensure the operator's competence is recommended in future studies investigating muscle ageing using SWE.

4.5.1 Limitations

The findings in this study are subject to several limitations. First, the three age groups were not matched in size. Middle-aged participants, especially males, were particularly challenging to recruit due to several work and life factors competing for their time. This difficulty was also experienced in a previous study [495]. Secondly, the study did not evaluate passive stretching on the BB or hamstring muscles to avoid long scanning time. Moreover, the study design does not represent the complete adulthood age-span since age was categorically analysed from three predetermined age groups. Although this incorporated the investigation of older age (i.e. >75 years), it lacked information on younger subjects 56–74 years. Another limitation is that inter-operator reproducibility was not verified. Additionally, it was impossible to blind the investigator to the participant's age groups. Finally, despite testing for muscle strength, the study did not control for physical activity. Though, self-reported exercise frequency does not seem to affect muscle stiffness [495].

4.6 Conclusions

In conclusion, ageing was associated with a decline in both lower and upper limb skeletal resting muscle stiffness as measured by SWE. The greatest reduction in muscle stiffness was found in elderly participants >75 years. This finding is in contrast with the current perception of increasing muscle stiffness with ageing reported in smaller sample size studies relying on mechanical in vitro testing of single muscle fibres. The decline correlated stronger with lower muscle strength than muscle mass. Sex and BMI did not influence muscle stiffness. The age-related changes in the mechanical properties of skeletal muscle may contribute to our understanding of the development of musculoskeletal disorders with age. The results highlight the needs for further research to investigate if decreased muscle stiffness could be a useful indicator for predicting fall risk in elderly individuals. Overall, the results emphasise the importance of controlling for the age variable in future muscle SWE studies. After highlighting the effect of age on muscle stiffness, the next chapter moves on to study the role of SWE in idiopathic inflammatory myopathies.

Chapter 5 Muscle shear wave elastography in idiopathic inflammatory myopathies.

This chapter describes a case-control study of patients with idiopathic inflammatory myopathy by investigating the diagnostic performance of shear wave elastography and correlating its results to magnetic resonance imaging. The results have been published as: Alfuraih, A.M., O'Connor, P., Tan, A.L., Hensor, E.M. Ladas, A., Emery, P. and Wakefield, R.J. (2019). Muscle Shear Wave Elastography in idiopathic inflammatory myopathies: a case-control study with MRI correlation. Skeletal Radiology, (in press).

5.1 Introduction

After investigating the reliability of muscle elastography (chapter 3) and highlighting the influence of ageing (chapter 4) on healthy cohorts, this chapter now looks at patients with a myopathic condition.

This chapter focuses on idiopathic inflammatory myopathies (IIM), a group of systemic autoimmune inflammatory muscle disorders characterised by muscle weakness, inflammation and structural changes [315]. The main subtypes of adult IIM are dermatomyositis, polymyositis and inclusion body myositis; it could also overlap with other systemic diseases. Although the subtypes may differ in pathology, they share similar features like muscle oedema and myofiber necrosis in addition to an elevation in muscle enzyme levels [323]. A recent systematic literature review demonstrated the rarity of IIM with an incidence rate up to 19/million/year and a prevalence ranging from 2 to 33 per 100,000 individuals [498]. It also highlighted a heterogeneity in the diagnosis and classification criteria. The complex inconsistent onset and progression of IIM can make it difficult to manage. Despite its rarity, patients with IIM may have a poor prognosis and life quality [317], which underlines the importance of research in this field.

Early accurate diagnosis is essential since IIM can be controlled effectively to prevent chronic complications such as severe atrophy and myosteatosis. The diagnostic methods for IIM were reviewed in chapter 2, which discussed their limitations such as invasiveness (muscle biopsy), poor sensitivity and specificity (serology for muscle enzymes and electromyography) [4]. Medical imaging has

a limited, albeit growing, role in the management of IIM. Magnetic resonance imaging (MRI) has emerged as a useful tool for mainly guiding muscle biopsy to regions of active muscle inflammation [499]. It is also helpful for providing evidence of morphological changes in localised regions missed on a negative biopsy [500]. Ultrasound, on the other hand, can reveal signs of increased echogenicity in cases of dermatomyositis and polymyositis [422]. Yet, no imaging investigations were recommended in the latest classification criteria of EULAR/ACR due to insufficient evidence of validity [323].

Pathological processes and disuse can cause structural alterations, which may affect the passive and active mechanical properties [501]. As highlighted in the literature review (chapter 2), muscle elasticity can become impaired by muscle inflammation. In IIM, multiple features including the presence of the destructive autoaggressive T cells, thickened capillaries, perifascicular atrophy and myofiber necrosis may alter the muscles' internal composition [502]. These features causing muscle oedema and atrophy suggest the occurrence of deleterious effects on the muscle's mechanical property.

Modern ultrasound technologies like shear wave elastography (SWE) can be helpful in the assessment and monitoring of myositis-induced muscle stiffness changes. It provides a quantitative measurement of the individual muscle stiffness with substantial reliability as shown in chapter 3. As reviewed in chapter 2, SWE has been found useful in the assessment of post-stroke muscle spasticity [269, 270] and Duchenne muscular dystrophy [277, 278].

There is limited published data evaluating muscle stiffness in patients with IIM. Previous studies used magnetic resonance elastography (MRE) [421] and strain elastography [83, 84, 503]. However, these studies are difficult to compare due to their varying design and methodologies. All lacked quantification of intrinsic muscle stiffness and comparison to a healthy control group. The quantitative characteristic of muscle elasticity in IIM is not well understood.

5.2 Aims

The study presented in this chapter aimed primarily to examine the quantitative characteristics of muscle stiffness in IIM patients compared to healthy controls.

This primary aim seeks to establish the face validity of muscle stiffness, measured using SWE, as an imaging biomarker. A secondary aim was to correlate SWE with MRI-reported features of muscle oedema, atrophy and fatty infiltration as well as to measures of muscle strength and function. This aim seeks to investigate the construct validity of muscle SWE to MRI and muscle strength.

5.3 Methods

5.3.1 Study design

The study was conducted prospectively as a case-control study because of the suitability of this design for investigating rare diseases such as IIM and the lack of similar study designs investigating SWE in IIM [504]. Patients and healthy participants provided written informed consent. The ethics of this study were granted under the same approval of the previous chapter's study. Recruitment began in May 2017 and stopped in August 2018.

5.3.2 Participants

Myositis patients were recruited from the outpatient rheumatology clinics and inpatient wards at Leeds Teaching Hospitals. Healthy controls were recruited in the same approach to the previous chapter. No formal sample size/power calculations were carried out due to a lack of available data. However, to estimate parameters for powering future clinical trials, published rules of thumb recommend between 12 and 30 subjects per group of interest [505, 506].

5.3.2.1 Inclusion/exclusion criteria

For IIM patients, the inclusion criteria were as follows:

1. Adult (aged >18 years);
2. Had an established diagnosis of adult IIM according to previously described criterion [318, 320];
3. Had an active disease, defined by the following criteria [507]:
    a. Presence of demonstrable muscle weakness determined subjectively by a qualified physician or quantitively with manual muscle test–8 score < 125/150;
    b. At least two abnormal measures from the following:

i. Elevation of serum creatine kinase (CK) at a minimum level of 1.3 times the upper limit of normal;
ii. Patient global visual analogue scale (VAS) score > 20mm/100mm;
iii. Physician global VAS score > 20mm/100mm [507].

The exclusion criteria were as follows:

1. Presence or history of spinal disease and neuropathy;
2. Presence of any contraindication to MRI (including but not limited to claustrophobia, implanted pacemaker, surgical clips within the head, metal fragments in the eye or head and pregnancy).

For healthy controls, asymptomatic adults (aged >18 years) with no previous history of muscle disorders, arthritis or neuropathy were recruited. None of the participants was on HMG-CoA reductase inhibitors (statins).

5.3.2.2 Matching

To reduce the risk of confounding, the patients were age and sex matched to healthy controls using the frequency-matching method because of its feasibility compared to the conventional individual-matching [508]. Initially, recruited patients were categorised as males and females then stratified onto ordinal age groups of five-year age increment. This a priori increment is generally acceptable to control confounding by age [509]. Next, matching healthy controls were assigned on each sex-age strata. This matching method ensured the same sex proportion and age frequency (± 5 years) between the patients and controls.

5.3.3 Clinical characteristics

Basic information was collected including age, sex, BMI, alcohol consumption, smoking and global VAS score. Additionally, the subtype of myositis, disease duration and current medications were recorded for IIM patients. The CK level closest to the time of SWE scan was recorded (within four weeks).

5.3.4 Shear wave elastography

The acquisition methods recommendations mentioned in the third chapter and utilised in the previous chapter were adapted. Briefly, the eight muscles tested were the vastus lateralis (VL), rectus femoris (RF), vastus medialis (VM), vastus intermedius (VI), biceps femoris (BF), semitendinosus (ST),

semimembranosus (SM) and biceps brachii (BB) of the dominant side. These muscles were chosen as proximal lower and upper limb muscles which are known to be commonly affected in IIM [320]. For the patients, the most symptomatic side was selected. The dominant side was selected when bilateral limbs have the same level of symptoms. All muscles were scanned in a relaxed position, except for the quadriceps group which was also assessed during passive stretching (90° passive knee flexion position). Assessing muscle during rest is important to highlight the biomechanical component when the muscle is not under any passive or active tension. This is also based on the notion that muscle quality is not limited to force production and functional capacity, but to other aspects such as metabolism and thermoregulation. Testing muscle stiffness in resting position ensures that elasticity is not confounded by structural-based tension. This may highlight an additional construct of muscle quality.

To avoid potential operator bias, the SWE was set at a high scale (0–7.1 m/s) above the expected ranges (<2.0 m/s) to suppress qualitative colour differences when collecting the SWE samples. The scale was retrospectively adjusted after the scan to an optimum level [0–2.9 m/s (equivalent to 0–25 kPa)] via the machine's software to export image examples.

5.3.5 Muscle assessments

Muscle weakness is a common symptom of myositis and is therefore always considered one of the first diagnostic criterion for IIM [315, 323]. All participants performed the same four muscle assessment tests in the previous chapter. First, handgrip strength was assessed as an indirect estimate of total body strength [383] using the Jamar Plus+® electronic hand dynamometer (Lafayette Instrument Company, Lafayette, USA). Next, participants performed the expanded timed get-up-and-go (ETGUG) test to assess essential functional tasks like standing, balance and walking.

The 30-second chair stand test was performed afterwards to test lower body strength and endurance [405]. This test had demonstrated good responsiveness and construct validity in IIM [405, 406]. Lastly, isokinetic knee extension/flexion strength was tested using the Biodex system 4 (IRPS Mediquipe, UK). Participants performed three sets of maximum effort

concentric knee extensions and flexions at an angular velocity of 60°/sec to calculate the peak torque [Newton-meters (Nm)] and average power (Watts) based on a mean of three repeated sets [482]. These strength and power measures were normalised to body weight (Nm/kg and W/kg). This test was previously recommended as one of the extended criterion for disease activity assessment in IIM clinical trials [378]. Moreover, it is one of the most sensitive methods for detecting muscle strength deficits in IIM patients [397].

Total body muscle mass was assessed prior to the above muscle tests using the Tanita DC-430 MA (Tanita Europe B.V., Manchester, UK) dual frequency (6.25kHz / 50kHz) 4 electrodes stand-on BIA system. The detailed protocol for each of the tests above is described in the previous chapter.

5.3.6 Magnetic resonance imaging

All IIM patients had a thigh MRI scan using the Siemens Magnetom Verio 3.0 T scanner (Siemens Healthcare, Germany) powered by the syngo (MR B17) software. The patients were laid supine with knees on full extension and were instructed to remain relaxed and still. Axial, coronal and sagittal images were acquired of the most symptomatic side using the MRI protocol in Table 5-1.

Table 5-1 Primary MRI acquisition parameters per sequence.

Sequence	Voxel size (mm)	FOV (mm)	Resolution (base × phase)	TR (ms)	TE (ms)	Slice thickness (mm)	Flip angle
T1_tse_COR	2.0×1.5×3.0	480	320 × 75%	658	8.8	3	150°
T1_tse_SAG	2.0×1.5×4.0	480	320 × 75%	658	8.8	4	150°
T1_tse_AX	1.2×1.2×5.0	300	256 × 100%	850	9.1	5	160°
STIR_AX	1.2×1.2×5.0	300	256 × 100%	6550	87.0	5	140°
T2_se_AX_FS	1.2×1.2×5.0	300	256 × 100%	1500	9.6	5	180°

COR= coronal; SAG= sagittal; AX= axial; TR= Repetition time; TE= Time to echo; tse= turbo spin echo; se= spin echo; STIR= short TI inversion recovery; FS= Fat suppression.

The MRI images of the quadriceps and hamstrings muscles were scored based on three main aspects: muscle oedema, fatty infiltration (myosteatosis) and muscle atrophy using previously described methods [414, 510, 511]. The scoring criteria are explained in Table 5-2. Semi-quantitative scoring was

performed by two experienced musculoskeletal radiologists (29 and 12 years of experience) from Chapel Allerton hospital. The radiologists were aware they were scoring IIM patients; however, they were blinded to other clinical, laboratory and muscle strength information.

Pre-scored example images were provided as a reference to standardise the scoring. Inter-reader reproducibility was analysed to assess scoring agreement. Each radiologist recorded the scores on a scoresheet per case. Post individual scoring, cases of disagreement between the radiologists were reconciled by consensus.

Table 5-2 Definition and scoring criteria of the evaluated MRI parameters.

Oedema	Definition	Increased intramuscular signal intensity within muscle tissues on STIR-weighted images.
	Scoring	0 = none. 1 = up to 1/3 of muscle volume involved. 2 = 1/3 – 2/3 of muscle volume involved. 3 = greater than 2/3 of muscle volume involved.
Fatty infiltration	Definition	Fatty replacement of muscle tissue, defined as intramuscular T1 hyperintense signal, which suppresses on STIR or fat-saturated images.
	Scoring	0 = none. 1 = up to 1/3 of muscle volume involved. 2 = 1/3 – 2/3 of muscle volume involved. 3 = greater than 2/3 of muscle volume involved.
Atrophy	Definition	Evident reduction of muscle volume based on the subjective assessment of the muscle's cross-sectional area at the mid-belly, compared to other muscle groups.
	Scoring	0 = none (no loss of bulk). 1 = up to 1/3 loss of bulk. 2 = 1/3 – 2/3 loss of bulk. 3 = greater than 2/3 loss of bulk.

5.3.7 Statistical analysis

Data analysis was performed using SPSS version 25 (Armonk, NY: IBM Corp) and GraphPad Prism version 7.00 (GraphPad Software, La Jolla California USA). Descriptive analysis was performed to report the main characteristics of each muscle SWV and graphically represented in box plots. Data normality distribution was checked by exploring histograms and the Shapiro-Wilk test to determine the choice of parametric or non-parametric approach for the following inferential statistical tests. The descriptive results were summarised as mean with standard deviations (SD) or median with interquartile range (IQR), depending on data distribution for continuous variables, and proportions with percentages for categorical variables. Intra-operator reproducibility of the three repeated measurements was analysed using intraclass correlations (ICC) for average measures of absolute agreement. Inter-reader agreement for the ordinal MRI scores was analysed using weighted Kappa coefficients (Kw). The results for these two tests were interpreted as follows: .00-.20 ‘poor agreement’, .21-.40 ‘fair agreement’, .41-.60 ‘moderate agreement’, .61-.80 ‘substantial agreement’ and >.80 ‘almost perfect agreement’ [436].

Independent sample Student’s t-test was used to determine if there was a significant difference in mean SWV values between patients and healthy controls per muscle. Besides, one-way analysis of covariance (ANCOVA) was employed to test if the mean SWV values are significantly influenced by age and sex as covariates. A receiver operating characteristic (ROC) curve was plotted to evaluate the ability of SWE to discriminate participants with and without IIM. The area under receiver operating characteristic (AUROC) were interpreted as follows: <0.5 ‘no discrimination’, 0.5–0.7 ‘poor discrimination’, 0.7–0.8 ‘acceptable discrimination’, 0.8–0.9 ‘excellent discrimination’ and >0.9 ‘outstanding discrimination’ [512].

The association between SWE and MRI scores was evaluated using the Jonckheere-Terpstra test. This test is suitable for detecting significant monotonic trend between a continuous variable (i.e. SWV) and an ordinal variable (i.e. MRI scores of IIM). It postulates an increasing or decreasing trend to the SWE values since there is a priori ordering of the MRI scores (normal, mild, moderate and severe). Additionally, Kendall’s tau-b correlation coefficients were calculated for the two variables. Furthermore, the Spearman’s

correlation coefficients were calculated to correlate SWV with CK levels, disease duration and the muscle tests results. This allows the investigation of the relationship between muscle elasticity to strength and disease activity. The 95% confidence intervals (CI) were calculated where appropriate. All tests were two-tailed. Absolute correlation coefficients ≥0.3 and statistical significance at $p<0.05$ was considered a potential effect worthy of further fully-powered investigation.

5.3.7.1 Missing data

Overall, less than 2% of the collected observations were missing. However, 18 participants (39%) were not assessed for body composition using the BIA due to the unavailability of the device at the time of their recruitment. This was considered as data missing completely at random (MCAR). The option of multiple imputations was evaluated but deemed unsuitable to impute 39% the BIA data considering the small sample size of the data to impute from. Therefore, the results of the BIA were omitted from the results.

On the other hand, five IIM patients failed to perform the ETGUG test, of whom two also failed to perform the knee extension/flexion due to severe muscle weakness. This missingness was considered as data missing not at random (MNAR). Since multiple imputations are not valid for predicting the values of MNAR, and due to the lack of acceptable alternative methods for analysing MNAR according to Bland (2015) [513], no other approaches were attempted to impute the data.

A single SWV observation was noted missing (MCAR) from different muscles of six participants. The value of multiple imputations was deemed negligible since it does not significantly improve the statistical power for this small quantity of missing data.

5.4 Results

5.4.1 Patients and characteristics

A total of 23 patients diagnosed with IIM volunteered to participate in this study [10 males and 13 females; mean age (SD)= 50.4 years (16.1)], including eight undifferentiated IIM, six polymyositis, four dermatomyositis, three inclusion body myositis and two overlap myositis. Clinical data of the recruited IIM

patients are listed in Table 5-3. Disease duration ranged from 1 week to 198 months with a median (IQR) of 8.1 months (33.2). CK levels were elevated for the majority of the patients with a median (IQR) of 757 (878). Four patients had a normal level of CK but represented with significant muscle weakness and were determined as clinically active by the treating physician similar to the others.

The patients were age- and sex-matched to healthy controls. Descriptive characteristics of the two groups are represented and tested for differences in Table 5-4. The table demonstrates that the controls were also matched for height, weight, BMI and waist-hip ratio as well as drinking and smoking habits. Five IIM patients failed to perform the ETGUG test, of whom two also failed to perform the knee extension/flexion due to severe muscle weakness. Nonetheless, all muscle tests showed that IIM patients performed considerably worse compared to the controls (p<0.002). Patients were 56% slower in the ETGUG test and had 56% weaker grip strength. They also performed on average 13 fewer stands in the 30-sec chair stand test. As for the knee extension/flexion strength, the patients performed 58%–78% worse than their matched controls.

Table 5-3 Clinical data of all IIM patients.

Case No	Sex	Age	Diagnosis	Disease duration (months)	CK level (IU/L)*	Treatment
1	Female	76.5	Undifferentiated IIM	20	601	Prednisolone.
2	Male	54.7	Undifferentiated IIM	1.1	708	Methylprednisolone, Prednisolone.
3	Female	58.6	Overlap myositis (Polymyositis and Rheumatoid arthritis)	0.2	2662	Methylprednisolone, Prednisolone.
4	Female	63.0	Undifferentiated IIM	6.5	324	Methotrexate, Prednisolone.
5	Male	38.2	Dermatomyositis	0.5	1375	None.
6	Female	50.9	Polymyositis	2.4	1000	Mycophenolate, Prednisolone.
7	Male	57.0	Polymyositis	108.7	757	Methotrexate.
8	Male	40.7	Undifferentiated IIM	34.8	12802	Methotrexate, Prednisolone.
9	Female	74.6	Undifferentiated IIM	2.1	777	Intravenous immunoglobulins, Prednisolone.
10	Female	35.8	Polymyositis	8.1	1205	Prednisolone, Azathioprine.
11	Female	59.1	Polymyositis	198.5	347	Methotrexate.

12	Male	77.9	Inclusion body myositis	6.1	190	Methotrexate.
13	Female	23.1	Dermatomyositis	0.4	4553	Prednisolone.
14	Female	40.5	Dermatomyositis	8.6	70	Hydroxychloroquine.
15	Male	52.7	Overlap myositis (mixed connective tissue disease and myositis)	64.3	692	Methotrexate, Hydroxychloroquine.
16	Female	49.1	Dermatomyositis	177.2	1784	Mycophenolate, Hydroxychloroquine, Prednisolone.
17	Male	58.4	Inclusion body myositis	19.9	399	Methotrexate.
18	Female	43.6	Undifferentiated IIM	1.6	763	Methotrexate, Hydroxychloroquine.
19	Female	53.5	Undifferentiated IIM	26.3	72	Mycophenolate, Prednisolone.
20	Male	49.8	Polymyositis	44.9	1225	Cyclophosphamide, prednisolone.
21	Female	21.0	Undifferentiated IIM	31.2	33	Hydroxychloroquine.
22	Male	60.5	Inclusion body myositis	0.4	1184	None.
23	Male	20.4	Polymyositis	2.1	634	Prednisolone.

* Normal value is 25–200 IU/L for females and 40–320 IU/L for males.

Table 5-4 Characteristics of the study participants.

Characteristic	IIM patients		Healthy controls		Difference	95% CI of the difference	p-value‡
	Mean*	95% CI	Mean*	95% CI			
Sex	13 Females (56.5%)	-	13 Females (56.5%)	-	-	-	1.00
Age (years)	50.4 (16.1)	43.4, 57.4	50.7 (16.2)	43.7, 57.7	-0.31 (-0.6%)	-9.9, 9.3	0.95
Males (years)	51.0 (15.4)	40.0, 62.0	52.1 (16.0)	40.7, 63.6	-1.1 (-2.1%)	-15.8, 13.6	0.87
Females (years)	49.9 (17.2)	39.6, 60.3	49.6 (17.0)	39.4, 59.9	0.3 (0.6%)	-13.5, 14.1	0.96
Height (cm)	169.0 (9.8)	164.7, 173.4	169.3 (10.5)	164.7, 173.8	-0.3 (-0.2%)	-6.3, 5.8	0.92
Weight (kg)	75.2 (11.2)	70.1, 80.2	72.9 (14.4)	67.0, 79.1	2.25 (3.2%)	-5.5, 10.0	0.56
Body mass index (BMI)	26.5 (5.4)	24.2, 28.8	25.3 (3.9)	23.6, 26.9	1.25 (4.7%)	-1.5, 4.0	0.37
Waist-hip ratio	0.90 (0.01)	0.86, 0.94	0.86 (0.01)	0.82, 0.90	0.04 (4.7%)	-0.01, 0.09	0.16
Smoking	9 (39%)	-	12 (52%)	-	-	-	0.37
Smoking pack-years	21.0 (15.6)	9.7, 33.7	13.1 (19.6)	0.7, 25.6	8.6 (60.3%)	-8.0, 25.2	0.29
Drinking alcohol	8 (35%)	-	5 (22%)	-	-	-	0.33
consumption (units/week)	3.7 (3.5)	0.7, 6.7	7.5 (2.5)	4.3, 10.7	-3.8 (-50.7%)	-7.9, 0.2	0.06
VAS score (mm)	53.2 (19.0)	45.0, 61.4	11.3 (16.0)	4.4, 18.3	41.8 (370%)	31.4, 52.3	**<0.001**

ETGUGT, sit to stand (sec)	2.5 (3.0)	1.0, 3.9	1.0 (0.3)	0.9, 1.1	1.5 (150%)	0.2, 2.7	**<0.001**
ETGUGT, Gait initiation (sec)	1.4 (0.9)	1.0, 1.9	0.9 (0.4)	0.7, 1.0	0.6 (55.6%)	0.1, 1.0	**<0.001**
ETGUGT, Walk 1 (sec)	6.2 (1.8)	5.4, 7.1	4.3 (0.8)	3.9, 4.7	1.9 (44.2%)	1.1, 2.8	**<0.001**
ETGUGT, Turn around (sec)	4.3 (1.4)	3.6, 4.9	3.0 (0.5)	2.8, 3.2	1.2 (43.3%)	0.5, 2.0	**0.002**
ETGUGT, Walk 2 (sec)	6.4 (1.9)	5.4, 7.4	4.4 (0.8)	4.1, 4.7	2.0 (45.5%)	1.0, 3.0	**<0.001**
ETGUGT, Slow, stop (sec)	4.5 (1.7)	3.7, 5.3	2.7 (0.6)	2.4, 2.9	1.8 (66.7%)	0.9, 2.6	**<0.001**
ETGUGT, Total time (sec)	25.3 (9.0)	20.8, 29.8	16.2 (2.7)	15.1, 17.4	9.1 (56.2%)	4.4, 13.7	**<0.001**
30 sec chair sit-to-stands	5.1 (5.4)	2.8, 7.5	18.6 (5.2)	16.3, 20.8	-13.4 (-72.6%)	-16.6, -10.3	**<0.001**
Handgrip strength (kg)	16.3 (10.4)	11.8, 20.8	37.6 (12.5)	32.0, 43.2	-21.3 (-56.6%)	-28.2, -14.4	**<0.001**
Knee extension torque (Nm/kg)	0.52 (1.02)†	0.29, 0.85	1.53 (0.70)†	1.25, 1.75	-1.01 (-66.0%)	-1.22, -0.53	**<0.001**
Knee flexion torque (Nm/kg)	0.36 (0.28)†	0.24, 0.45	0.86 (0.43)†	0.70, 0.99	-0.5 (-58.1%)	-0.64, -0.29	**<0.001**
Knee extension power (W/kg)	0.20 (0.62)†	0.06, 0.55	0.92 (0.43)†	0.72, 1.09	-0.72 (-78.3%)	-0.82, -0.38	**<0.001**
Knee flexion power (W/kg)	0.17 (0.21)†	0.10, 0.26	0.55 (0.21)†	0.47, 0.63	-0.38 (-69.1%)	-0.46, -0.24	**<0.001**

* Data in brackets represent standard deviations for means or percentages for ratio.
† Median and interquartile range (95% confidence interval for the median values is generated based on 1000 bootstrap samples).
‡ p-values significant at 95% are highlighted in bold. Continuous variables tested via independent t-test or Mann-Whitney, and categorical data tested using Chi-square test.

5.4.2 Muscle shear wave elastography

The descriptive data for the SWV measurements are reported in Table 5-5. Inspecting the normality of the data revealed a level of skewness which was resolved by performing a natural log-transformation. An independent sample t-test was run to determine if there were differences in SWV readings between the two groups of participants. Inspecting the test results showed that variances were homogeneous, as assessed by Levene's test for equality of variances (p>0.05) for most of the variables. However, the SWV for the VI violated this assumption. Thus, the output for the unequal assumption of variances was reported instead.

The independent sample t-test demonstrated that muscle stiffness was significantly lower in IIM across all the quadriceps and hamstrings in the resting position (p<0.05) (Table 5-5). In contrast, there was no significant difference for the BB or the quadriceps during passive stretching. The BF exhibited the greatest SWV difference between IIM patients (1.35 m/s IQR=0.32 m/s) and healthy (1.86 m/s IQR=0.32 m/s) with a difference of -0.37 m/s (95% CI, -0.44 to -0.26) p<0.001. The percentage of a significant reduction in SWV ranged from -22.2% to -12.9% for the BF and VI respectively. The hamstrings demonstrated a relatively similar loss of muscle stiffness (-19.9% to -22.2%) in contrast to the quadriceps where they varied slightly (-12.9% to -19.6%). As for the BB, the marginal reduction of -0.07 m/s (95% CI, -0.08 to 0.14) did not yield a statistically significant difference (p=0.509). The clustered boxplots in Figure 5-1 graphically represent the SWV results for the various muscles of the two groups. Examples of SWE images from IIM patients and their matching controls are shown in Figure 5-2. Sample size was too small to compare SWV between IIM subtypes meaningfully.

The ANCOVA test was attempted to evaluate the effect of sex and age as independent variables on the dependent variable (i.e. SWV). However, the SWV data across the muscles violated the assumptions of ANCOVA for linearity and homogeneity of regression slopes. Therefore, the test was not conducted, and the independent variables can be assumed to have no significant effect on SWV evident by the lack of linearity between them.

Table 5-5 Shear wave elastography measurements of the scanned muscles for the IIM patients and healthy controls.

Muscle	IIM patients		Healthy controls		Difference	95% CI of the difference†	p-value‡
	Median*	95% CI	Median*	95% CI			
Vastus lateralis (VL)	1.35 (0.32)	1.26, 1.44	1.68 (0.23)	1.62, 1.76	-0.33 (-19.6%)	-0.42, -0.20	**<0.001**
passively stretched	2.60 (0.68)	2.36, 2.93	2.65 (0.51)	2.56, 2.81	-0.05 (-1.9%)	-0.31, 0.21	0.504
Rectus femoris (RF)	1.52 (0.33)	1.43, 1.65	1.81 (0.23)	1.71, 1.85	-0.29 (-16.0%)	-0.32, -0.10	**0.006**
passively stretched	2.23 (0.53)	2.05, 2.43	2.20 (0.36)	2.12, 2.27	0.03 (1.4%)	-0.20, 0.21	0.989
Vastus Medialis (VM)	1.36 (0.16)	1.33, 1.46	1.60 (0.21)	1.55, 1.74	-0.24 (-15.0%)	-0.34, -0.13	**0.002**
passively stretched	2.28 (0.49)	2.10, 2.48	2.39 (0.38)	2.29, 2.58	-0.11 (4.6%)	-0.39, 0.03	0.091
Vastus Intermedius (VI)	1.62 (0.49)	1.46, 1.82	1.86 (0.22)	1.78, 1.95	-0.24 (-12.9%)	-0.42, -0.08	**0.038**
passively stretched	2.37 (0.39)	2.30, 2.56	2.36 (0.28)	2.25, 2.47	0.01 (0.4%)	-0.12, 0.23	0.454
Biceps Brachii (BB)	1.85 (0.28)	1.72, 1.90	1.78 (0.20)	1.75, 1.90	0.07 (3.9%)	-0.08, 0.14	0.509
Biceps Femoris (BF)	1.30 (0.14)	1.28, 1.45	1.67 (0.20)	1.58, 1.76	-0.37 (-22.2%)	-0.44, -0.26	**<0.001**
Semitendinosus (ST)	1.33 (0.31)	1.26, 1.40	1.66 (0.23)	1.58, 1.70	-0.33 (-19.9%)	-0.42, -0.187	**0.001**
Semimembranosus (SM)	1.36 (0.28)	1.28, 1.51	1.71 (0.18)	1.63, 1.76	-0.35 (-20.5%)	-0.44, -0.23	**<0.001**

* Data in m/s with interquartile range (95% confidence interval for the median values is generated based on 1000 bootstrap samples).
† The 95% confidence intervals (CI) for the difference between the medians is calculated based the Hodges-Lehmann method [514].
‡ p-values significant at 95% are highlighted in bold. Results are based on independent sample t-test of natural log-transformed values.

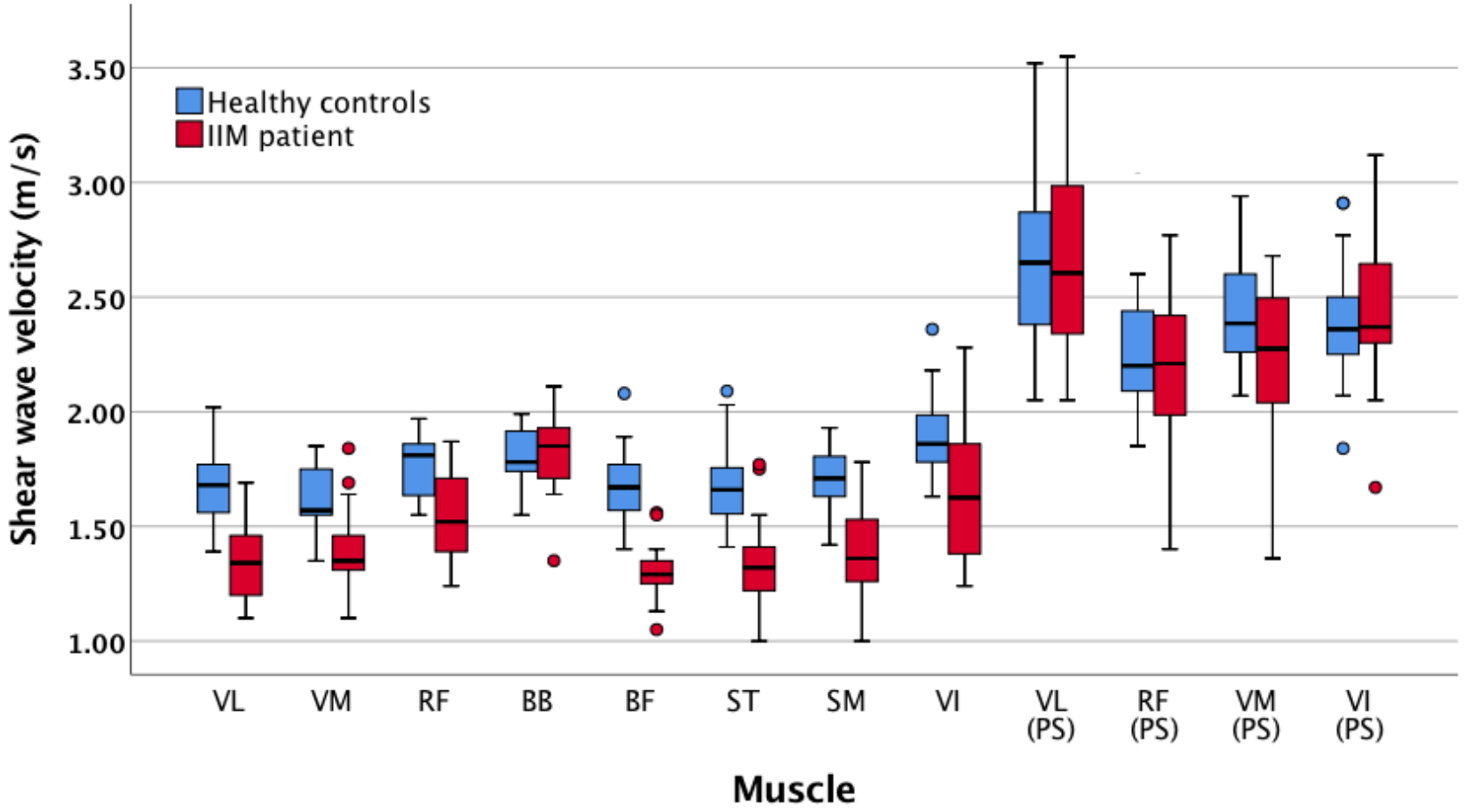

Figure 5-1 Clustered boxplot of shear wave velocity (m/s) by participant type.

VL: vastus lateralis, RF: rectus femoris, VM: vastus medialis, VI: vastus intermedius, BF: biceps femoris, ST: semitendinosus, SM: semimembranosus, BB: biceps brachii, PS: passively stretched.

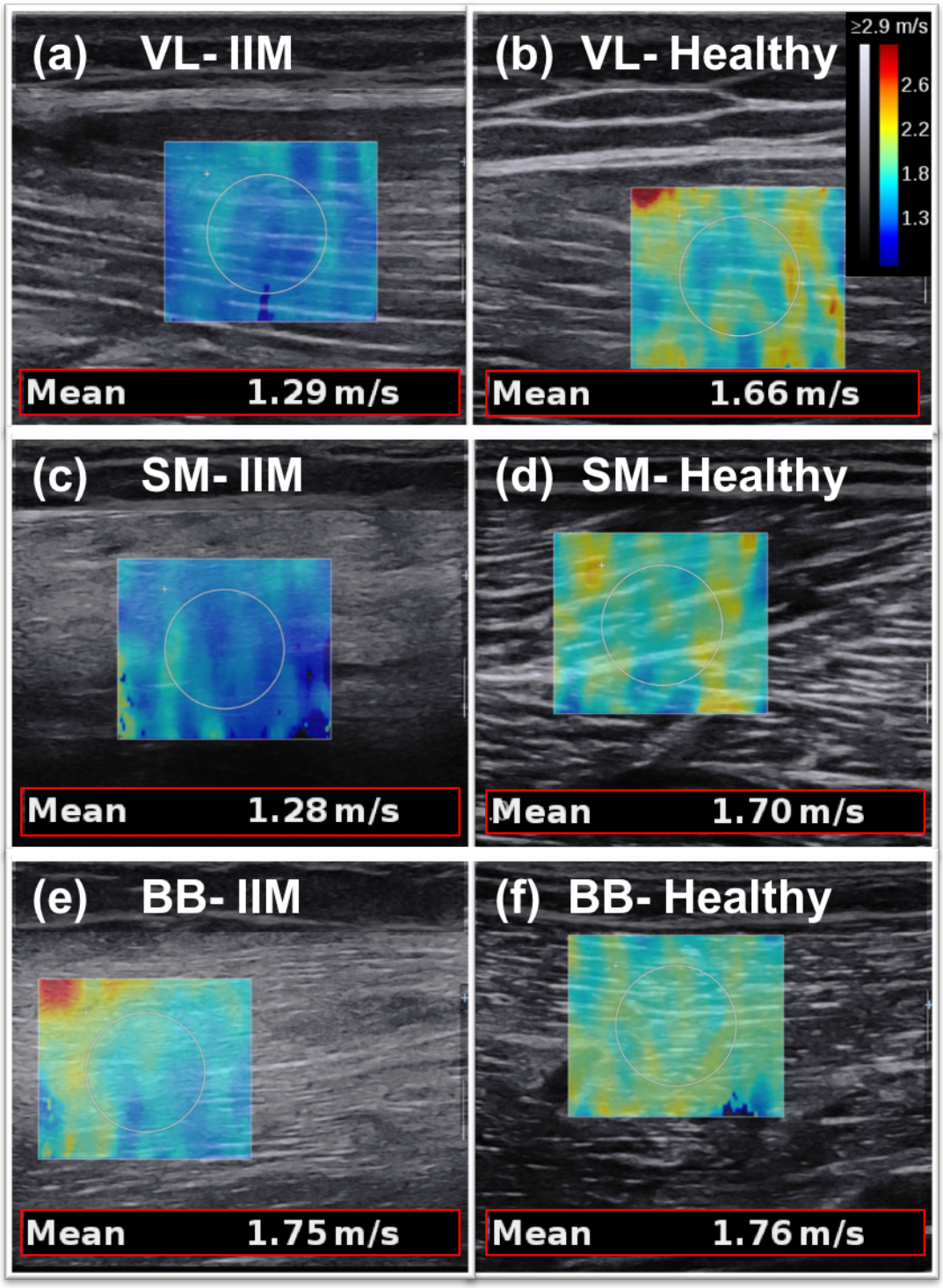

Figure 5-2 SWE images from three IIM patients compared to their matching healthy controls' muscles.

The figure shows two examples of significant differences from the quadriceps and hamstrings (a versus b for the vastus lateralis and c versus d for the semimembranosus) and a non-significant difference (e versus f for the biceps brachii). The SWE scale is set to 0–2.9 m/s to accentuate the qualitative colour differences.

Intra-operator reproducibility showed almost perfect reliability in the readings with ICC >0.95 for all muscles within each participant group except for the stretched RF that had a slightly lower ICC of 0.84.

ROC curve for SWE was plotted in Figure 5-3 using clinical diagnosis (based on a composite of clinical assessments and investigations) as the reference standard. SWE had AUROC results demonstrating an excellent level of discrimination for the quadriceps and hamstrings in the resting position (Table 5-6). The BB and the quadriceps in a passive stretching had a poor discriminatory performance. The SM yielded the best AUROC of 0.925 (95% CI 0.846, 1.00), which can be interpreted as outstanding discrimination according to Hosmer et al. [512].

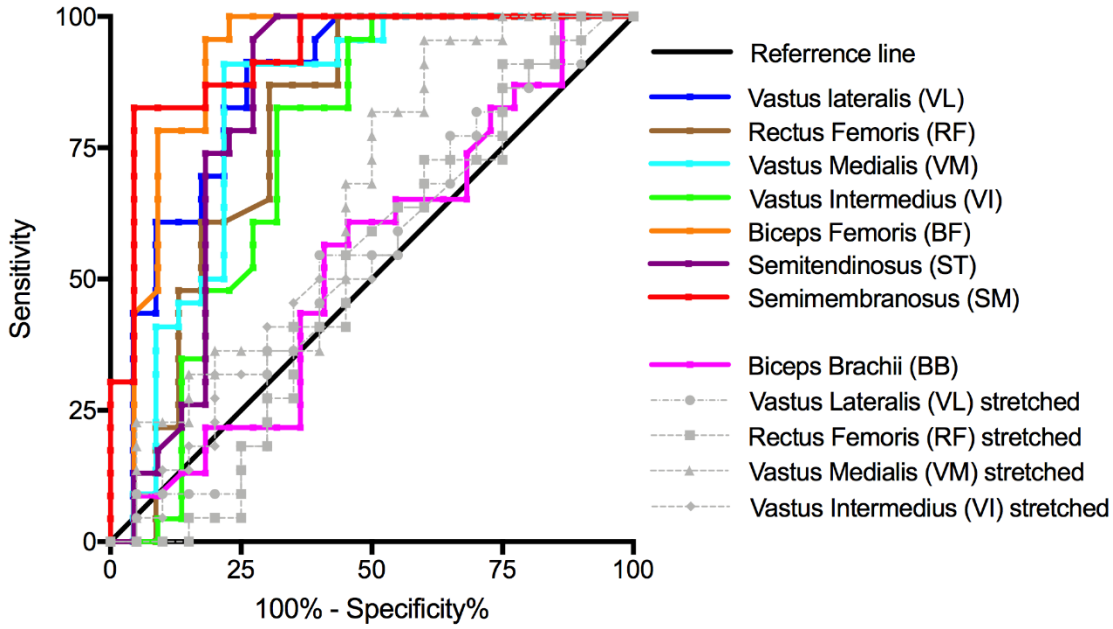

Figure 5-3 ROC curve for SWE performance in discriminating IIM and healthy muscles.

Table 5-6 AUROC results for the muscles tested using SWE.

Muscle	AUROC	95% CI	*p*-value*
Vastus lateralis (VL)	0.865	0.754, 0.975	**<0.001**
passively stretched	0.525	0.344, 0.705	0.782
Rectus femoris (RF)	0.790	0.649, 0.930	**<0.001**
passively stretched	0.507	0.324, 0.689	0.940
Vastus Medialis (VM)	0.822	0.689, 0.954	**<0.001**
passively stretched	0.644	0.471, 0.817	0.110
Vastus Intermedius (VI)	0.746	0.590, 0.901	**0.005**
passively stretched	0.548	0.370, 0.725	0.560
Biceps Brachii (BB)	0.532	0.359, 0.704	0.717
Biceps Femoris (BF)	0.908	0.806, 1.000	**<0.001**
Semitendinosus (ST)	0.822	0.681, 0.963	**<0.001**
Semimembranosus (SM)	0.925	0.846, 1.000	**<0.001**

* Significant *p* values are highlighted in bold.

5.4.3 SWE correlations with clinical variables and muscle tests.

The Spearman's correlation coefficient for the association between muscle SWV and the multiple clinical and strength variables are listed in Table 5-7. The SWV correlations with CK and disease duration were generally weak and insignificant ($r<0.30$; $p>0.05$). The RF, VM and ST did not significantly correlate with any of the analysed outcomes.

Slower walking speeds in the ETGUG were significantly associated with lower SWV for the VL, VI and RF with r_s coefficients of -0.56, -0.64 and -0.51 respectively. In contrast, stronger grip strength was associated with higher SWV for the VL, BF and SM. Another positive correlation was detected between the chair stand test and SWV for VL ($r_s=0.51$, $p=0.012$). The knee strength test correlated only with the BF; the correlations were explicably stronger for the flexion movement (peak torque $r_s=0.60$, power $r_s = 0.53$) compared to the extension movement (peak torque $r_s=0.47$, power $r_s = 0.48$).

Table 5-7 SWE correlations with clinical and muscle test variables for the IIM patients.

		VL	RF	VM	VI	BF	ST	SM
Age	Coeff	-.31	-.22	-.25	-.18	-.34	-.05	-.34
	p value	.15	.3	.26	.42	.12	.82	.13
BMI	Coeff	-.08	-.39	.21	**-.52***	-.08	-.2	-.19
	p value	.72	.07	.33	.013	.73	.38	.41
Disease duration (months)	Coeff	.01	-.03	.1	-.17	.26	-.09	.14
	p value	.98	.91	.66	.46	.24	.68	.53
Creatine kinase (IU/L)	Coeff	.02	.13	.28	.04	-.3	-.34	-.2
	p value	.92	.56	.19	.86	.17	.12	.37
ETGUGT, Total time (sec)	Coeff	**-.56***	-.37	.02	**-.64****	**-.51***	-.17	-.32
	p value	.017	.14	.94	.006	.036	.52	.21
30-sec Chair stand test	Coeff	**.51***	-.07	.37	.14	.4	.08	.31
	p value	.012	.74	.08	.53	.07	.73	.15
Handgrip Strength (kg)	Coeff	**.47***	-.02	.01	.05	**.62****	.27	**.45***
	p value	.025	.94	.97	.83	.002	.22	.033
Knee extension torque (Nm/kg)	Coeff	.33	-.12	-.06	-.02	**.47***	.32	.38
	p value	.15	.62	.79	.95	.034	.16	.09
Knee flexion torque (Nm/kg)	Coeff	.42	.11	.01	.19	**.60****	.2	.31
	p value	.06	.64	.97	.42	.005	.4	.18
Knee extension power (W/kg)	Coeff	.33	-.09	-.06	.02	**.48***	.26	.36
	p value	.14	.71	.8	.94	.033	.26	.12
Knee flexion power (W/kg)	Coeff	.43	.09	.12	.19	**.53***	.19	.25
	p value	.05	.71	.6	.42	.015	.42	.3

Coeff= correlation coefficient.
*. Correlation is significant at the 0.05 level (2-tailed).
**. Correlation is significant at the 0.01 level (2-tailed).

5.4.4 Magnetic resonance imaging

Inter-reader agreement between the two radiologists was ‘almost perfect’ for the overall MRI scoring of oedema, fatty infiltration and atrophy with Kw scores

(95% CI) of 0.88 (0.83, 0.94), 0.88 (0.83, 0.93) and 0.83 (0.76, 0.90) respectively. The detailed agreement coefficients for each muscle are listed in Table 5-8. The MRI results for the consensus scores are presented in Table 5-9.

Table 5-8 Inter-reader agreement for MRI scores of IIM.

Muscle	Oedema		Fatty infiltration		Atrophy	
	Kw*	95% CI	Kw*	95% CI	Kw*	95% CI
Vastus lateralis (VL)	.89	.79, .99	.96	.89, 1.0	.80	.65, .95
Rectus Femoris (RF)	.89	.75, 1.0	1.0	1.0, 1.0	.90	.77, 1.0
Vastus Medialis (VM)	.96	.87, 1.0	.87	.71, 1.0	.88	.78, .99
Vastus Intermedius (VI)	.93	.84, 1.0	.88	.76, .99	.91	.80, 1.0
Biceps Femoris (BF)	.73	.49, .96	.83	.59, 1.0	.60	.23, .96
Semitendinosus (ST)	.87	.71, 1.0	.74	.52, .96	.75	.53, .96
Semimembranosus (SM)	.90	.76, 1.0	.80	.56, 1.0	.88	.72, 1.0

* Weighted Kappa coefficient of inter-reader agreement.

Table 5-9 MRI muscle characteristics of the IIM patients.

Muscle | MRI score		Oedema		Fatty infiltration		Atrophy	
		Count	%	Count	%	Count	%
Vastus lateralis (VL)	Normal	12	52.2%	8	34.8%	15	65.2%
	Mild	5	21.7%	9	39.1%	2	8.7%
	Moderate	0	0%	1	4.3%	2	8.7%
	Severe	6	26.1%	5	21.7%	4	17.4%
Rectus Femoris (RF)	Normal	13	56.5%	13	56.5%	15	65.2%
	Mild	4	17.4%	7	30.4%	4	17.4%
	Moderate	0	0%	2	8.7%	2	8.7%
	Severe	6	26.1%	1	4.3%	2	8.7%
Vastus Medialis (VM)	Normal	14	60.9%	12	52.2%	17	73.9%
	Mild	4	17.4%	6	26.1%	2	8.7%
	Moderate	2	8.7%	3	13.0%	3	13.0%
	Severe	3	13.0%	2	8.7%	1	4.3%
Vastus Intermedius (VI)	Normal	12	52.2%	14	60.9%	16	69.6%
	Mild	3	13.0%	3	13.0%	2	8.7%
	Moderate	3	13.0%	2	8.7%	1	4.3%
	Severe	2	21.7%	4	17.4%	4	17.4%

Biceps Femoris (BF)	Normal	10	43.5%	6	26.1%	15	65.2%
	Mild	7	30.4%	15	65.2%	6	26.1%
	Moderate	5	21.7%	2	8.7%	1	4.3%
	Severe	1	4.3%	0	0%	1	4.3%
Semitendinosus (ST)	Normal	13	56.5%	7	30.4%	13	56.5%
	Mild	7	30.4%	10	43.5%	6	26.1%
	Moderate	3	13.0%	5	21.7%	3	13.0%
	Severe	0	0%	1	4.3%	1	4.3%
Semimembranosus (SM)	Normal	12	52.2%	6	26.1%	13	56.5%
	Mild	7	30.4%	14	60.9%	7	30.4%
	Moderate	3	13.0%	2	8.7%	3	13.0%
	Severe	1	4.3%	1	4.3%	0	0%

The results of the consensus scores on the Jonckheere-Terpstra test and Kendall's tau-b correlations for the associations between SWV and MRI were analogous (Table 5-10). They determined a statistically significant decreasing monotonic trend and a negative correlation between MRI-muscle oedema and SWV for the VL, VM and BF with *p*-values of 0.008, 0.001 and 0.002 respectively. The results were also significant in muscle atrophy for ST and SM with *p*-values of 0.038 and 0.006 respectively. However, the correlations between SWV and fatty infiltration across all muscles were weak ($r<0.3$; $p>0.05$). Figure 5-4 displays an example of the decreasing SWV scores with higher muscle oedema.

Table 5-10 The relationship between MRI and shear wave elastography in IIM patients

Muscle		Oedema	Fatty infiltration	Atrophy
Vastus Lateralis (VL)	Monotonic trend *p*-value †	**0.008**	0.27	0.14
	Correlation, (*p*-value) ‡	**-0.405** (0.008)**	-0.099 (0.28)	-0.181 (0.14)
Rectus Femoris (RF)	Monotonic trend *p*-value	0.26	0.42	0.33
	Correlation, (*p*-value)	0.112 (0.26)	-0.036 (0.42)	0.075 (0.33)
Vastus Medialis (VM)	Monotonic trend *p*-value	**<0.001**	0.44	0.19
	Correlation, (*p*-value)	**-0.553** (0.001)**	-0.019 (0.45)	-0.148 (0.19)

Vastus Intermedius (VI)	Monotonic trend *p*-value	0.40	0.07	0.32
	Correlation, (*p*-value)	-0.042 (0.40)	-0.252 (0.07)	-0.083 (0.32)
Biceps Femoris (BF)	Monotonic trend *p*-value	**0.000**	0.054	0.20
	Correlation, (*p*-value)	**-0.489** (0.002)**	-0.288 (0.054)	-0.150 (0.20)
Semitendinosus (ST)	Monotonic trend *p*-value	0.45	0.21	**0.037**
	Correlation, (*p*-value)	0.022 (0.45)	-0.137 (0.21)	**-0.312* (0.038)**
Semimembranosus (SM)	Monotonic trend *p*-value	0.10	0.11	**0.006**
	Correlation, (*p*-value)	-0.219 (0.10)	-0.212 (0.11)	**-0.444** (0.006)**

† The *p* value (1-sided test) of the Jonkheere-Terpstra test *p* value (significant at p<0.05).
‡ The correlation coefficient and *p* value of the Kendall's tau-b correlations (significant at p<0.05). *. Correlation is significant at the 0.05 level (2-tailed). **. Correlation is significant at the 0.01 level (2-tailed).

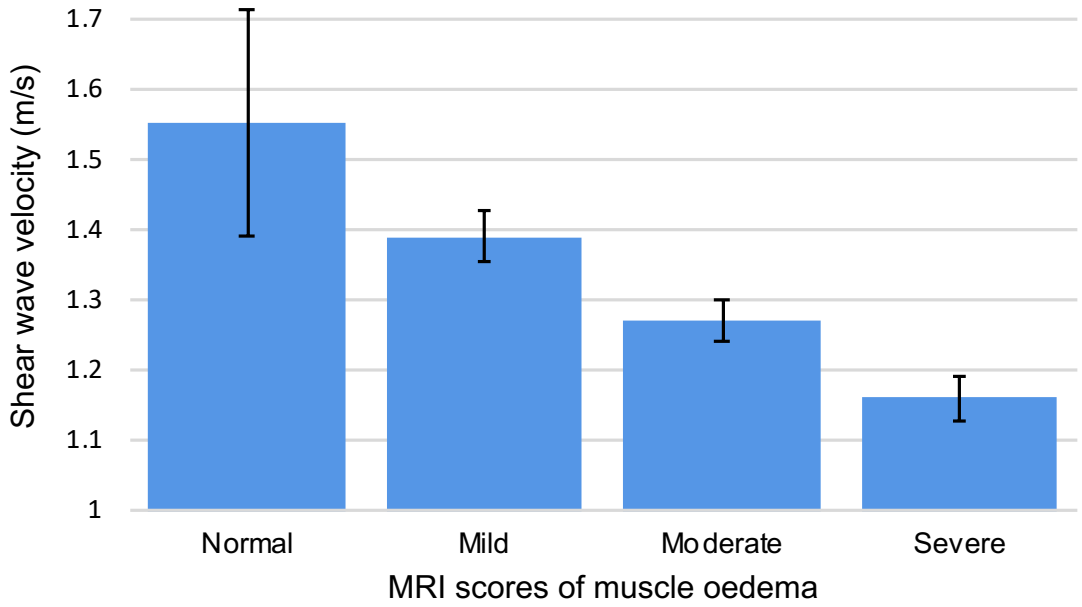

Figure 5-4 Bar graph of the significant decreasing monotonic trend between muscle stiffness and MRI oedema.

The data shown is for the VM muscle in IIM patients. Error bars represent the standard deviation.

5.5 Discussion

Over the past 50 years, more than a dozen attempts have been conducted to establish and develop the diagnostic and classification criteria for IIM. Experts are still calling for the development of novel diagnostic methods to distinguish IIM from other mimicking conditions as well as developing the classification criteria to characterise IIM subgroups [515]. The work conducted in this chapter is original as it is the first case-control study investigating muscle elasticity using SWE in IIM patients. It is also the first to study the association of SWE with muscle strength and MRI features.

The results, particularly the lower muscle stiffness measurements in IIM during the resting position across the tested lower limb muscles, support the face validity of SWE. This is considered the main finding and most important contribution of this chapter. Various pathological processes could have induced this abnormality including muscle atrophy and the presence of destructive inflammatory infiltrates causing oedema [502].

The diagnostic performance of SWE was strong for discriminating IIM from healthy controls in the muscles that showed significant differences. For the best performing muscle (SM), there was a 92% chance of correctly distinguishing IIM from healthy muscle. But the diagnostic performance of BB and stretched quadriceps was not much better than a coin toss. The substantial performance lends credence to SWE as a promising non-invasive and quantitative method for detecting active IIM. However, it should be noted that an extreme design such as this (healthy compared to diagnosed IIM) may not measure clinically relevant diagnostic performance.

These exploratory muscle assessments suggest that IIM patients lost, on average, half of their strength and functional performance compared to healthy controls. The moderate correlations with muscle stiffness were heterogeneous and inconsistent across the different tests and muscles. A potential bias can be expected due to the inevitable failure of few patients to perform two of the required tests due to severe muscle weakness as stated previously. Such patients are expected to perform worse than the recorded measurements. Nevertheless, all tests revealed a significant correlation with SWE indicating a clinical relevance in terms of construct validity for SWE in IIM. Abnormal

muscle stiffness can be a precursor to the commonly observed muscle weakness. It can be hypothesised that the loss in muscle stiffness limits force transmission capability and can be responsible for diminished muscle strength and functional capacities.

Despite the significant abnormal findings, these preliminary findings indicate that the stretched muscle stiffness was preserved and unaffected by IIM. If confirmed, there are two explanations for this finding. Firstly, the functional stretching property of individual muscle fibres remains intact in IIM [516]. Secondly, infiltrative inflammatory cells are known to attack passive components such as the extracellular matrix, which has a role in providing the resting passive elastic property for muscle [517]. This calls for research geared towards exploring the passive resting muscle components such as structural proteins and their potential impact on muscle elasticity.

The results of reduced muscle stiffness match those observed by McCullough et al. [421] in a case-control study of nine active IIM patients using MRE, which also only observed a statistically significant stiffness difference during the relaxed resting position. The application of SWE is more clinically feasible than MRI for bedside applications. Overall, these trends of altered muscle stiffness support the concept of the detrimental effects of IIM on muscle tissue and its biomechanical aptitude.

Not all studies have observed a reduction in muscle stiffness. On the contrary, Song et al. [503] compared affected versus normal muscles within each IIM patient and reported that the affected muscles had a higher stiffness than adjacent healthy muscles as indicated by high strain ratios of semi-quantitative strain elastography. The discrepancy could be due to the different elastographic modalities used as well as a potential sampling bias in the placement of the small ROI within the assumed “nearby normal muscle” on ultrasound. The current study systematically investigated the selected muscles and showed that all quadriceps and hamstrings exhibited relatively similar levels of reduced stiffness.

Of particular interest was the normal BB stiffness in IIM patients, which could be attributed to the disease’s relative predilection for the proximal lower thigh and hip girdles muscles [320]. There is so far only one study, Bachasson et al.

[518] that utilised SWE in myositis, which focused on the BB in inclusion body myositis patients. Although their study design lacked a control group, the researchers reported a significant but weak correlation between BB stiffness and muscle weakness (r_s=0.36, p<0.05). Additionally, they reported substantial within-day reliability [intraclass correlation (ICC)=0.83] and moderate between-day reliability (ICC=0.64).

Although the altered stiffness can be linked primarily to the IIM pathological processes, secondary confounders and underlying factors cannot be ruled out. For example, the majority of IIM patients are on a treatment regimen, some of which may induce drug myopathies especially corticosteroid-induced myopathy. This topic will be the focus of the next chapter. However, approximately one-third of the recruited patients can be considered newly diagnosed and less exposed to potential drug myopathies.

This is the first study to analyse the multimodality correlation between SWE and MRI to characterise IIM. The results indicated that increased muscle inflammation (i.e. oedema) and loss of muscle mass (i.e. atrophy) were associated with lower muscle stiffness in IIM on a number of the investigated muscles. This is in contrast to the findings of Song et al. [503] and Berko et al. [84] who reported no statistically significant correlation using strain elastography, although power was low and they did not report the actual correlation coefficients. The technical and mechanical factors of strain elastography, used by both studies, may have limited its capability to detect the myositis-induced elasticity changes. Using SWE, a recent study on delayed onset muscle soreness reported a significant 19% reduction in SWV (p=0.008), which corresponded with MRI signs of muscle oedema [283]. Previous research shows that the pattern of MRI muscle involvement can vary depending on IIM subtypes [519]. This could explain the inconsistent SWE-MRI correlations across all muscles.

This study only incorporated CK serum levels into the analysis since they are the most frequently requested blood markers to monitor disease activity. The failure of muscle elastography to correlate with IIM disease activity was also reported by Song et al. [503] and Berko et al. [84]. The latter, however, used the physician’s grading of disease activity as the measure instead of CK. On the other hand, Botar et al. [83] demonstrated a close graphical proportionality

between CK serum levels and average hue values of the strain elastography box. This was not substantiated by a statistical test. The failure to correlate with CK was also reported in a previous study using MRI [520].

Out of the four muscle tests, the ETGUG (total time) and grip strength tests demonstrated the best correlation outcomes. These tests, combining functional and strength assessments, can be recommended in future research due to ease of application and positive outcomes. Regarding muscles, the VL showed a substantive difference in SWV between the groups and was associated with muscle strength impairment and moderate correlations with MRI oedema. It is a more accessible and easier muscle to scan due to its location and size and also does not require a special positioning like the hamstrings. Therefore, it is recommended that future research focuses on VL as the most reliable muscle to be assessed.

This study is one of the first steps towards evaluating SWE muscle stiffness as an imaging biomarker in IIM. The work has revealed the common muscles affected and the best muscle position to detect the changes in. The findings contribute towards defining and developing the limited role of ultrasound in managing IIM. SWE is expected to be most useful in monitoring disease activity since several available methods, including biopsy, may not be feasible on a routine basis. The correlations with MRI suggest that SWE could be useful in guiding muscle biopsy to regions of active muscle inflammation. With further research, SWE can be incorporated into the diagnostic criteria of IIM.

Notwithstanding the limitations below, the significant results in this study have suggested multiple questions warranting further investigation. Future studies should evaluate newly suspected and treatment naïve IIM patients with SWE then follow them prospectively to first, determine if SWE readings predict a future diagnosis of IIM and second, if SWE is responsive to treatment changes. To achieve a power of 90% (alpha 0.05), the required sample sizes in future studies to detect 20%, 15% and 10% SWV difference in the VL are 50, 80 and 154 participant per group respectively. Further powered studies are needed to investigate disease duration and IIM subtypes on SWE. Moreover, it is unknown if inactive patients will exhibit the same reduction in muscle stiffness. More broadly, testing muscle echogenicity on B-mode can provide a composite of useful ultrasonographic features alongside SWE.

5.5.1 Limitations

The findings of this study are subject to several limitations. The study is considered relatively small; nevertheless, the sample size is larger than previous studies on older modalities. The differences between the types of myositis and the effects of the medications including steroid and disease-modifying agents are unknown. Furthermore, the CK values were not tested on the same day due to feasibility and funding limitations. Rather, they were extracted from the latest requested laboratory test. This may have affected the accuracy of its related results.

Furthermore, inter-reader reproducibility was not analysed due to the unavailability of a secondary reader. Cut off values were also not computed to calculate sensitivity and specificity as well as positive predictive value and negative predictive value due to the unbefitting study design and small sample size. Hence, only the AUROC was reported to evaluate the diagnostic performance of SWE. It was not possible to blind the SWE operator to the participants' disease status due to being actively involved in recruitment. However, the results of the MRI scores and muscle assessment were not available during the scan. Despite these limitations, the study included well-matched healthy controls and tested the correlations with strength, CK and MRI to provide an extensive assessment of SWE for the first time.

5.6 Conclusions

In conclusion, muscle stiffness, as quantitatively measured by SWE, appears to be lower in active IIM patient compared to matched healthy controls. Reduced muscle stiffness is likely to be associated with muscle weakness and MRI signs of oedema and atrophy. SWE shows promise as a non-invasive tool for the investigation of biomechanical changes in muscle in patients with IIM. This research is one of the first steps towards validating the usefulness of SWE in the management of IIM. Further studies are needed to confirm these findings and to investigate the responsiveness of SWE for monitoring disease activity.

Chapter 6 Corticosteroids effect on muscle stiffness

This chapter describes a prospective longitudinal cohort study investigating muscle stiffness in patients receiving high doses of oral corticosteroid medication at risk of developing steroid-induced myopathy. Muscle stiffness in addition to relevant muscle characteristics are followed-up and analysed after three and six months of commencing treatment.

6.1 Introduction

The previous two chapters explored the influence of ageing on muscle stiffness and established the face validity of shear wave elastography (SWE) after detecting altered muscle stiffness in patients with myositis. This chapter looks at the responsiveness aspect of SWE.

Exogenous corticosteroids are analogous synthetic pharmaceutical medications to the naturally occurring hormones produced by the adrenal glands. Corticosteroids therapy is commonly used for a range of medical conditions due to its powerful anti-inflammatory and immunosuppressive effects [521]. Reports from 1989 to 2008 estimated the prevalence of corticosteroid usage at 0.85% of the population in the UK [522] whereas in the USA the percentage is slightly higher at 1.2% of which 65.2% reported usage duration ≥90 days and 42.2% ≥2 years [523].

Despite the efficacy of corticosteroids, they are linked to numerous side effects, most notably osteoporosis, adrenal suppression, diabetes and myopathy. As a whole, these effects have been estimated to cost the UK at least £165 per patient annually to manage [524]. This chapter focuses on corticosteroid-induced myopathy (CIM), a non-inflammatory condition affecting largely the proximal muscles and associated with muscle weakness, wasting and fatigability.

Skeletal muscle is a major target of corticosteroid hormones to regulate protein and glucose metabolism. Loss of muscle mass and function occurs in multiple catabolic diseases (e.g. cancer cachexia and sepsis) when endogenous corticosteroid levels are elevated [525]. CIM is historically associated with fluorinated corticosteroids, but can also occur in other non-fluorinated

formulations [525]. For example, prednisolone, an oral corticosteroid drug with predominant glucocorticoid and low mineralocorticoid activity, is linked with myopathic side effects like weakness and atrophy [345, 526-534]. This commonly prescribed drug will later be the focus of this study.

The mechanisms of CIM are associated with two primary actions. First, the decline in protein synthesis by inhibiting the transport of amino acids into the muscle (anti-anabolic action) [535]. Secondly, the rise in the catabolic rate of protein breakdown by activating the release of major proteolytic systems (catabolic action) [536]. These two actions lead to muscle atrophy, predominantly in type IIb muscle fibres [358, 537]. Further details on the underlying mechanisms are explained in Schakman et al.'s review [538].

The risk of CIM appears to be higher in elderly and inactive patients [525]. Research into the epidemiology of this acquired myopathy is scarce. Clinical presentation is insidious; it usually starts with proximal lower limb muscle weakness with/without pain [539]. A common complaint is a difficulty standing from a chair and climbing stairs. Acute forms of CIM may occur and have significant consequences such as rhabdomyolysis, which can lead to kidney failure [346]. Additionally, patients can have severe dyspnoea when the respiratory muscles become affected [347]. Therefore, CIM have significant clinical implications.

There is a wealth of evidence substantiating the association between oral corticosteroids and myopathy. Multiple case studies were published, but Bowyer et al. [532] in 1985 was one of the first to investigate this association on a larger group of 60 subjects treated with oral-corticosteroids. They reported a significant reduction in muscle strength in 64% of the 25 patients taking ≥40mg/day compared to healthy controls. Later, in 1994 Decramer et al. [528] tested 21 patients on corticosteroids for asthma; they reported the incidence of muscle weakness in 8 subjects (38%).

In a matched case-control study of 367 chronic lung disease patients on long-term corticosteroids, Walsh et al. [345] found that patients had a high incidence of muscle weakness (59.8%) compared to controls (19.3%) (p<0.001). This derived an odds ratio of 6.7 (95% CI 4.8 to 9.3) for the risk of developing CIM. More recently, Levine et al. [540] reported that 60% of their patients

complained of leg weakness and 20% them demonstrated objective signs of weak muscle strength. Not all studies have reported high incidence rates like the ones described above. For example, two previous studies reported incidence rates of only 2% and 13% [526, 527]. This disparity can be related to the underlying conditions treated by corticosteroids as well as the methods used to determine CIM.

In rheumatology, corticosteroids are the backbone of the management for a number of inflammatory-mediated disorders. In many cases, the steroids are used only for short periods and at a relatively low dose. However, more serious conditions such as vasculitis require much higher doses and for longer periods. This is particularly true for patients with giant cell arteritis (GCA), an inflammatory, autoimmune vasculitis affecting predominantly large and medium-sized arteries. This potentially life and sight-threatening condition require prompt commencement of ‘high-doses’ of prednisolone (often at 40–60 mg) with prolonged treatment thereafter at a reduced dose.

Few studies had looked at corticosteroid side effects in GCA. However, the majority overlooked the myopathic side effects in their methodologies [541-543]. Nevertheless, Proven et al. [544] prospectively assessed 125 GCA patients for muscle weakness based on the physician’s physical examination of proximal muscles. They reported that “most patients” developed muscle weakness; the exact incidence and severity were not mentioned due to poor data recording.

Currently, the identification of muscle involvement is largely based on patient-reported symptoms and physical evidence of weakness using manual muscle testing methods. However, the diagnosis and monitoring of CIM may be challenging as these features can be non-specific and poorly sensitive to change. The literature reviewed above demonstrated an apparent discrepancy in the methods utilised for identifying CIM. For example, Walsh et al. [345] diagnosed myopathy based on a questionnaire asking the patients “whether they had difficulty getting out of a chair or climbing stairs compared with others of their own age”. In contrast, Decramer et al. [528] measured quadriceps strength on a dynamometer, whereas Boyer et al. [532] used dynamometry to evaluate the hip flexors and extensors in addition to manual muscle testing.

Proven et al. [544] used the physician's subjective muscle strength assessment as their evaluation tool.

There are no established guidelines for workup and management of CIM. In the meantime, the diagnosis depends on the clinical diagnosis of characteristic symptoms of disease onset to exclude other likely alternative causes. Strength regeneration within 3 to 4 weeks post-tapering of corticosteroids helps in establishing the diagnosis. Creatine kinase is typically unremarkable as well as other muscle enzymes [356]. Muscle biopsy can reveal atrophy of type IIb fibres with significant size variation as well as an absence of inflammatory infiltrates [358].

The role of imaging is so far limited to assessing muscle mass since CIM can consequently lead to muscle atrophy. Electromyography (EMG) had been used extensively in old studies to diagnose CIM and was stated that it "provides the only reliable means of diagnosis and assessment" [533, 534]. However, its usefulness was contested in later reviews after establishing that EMG is normal in most cases or yields inconsistent findings [545, 546]. A recent review by Minetto et al. [547] has reviewed various tools for diagnosing and monitoring CIM. It highlighted the importance of quantitative tests and the lack of predictive and prognostic tools for the steroid myopathic process.

The morphological alterations observed in histological evidence supports a hypothesis of altered muscle elasticity in CIM [358, 537]. A recent preclinical study subjected eighteen rats to a 10-day glucocorticoids treatment to study its effect on muscles' biomechanical properties [548]. It showed a significant 10% reduction in muscles' elasticity ($p<0.001$). This finding supports the hypothesis and reveals promise for the use of SWE clinically to monitor muscles' response to treatment before the development of CIM.

It is so far unknown if the use of oral corticosteroids alters muscle elasticity in human subjects. To date, no studies have utilised SWE for this purpose. Moreover, limited research has included a combined assessment of muscle mass, strength and performance as recommended in the diagnostic workup of CIM [547]. Investigating the combination of these muscle aspects in patients taking high corticosteroid doses could provide new insights into the mechanism of CIM development.

6.2 Aims

The main aim of the study in this chapter was to investigate the responsiveness of muscle stiffness as measured by SWE and physical strength tests in patients exposed to high doses of corticosteroid treatment.

6.3 Methods

6.3.1 Study design

This study was conducted as a longitudinal cohort study at Leeds Teaching Hospitals in the UK between May 2017 to October 2018. GCA was the targeted pathology for this study since patients affected require high-dose corticosteroid treatment over prolonged periods of a few months or years [352]. Moreover, GCA is not known to be primarily associated with muscle conditions, making it ideal for the investigation of iatrogenic muscular side effects.

GCA patients were examined at the baseline (up to 14 days post-treatment initiation) then followed-up after three and six months (± 15 days). These follow-up time points were selected based on the suspected onset of early signs of myopathy [534]. Patients were compared at baseline to age and gender-matched healthy controls to evaluate their muscle characteristics. The frequency matching method was employed as described in the previous chapter. Healthy controls were only evaluated at baseline and not followed-up.

No formal sample size/power calculations have been carried out due to a lack of available data. However, to estimate parameters for powering future research on CIM, published rules of thumb recommend a minimum of 12 subjects per group of interest to provide a reasonable effect size estimate [505, 506]. Written informed consent was obtained from all participants. The study had been approved by a UK research ethics committee under the same approval to the previous two studies.

6.3.2 Patients

6.3.2.1 Inclusion criteria

1. 18 years or older.

2. suspected or diagnosed with GCA according to the American College of Rheumatology (ACR) classification guidelines [549].
3. Due to start or started (≤14 days) on prednisolone (≥40 mg/day).

6.3.2.2 Exclusion criteria

1. Presence or history of any muscle condition.
2. On or had corticosteroid treatment >5 mg/day for more than three months in the past five years.
3. Taking corticosteroid for a chronic obstructive pulmonary disease for more than six months in the past five years.

Matched healthy controls were eligible if they were asymptomatic adults, not had any dose of corticosteroids as a treatment in the past five years and did not have a history of any muscle condition.

6.3.2.3 Recruitment

Patients were approached if the referring rheumatologists deemed the case as a ‘possible GCA’ and immediately initiated treatment to avoid irreversible complications before undergoing a temporal artery biopsy to establish the diagnosis. Patients were commenced on prednisolone 40–60 mg/day according to the followed established guidelines. The higher dosage (60 mg/day) was prescribed in complicated GCA cases with vision loss symptoms. The corticosteroids were rapidly tapered to stop the treatment if the subsequent temporal biopsy results were negative and the clinical suspicion was not high. Otherwise, the patient continued on the corticosteroids regimen and gradually tapered (unless relapse occurs) according to the management guidelines [352] as follows:

1. Initial prednisolone dose (40–60 mg/day) continued for four weeks until resolution of symptoms and laboratory abnormalities.
2. Dose reduced by 10 mg every two weeks to 20 mg;
3. then reduced by 2.5 mg every 2–4 weeks to 10 mg;
4. then reduced by 1 mg every 1–2 months provided there is no relapse.

6.3.3 Clinical characteristics

Relevant patient characteristics were collected including age, gender, body mass index (BMI). Additionally, muscle mass and fat mass were analysed

using a bioelectrical impedance analyser [Tanita DC-430 MA (Tanita Europe B.V., Manchester, UK)]. The cumulative dose of corticosteroids and average daily dosage were noted. The previous and following variables were assessed at each visit.

6.3.4 Shear wave elastography

The SWE methodology is described in detail in chapter 4 and follows the acquisition technique recommendations of chapter 3. As CIM mostly affects proximal muscles [539], the scanned muscles included the quadriceps [vastus lateralis (VL), rectus femoris (RF), vastus medialis (VM) and vastus intermedius (VI)], the hamstrings [biceps femoris (BF), semitendinosus (ST) and semimembranosus (SM)] and the biceps brachii (BB). The muscles were scanned in a relaxed resting position with no active contraction. The quadriceps were also scanned with the knee flexed at 90° in a sitting position to assess the muscles' passive elastic property. Only the dominant side was assessed due to time constraints and the previous evidence reporting pronounced muscle atrophy at the dominant leg in patients with CIM [540].

6.3.5 Muscle assessments

The review by Minetto et al. [547] suggested the combined assessment of muscle strength and physical performance and recommended the incorporation of dynamometers in the diagnosis and monitoring of CIM. Therefore, handgrip strength was assessed using an isometric dynamometer [386]. Isokinetic knee extension and flexion was used to determine the quadriceps and hamstrings strength [482]. Previous evidence showed that this test demonstrated diminished strength in CIM [528, 532]. Muscle function and performance were evaluated using the 30-second chair stand test (CST) [405] and the expanded timed get-up-and-go (ETGUG) test [469]. The detailed protocol for each test is described in the methodology section of chapter 4.

6.3.6 Statistical analysis

Descriptive statistics were expressed as frequencies for categorical data and as means (standard deviations) or medians for continuous data depending on the distribution. Independent sample t-test was employed to test for difference between healthy controls and patients at the baseline.

The difference in SWV between the timepoints was correlated with the differences in muscle strength and functional tests using the Pearson's correlation coefficients. This analysed whether the longitudinal changes in SWV were associated with changes in muscle strength and function. The effect of cumulative corticosteroid dose at 3 and 6 months on SWV changes of each patient was plotted in a line chart.

Appropriate assumptions for each statistical tests were verified. The tests were conducted and reported on each muscle separately. An alpha level (p-value) <0.05 was considered statistically significant. Statistical analysis was performed using SPSS version 25 (Armonk, NY: IBM Corp).

6.3.6.1 Linear mixed models

In longitudinal data, the observations for each participant usually correlate since they share the same subject attributes. Ignoring these within-participant correlations, as in repeated measures ANOVA, can result in reduced statistical power and bias towards non-significance. Moreover, observations taken closer together are expected to be more correlated compared to observations taken further apart as several influential and confounding factors may change over time. Linear mixed models, a form of multilevel modelling based on regression methods, takes this into account by modelling the within-participant correlations using the covariance structure. The variance around the outcome measure (i.e. SWV) at each visit and the within-participant correlations are incorporated in the covariance structure.

The longitudinal data for the GCA patients were analysed using linear mixed models to test if SWV significantly changes after three and six months of corticosteroid treatment following previously described guidance [550]. This multilevel modelling technique evaluates the dependent variable (i.e. SWV) initially then adds the longitudinal timepoints to test if the data fit the regression model. It is flexible, makes fewer assumptions about homogeneity of variance and is more tolerant of the missing data at the last visit compared to other methods such as repeated measures analysis of variance (ANOVA) [550].

The models were estimated using the restricted maximum likelihood method due to its suitability for small sample sizes. Each model was initially conducted as an unconditional base growth model then repeated in a second model after

adding the time variable to determine if adding the follow-up visits will result in a significantly better model fit by comparing their -2 log likelihood (-2LL). No other variables were included due to the small sample size limiting statistical power. The autoregressive covariance structure [AR(1)] was selected due to its suitability in longitudinal studies.

6.4 Results

Seventy-nine patients with GCA were screened to take part in the study; 20 patients met the eligibility criteria and agreed to take part in the study; 6 were lost before the 3-month follow-up. Therefore, a total of 14 patients formed the basis of this study and were followed-up. The flowchart below in Figure 6-1 highlights the recruitment timeline including the 7 patients dropped out before the 6-months visit.

The mean ± SD age of the GCA cohort was 68.2 ± 4.3 years (range 61.3–76.5); ten (72%) of the cohort were female. The patient characteristics and corticosteroid information are listed in Table 6-1. They were recruited on average seven days (range -1 to 12 days) after commencing corticosteroid treatment. The mean (SD, range) for cumulative steroid dose was 2701 mg (619, 2280–4190) and 4233 (926, 2962–5632) at 3 and 6-months respectively. Two patients had hypertension, one had prostate hypertrophy and one had hypothyroidism. Ten patients (72%) started on 40 mg of prednisolone, one (7%) on 50 mg and three (21%) on 60 mg. Additional prescribed medications included Alendronic acid (n=7, 50%), Omeprazole (n=3, 21%), Calceos (n=3, 21%), vitamin D (n=1, 7%), Lansoprazole (n=1, 7%), Aspirin (n=1, 7%), Co-codamol (n=1, 7%) and Levothyroxine (n=1, 7%).

All of the patients fulfilled the ACR classification criteria of GCA. Half of the patients had a positive temporal artery biopsy, one refused the procedure and the remaining six had a negative biopsy but were clinically diagnosed as GCA (strong clinical symptoms and rapid response to prednisolone). None of the patients complained of limb claudication. Two patients presented with symptoms of polymyalgia rheumatica (both had positive temporal biopsies).

The GCA cases were matched to healthy controls to evaluate their muscle condition at baseline. Table 6-2 shows the demographics and baseline

characteristics of the participants. It demonstrates that they were matched in age, gender and other body characteristics. In the muscle assessments, the GCA patients generally performed less well than controls; however, this difference did not reach statistical significance for most variables (Table 6-2).

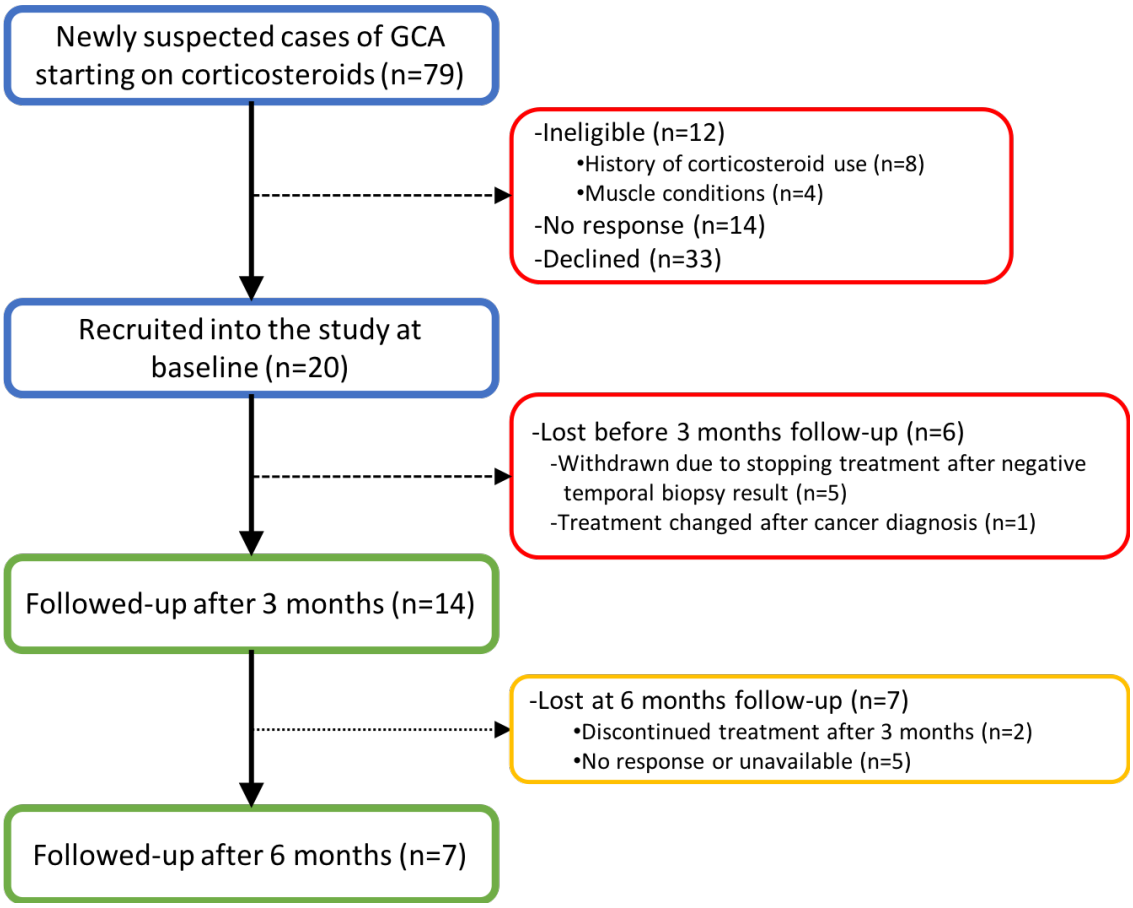

Figure 6-1 A flowchart of GCA patients screening, recruitment and follow-up.

Table 6-1 Clinical and corticosteroid dose information of the giant cell arteritis patients.

Case No	Sex	Age	Starting dose	Daily dose at 3m	Cumulative dose at 3m	Daily dose at 6m	Cumulative dose at 6m
1	Female	76.5	60	30	3935	7.5	5632
2	Male	63.0	40	10	2280	1	2962
3	Female	66.5	40	8	2723	10	4422
4	Female	69.2	40	12.5	2415	-	-
5	Female	74.3	40	15	2543	7	3474
6	Female	61.3	50	17.5	4190	-	-
7	Female	70.4	40	15	2690	10	3606
8	Female	67.8	60	15	3850	9	4767
9	Male	65.7	40	15	2990	-	-
10	Male	65.3	40	5	2375	-	-
11	Female	70.5	40	10	2712	-	-
12	Female	71.2	40	12.5	2528	17.5	4770
13	Female	69.5	40	15	2680	-	-
14	Male	63.7	60	60	3080	-	-

Dose unit is milligram. 3m= 3-months. 6m= 6-months. The dashes indicate data unavailability for the patients that missed the 6-months visit.

Table 6-2 Demographics and baseline characteristics of the GCA patients and healthy controls.

Characteristic	GCA patients*	Healthy controls*	*p*-value‡
Sex	10 Females (71%)	10 Females (71%)	1.00
Age (years)	68.2 (4.3)	68.0 (6.0)	0.91
Height (cm)	166.3 (11.9)	163.8 (8.7)	0.53

Weight (kg)	75.4 (16.8)	72.1 (9.7)	0.52
Body mass index (BMI)	26.6 (4.3)	27.0 (4.5)	0.79
Waist-hip ratio	0.90 (0.09)	0.90 (0.10)	0.95
Fat mass (kg) †	28.9 (13.8–31.8)	27.3 (24.4–29.3)	0.66
Muscle mass (kg) †	44.9 (37.7–52.0)	42.7 (38.6–44.2)	0.53
Muscle mass index	16.8 (1.8)	17.0 (2.5)	0.83
Ever smoked (yes)	7 (50%)	9 (64%)	0.44
Smoking pack-years †	12.0 (7.5–45.0)	8.8 (2.0–33.0)	0.63
Drinking alcohol	5 (35%)	5 (35%)	1.00
consumption (units/week) †	2.0 (1.0–13.0)	10.0 (1.5–38.0)	0.07
Visual analogue score of health (mm) †	25 (10–40)	4.5 (1–18)	0.07
ETGUGT, sit to stand (sec)	1.4 (0.4)	1.2 (0.4)	0.24
ETGUGT, Gait initiation (sec)	1.1 (0.5)	0.9 (0.3)	0.37
ETGUGT, Walk 1 (sec)	5.4 (1.6)	4.2 (1.0)	**0.027**
ETGUGT, Turn around (sec)	3.8 (1.1)	3.4 (1.4)	0.44
ETGUGT, Walk 2 (sec)	5.4 (1.6)	4.5 (1.0)	0.09
ETGUGT, Slow, stop (sec)	3.2 (0.9)	2.8 (0.8)	0.16
ETGUGT, Total time (sec)	21.0 (5.7)	17.0 (3.3)	**0.038**
30 sec chair sit-to-stands	12.2 (6.5)	16.1 (3.9)	0.06
Handgrip strength (kg)	25.9 (13.2)	29.7 (11.0)	0.42
Knee extension torque (Nm/kg)	1.03 (0.33)	1.18 (0.33)	0.23
Knee flexion torque (Nm/kg)	0.53 (0.21)	0.68 (0.22)	0.07
Knee extension power (W/kg)	0.57 (0.24)	0.71 (0.18)	0.09
Knee flexion power (W/kg)	0.29 (0.15)	0.40 (0.12)	**0.032**

* Data presented as mean and standard deviation unless otherwise stated.
† Median and interquartile range.
‡ *p*-values significant at 95% are highlighted in bold. Continuous variables tested via independent t-test or Mann-Whitney, and categorical data tested using Chi-square test.

6.4.1 Shear wave elastography

The baseline SWE readings for the GCA patients compared to matched healthy at baseline are represented in Table 6-3. It demonstrates no significant muscle stiffness differences (all $p>0.05$). For the patients, the mean and differences in SWV between the visits are listed in Table 4-4. The results are also graphically illustrated in the line charts for the muscles in the resting position in Figure 6-2 and during passive stretching in Figure 6-3.

In general, significant and consistent reductions were noted in the resting SWV measurements (Figure 6-2); the quadriceps readings under passive stretching showed greater variability (Figure 6-3). From baseline to 3 months, and to 6 months, there was a significant reduction in SWV in all the thigh muscles, but not in the BB muscle. During the resting position in the quadriceps and hamstrings, SWV decreased on average by 14% (range 8.3% – 17.3%) after 3 months and 18% (range 10.2% – 25.3%) after 6 months (Table 4-4).

SWE image examples from the quadriceps, hamstrings and BB are displayed in Figure 6-4. The two patients with PMR symptoms did not exhibit any different patterns compared to others.

Table 6-3 Shear wave elastography readings at the baseline for the GCA patients compared to healthy.

Muscle	GCA patients		Healthy controls		Difference	95% CI of the difference	*p*-value‡
	Mean*	95% CI	Mean*	95% CI			
Vastus lateralis (VL)	1.62 (0.16)	1.52, 1.71	1.68 (0.20)	1.56, 1.79	0.06	-0.08, 0.20	0.39
passively stretched	2.67 (0.33)	2.46, 2.88	2.80 (0.33)	2.60, 3.00	0.13	-0.14, 0.41	0.33
Rectus femoris (RF)	1.68 (0.11)	1.62, 1.74	1.74 (0.15)	1.65, 1.83	0.06	-0.05, 0.16	0.28
passively stretched	2.28 (0.63)	1.87, 2.68	2.19 (0.26)	2.03, 2.35	-0.09	-0.48, 0.31	0.66
Vastus Medialis (VM)	1.70 (0.33)	1.51, 1.88	1.60 (0.18)	1.48, 1.71	-0.10	-0.31, 0.11	0.34
passively stretched	2.41 (0.28)	2.23, 2.59	2.36 (0.21)	2.23, 2.49	-0.05	-0.25, 0.16	0.63
Vastus Intermedius (VI)	1.96 (0.33)	1.77, 2.15	1.85 (0.11)	1.79, 1.92	-0.11	-0.30, 0.09	0.26
passively stretched	2.42 (0.22)	2.28, 2.56	2.40 (0.28)	2.23, 2.57	-0.02	-0.23, 0.19	0.85
Biceps Brachii (BB)	1.83 (0.30)	1.66, 2.01	1.87 (0.23)	1.74, 2.00	0.04	-0.17, 0.25	0.71
Biceps Femoris (BF)	1.62 (0.17)	1.52, 1.72	1.65 (0.22)	1.52, 1.78	0.03	-0.12, 0.18	0.69
Semitendinosus (ST)	1.58 (0.15)	1.49, 1.66	1.65 (0.24)	1.51, 1.78	0.07	-0.09, 0.22	0.37
Semimembranosus (SM)	1.59 (0.15)	1.51, 1.68	1.58 (0.13)	1.51, 1.66	-0.01	-0.12, 0.10	0.81

* Data in m/s with standard deviation. ‡ Results are based on independent sample t-test.

Table 6-4 Mean muscle shear wave velocity in the GCA patients at each visit.

Muscle	Baseline		3 Months			6 Months			
	Mean (SD)	95% CI	Mean (SD)	95% CI	Difference to baseline	Mean (SD)	95% CI	Difference to 3 months	Difference to baseline
Vastus lateralis	1.62 (0.16)	1.52, 1.71	1.40 (0.10)	1.35, 1.46	-0.22 (-13.6%) ***p*<0.001**	1.31 (0.06)	1.26, 1.36	-0.09 (-6.4%) ***p*=0.037**	-0.31 (-19.1%) ***p*<0.001**
passively stretched	2.67 (0.33)	2.46, 2.88	2.66 (0.33)	2.46, 2.86	-0.01 (-0.4%) p=0.96	2.50 (0.34)	2.19, 2.81	-0.16 (-6%) *p*=0.91	-0.17 (-6.4%) *p*=0.30
Rectus femoris	1.68 (0.11)	1.62, 1.74	1.54 (0.13)	1.47, 1.62	-0.14 (-8.3%) ***p*=0.010**	1.41 (0.15)	1.28, 1.55	-0.13 (-8.4%) *p*=0.25	-0.27 (-16.1%) ***p*=0.002**
passively stretched	2.28 (0.63)	1.87, 2.68	1.99 (0.28)	1.82, 2.16	-0.29 (-12.7%) p=0.08	2.05 (0.11)	1.95, 2.15	0.06 (3%) *p*=0.99	-0.23 (-10.1%) *p*=0.16
Vastus Medialis	1.70 (0.33)	1.51, 1.88	1.36 (0.12)	1.29, 1.43	-0.34 (-20%) ***p*=0.001**	1.41 (0.15)	1.27, 1.55	0.05 (3.7%) *p*=0.99	-0.29 (-17.1%) ***p*=0.012**
passively stretched	2.41 (0.28)	2.23, 2.59	2.30 (0.22)	2.17, 2.43	-0.11 (-4.6%) p=0.07	2.30 (0.15)	2.16, 2.43	0 (0%) *p*=1.00	-0.11 (-4.6%) *p*=0.18
Vastus Intermedius	1.96 (0.33)	1.77, 2.15	1.62 (0.19)	1.51, 1.73	-0.34 (-17.3%) ***p*<0.001**	1.76 (0.22)	1.56, 1.96	0.14 (8.6%) ***p*=0.030**	-0.20 (-10.2%) *p*=0.26
passively stretched	2.42 (0.22)	2.28, 2.56	2.37 (0.34)	2.16, 2.58	-0.05 (-2.1%) p=0.39	2.08 (0.34)	1.77, 2.39	-0.29 (-12.2%) *p*=0.08	-0.34 (-14%) ***p*=0.013**
Biceps Brachii	1.83 (0.30)	1.66, 2.01	1.82 (0.18)	1.72, 1.93	-0.01 (-0.5%) *p*=0.94	1.84 (0.28)	1.58, 2.10	0.02 (1.1%) *p*=0.99	0.01 (0.5%) *p*=0.92
Biceps Femoris	1.62 (0.17)	1.52, 1.72	1.37 (0.09)	1.31, 1.42	-0.25 (-15.4%) ***p*<0.001**	1.21 (0.10)	1.12, 1.31	-0.16 (-11.7%) ***p*=0.022**	-0.41 (-25.3%) ***p*<0.001**
Semitendinosus	1.58 (0.15)	1.49, 1.66	1.36 (0.08)	1.31, 1.41	-0.22 (-13.9%) ***p*<0.001**	1.26 (0.08)	1.18, 1.33	-0.10 (-7.4%) ***p*=0.043**	-0.32 (-20.3%) ***p*<0.001**
Semimembranosus	1.59 (0.15)	1.51, 1.68	1.41 (0.11)	1.34, 1.47	-0.18 (-11.3%) ***p*<0.001**	1.35 (0.10)	1.26, 1.44	-0.06 (-4.3%) *p*=0.66	-0.24 (-15.1%) ***p*<0.001**

P-values computed using linear mixed models from the significance of difference estimates at 3 and 6-months. *P*-values significant at 95% are highlighted in bold.

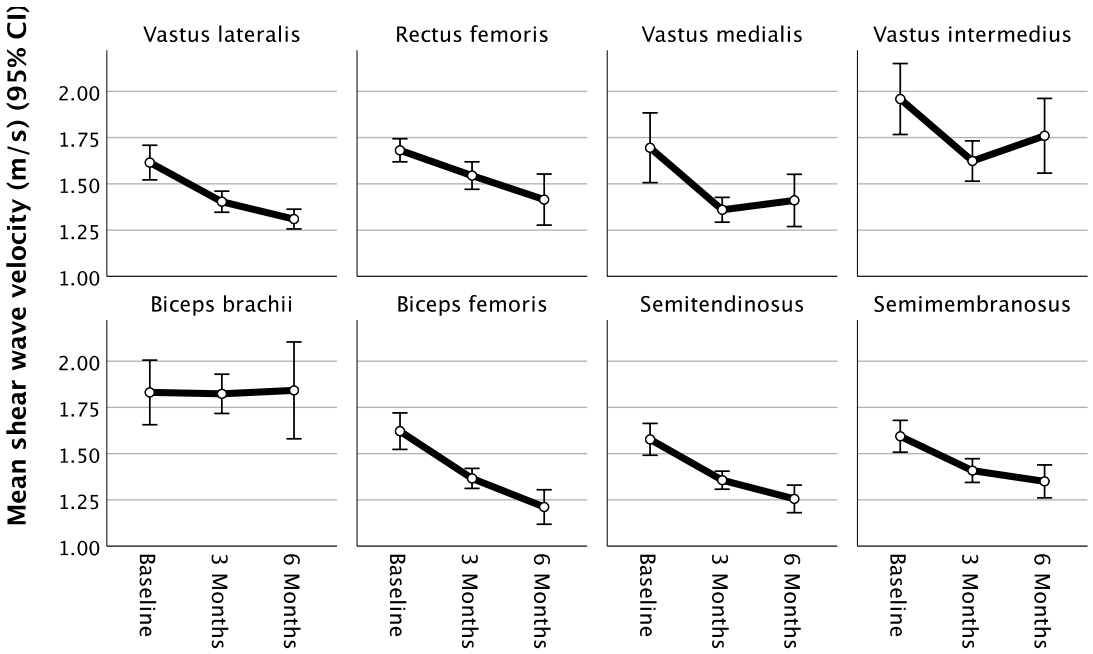

Figure 6-2 Muscle stiffness changes during the resting position in the GCA patients.

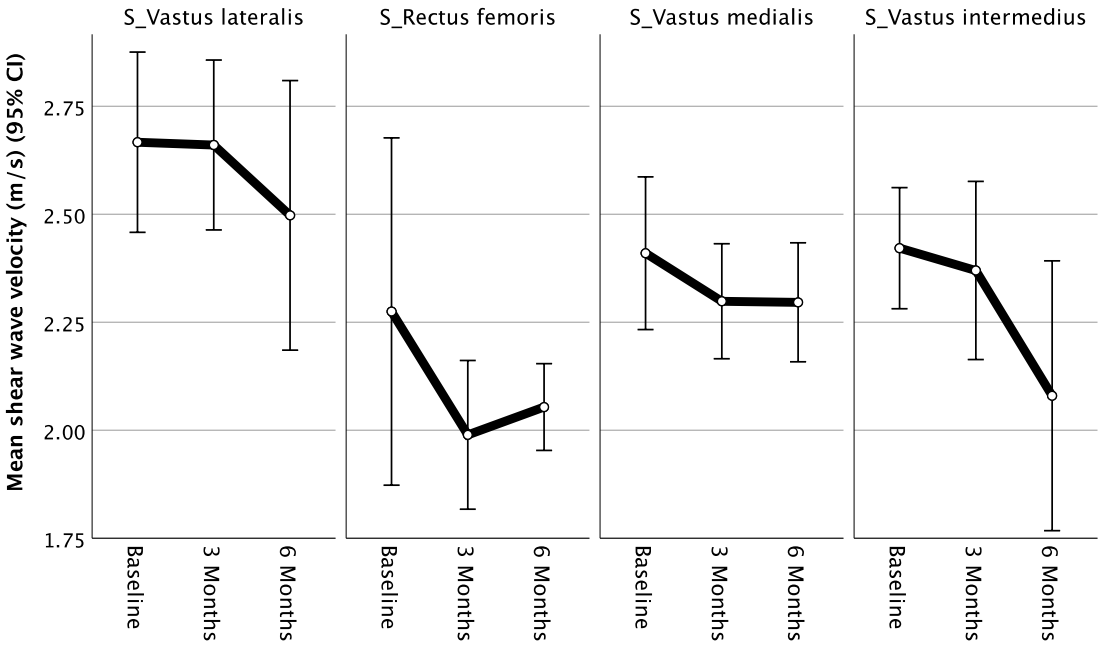

Figure 6-3 Quadriceps stiffness changes under passive stretching in the GCA patients.

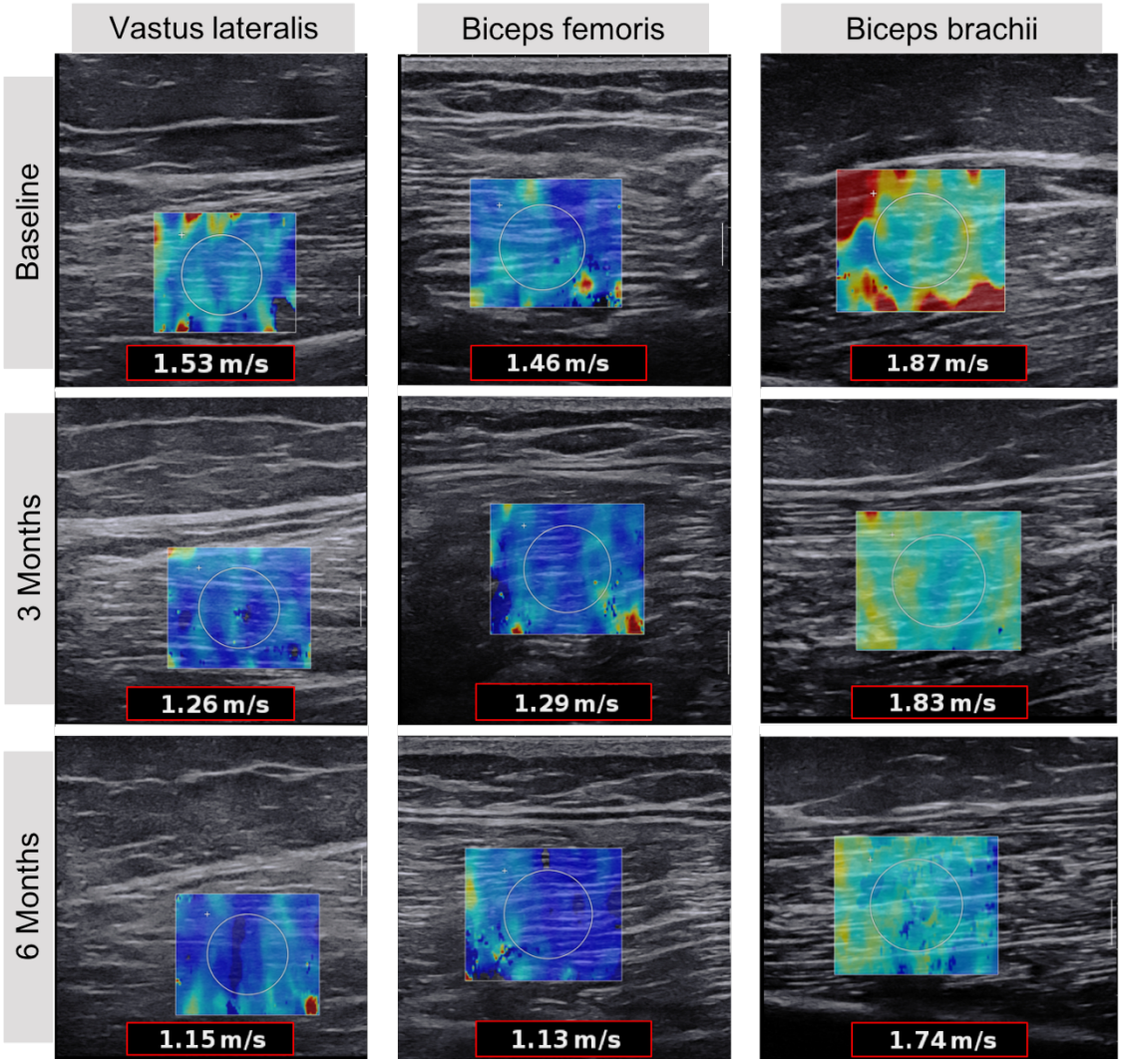

Figure 6-4 Longitudinal shear wave elastography examples with shear wave velocity measurements from several muscles.

The figure highlights the significant reduction with time in the VL and BF compared to the insignificant change in BB. SWE scale is 0–2.9 m/s on all images.

Linear mixed models were used to test the corticosteroids effect on SWV with time added as a fixed effect. The unconditional base model and time-factored model are represented in Table 6-5. Adding the longitudinal time-points in the second model explained a significant variation in the change of model fit (Δ fit) for most of the muscles. For example, in the VL, the SWV at 3-months was -0.21 m/s (95% CI -0.31 to -0.11) significantly lower than at baseline (p<0.001). At 6-months, the SWV was on average -0.31 m/s significantly lower than the baseline SWV of 1.62 m/s.

Inspecting the BB shows that time did not explain any significant variation. Moreover, the changes observed in the quadriceps during passive stretching

were generally variable and insignificant. In RF (stretched), although the model fit improved significantly, the estimates were generally weak. However, in the VI (stretched), the -0.34 m/s (-14%) reduction at 6 months was significantly lower than the baseline reading (p=0.001).

The Bonferroni-corrected multiple pairwise comparisons showed that the *p*-values for SWV difference between the 3 and 6 months were 0.037 (VL), 0.25 (RF), 0.99 (VM), 0.030 (VI), 0.99 (BB), 0.022 (BF), 0.043 (ST), 0.66 (SM), 0.91 (VL-stretched), 0.99 (RF-stretched), 0.99 (VM-stretched) and 0.08 (VI-stretched).

The age variable was initially considered to be adjusted for as a covariate in the model. However, it violated the assumption of linearity with the dependent variable (SWV) and was therefore dropped and considered an insignificant predictor in the longitudinal change of SWV.

Table 6-5 Mixed linear models and fixed effect estimates for shear wave velocity on the various tested muscles.

Vastus lateralis			
	Estimate (SE)	**95% CI**	***p*-value**
Model 1: unconditional growth.			
Fit (-2LL)= -18.938			
Intercept	1.47 (0.03)	1.41, 1.53	<0.001
Model 2: (time)			
Fit (-2LL)= -43.958			
Δ fit= 25.02 *p*-value= **<0.001**			
Intercept	1.62 (0.04)	1.52, 1.71	<0.001
Time=baseline	ref	ref	ref
Time=3 months	-0.21 (0.05)	-0.31, -0.11	**<0.001**
Time=6 months	-0.30 (0.05)	-0.41, -0.20	**<0.001**
Time (type III test of fixed effect*)	-	-	**<0.001**
Rectus femoris			
	Estimate (SE)	**95% CI**	***p*-value**
Model 1: unconditional growth.			
Fit (-2LL)= -25.294			
Intercept	1.57 (0.03)	1.52, 1.63	<0.001
Model 2: (time)			
Fit (-2LL)= -36.027			
Δ fit= 10.73 *p*-value= **<0.05**			
Intercept	1.68 (0.03)	1.62, 1.74	<0.001
Time=baseline	ref	ref	ref
Time=3 months	-0.14 (0.05)	-0.24, -0.04	**0.010**
Time=6 months	-0.27 (0.06)	-0.41, -0.12	**0.002**

Time (type III test of fixed effect)	-	-	**0.002**
Vastus medialis			
	Estimate (SE)	**95% CI**	***p*-value**
Model 1: unconditional growth.			
Fit (-2LL)= 12.248			
Intercept	1.50 (0.05)	1.41, 1.60	<0.001
Model 2: (time)			
Fit (-2LL)= -11.718			
Δ fit= 23.97 *p*-value= **<0.001**			
Intercept	1.70 (0.09)	1.51, 1.88	<0.001
Time=baseline	ref	ref	ref
Time=3 months	-0.34 (0.08)	-0.51, -0.16	**0.001**
Time=6 months	-0.28 (0.10)	-0.49, -0.07	**0.012**
Time (type III test of fixed effect)	-	-	**0.005**
Vastus intermedius			
	Estimate (SE)	**95% CI**	***p*-value**
Model 1: unconditional growth.			
Fit (-2LL)= 17.310			
Intercept	1.78 (0.05)	1.68, 1.89	<0.001
Model 2: (time)			
Fit (-2LL)= -0.594			
Δ fit=17.9 *p*-value= <0.001			
Intercept	1.96 (0.09)	1.76, 2.16	<0.001
Time=baseline	ref	ref	ref
Time=3 months	-0.34 (0.07)	-0.49, -0.18	**<0.001**
Time=6 months	-0.12 (0.10)	-0.32, 0.09	0.26
Time (type III test of fixed effect)	-	-	**<0.001**
Biceps brachii			
	Estimate (SE)	**95% CI**	***p*-value**
Model 1: unconditional growth.			
Fit (-2LL)= 5.630			
Intercept	1.83 (0.04)	1.74, 1.92	<0.001
Model 2: (time)			
Fit (-2LL)= 7.819			
Δ fit=2.19 *p*-value= >0.05			
Intercept	1.83 (0.08)	1.65, 2.01	<0.001
Time=baseline	ref	ref	ref
Time=3 months	-0.01 (0.09)	-0.2, 0.19	0.94
Time=6 months	0.01 (0.13)	-0.27, 0.30	0.92
Time (type III test of fixed effect)	-	-	0.98
Biceps femoris			
	Estimate (SE)	**95% CI**	***p*-value**
Model 1: unconditional growth.			
Fit (-2LL)= -7.065			
Intercept	1.44 (0.03)	1.37, 1.51	<0.001
Model 2: (time)			
Fit (-2LL)= -37.098			

Δ fit=30.03 *p*-value= **<0.001**			
Intercept	1.62 (0.05)	1.52, 1.72	<0.001
Time=baseline	ref	ref	ref
Time=3 months	-0.26 (0.05)	-0.37, -0.14	**<0.001**
Time=6 months	-0.41 (0.06)	-0.53, -0.29	**<0.001**
Time (type III test of fixed effect)	-	-	**<0.001**
Semitendinosus			
	Estimate (SE)	**95% CI**	***p*-value**
Model 1: unconditional growth.			
Fit (-2LL)= -19.407			
Intercept	1.42 (0.03)	1.37, 1.48	<0.001
Model 2: (time)			
Fit (-2LL)= -48.795			
Δ fit=29.39 *p*-value= **<0.001**			
Intercept	1.58 (0.04)	1.50, 1.66	<0.001
Time=baseline	ref	ref	ref
Time=3 months	-0.22 (0.03)	-0.30, -0.15	**<0.001**
Time=6 months	-0.34 (0.05)	-0.44, -0.23	**<0.001**
Time (type III test of fixed effect)	-	-	**<0.001**
Semimembranosus			
	Estimate (SE)	**95% CI**	***p*-value**
Model 1: unconditional growth.			
Fit (-2LL)= -24.429			
Intercept	1.47 (0.03)	1.42, 1.53	<0.001
Model 2: (time)			
Fit (-2LL)= -37.704			
Δ fit=13.28 p-value= **<0.025**			
Intercept	1.59 (0.04)	1.51, 1.68	<0.001
Time=baseline	ref	ref	ref
Time=3 months	-0.19 (0.04)	-0.28, -0.09	**0.001**
Time=6 months	-0.24 (0.05)	-0.35, -0.13	**<0.001**
Time (type III test of fixed effect)	-	-	**0.001**
Vastus lateralis (stretched)			
	Estimate (SE)	**95% CI**	***p*-value**
Model 1: unconditional growth.			
Fit (-2LL)= 21.913			
Intercept	2.63 (0.06)	2.51, 2.74	<0.001
Model 2: (time)			
Fit (-2LL)= 24.783			
Δ fit=2.87 *p*-value= >0.05			
Intercept	2.67 (0.09)	2.46, 2.88	<0.001
Time=baseline	ref	ref	ref
Time=3 months	-0.01 (0.13)	-0.28, 0.27	0.96
Time=6 months	-0.17 (0.16)	-0.52, 0.17	0.30
Time (type III test of fixed effect)	-	-	0.51
Rectus femoris (stretched)			
	Estimate (SE)	**95% CI**	***p*-value**

Model 1: unconditional growth.			
Fit (-2LL)= 40.455			
Intercept	2.11 (0.08)	1.95, 2.27	<0.001
Model 2: (time)			
Fit (-2LL)= 17.862			
Δ fit= 22.59 *p*-value= **<0.001**			
Intercept	2.30 (0.17)	1.93, 2.67	<0.001
Time=baseline	ref	ref	ref
Time=3 months	-0.29 (0.15)	-0.63, 0.04	0.08
Time=6 months	-0.25 (0.17)	-0.62, 0.11	0.16
Time (type III test of fixed effect)	-	-	0.18
Vastus medialis (stretched)			
	Estimate (SE)	**95% CI**	***p*-value**
Model 1: unconditional growth.			
Fit (-2LL)= 0.698			
Intercept	2.34 (0.04)	2.26, 2.42	<0.001
Model 2: (time)			
Fit (-2LL)= -3.832			
Δ fit=4.53 *p*-value= >0.05			
Intercept	2.43 (0.08)	2.26, 2.59	<0.001
Time=baseline	ref	ref	ref
Time=3 months	-0.13 (0.07)	-0.27, 0.01	0.07
Time=6 months	-0.12 (0.09)	-0.3, 0.06	0.18
Time (type III test of fixed effect)	-	-	0.18
Vastus intermedius (stretched)			
	Estimate (SE)	**95% CI**	***p*-value**
Model 1: unconditional growth.			
Fit (-2LL)= 20.815			
Intercept	2.33 (0.06)	2.21, 2.44	<0.001
Model 2: (time)			
Fit (-2LL)= 8.673			
Δ fit=12.14 *p*-value= **<0.05**			
Intercept	2.42 (0.06)	2.29, 2.55	<0.001
Time=baseline	ref	ref	ref
Time=3 months	-0.07 (0.08)	-0.23, 0.09	0.39
Time=6 months	-0.34 (0.11)	-0.60, -0.09	**0.013**
Time (type III test of fixed effect)	-	-	**0.028**

-2LL= −2 restricted log-likelihood (estimate of the model fit displayed in smaller-is-better form). SE= standard error. * Omnibus test of significance for the time variable. Δ fit= change in model fit [significance determined comparing the Δ fit value to the chi-square statistic critical values for 0.001 (99%), 0.025 (97.5%) and 0.05 (95%)].

Figure 6-5 below shows the profile of relative change (unitless) in SWV plotted as a function of cumulative corticosteroid dose received over the entire duration. No distinct pattern can be depicted. In other words, receiving a high cumulative corticosteroid dose did not result in a greater change in SWV and vice versa.

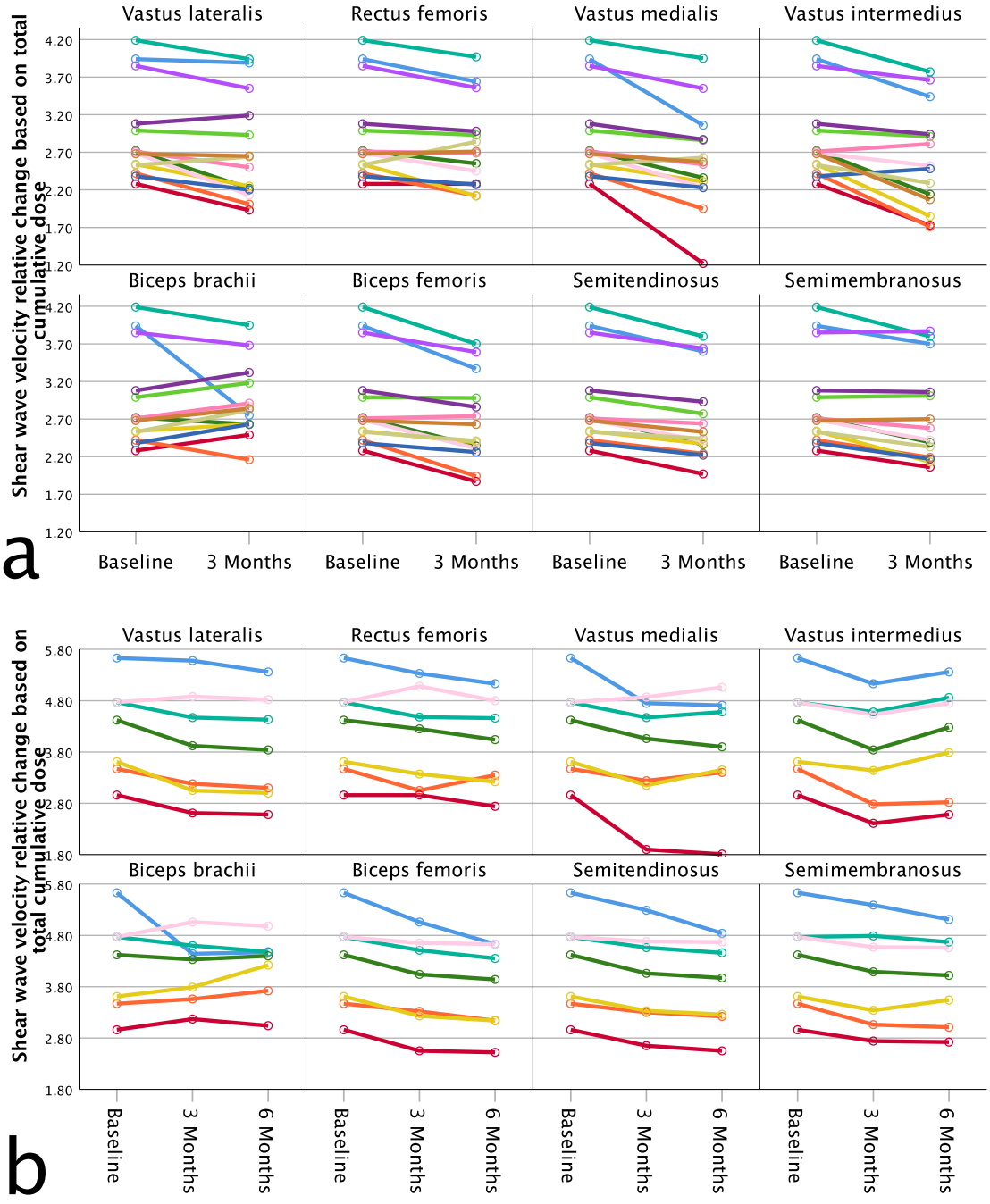

Figure 6-5 Change in shear wave velocity relative to the total cumulative dose received (grams) for each GCA patient at 3 (a) and 6 (b) months.

6.4.2 Muscle assessments

The longitudinal data for the muscle assessments are listed in Table 6-6. The results show unremarkable fluctuations in body composition. Functional and strength results generally remained similar to baseline.

Pearson's correlation coefficients were used to evaluate the association between SWV and muscle performance differences at the follow-up visits. The difference at 3-months for the isokinetic knee extension strength correlated significantly with SWV differences in VL, VI and SM with coefficients (*p*-value) of 0.54 (0.048), 0.69 (0.006) and 0.60 (0.022) respectively. Similar results were observed for the same muscles with isokinetic knee extension power. Weaker grip strength after 3-months correlated with lower SWV for ST (r=0.56; *p*=0.009).

For the changes after 6-months, the VL strongly correlated with isokinetic knee extension strength (r=0.93; *p*<0.001). Moreover, longer walking times in the ETGUG test after 6-months were associated with lower SWV in the VL (r=-0.80; *p*=0.031). The VM difference correlated with isokinetic knee extension power (r=0.84; *p*=0.017). The patients that performed fewer chair stands had a greater reduction in SWV for SI and SM with coefficients (*p*-value) of 0.79 (p=0.035) and 0.88 (0.008) respectively. The correlation coefficients for changes between the other muscles and tests were generally weak (r <0.30) or insignificant (p >0.05).

Table 6-6 Clinical and muscle assessment results at each visit for the GCA patients.

Muscle	Baseline	3 Months		6 Months		
	Mean (SD)	Mean (SD)	Difference to baseline	Mean (SD)	Difference to 3 months	Difference to baseline
Weight (kg)	75.5 (16.8)	77.6 (16.4)	2.1 (2.8%)	75.2 (15.1)	-2.4 (-3.1%)	-0.3 (-0.4%)
Body mass index (BMI)	27.1 (4.0)	27.9 (4.2)	0.8 (2.9%)	28.0 (4.3)	0.1 (0.3%)	0.9 (3.3%)
Fat mass (kg) *	29.0 (13–31)	28.5 (21–31)	-0.5 (-1.7%)	27.1 (22–32)	-1.4 (-4.9%)	-1.9 (-6.5%)
Muscle mass (kg) *	45.0 (38–52)	46.6 (42–55)	1.6 (3.6%)	45.5 (41–47)	-1.1 (-2.4%)	0.5 (1.1%)
Muscle mass index	16.8 (1.8)	17.5 (2.1)	0.7 (4.2%)	17.3 (2.1)	-0.2 (-1.1%)	0.5 (3.0%)
Visual score of health (mm) *	25 (10–40)	19 (8–46)	-6 (-24%)	15 (4–21)	-4 (-21.0%)	-10 (-40%)
ETGUGT, Total time (sec) †	21.0 (5.7)	21.2 (6.3)	0.2 (0.9%)	19.3 (5.4)	-1.9 (-9.0%)	-1.7 (-8.1%)
30 sec chair sit-to-stands	12.2 (6.5)	11.0 (4.5)	-1.2 (-9.8%)	10.7 (2.4)	-0.3 (-2.7%)	-1.5 (-12.3%)
Handgrip strength (kg)	25.9 (13.2)	26.7 (12.7)	0.8 (3.10%)	28.8 (11.3)	2.1 (7.9%)	2.9 (11.2%)
Knee extension torque (Nm/kg)	1.03 (0.34)	1.04 (0.33)	0.01 (1.0%)	1.07 (0.40)	0.03 (2.9%)	0.04 (3.9%)
Knee flexion torque (Nm/kg)	0.53 (0.22)	0.60 (0.25)	0.07 (13.2%)	0.63 (0.16)	0.03 (5.0%)	0.1 (18.9%)
Knee extension power (W/kg)	0.57 (0.24)	0.56 (0.26)	-0.01 (1.8%)	0.57 (0.24)	0.01 (1.8%)	0 (0%)
Knee flexion power (W/kg)	0.29 (0.15)	0.34 (0.17)	0.05 (17.2%)	0.34 (0.09)	0 (0%)	0.05 (17.2%)

† Median and interquartile range. * Other ETGUG test components had similar trends and were therefore omitted.

6.5 Discussion

This study aimed to investigate muscle stiffness changes in patients receiving high doses of corticosteroids after 3 and 6-months. This is the first study to conduct this type of quantitative analysis research. The main result indicates that the proximal lower limb muscles of GCA patients can lose on average 15% and up to one-quarter of its stiffness after being exposed to high corticosteroid dose therapy for 3 and 6-months. Additionally, this loss correlated with muscle strength.

Corticosteroids are one of the commonest medications causing proximal myopathy in clinical practice, which is largely due to a high volume of prescriptions [551]. The diagnosis of CIM currently is merely based on evaluating the temporal onset of muscle weakness symptoms relative to commencement of corticosteroids. Generally, there is no agreement on the exact onset of CIM. Old studies mentioned that steroid myopathy symptoms usually start after 3–6 months for doses higher than 15–20 mg/day [349].

In this study, there was evidence of muscle stiffness changes after 3 and 6-months. These changes might be explained by the microscopic morphological alterations induced by the catabolic and anti-anabolic effects of corticosteroids on skeletal muscle [358, 537]. However, the cumulative dose of corticosteroids received either at 3 or 6-months was not related to the magnitude of the detected stiffness changes.

No studies thus far have been conducted to investigate the usefulness of SWE or similar imaging modalities for diagnosis or monitoring of CIM on humans. Nonetheless, the findings are in line with a recent preclinical study on rats, which demonstrated a significant reduction in muscle stiffness after glucocorticoid treatment [548]. Their reported reduction of 10% is close to the average change of 15% in this study regardless of the relatively different follow-up durations. They also stated that dosage (100ug/100g vs 50ug/100g) did not influence muscle stiffness which is in agreement with the presented results.

A recent case study of Cushing's syndrome myopathy suggested the usefulness of muscle echo intensity as a recovery sign after resolution of the hypercortisolaemic state [552]. Moreover, Nawata et al. [529] recently used

computed tomography and showed a significant reduction in muscle mass (p=0.039) in a mixed group of patients taking corticosteroids (>30 mg/day) for an average of three months. The usefulness of computed tomography, however, is complicated by the cost and exposure to ionising radiation.

A meta-analysis has shown that the rate of musculoskeletal side effects in low (≤7.5 mg) to medium doses (7.5 – <30 mg) is low at 12 cases per 100 patients a year compared to psychological and behavioural side effects with double the incidence [553]. For prolonged high-dose corticosteroid exposure, the reported prevalence of CIM is remarkably variable in the literature ranging from 2% to 60% [345, 526, 527, 540]. In this study, there was no significant muscle weakness observed in the follow-up visits suggestive of CIM. The patients performed on average similar to the baseline, except for the number of chair stands that decreased gradually at follow-up visits. Nawata et al. [529] reported an improvement in muscle strength after 3-months of corticosteroid treatment despite a significant reduction in muscle volume.

In the present study, the changes in muscle strength were significantly associated with changes in muscle stiffness whereby patients who performed worse in the follow-ups lost more muscle stiffness. At baseline, the patients presented with a headache and pain due to the GCA symptoms and were generally feeling lethargic and malaise. This may have diminished their actual physical performance in the muscle assessments. Indeed, the self-reported general state of health rating (VAS score) improved gradually at the follow-ups. Furthermore, they performed on average worse than the healthy controls at baseline. It can be argued that if the patients' baseline muscle performance was normal, the correlations between SWV and muscle assessment differences would have been stronger and more consistent. However, it was not possible to test the patients in an asymptomatic state without sacrificing the enrolment time at baseline and potentially missing muscle stiffness changes due to the corticosteroids.

Age was not associated with muscle stiffness in this study. This can be expected considering the small sample size and range of ages involved. However, it may still influence muscle elasticity if future studies recruit a broader range of ages based on the findings in chapter 4. The preclinical study cited above showed that older rats were more prone to lose their muscle

stiffness than younger rats [548]. Therefore, the exact effect of ageing on muscle stiffness changes in CIM should be evaluated in the future.

Steroid-induced atrophy seems to affect glycolytic fast-twitch fibres (i.e. type IIb) [537]. The BB has a high proportion (>60%) of type II fibres [554] compared to a balanced ratio in the quadriceps and hamstrings [555]. This knowledge does not support the current results of preserved muscle stiffness in BB and diminished stiffness in quadriceps and hamstrings. The lack of muscle stiffness alteration in BB was also reported in the previous chapter on myositis patients. The reason behind the difference is therefore not clear. Overall, the VL and BF demonstrated the least variability and most consistent significant changes between the time points. Moreover, the muscle stiffness changes were observed during resting and passive stretched positions. However, the readings variation during passive stretching was large, and the changes were less consistent compared to the resting position.

The patients in this study were followed-up after 3 and 6-months. This was decided based on previous evidence of symptom manifestation after this period [349]. However, other studies indicate that CIM onset may take as long as one year [351]. With regard to dose, several reports support its significant role in CIM [346, 350]. For example, Walsh et al. [345] mentioned that the risk of myopathy is sevenfold higher in patients consuming 60 mg/day compared to 5 mg/day. Moreover, Decramer et al. [528] found a significant negative correlation between the average daily dose of corticosteroids and muscle strength. Therefore, this study focused on patients taking high doses of corticosteroids (>40 mg/day). However, the results highlighted that changes in SWV were not influenced by cumulative received dose at both visits. It would be interesting to compare the present changes to patients receiving lower doses (e.g. 10 mg/d) for the same duration.

Clinically, the tools to monitor or diagnose CIM are extremely limited and inadequate. EMG does not offer positive findings until late chronic stages of CIM [357]. Muscle enzymes such as CK and aldolase usually appear within normal limits [356]. Muscle biopsy can show signs of type IIb myofibre atrophy but is not feasible as a monitoring tool. No evidence has previously demonstrated the clinical usefulness for quantitative or qualitative MRI in CIM.

The clinical goal in CIM is to prevent any myopathic changes. Changes in muscle stiffness could be a useful early sign for physicians to be aware of CIM and supports a decision to help taper the corticosteroid dose promptly. In cases where dose reduction is not possible, physicians may consider alternative prophylactic strategies (e.g. physiotherapy and high protein diet) [556]. This focuses on the prevention of CIM rather than identifying it at later stages when atrophy has occurred. The presented results highlight that the muscle strength loss was marginal compared to the SWV observed differences. This may suggest that muscle stiffness alterations may precede CIM symptoms of muscle weakness. However, this has to be validated in a future study to establish the usefulness of SWE for evaluating early signs of subclinical CIM.

The promising findings demonstrated in this chapter call for future cohort studies to follow-up a larger sample of patients for a longer duration to assess if decreased muscle stiffness is a valid and reliable early sign for steroid myopathy. To detect a 15% difference in the stiffness of VL after 3 months with 90% power and 0.05 alpha level, a future study should aim to recruit a minimum of 63 GCA patients. Most of the recruited GCA patients would have stopped corticosteroids treatment soon after the last follow-up. Future studies should also aim to investigate the results in younger cohorts and on patients with other underlying pathologies that are expected to be on corticosteroids for long durations such as myositis, rheumatoid arthritis and chronic obstructive pulmonary disease.

6.5.1 Limitations

The results in this chapter are subject to a number of limitations. It was not pragmatically possible to blind the SWE operator to the patients' condition due to direct involvement in recruitment. However, the SWE operator was not aware of the participants' muscle performance at the time of scanning to minimise potential bias. Inter-operator reproducibility was not evaluated in this study. However, the decreasing trend observed on most muscles suggests that the changes were not merely due to day-to-day reading variability.

It was not feasible to study the patients before commencing treatment as the management guidelines recommend the immediate start of corticosteroids to prevent sight loss [352]. Corticosteroids can be commenced as a precautionary

measure in primary care centres before being seen by specialised rheumatologists and be screened for eligibility to participate in this study.

This study was designed as a prospective cohort study. The control group was only tested at the baseline to evaluate the baseline muscle stiffness measurements compared to the GCA cohort. It was not possible to follow-up the control group due to time limit constraints to complete the project. Although GCA rarely develops below 50 years, the sample included an old cohort with a mean age of 68.2 and comprised predominantly of female patients where risks of CIM are relatively higher [525]. Therefore, caution is advised when extrapolating these results to other cohorts of different demographics.

6.5.1.1 Sample size

The small sample size is acknowledged as a major limitation of the results. An attempt to improve the overall statistical power was made by employing multilevel modelling statistics. The mixed linear model improves the overall statistical power by accounting for within-subject correlations as it models the data using a covariance structure unlike repeated measures ANOVA [557].

Estimating the required sample size in multilevel models is complicated. Additionally, Kreft and de Leeuw [558] state that it may be impossible to suggest meaningful rules of thumb. This prevented the investigation of random effects associated with individual intercepts and slopes of each subject in the linear mixed model. In other words, it was not statistically feasible to test if different patients start at different points (intercepts) and respond differently to the corticosteroids (slopes). This can be tested in the future to evaluate if patients with a high baseline SWV lose their muscle stiffness faster compared to patients starting with low SWV.

The small sample size and number of longitudinal timepoints limited the investigation of further polynomial patterns in the applied growth model such as quadratic, cubic or logarithmic patterns. Hence, the data was only investigated for linear patterns. Moreover, the small sample size limited the evaluation of factor interactions in the model (e.g. sex*dose). Overall, statistical analysis was conducted conservatively to avoid weak or flawed inferences that the study power cannot support. Hence, risk analysis was not carried due to the small sample and lack of cut-off values.

6.6 Conclusions

In conclusion, the results show that muscle stiffness measured by SWE may become significantly reduced in GCA patients receiving high doses of corticosteroid after 3 and 6-months of treatment. Furthermore, higher reduction appeared to correlate with worse physical performance at the follow-up visits. Future research should study the results in a larger sample of patients for a longer duration to investigate if diminished muscle stiffness precedes CIM signs of muscle weakness. Assuming the preliminary results are validated by other studies, SWE has the potential to serve as a non-invasive clinic-based tool for detecting and monitoring early signs of the corticosteroid-induced myopathic process. Additionally, it may aid a physician's decision to taper corticosteroids more promptly. In the context of this thesis, the results demonstrated preliminary evidence of responsiveness validity for SWE in skeletal muscle.

Chapter 7 Muscle Stiffness in Rheumatoid Arthritis

This chapter describes a case-control study of rheumatoid arthritis patients of various disease activity. It includes an investigation of their muscle elasticity using shear wave elastography as well as an assessment of muscle strength.

7.1 Introduction

The previous chapters showed how muscle stiffness could be influenced by ageing (chapter 4), muscle inflammation (chapter 5) and corticosteroids (chapter 6). This chapter explores the potential muscle involvement in terms of abnormal muscle stiffness in patients with rheumatoid arthritis (RA).

Systemic extra-articular manifestations of RA are well described in the literature including cardiovascular disease, anaemia, interstitial lung disease, vasculitis, osteoporosis and ocular complications [559]. These are associated with reduced life quality, significant morbidity and increased mortality. The incidence of such nonarticular manifestation is approximated to be up to 40% in RA patients over the lifetime of the disease [560].

Myopathy is a recognised but less investigated symptom of rheumatoid arthritis compared to other extra-articular manifestations. Its aetiology is thought to be multi factorial including joint inflammation, myositis, vasculitis and drug-induced myopathies [338, 340]. Chapter 2 underlined the research activity focused on investigating muscle involvement in RA since 1940. Despite the early recognition, relatively little work has been conducted to characterise it further.

Few studies have investigated the frequency of muscle involvement occurring in RA [330, 331, 337-340, 367, 561]. Most have estimated the prevalence between 6% and 19% [330, 331, 367] whereas others reported it higher at 50%–70% [337, 340, 561]. All studies utilised invasive muscle biopsy to investigate the histological and immunohistochemical characteristics. They reported the presence of inflammatory cell infiltrates [330, 331, 338-340], muscle fibre atrophy [330, 338-340] and fibre size variability [330, 340]. Although the prevalence rates of abnormal biopsy results varied considerably, they were common findings across the studies. Besides, muscle weakness is a commonly reported complaint in RA patients, which not only reduces the quality

of life, but may also impose a burden on the society due to impaired work capacity [562]. Reports show that RA patients have 25%–70% weaker muscles compared to healthy matched controls [340, 562].

Rheumatoid myositis and rheumatoid cachexia are two recently introduced terms describing muscle inflammation and the loss of muscle mass with little or no loss in fat mass respectively [337, 367, 563]. Kramer et al. [564] showed that muscle density in RA, as assessed using computed tomography, is strongly associated with physical performance and disability. The literature reviewed above and in Chapter 2 call for further research to understand the myopathic characteristics in RA.

RA-associated myopathy can occur with the absence of obvious clinical symptoms, and the presence of arthralgia can complicate its detection. Despite the present knowledge, muscle biopsy is currently the only available method to detect subclinical muscle involvement. To date, the documentation of myopathic features in RA is poorly detailed. No studies have yet utilised a non-invasive quantitative method to define and investigate it.

New biomarkers such as muscle stiffness can now be assessed non-invasively using shear wave elastography (SWE), which may offer new insights into the biomechanical state of RA muscles. The combination of inflammation, atrophy, muscle weakness and lower muscle density [361, 562] may hypothesise an impaired elastic property of RA muscles. Understanding muscle involvement in RA via SWE can help in developing prevention and therapeutic strategies. Additionally, it can emphasise the breadth of extra-articular manifestations of RA as a systemic inflammatory disease.

7.2 Aims

The hypothesis underlying the study carried in this chapter is that patients of variable disease activity will exhibit different muscle stiffnesses. The first aim was to define muscle stiffness and strength in three cohorts of RA patients: newly diagnosed untreated, those in disease remission and those who have an ongoing active disease. The second aim was to compare and correlate the results amongst the RA subgroups.

7.3 Methods

7.3.1 Study design

This study was conducted in a case-control design. Patients were prospectively recruited from a single centre (Chapel Allerton Hospital, part of Leeds Teaching Hospitals NHS Trust) between May 2017 and August 2018. The investigations took place in the research facility based at the same centre (Leeds Biomedical Research Centre). The ethical approval for this study was covered by the same ethical approval granted to the previous three studies. Healthy controls were enrolled to compare the RA patients' muscle characteristics against. All participants provided written informed consent prior to enrolment. No power calculations were carried out to determine a sample size Due to the lack of prior information and similar studies. However, the same recommended rule of thumb in previous studies was followed by recruiting between 12 – 30 per group of interest to provide an acceptable precision around the estimates [505, 565].

7.3.2 Patients

To test muscle characteristics in RA patients, three main groups of varying disease activities were specified: a- newly diagnosed and untreated (new RA), b- diagnosed over 1 year and in remission (remission RA), and c- diagnosed over 1 year and is active (active RA). The eligibility criteria are detailed below for each group.

7.3.2.1 Inclusion/exclusion criteria

The inclusion criteria for the RA patients were as follows:

1. ≥18 years old.
2. Have an established diagnosis of RA based on the adopted criteria [38].
3. For new RA:
   3.1. Newly diagnosed with RA.
   3.2. Disease-modifying antirheumatic drugs (DMARD)-naïve.
4. For active RA:
   4.1. Diagnosed with RA for at least 12 months.
   4.2. Disease activity score-28 (DAS28) ≥3.2 at the time of recruitment [566].
   4.3. At least two of the following markers of active disease within the past 12 months:

4.3.1. DAS28 ≥3.2 in at least one additional clinic visit prior to recruitment.
4.3.2. Raised inflammatory markers.
4.3.3. Required corticosteroid therapy (intra-muscular or oral) to control the disease.
4.3.4. Ultrasound evidence of active disease.
4.3.5. A physician's determined long-standing active disease for more than one year (based on clinical RA symptoms, early morning stiffness, joint pain and swelling).
4.3.6. Escalation to, or recent changes in biologic medication.

5. For remission RA:
   5.1. Diagnosed with RA for at least 12 months.
   5.2. Achieved remission for the past 12 months with a DAS28 <2.6 [567].
   5.3. No disease flairs during the past 12 months.

The exclusion criteria were pregnancy or a history of any muscle disease or neuropathy. The eligibility conditions described above were adapted from the established definitions of RA disease activity [38, 567-569]. The eligibility for the active RA group was set to ensure the inclusion of a prolonged active disease. As for healthy controls, eligibility was similar to the described in the previous chapters.

7.3.3 Shear wave elastography

SWE was performed using the Aixplorer system (Supersonic Imagine, Aix-en-Provence, France) operating the SuperLinear™ SL10–2MHz probe. Three repeated measurements of shear wave velocity (SWV) were recorded. The detailed SWE acquisition methods and protocol are described in chapter 4. The investigated muscles were the vastus lateralis (VL), rectus femoris (RF), vastus medialis (VM), vastus intermedius (VI), biceps femoris (BF), semitendinosus (ST), semimembranosus (SM) and biceps brachii (BB) of the dominant side. All muscles were tested in the most relaxed resting position only. The quadriceps were not tested during passive stretching for the patients recruited during the first months since this position was decided at a later stage of the project. The poor predictive value obtained using this position in the previous chapters did not encourage any attempt to impute the missing data. Therefore, only the

complete set of SWE readings during the resting position are reported in this study.

7.3.4 Clinical and muscle assessments

Age, sex, body mass index (BMI), global visual analogue scale (VAS) 100 mm score of general health, smoking status (pack-years) and alcohol intake (units/week) were documented. To evaluate the relationship between muscle stiffness and the patients' disease status, the DAS28 score, swollen joint count and tender joint count were reviewed by board-certified rheumatologists. In addition, the main inflammatory blood markers [C-reactive protein (CRP) and Erythrocyte sedimentation rate (ESR)] were recorded.

As muscle weakness is a common symptom in RA, muscle strength and function were assessed by a series of four tests. This included the isometric handgrip strength, expanded timed get-up-and-go (ETGUG) and 30-sec chair stand test (CST). Moreover, isokinetic knee extension/flexion torque and power were measured since it provides an accurate assessment of muscle strength in RA and correlates with disease activity [396]. The protocols for the four tests are described in chapter 4.

7.3.5 Statistical analysis

Descriptive results were summarised as mean with standard deviations for continuous variables, and proportions with percentages for categorical variables. The significance of the differences in muscle stiffness (i.e. SWV) and strength assessments amongst the various groups were tested using one-way analysis of variance (ANOVA) followed by Tukey-Kramer post-hoc multiple comparisons to highlight between groups differences. Further analyses using two-way analysis of covariance (ANCOVA) were employed to adjust for the independent effects of age (covariate) and sex (moderator variable).

To test the difference between patients and healthy controls, RA groups were pooled in one category and compared using independent sample-test. The correlations of SWV with the disease activity variables (i.e. DAS-28 and CRP) and muscle strength tests were analysed using Pearson's correlation coefficients.

Intra-operator reliability for the three repeated measurements were evaluated using intraclass correlation coefficients (ICC). The tests mentioned above were

repeated for each muscle evaluated by SWE. *P*-values <0.05 were regarded as statistically significant. All statistical analyses were performed on SPSS version 25 (Armonk, NY: IBM Corp).

7.4 Results

A total of 80 RA patients have been recruited, of whom 29 new RA, 18 active RA and 33 remission RA. Additionally, 40 healthy controls were recruited with a similar age distribution to the RA groups. The demographic and clinical characteristics of all participants are listed in Table 7-1. The age of the control group (61.5 ±10.5 years) was not significantly different from the new RA (56.7 ±10.6 years; *p*=0.85), active RA (60.8 ±15.9 years; *p*=0.94) or remission RA (65.9 ±11.6 years; *p*=0.07). However, the new RA group was younger (-9.2 years; *p*=0.011) than the remission RA group.

Median duration since RA diagnosis and range was 88 month (12–347 month) for active RA and 59 month (12–212 month) for remission RA. Early morning stiffness median (interquartile range) was 60 minute (29–60 minute) and 45 minute (30–60) for the active and new RA groups respectively. No patients in the remission RA group complained of early morning stiffness. Regarding treatment, the active RA group were on methotrexate (n=8), prednisolone (n=4), rituximab (n=3), etanercept (n=2), tocilizumab (n=2), hydroxychloroquine (n=2), sulfasalazine (n=1), tofacitinib (n=1), adalimumab (n=1) and abatacept (n=1). As for the remission RA group, they were on methotrexate (n=26), hydroxychloroquine (n=8), sulfasalazine (n=5), etanercept (n=4), adalimumab (n=2), infliximab (n=2) and prednisolone (n=1).

Table 7-1 Demographic and clinical characteristics of the rheumatoid arthritis patients and healthy controls.

Characteristic	Healthy controls (a) (n=40)	New RA (b) (n=29)	Active RA (c) (n=18)	Remission RA (d) (n=33)	*p*-value†	Post hoc‡
Sex	12 Males (30%)	8 Males (28%)	4 Males (22%)	19 Males (58%)	**0.026**	d>a,b,c
Age (years)	61.5 (10.5)	56.8 (10.6)	60.9 (15.9)	65.9 (11.6)	**0.030**	d>b
Height (cm)	166.4 (9.6)	163.9 (12.0)	164.1 (9.6)	167.8 (9.5)	0.41	-
Weight (kg)	75.2 (14.1)	80.4 (17.7)	74.3 (18.6)	76.8 (16.0)	0.53	-
BMI	27.2 (4.6)	30.2 (7.6)	27.4 (5.7)	27.1 (4.2)	0.10	-
Waist-hip ratio	0.88 (0.09)	0.88 (0.08)	0.88 (0.10)	0.92 (0.07)	0.24	-
Ever smoked	17 (42%)	16 (55%)	10 (55%)	22 (67%)	0.27	-
pack-years *	2.5 (1.8–4.0)	18.8 (9.3–30.2)	19.7 (6.4–39.0)	10.2 (3.7–28.1)	**0.037**	a<b,c,d
Drinking alcohol	23 (57%)	15 (52%)	9 (50%)	25 (75%)	0.17	-
(units/week) *	8 (6–15)	6 (1–15)	13 (3–20)	10 (4–18)	0.80	-
VAS health (mm) *	10 (3–22)	27 (15–50)	47 (31–58)	9 (3–18)	**<0.001**	a,d<b,c
Months since diagnosis *	-	0	88 (45–163)	59 (38–77)	**<0.001**	b<d<c
DAS-28	-	4.7 (1.2)	4.6 (1.0)	1.8 (0.3)	**<0.001**	d<b,c
Swollen joints	-	8.0 (5.9)	4.4 (3.5)	0	**<0.001**	d<c<b
Tender joints	-	9.7 (7.0)	10.2 (5.9)	0	**<0.001**	d<b,c
CRP (mg/l)*	-	10 (5–23)	6 (5–25)	<5.0	**0.003**	b>d
ESR (mm/hr)*	-	26 (13–48)	13 (5–32)	11 (8–17)	**0.018**	b>d

Data in brackets represent standards deviation for means, or percentages for ratio.

* Median (interquartile range).

† *p*-values significant at 95% are highlighted in bold. Continuous variables tested via one-way ANOVA, and categorical data tested using Chi-square test.

‡ The signs > or < indicate that the group(s) are significantly higher or lower at 0.05 significance level compared to others.

VAS=Visual analogue scale of health; DAS=Disease activity score; CRP= C-reactive protein; ESR= Erythrocyte sedimentation rate.

7.4.1 Shear wave elastography

The SWE for the healthy controls and RA groups are presented in Table 7-2 and Figure 7-1. The results of the one-way ANOVA in the last column of the table showed no significant differences between the groups (p>0.05). However, the tendency observed in the VM muscle (p=0.052) was further analysed after adjusting for age using the ANCOVA test which confirmed the lack of SWV statistical difference (p=0.149) amongst the participants. Age, however, had a significant effect on SWV measurements in VM (p<0.001). This significant effect of age was also observed after further analysis on VL (p=0.011), RF (p<0.001), VI (p=0.014), BB (p<0.001), BF (p=0.003), ST (p<0.001) and SM (p=0.029), but not in BB (p=0.86). In contrast, sex had no significant impact on SWV measurements (all p>0.10).

Despite the lack of statistically significant differences, the descriptive statistics in Table 7-2 showed that the active group had on average 5% difference in the quadriceps and hamstrings SWV compared to healthy controls. The difference was highest over the SM muscle at 7.5% (1.60 versus 1.48 m/s), but was not statistically significant in post hoc multiple comparisons (p=0.34). A higher difference at 8.6% (p=0.21) in the same muscle was noted between the active RA (1.48 m/s) and remission RA (1.62 m/s).

Comparing the healthy controls to a pooled group of all RA patients also showed no significant differences between their mean SWV measurements [VL (p=0.24), RF (p=0.86), VM (p=0.08), VI (p=0.97), BB (p=0.35), BF (p=0.27), ST (p=0.23) and SM (p=0.47)]. A lack of significant difference was also observed when comparing RA groups amongst each other [VL (p=0.41), RF (p=0.87), VM (p=0.14), VI (p=0.14), BB (p=0.50), BF (p=0.34), ST (p=0.37) and SM (p=0.22)].

Correlation analysis showed no significant associations between SWV and DAS-28 across all muscles. Similar results of poor (r<0.2) and insignificant (p>0.05) coefficients were observed between SWV and CRP as well as ESR. Moreover, early morning stiffness was not associated with SWV (r<0.2; p>0.05).

Intra-operator reliability for the repeated measurements were all above 0.90 indicating ‘almost perfect’ reliability. The ICC were 0.97 for VL, 0.95 for RF, 0.99 for VM, 0.93 for VI, 0.94 for BB, 0.97 for BF, 0.95 for ST and 0.96 for SM.

Table 7-2 Shear wave velocity measurements for all participants.

Muscle	Healthy controls		New RA		Active RA		Remission RA		*p*-value†
	Mean (SD)	95% CI	Mean (SD)	95% CI	Mean (SD)	95% CI	Mean (SD)	95% CI	
Vastus lateralis	1.64 (0.15)	1.59 ,1.69	1.63 (0.26)	1.54 ,1.73	1.55 (0.17)	1.47 ,1.64	1.58 (0.21)	1.5 ,1.65	0.32
Rectus femoris	1.69 (0.15)	1.64 ,1.74	1.68 (0.18)	1.61 ,1.75	1.70 (0.16)	1.62 ,1.78	1.68 (0.14)	1.63 ,1.73	0.96
Vastus medialis	1.62 (0.17)	1.57 ,1.68	1.62 (0.32)	1.49 ,1.76	1.52 (0.20)	1.42 ,1.62	1.50 (0.18)	1.44 ,1.57	0.052
Vastus intermedius	1.84 (0.19)	1.78 ,1.91	1.78 (0.22)	1.70 ,1.87	1.93 (0.25)	1.80 ,2.06	1.85 (0.25)	1.76 ,1.94	0.21
Biceps brachii	1.83 (0.18)	1.78 ,1.89	1.92 (0.36)	1.78 ,2.06	1.81 (0.14)	1.74 ,1.88	1.89 (0.35)	1.77 ,2.01	0.45
Biceps femoris	1.57 (0.18)	1.52 ,1.63	1.56 (0.23)	1.47 ,1.64	1.46 (0.21)	1.36 ,1.57	1.54 (0.21)	1.47 ,1.62	0.30
Semitendinosus	1.56 (0.17)	1.51 ,1.62	1.53 (0.16)	1.47 ,1.59	1.45 (0.17)	1.37 ,1.54	1.54 (0.25)	1.45 ,1.63	0.30
Semimembranosus	1.60 (0.16)	1.55 ,1.65	1.54 (0.15)	1.48 ,1.60	1.48 (0.18)	1.38 ,1.57	1.62 (0.41)	1.48 ,1.77	0.21

Mean values represent shear wave velocity in units of m/s.

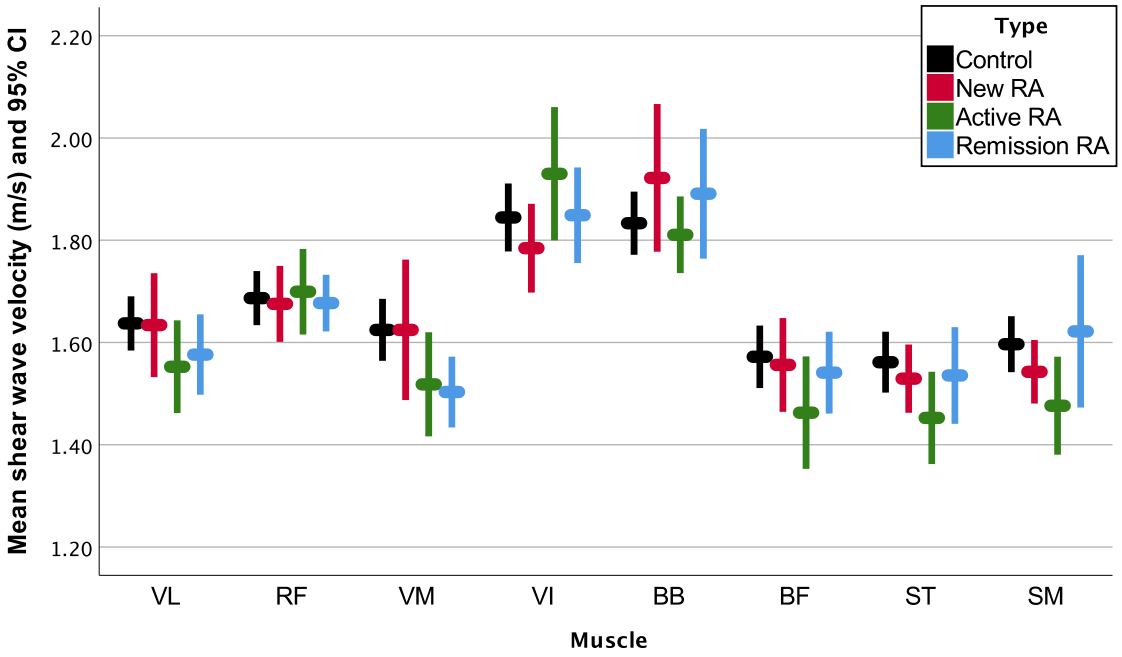

Figure 7-1 Shear wave velocity means and 95% CI for each participant group.

7.4.2 Muscle assessments

The participants' performance in the muscle assessment tests are described and compared in

Table 7-3. The results are also graphically represented in Figure 7-3 and Figure 7-2. A summary of the mean difference percentages for the RA groups compared to the healthy control group are displayed in Figure 7-4.

Overall, the RA patients' performance was worse than healthy controls across all tests. Though, the remission RA patients performance was not significantly different to the healthy control group except in the isokinetic knee flexion strength (-21%, p=0.027). In contrast, the new and active RA groups exhibited significant muscle weakness. They had a weaker isokinetic knee flexion and extension strength by 29% (p=0.013) and 28% (p=0.040) respectively. Moreover, their grip strength was weaker by more than 45% (both p<0.001). The active RA group performed considerably worse than all other groups in the number of chair stands (-44%, p<0.001).

The correlations in Table 7-4 indicates that the SWV measurements were not associated with significant positive or negative changes in any of the muscle test results in RA patients.

Table 7-3 Muscle assessment results for all participants.

Test	Healthy controls (a)		New RA (b)		Active RA (c)		Remission RA (d)		p-value	Post hoc*
	Mean (SD)	95% CI	Mean (SD)	95% CI	Mean (SD)	95% CI	Mean (SD)	95% CI		
ETGUGT, Total time (sec)	16.6 (4.3)	15.3, 18.0	20.7 (5.7)	18.7, 22.9	21.5 (6.3)	18.7, 24.5	18.2 (4.5)	16.6, 19.7	**0.002**	a>b,c
Number of chair stands in 30 sec	17.0 (5.8)	15.2, 18.8	12.3 (6.0)	10.1, 14.5	9.5 (6.3)	6.6, 12.4	14.0 (5.4)	12.1, 15.8	**<0.001**	a>b,c
Handgrip strength (kg)	31.5 (13.7)	27.4, 35.9	17.3 (8.1)	14.6, 20.5	17.3 (8.4)	13.7, 21.5	26.6 (10.9)	23.1, 30.6	**<0.001**	a,d>b,c
Knee extension torque (Nm/kg)	1.29 (0.42)	1.16, 1.42	1.06 (0.45)	0.89, 1.22	0.93 (0.47)	0.72, 1.15	1.20 (0.40)	1.06, 1.33	**0.026**	a>c
Knee flexion torque (Nm/kg)	0.75 (0.27)	0.66, 0.83	0.53 (0.27)	0.43, 0.63	0.60 (0.29)	0.46, 0.73	0.59 (0.25)	0.50, 0.67	**0.006**	a>b,d
Knee extension power (W/kg)	0.75 (0.29)	0.66, 0.84	0.58 (0.30)	0.47, 0.69	0.52 (0.32)	0.37, 0.67	0.68 (0.28)	0.59, 0.78	**0.029**	a>c
Knee flexion power (W/kg)	0.47 (0.18)	0.41, 0.52	0.32 (0.19)	0.25, 0.39	0.34 (0.21)	0.25, 0.44	0.34 (0.18)	0.28, 0.40	**0.005**	a>b,d

Mean results are presented as unweighted marginal means adjusted by sex and age in two-way ANCOVA.
* The signs > or < indicate that the group(s) are significantly higher or lower at 0.05 significance level compared to others.

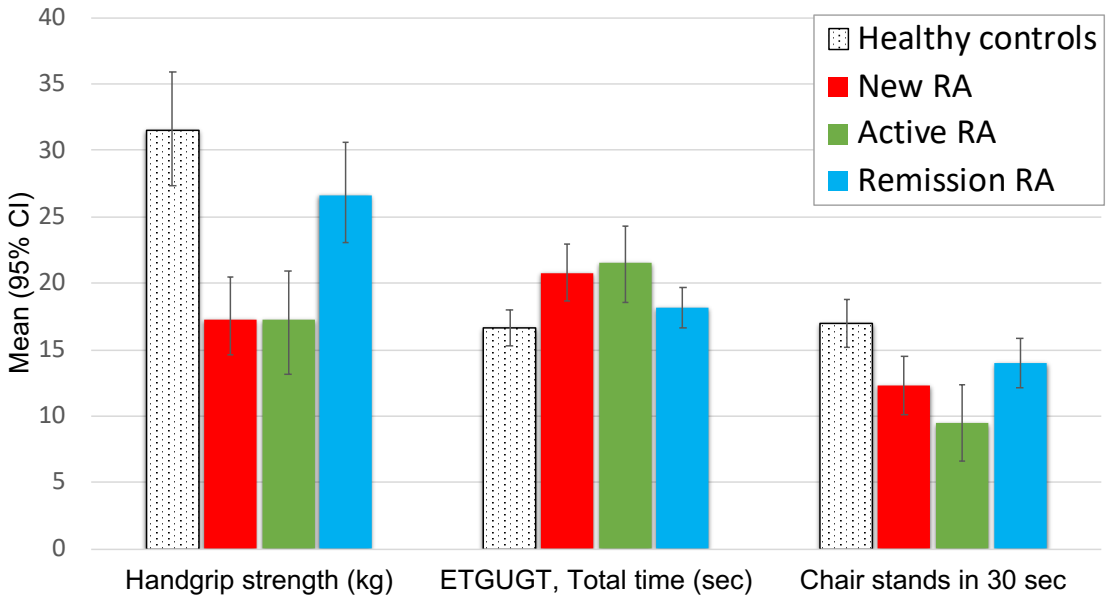

Figure 7-2 Participants' performance in handgrip strength, walking time and number of chair stands in 30 seconds.

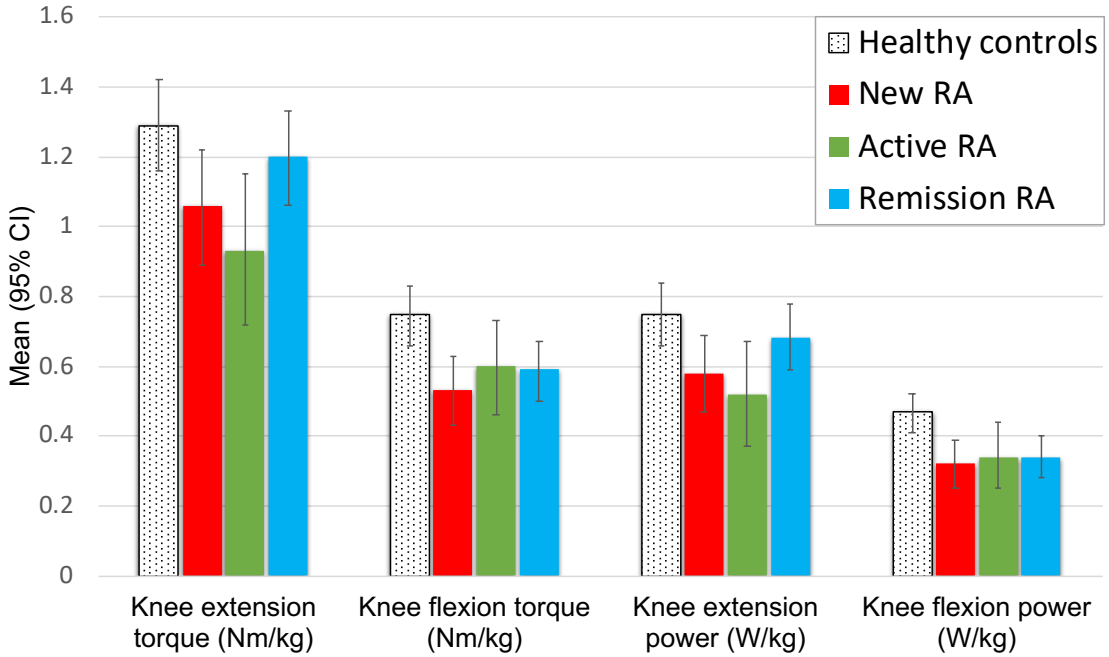

Figure 7-3 Isokinetic knee strength during flexion and extension for the healthy controls and RA patients.

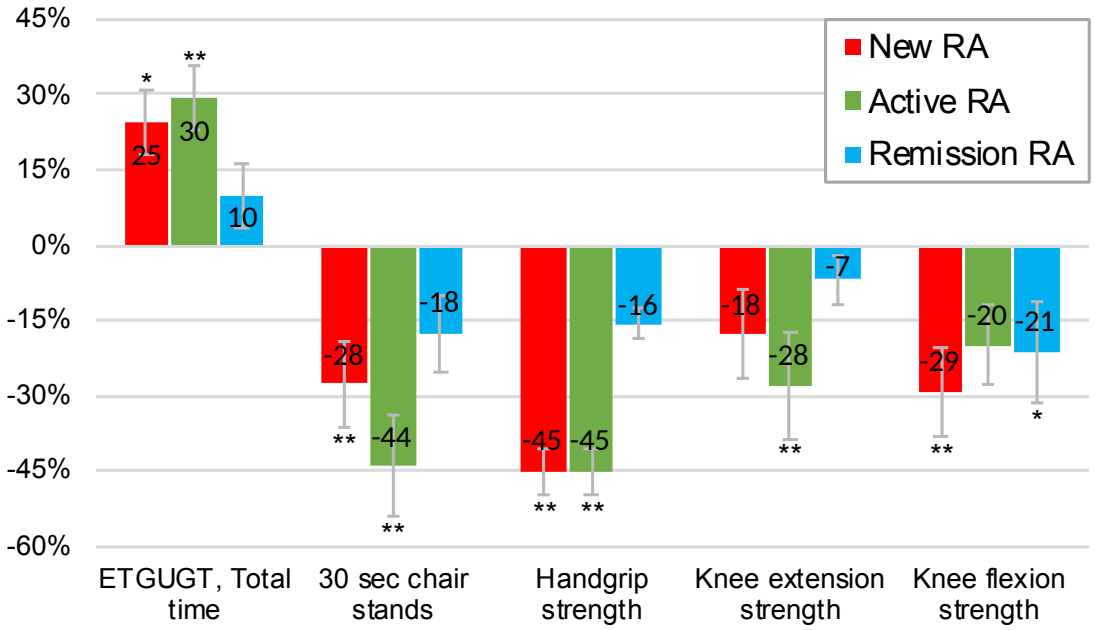

Figure 7-4 Percentages of difference in muscle assessment results for the RA patients relative to the healthy control group.

(*) significant at $p<0.05$, (**) significant at $p<0.001$.

Table 7-4 Correlation coefficients showing no significant association between shear wave velocity and results of the muscle assessment tests in RA patients.

	VL	RF	VM	VI	BB	BF	ST	SM
ETGUGT, Total time (sec)	-0.02 (p=0.83)	-0.12 (p=0.3)	0.02 (p=0.87)	-0.17 (p=0.13)	-0.18 (p=0.11)	0.13 (p=0.26)	0.05 (p=0.63)	-0.01 (p=0.91)
30-sec Chair stand test	-0.18 (p=0.12)	-0.08 (p=0.46)	-0.05 (p=0.66)	-0.09 (p=0.43)	-0.04 (p=0.71)	0.1 (p=0.38)	0.02 (p=0.89)	0.12 (p=0.31)
Handgrip Strength (kg)	0.02 (p=0.86)	-0.07 (p=0.56)	-0.02 (p=0.88)	0.02 (p=0.88)	-0.22 (p=0.05)	0.11 (p=0.35)	0.08 (p=0.51)	0.01 (p=0.93)
Knee extension torque (Nm/kg)	-0.03 (p=0.78)	-0.04 (p=0.75)	-0.17 (p=0.14)	-0.01 (p=0.9)	-0.17 (p=0.14)	0.1 (p=0.39)	0.18 (p=0.13)	0.14 (p=0.22)
Knee flexion torque (Nm/kg)	0.01 (p=0.96)	0.01 (p=0.94)	-0.01 (p=0.9)	0.01 (p=0.99)	-0.2 (p=0.08)	0.12 (p=0.28)	0.08 (p=0.49)	-0.02 (p=0.85)

Knee flexion power (W/kg)	-0.05 (p=0.68)	-0.02 (p=0.89)	-0.11 (p=0.36)	-0.04 (p=0.71)	-0.17 (p=0.15)	0.09 (p=0.42)	0.09 (p=0.43)	0.03 (p=0.78)
Knee extension power (W/kg)	-0.02 (p=0.83)	-0.12 (p=0.3)	0.02 (p=0.87)	-0.17 (p=0.13)	-0.18 (p=0.11)	0.13 (p=0.26)	0.05 (p=0.63)	-0.01 (p=0.91)

Data presented as correlation coefficients (*p*-value) based on Pearson's test.

Evaluating the association between disease activity (i.e. DAS-28) and the muscle assessment outcomes showed that it moderately correlated with ETGUG total walking time (r=0.473; $p<0.001$), number of chair stands (r= -0.369; $p=0.001$), handgrip strength (r= -0.609; $p<0.001$), knee extension torque (r= -0.356; $p<0.001$) and knee flexion torque (r= -0.249; $p=0.001$).

7.5 Discussion

The main aim of the work in this chapter was to explore muscle stiffness in RA patients. Despite the tendency for RA patients to have a lower muscle stiffness (i.e. lower SWV) compared to healthy controls, especially those with active disease, the differences were not statistically significant. This main finding does not substantiate the initially proposed hypothesis of altered muscle stiffness in RA. Though, it confirms the results from chapter 4 regarding the effect of ageing on muscle stiffness.

The normal muscle stiffness in RA may indicate that the degree of reported muscle fibre atrophy and inflammatory cell infiltrates in RA subjects might not be profound enough to detrimentally affect the biomechanical properties of skeletal muscles. This argument can be supported by the results reported in chapter 5 on myositis patients, where significant structural changes (i.e. fibre atrophy) and inflammation (i.e. oedema) were associated with abnormal SWE results. Additionally, the prevalence of such myopathic features in RA was also low as reported previously [330, 331].

The second main finding was that all RA patients exhibited a significantly lower strength and functional performance based on the objective muscle assessment tests employed. The positive muscle weakness, but lack of abnormal SWV, may suggest other primary intrinsic (intracellular) muscular dysfunction factors rather

than an altered biomechanical property in skeletal muscle. For example, impairment in the metabolic process of reactive nitrogen species in RA muscles can attack the proteins responsible for force production (actin and myosin) [570]. Similarly, a molecular imbalance in calcium ions (Ca^{2+}) release can cause myofibrillar dysfunction [562].

By contrast, other researchers support the theory that secondary factors promote muscle weakness in RA. For instance, the disuse due to a sedentary lifestyle, joint deformity, pain and stiffness, and the increase in energy expenditure during rest are all factors attributable to muscle deconditioning and subsequent weakness in RA [361, 571, 572]. These factors might lead to secondary muscle wasting [571]. Indeed, Baker et al. [361] showed that RA patients have a significant skeletal muscle mass deficit compared to healthy controls ($p<0.001$). However, Helliwell and Jackson [572] argued that the reduction in strength is often greater and precedes what could be explained by muscle mass decline in RA. Their argument was later supported by others [573, 574]. Furthermore, it reinforces what has been discussed in chapter 4 explaining how loss of strength precedes the loss of muscle mass in the elderly.

It is important to highlight the difficulty of directly assessing the influence of inflammation on the results of strength assessments due to the secondary factors mentioned above. The results revealed that the weakness might vary depending on disease activity. The presented percentages of muscle weakness deficits match those observed in previous studies. In isokinetic knee strength testing, Madsen et al. [575] reported a -32% reduction in extension strength (-28% in this study) and -28% reduction in flexion strength (-20% in this study) over a group of active RA. A lesser reduction of -22% in extension strength and -28% in flexion strength was reported by Meireles et al. [395]. In remission RA, another study found comparable differences in flexion strength of -29% (-21% in this study) and extension strength of -9% (-7% in this study) [394].

As for grip strength weakness, the presented difference of -45% in the new and active RA is in agreement with the -43% average reduction calculated in a large meta-analysis of more than 10 thousand RA patients [362]. Using another variation of the chair stand test, one study found a slightly worse performance of -23% in remission RA compared to -18% in this study [394]. Similar to the current observations, Bohler et al. [400] used the chair stand test and a shorter

version of the ETGUG, and demonstrated that RA patients in higher disease activity categories generally performed worse than patients in remission. They reported a significant correlation for DAS-28 with chair standing and walking time of -0.314 (p<0.05) and 0.437 (p<0.001) respectively, which are close to what were reported in this study (-0.369 for chair stand; 0.473 for ETGUG).

Although the remission patients had better results in most of the tests compared to the new and active RA, they performed worse than controls in all strength and function assessments. This raises a doubt that modern therapies are effective in counteracting disease activity yet seems to partially fail in recovering RA-induced weakness [562]. Thus, future RA therapies could trial the use of conventional effective therapies coupled with resistance exercises to control disease activity and improve muscular strength respectively, and perhaps consider muscle protein stabilising compounds. Eventually, this hybrid therapy may reduce risks of injurious falls and subsequent disability as well as enhance life quality and decrease the burden on society by increasing work capacity amongst those afflicted patients.

Since the biomechanical properties of skeletal muscles do not appear to be compromised in RA, the focus of future SWE research could be directed at pathologies of primary muscle disease, where elastography demonstrated signs of promise such as in chapter 5 for idiopathic inflammatory myopathies [84], Duchenne muscular dystrophy [278] and muscle spasticity [269]. Besides, the scale of observed muscle weakness calls for researchers to develop assessment methods that can readily assist healthcare professionals in identifying patients at risk. Also, a better understanding of the various aspects associated with muscle quality in RA is vital for developing novel muscle-related interventions. Stanmore [576] has published useful recommendations for assessing and preventing falls in RA, which could be a helpful resource for RA-associated muscle impairment.

7.5.1 Limitations

The study conducted in this chapter has several limitations. Achieving an equal number of participants in each category is challenging in observational studies in contrast to experimental studies [577]. Though not extremely remarkable, the unbalanced design is noticeable in this study, and is acknowledged as a limitation of the results. It was particularly difficult to recruit the active RA

patients (smallest group, n=18) since cases seldom persist with such prolonged and uncontrolled disease activity. To mitigate the effect of this limitation on the results, type III sums of squares and unweighted marginal means were used in the statistical analysis when possible. This also addressed the larger ratio of male patients in the remission group.

Besides, the results are limited to large upper and lower limb muscles. Smaller muscles, such as the hand muscles, were not evaluated. Moreover, SWE was not investigated in the tendons of RA patients since it is outside the scope of this thesis. SWE may potentially be a relatively cheaper and feasible option for RA tendinopathies compared to MRI, where baseline tendinopathy was shown to be suggestive of tendon rupture in the long term [578].

7.6 Conclusions

In conclusion, muscle stiffness, as evaluated using SWE, did not appear to be affected in RA patients from various disease activity groups compared to healthy controls. However, muscle strength and physical performance were significantly reduced in RA patients. This reduction did not correlate with SWE measurements of muscle stiffness. Rather, the weakness is believed to be a result of a complicated mixture of primary (e.g. intracellular molecular imbalance) and secondary (e.g. myofibre deconditioning due to disuse) factors. Doubts remain regarding muscle quality in RA considering the lack of clinically meaningful criteria to define RA-associated muscle impairment. The muscle weakness results call for interventions focused on improving muscle strength and physical function in RA to prevent consequent disability.

Chapter 8 Discussion, future directions and conclusions

This final chapter presents a summary of the main findings arising from this thesis, discussing the results in the context of existing literature and suggests future research directions in muscle elastography.

8.1 Thesis synopsis

This thesis is centred around the development of a reliable muscle shear wave elastography (SWE) technical protocol and exploring SWE use in healthy and diseased skeletal muscles. The key findings from the observations in chapters 3, 4, 5, 6, and 7 are summarised below.

Chapter 3 - Reliability of shear wave elastography in healthy skeletal muscles.

This chapter comprised two studies that aimed to 1) determine and compare the reliability of two SWE systems on healthy skeletal muscles, and 2) investigate the effects of probe location, orientation, load, region of interest (ROI) size, depth and measurement units on the reliability of the readings. This chapter included 40 healthy participants divided between the two studies.

- The internal reliability of the two SWE systems using the best acquisition method was high; however, the 95% limits of agreement were wide, and results may vary by up to 26%.
- There was a reasonable advantage for the older (more established) system by Supersonic Imagine, which supported its purchase to be used for the remaining studies in the thesis.
- The results regarding the technical factors recommended: 1) orienting the probe along the muscle fibres direction; 2) acquiring SWE measurements in locations free from myotendinous or myoaponeurotic structures; 3) avoiding the use of small ROI sizes (e.g. 15mm^2); 4) placing the probe in direct contact with the skin using minimal pressure; 5) being aware that readings variability can increase proportionally with depth; 6) recording the readings in the original SWE unit of meters per second (m/s).

- These recommendations informed the technical acquisition methodology for the remainder studies in succeeding chapters.

Chapter 4 - The effect of ageing on shear wave elastography muscle stiffness in adults.

This chapter described a cross-sectional study that aimed to investigate muscle stiffness changes throughout adulthood amongst healthy young, middle-aged and elderly cohorts. Additionally, to explore muscle stiffness association with strength and muscle mass. The SWE analysis included the quadriceps, hamstrings and biceps brachii of 77 healthy volunteers.

- Ageing was associated with a gradual decline in muscle stiffness with significant reductions appearing in elderly subjects (>75 years).
- The decline is muscle stiffness correlated more strongly with muscle strength than mass, in contrast to sex and body mass index which were not associated with muscle stiffness.
- This chapter emphasised the importance of accounting for age-related changes in muscle stiffness when conducting muscle SWE studies, especially when the recruited cohort's age range is wide.

Chapter 5 - Muscle shear wave elastography in idiopathic inflammatory myopathies.

The chapter aimed to investigate muscle stiffness in subjects with active idiopathic inflammatory myopathies (IIM). The objectives were to determine if there was evidence of face and construct validity by comparing IIM patients (n=23) to matched healthy controls (n=23) and analysing the association of SWE with measures of muscle strength and magnetic resonance imaging (MRI) outcomes.

- The results indicated that IIM patients had a significantly lower muscle stiffness compared to the healthy controls group.
- In the quadriceps and hamstrings during the relaxed position, SWE had an excellent performance for differentiating IIM from healthy muscles (AUROC= 0.790–0.908).
- Higher muscle oedema and atrophy scores on MRI seemed to be associated with lower muscle stiffness measurements. However, there

was no evidence of significant association with MRI scores of fatty infiltration.

- There were signs of a negative correlation between muscle strength and SWE measurements whereby lower muscle stiffness was observed in weaker patients.

Chapter 6 - Corticosteroids effect on muscle stiffness.

The cohort study in this chapter aimed to test the effect of high dose corticosteroid treatment on muscle stiffness and strength. The objective was to look for evidence of SWE responsiveness to changes in the muscle elastic properties as an imaging biomarker for detecting corticosteroid-induced myopathy. The study was conducted on 14 giant cell arteritis (GCA) patients that were followed-up after three months, and half of them after six months.

- After normal muscle stiffness at the baseline, shear wave velocity (SWV) decreased on average by 14% after three months and 18% after six months of treatment in the quadriceps and hamstrings.
- Muscle strength was generally preserved at follow-ups. However, there were moderate to strong correlations (r= 0.54–0.96) between exhibiting weaker muscle strength at follow-up visits and a greater reduction in SWV.
- The findings suggest that abnormal SWE measurements of muscle stiffness may potentially detect preclinical signs of corticosteroid-induced myopathy.

Chapter 7 - Muscle Stiffness in rheumatoid arthritis.

The aim of this chapter was to explore muscle stiffness in rheumatoid arthritis (RA) patients using SWE and examine muscle strength and its association with SWE results. This study included 80 new, active and remission RA patients as well as 40 healthy controls.

- The SWE results did not substantiate the hypothesis of altered muscle stiffness in RA patients regardless of their disease activity.
- However, muscle strength and physical performance were significantly diminished in RA patients especially in the new and active groups.

- The lack of association between SWE results and muscle strength may indicate that the diminished strength could be attributed other factors besides an abnormal muscle stiffness.

8.1.1 Addressing the central hypothesis

The central hypothesis underlining this thesis was that **"Shear wave elastography is reliable and able to detect altered skeletal muscle elasticity in various established and suspected muscle conditions".**

The reliability analyses conducted in Chapter 3 and later chapters has indeed demonstrated evidence of SWE reliability. In the established muscle disease in Chapter 5, SWE has shown its ability to detect an abnormal muscle elasticity. Moreover, in suspected biomechanical changes with ageing and corticosteroid use, SWE was able to detect signs of decreasing muscle stiffness. However, it did not detect any SWE abnormality in RA patients (Chapter 7) despite reduced muscle strength. In general, the overall results support the central hypothesis except for the findings in Chapter 7.

8.1.2 Originality and contribution

The originality of the work conducted in this thesis arises from several aspects. Firstly, combining muscle elasticity and strength as well as MRI in the methodology of Chapter 5 is an original approach. Secondly, the exploration of a novel imaging technology in suspected areas that have not been investigated before such as steroid-induced myopathy and rheumatoid arthritis. Furthermore, the methodological SWE techniques in the later chapters were adopted from the original research investigating the reliability and acquisition techniques in Chapter 3.

Overall, each study chapter provides novel contributions to its research area. For example, before conducting the study in Chapter 3, the reliability of the LOGIQ-E9 SWE system was not evaluated in skeletal muscles. Moreover, SWE inter-system agreement has not been reported before. Next, in Chapter 4, it was not clear to what extent muscle stiffness measured by SWE differed amongst various age groups. The chapter addressed this question and evaluated its association with muscle strength and mass. Later, Chapter 5 evaluated, for the first time, the difference between myositis and healthy muscles, and demonstrated signs of construct validity. Chapter 6 then

demonstrated a potential SWE usefulness for detecting subclinical signs of corticosteroid-induced myopathy. This is a promising finding considering the poor tools available today for evaluating such types of drug myopathies. Finally, Chapter 7 showed that muscle stiffness in RA subject is unlikely related to the underlying causes of weakness. On the whole, these contributions can improve our understanding of how muscle stiffness relates to such pathological aetiologies and how SWE might be a useful imaging biomarker for diagnosis and monitoring. Additionally, it will inform the literature regarding the future research directions, which will be discussed later in this chapter.

The work in this thesis relates to the domain of developing biomarkers within the core area of pathophysiological manifestations in the context of the Outcome Measures in Rheumatology (OMERACT) conceptual framework [579]. The OMERACT working group has developed a filter for developing surrogate outcome measures. The filter is based on three pillars: truth (validity), discrimination (reliability and responsiveness) and feasibility (accessibility, cost, burden etc.). The contributions of this thesis' work regarding each aspect are summarised below.

In terms of validity, Chapters 4 and 5 demonstrated face validity for detecting muscle stiffness changes as a result of ageing and muscle inflammation. The moderate, albeit inconsistent, correlations with the muscle assessments tests (in chapters 4, 5 and 6) and MRI (in Chapter 5) showed signs of SWE construct (convergent) validity. Construct validity was supported in the case-control study of Chapter 5 as SWE had a high area under the curve for discriminating healthy from diseased muscles. Content validity was hard to determine since SWV as a surrogate measure for tissue elasticity may not necessarily account for anisotropy, inhomogeneity and viscoelasticity of skeletal muscles, as explained previously in Chapter 2. Investigating content validity was beyond the scope of this thesis. Generally, establishing validity for muscle SWE is challenging since there are no gold-standard tools for clinically assessing muscle stiffness.

Regarding reliability, the results in Chapter 3 and later chapters substantiated the intra-operator reliability. However, other constituents of reliability were not evaluated. As for responsiveness (also called longitudinal construct validity), SWE displayed the ability to detect muscle stiffness changes in patients under

corticosteroid treatment. Still, this evidence is not sufficient enough to verify SWE sensitivity to change in the context of a randomised controlled trial.

Regarding feasibility, the relative cost of SWE is low compared to other more expensive muscle imaging techniques like MRI. SWE provides real-time quantitative results that are easily interpretable. The time to carry a muscle SWE scan depends on the number of muscles tested but should not exceed 30 minute if less than ten muscles are evaluated. This includes the time to explain the scan and position the patient and as well as the hands-on time. Although SWE is less operator dependent than strain elastography, it still requires training and knowledge about probe-handling and muscle anatomy. SWE scanning carries virtually no burden on the patient or operator. Although not appraised systematically, the feasibility of SWE can be deemed satisfactory.

8.2 Thesis discussion

The findings derived from the thesis are discussed in this sub-section and supplemented by an update of the extant literature since Chapter 2 was written.

8.2.1 Reliability and techniques

Since publishing the two studies in Chapter 3, they received multiple citations. In reference to the first reliability study, one paper has tested the reliability of SWE on the gastrocnemius muscle in the relaxation and submaximal contraction states [580]. The researchers oriented the probe transversely despite acknowledging our recommendation of using the longitudinal orientation. They questionably justified this “for the convenience of the measurements”. It should be noted that not only this improper orientation produces lower reliability results, but also fails to accurately track the proportional increase in muscle stiffness during high active contraction forces [88].

Aslan et al. [581] have recently supported the recommendation of using SWV instead of Young’s modulus (kPa) in SWE of the brachial plexus. They have cited and confirmed the results of the second reliability study by reporting a better reliability coefficient using SWV (ICC=0.587) compared to kPa (ICC=0.456). Their study was one of a few comparing SWE to strain elastography, which also demonstrated an overall superior performance and

feasibility for SWE, further supporting the rationale behind selecting SWE for this thesis.

A recent study [582] has also adopted our recommendations regarding the acquisition techniques from Chapter 3. They mentioned that the recommendations on location, probe load and orientation had improved the repeatability of their readings. Additionally, they confirmed the lack of significant differences between dominant and non-dominant limb muscles (p=0.12). Notably, they reported the seldom investigated inter-day repeatability, which ranged from moderate to almost perfect (ICC=0.69–0.91). Their results were conducted on the hamstring muscles of healthy individuals during active contraction, which can support the generalisability of Chapter 3 results to this group of muscles.

Another recent study by Liu et al. [583] has cited the work in Chapter 3 and followed the recommendations on location and probe orientation. Similar to the objective in Chapter 3, they investigated the effect of orienting the probe along, oblique and transverse to the muscle fibres but during passive load forces on swine muscles. When the probe was beyond the longitudinal orientation, the linearity for the association between muscle stiffness and passive force decreased drastically and the observations became more scattered (Figure 8-1). This further supports the significant effect of probe orientation and the evidence mentioned above regarding the major influence of the probe load for acquiring accurate results during active contraction forces or passive stretching.

Liu et al. [583] used a standoff gel layer between the probe and skin, which contrasts with this thesis' recommendation of placing the probe in direct contact with the skin using no more than the probe load for more reliable results. Nevertheless, their methodology derived almost perfect ICC results ranging from 0.985 to 0.999. Using a probe holding actuator and the in vitro controlled settings on excised muscles from only four swines might explain their observed high reliability.

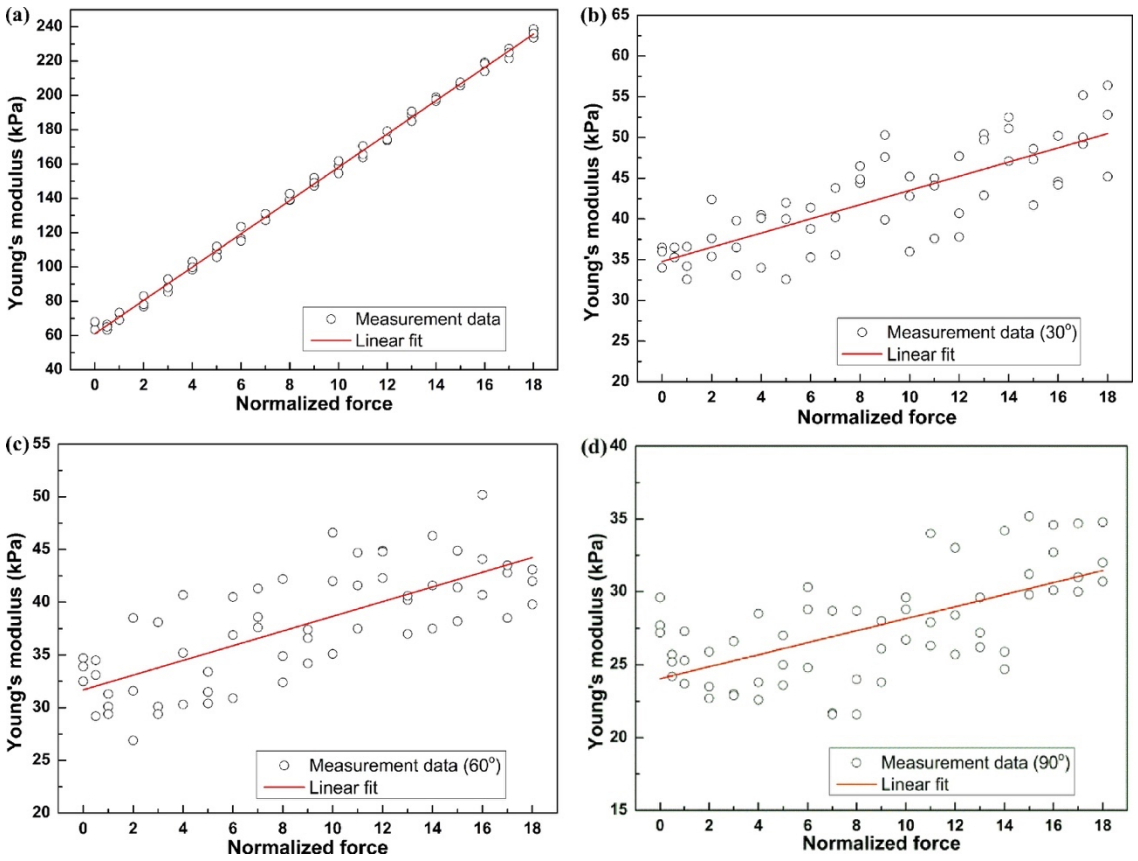

Figure 8-1 Association between muscle stiffness and passive normalised force at different probe angles: longitudinal-0° (a), oblique-30° (b), oblique-60° (c) and transverse-90°(d).

Reprinted with permission from Elsevier, Ultrasound in Medicine & Biology [583].

Carlsen and Ewertsen et al., known for their work on muscle SWE, have also recently investigated probe orientation but on the neck and shoulder muscles in healthy individuals [584]. Using the same LOGIQ-E9 system in Chapter 3, they found a significant difference in mean SWV between longitudinal and transverse planes. Additionally, they reported that day-to-day reading differences were not clinically significant. Despite the relative novelty of their work, their data analysis approach can be criticised. Merely reporting that one approach produces different readings to another is fruitless. It does not present any validity or superior performance (i.e. which one is better and should be used). Hence, when investigating the probe orientation, for example, researchers should investigate the most valid and reliable technique. The statistical hypothesis should focus on investigating the reliability between the reading rather than the differences. Similarly, for the day-to-day variation, the emphasis should be placed on the repeatability and agreement between the

SWE results. Unfortunately, their inaccurate approach is not uncommon in the SWE literature and should be avoided.

More work has been published on the effects of acquisition techniques. In an ex vivo experiment on porcine muscles using the LOGIQ-E9, a recent study [585] investigated the influence of probe orientation, probe pressure, depth and ROI size. As expected for the probe orientation, the longitudinal direction produced less variation. Variability increased gradually with depth. In contrast to Chapter 3 results, the mean SWV significantly decreased at greater depths (p<0.001). The ROI size did not influence the SWV measurements but increasing it had a positive effect on the readings variation. They also reported that using a lower frequency on a different probe (2.5 MHz, C1-6 convex) produced significantly lower SWV values. A manual increase in probe pressure resulted in higher muscle stiffness most pronounced between no load applied to 500 grams of added weight. Interestingly, it was recently reported that probe pressure might be beneficial in liver SWE to reduce the number of erroneous SWE acquisitions [586].

On the whole, recently published articles supported Chapter 3 findings regarding reliability and the importance of accounting for technical acquisition methods to yield valid readings of optimum reliability. These recommendations should hopefully contribute to muscle SWE acquisition guidelines when more research on musculoskeletal SWE is available.

8.2.2 Elastography in healthy and diseased skeletal muscles

Now turning to the work after the reliability chapter researching the topics of ageing (Chapter 4), myositis (Chapter 5), corticosteroids (Chapter 6) and rheumatoid arthritis (Chapter 7). These consecutive topics were selected to investigate SWE on a range of normal, established myopathy and suspected cases. Although the work carried out in these chapters shared a generally similar SWE and muscle assessment methodology, they had different study designs and focused on fundamentally different cases. This was the justification behind allotting a chapter for each instead of grouping them. The similar SWE and muscle assessment methodology was intended to allow comparison of the results. Besides, multiple muscles were scanned to provide integrity to the results.

The ageing effect on SWE-derived resting muscle stiffness was a significant finding with an important retrospective and prospective implications. Retrospectively, doubt can be placed on the results of studies that recruited a wide range of ages without accounting for the age variable. This applies to the numerous studies reviewed in Chapter 2. Moreover, a recent study [587] has presented interesting findings on SWE ability to identify muscle weakness in chronic heart failure patients. The study found that chronic heart disease patients displayed a significantly lower gastrocnemius muscle stiffness. However, the control group was noticeably younger [mean=55.8 years (range 24–78)] than the diseased group [mean=64.9 years (range 38–83)]. Indeed, their results could have been possibly confounded by age.

Prospectively, future muscle SWE should consider adjusting for age as a covariate in their analysis or rule-out its effect by matching their controls. The results in Chapter 7 confirmed the effect of ageing on the SWV readings as the tendency observed in the RA patients was excluded after adjusting the results. Indeed, age was a significant independent factor for explaining the variation in SWE results across the muscles.

Sex, in contrast, had no significant influence on SWV results. Male and female adults appeared to have the same normal resting muscle stiffness. Also, the results in the later chapters showed that both sexes are affected to the same degree by ageing, myositis and corticosteroid treatment. The literature is still inconclusive on this matter, but the presented results agree with the majority [186, 207, 251, 252]. Nevertheless, there is consensus on active muscle elasticity differences since this active state is controlled by the applied muscle contraction forces [205].

One of the limitations in Chapter 4 was the missing information on cohorts aged 55–75 years. Data on the healthy controls in Chapter 6 included subjects in their 60s. Comparing their results show that they are close to the muscle stiffness values of the middle-aged group (40–55 years) in Chapter 4. For example, the vastus lateralis and rectus femoris SWV were 1.64 m/s and 1.72 m/s respectively in the middle-aged group compared to 1.68 m/s and 1.74 m/s in the healthy controls from Chapter 6. This could support the finding that significant declines in muscle stiffness occur in elderly participants >75 years. Additionally, it is in line with other longitudinal evidence reporting a

considerable loss of strength and mass above 75 years [464]. The results from Chapter 7 in RA patients could indicate that the suspected concomitant arthritis in the elderly group from Chapter 4 did not have a substantial effect on SWV.

As the world's population is growing rapidly, the advent of novel assessment methods and interventions is necessary to prevent health and economic consequences associated with disability and loss of independence. The results of this thesis hold promise for SWE in evaluating the ageing effects on the biomechanical properties of skeletal muscles. A recent interesting study aimed to identify sarcopenia in elderly individuals (mean age 82 years) by calculating the speed of sound [588]. The velocity at which ultrasound waves travel in the gastrocnemius muscle was obtained by calculating the radiofrequency ultrasound data. In agreement with the SWE data in this thesis, the elderly subjects had a significantly lower speed of sound (1516 m/s) compared to young subjects (1545 m/s; $p<0.01$). Despite the convoluted setup required to collect the data, this new technique may overcome some SWE limiting factors such as ROI position, probe handling and muscle activation state.

Other relevant quantitative ultrasound parameters may also add a great value to the assessment of muscle ageing such as myofibres pennation angle. This specific property can provide information about the mechanical and contractile properties of skeletal pennate muscle [589]. Together with SWE, these assessment techniques may provide a feasible bed-side tool for assessing patients at risk to initiate timely interventions then monitor their progress.

Muscle SWE is somewhat in its infancy for a clinical application. However, the presented findings in Chapter 5 on SWE ability to identify IIM muscles can be considered the most promising and least far from clinical use compared to the assessment of ageing or corticosteroids myopathy. This is because the study defined the quantitative muscle elasticity characteristic in IIM compared to healthy controls and included strength and MRI validation.

The results determined that IIM patients have significantly reduced muscle stiffness. This altered property can be attributed to the increased volume of intra- and extra-cellular water content, atrophy and necrosis [502]. It may be suggested that these pathological features could impair the elastic proteins (e.g. titin) responsible for the muscle contractile properties. However, the intact

muscle stiffness during passive stretching was puzzling; Chapter 5 presented possible explanations. This preserved property was also found in chapters 4 and 6. The muscle fascia might have a fundamental role since it surrounds muscle fascicles and provides mechanical support during stretching as well as helps in force transmission [590]. In vitro analysis of IIM myofibres subjected to passive loads might explain the underlying mechanisms.

The role of medical imaging in IIM, particularly MRI, is growing rapidly for diagnosing and monitoring this disease. However, SWE is more clinically feasible compared to MRI and MR elastography (MRE). The agreement between SWE and MRE is unknown in skeletal muscle as well as other organs. Both techniques evaluate shear wave propagation but use principally different methods to estimate tissue displacement. SWE may play a vital role in management of IIM in the same way it has for liver fibrosis. Additionally, it may complement the limited clinical role of ultrasonography in IIM.

Next, Chapter 6 addressed the responsiveness of SWE for detecting muscle stiffness changes associated with corticosteroid use. The diagnosis of CIM may be challenging due to the insidious occurrence and the lack of diagnostic biomarkers to detect subclinical signs prior to consequent myopathy. Currently, the diagnosis depends on the clinical diagnosis of characteristic symptoms of disease onset to exclude other likely alternative causes. These points motivated the research carried in Chapter 6.

Relying exclusively on muscle strength to diagnose or monitor CIM can be misleading. Diminished muscle strength can be confounded by multiple factors such as age, psychological health and nutrition. Therefore, identifying novel methods that look beyond strength and muscle morphology might provide an invaluable clinical benefit. In the view of the results mentioned in Chapter 6, SWE evaluation may be useful for detecting decreased muscle stiffness as an early sign of CIM.

It seems that corticosteroid use, ageing and IIM all induce a loss in muscle stiffness. On the contrary, a rise in muscle stiffness can be observed in various myopathies. Patients with chronic neck pain have an approximately 0.5 m/s (15%) higher muscle stiffness compared to asymptomatic individuals ($p=0.001$) [591]. Similarly, masticatory myofascial pain patients have a significantly higher

masseter muscle SWV (2.00 m/s) compared to healthy controls (1.27 m/s) [592]. Kimura et al. [593] suggested that the increase in muscle stiffness occurs when intramuscular pressure increases due to a rise in blood perfusion and restricted venous outflow. However, this opinion does not correspond with the lower stiffness readings observed in IIM patients where increased muscle blood perfusion as a result of active inflammation is expected. For the topics investigated in this thesis, decreased muscle stiffness is likely to be the result of increased muscle water content and breakdown of contractile muscle elements. More discussion on these probable mechanisms is described in the previous chapters.

Muscle stiffness in RA patients was not altered or associated with diminished muscle strength. Comparing the results of SWE on myositis and RA could suggest that the degree of reported fibre atrophy and inflammatory infiltrates in RA is not likely as high as that in myositis to alter the biomechanical properties. This may suggest that the muscle weakness observed in RA could be related to intracellular metabolic impairment rather than RA-induced muscle atrophy. A recent study [594] has investigated the association between the gastrocnemius muscle SWV and ankle joint stiffness (as predicted in a biomechanical model) on four healthy volunteers. It reported a strong linear relationship (R^2=0.66; p=0.001) between them. On the contrary, the results in Chapter 7 showed no such association using patient-reported early morning joint stiffness. Theoretically, joint stiffness relies on multiple factors including passive elements such as the joint capsule, friction, ligaments and fascia as well as the muscle-tendon unit. Estimating these elements in a single model, similar to the cited study methodology, may yield positive results.

There are multiple challenges inherent in scanning musculoskeletal tissues that should be highlighted after examining more than 1000 muscles in this thesis. Firstly, muscles are extremely heterogeneous compared to other structures like the liver and thyroid. Muscle fibres are surrounded by the endomysium grouping them into muscle fascicles that are enclosed within the perimysium forming the muscle belly that is enclosed by the outer epimysium layer. Such heterogeneity is further complicated by the muscle-tendon orientations in uni-, bi- and multi-pennate muscles where fibres run at different directions. Furthermore, neurovascular structures course between the muscle fascicles.

These structures may inadvertently be included within the SWE acquisition box. Secondly, controlling muscle activation can be challenging especially in restless participants. A high resting SWV might be due to the patient isometrically contracting the muscle unintentionally. This was common during the hamstring positioning where participants may struggle to fully rest their legs against the wall at first-hand. Also, high SWV readings in the quadriceps can be detected when the patients' feet accidentally touch or push against the wall in the supine position. Therefore, it is essential to clearly instruct participants to relax and be aware of unexpected high SWV readings.

Moreover, muscle depth can represent a real challenge. This can be particularly problematic in obese patients where the subcutaneous fat layer is thick. Readings deeper than 6 or 7 cm using linear 9–12 MHz frequency may be inaccurate. A novel sonoelastography technology called crawling wave elastography may overcome the depth limitation of SWE systems based on external acoustic force pulses [595]. It is based on using two mechanical vibration sources operating at different frequencies sending sinusoidal waves that produce a shifting interference pattern (hence crawling waves) which can be used to estimate SWV. However, this technology has not yet been commercialised and its clinical usefulness in obese patients is not validated.

Users should be mindful of these challenges and their effects on the acquired SWE image. Correct probe orientation, optimum probe handling, careful patient positioning, appropriate ROI placement and use of SWV rather than Young's modulus (kPa) should yield valid and reliable muscle SWE readings. Based on the SWE results and practising experience throughout this thesis, the vastus lateralis muscle was the most accessible and easiest to scan. It also consistently produced positive results across the studies. The resting position yielded better results across the chapters and can be easily followed by subjects.

Overall, the thesis focused on adults. It is not certain that the recommended SWE acquisition techniques have the same performance on paediatrics. In addition, it is unknown how muscle stiffness behaves in juvenile myositis. Similarly, muscle stiffness might respond differently in children taking corticosteroid treatment. Therefore, the results should not be generalised to this

demographic. Future research should investigate muscle SWE on paediatric myopathies.

8.3 Limitations of the current work

The specific limitations of preceding studies were mentioned in each corresponding chapter. The overall thesis limitations are presented below.

8.3.1 Sample size

Considering the novelty of the work conducted in this thesis, no similar data were available to conduct formal sample size/power calculations for the majority of the studies. Clinically meaningful differences in SWV for the conditions investigated were unknown prior to starting this thesis. Therefore, published rules of thumb for study sample sizes were followed, which recommend between 12 and 30 subjects per group of interest to estimate parameters for powering future clinical trials [505, 506]. The results reported in this thesis, after exploring a multitude of potential muscle SWE applications, will inform power analysis of future trials. Despite the lack of sample size/power calculations, more than 1000 muscles were scanned from around 250 participants.

IIM is a rare disease, and its low prevalence limited recruiting more patients. Likewise, the incidence of GCA is relatively low. Recruiting GCA patients was challenging considering their symptoms at baseline. Nevertheless, the ageing study in Chapter 4 benefited from pre-existing data to power an appropriate sample size.

8.3.2 Blinding

A noticeable drawback is the lack of SWE operator blinding across all studies. This was not pragmatically feasible due to direct involvement in recruitment and scanning. To mitigate this limitation, the SWE acquisition scale was set at a large scale (0–7.1 m/s) above the expected ranges (<3.0 m/s) when collecting the data to suppress qualitative colour differences in the SWE colour box. Then, to use example images in the studies, the scale was retrospectively adjusted to an optimum level (0–2.9 m/s) via the machine's software.

8.3.3 Inter-operator reproducibility

The lack of inter-operator reproducibility testing is a limitation shared across the study chapters. No secondary sonographer was available to perform dual readings to verify this important reliability aspect. Nevertheless, various studies reported substantial inter-operator reproducibility for muscle SWE [202, 206, 209, 212, 213, 223, 225, 240, 242]. The studies reported ICC coefficients ranging from 0.57 to 0.99.

8.3.4 Physical activity

It is plausible to hypothesise that high levels of physical activity promotes muscle conditioning and changes the biomechanical properties of skeletal muscles. Indeed, a study has found that participants who perform physical activity for at least 6 hours per week have a significantly higher SWV ($p=0.023$) [222]. However, this difference was detected in only one of the two muscles tested (erector spinae muscle). In contrast, another study tested the biceps femoris and gastrocnemius and reported no difference in SWV based on physical activity levels ($p=0.314$) [252].

Physical activity of all participants was not recorded. It could have been evaluated using established questionnaires. Unfortunately, this was not considered during the design of the studies. It is worth noting, however, that none of the participants was considered a professional athlete.

8.4 Directions for future research

8.4.1 Muscle SWE acquisition and variability

Despite investigating the variability between two SWE systems in Chapter 3, the degree of agreement between other systems in skeletal muscles is unknown. This is currently important with the availability of more than seven SWE systems from various manufacturers each operating its unique patent-protected shear wave excitation and tracking technology. A recent study investigating the inter-system variability between six SWE systems in the liver demonstrated a good to excellent agreement [596]. However, this may not be true in skeletal muscles for the inherent challenges described before. Suggesting universal cut-off values for a specific myopathy is challenged by the variability and dependence on the elastography technique, system and

acquisition methods. Henceforward, researchers should develop variability correction formulas to accelerate clinical applicability.

All of the results were acquired using transient stress forces generated by acoustic radiation force impulses of a limited frequency range (120–160 Hz). This technique generates short-lived shear waves that get attenuated within 5mm approximately. Hence, most two-dimensional SWE systems send multiple consecutive pulses to generate stronger shear waves though this is still limited to a relatively small area (2–3 cm approximately). Therefore, alternative techniques such as the mechanical stress method used in MRI uses continuous mechanical vibrations at lower frequencies (as low as 20 Hz) to generate shear waves that can travel for longer durations and extend over larger areas. This continuous mechanical stress method has recently been used in a new elastography technique called time-harmonic elastography in the liver and demonstrated excellent results [597]. This method also enables varying the stress frequency, which can offer additional information on the biomechanical property of different tissues since shear wave velocity depends on the frequency. It would be interesting to investigate in future research the value of this method in diffuse muscle diseases where larger elastography coverage area is desired.

The usefulness of novel SWE technologies such as three-dimensional SWE should be investigated. This technology is so far only available on the Aixplorer system from Supersonic Imagine, which operates mechanical sweeping to acquire the volumetric data. Its feasibility on healthy skeletal muscles has been demonstrated recently [598]. Multiplanar elastography views could provide additional diagnostic value for muscle and soft tissue masses. Future studies are encouraged to research and analyse the cost-effectiveness of this latest development in SWE technology.

More broadly, the effect of surrounding structures (bone, subcutaneous tissue, fascia) on the muscle SWE measurements needs to be clarified. Future research should evaluate their impact on SWE image quality (e.g. artefacts) and define instances where measurements inaccuracy are common.

8.4.2 Elastography in muscle diseases

Experts believe that ultrasonography is a valuable tool for the screening and diagnosis of sarcopenia. Steps towards standardised measurements have begun [599]. However, too little is currently known regarding the usefulness of SWE in the context of sarcopenia assessment. There is a particular emphasis amongst researchers on the aspects of muscle quality in sarcopenia. The promising results in Chapter 4 highlight the impact of ageing on muscle elasticity.

Future research should aim to compare sarcopenic versus non-sarcopenic subjects. Studies should incorporate resting and passive stretching conditions since this thesis demonstrated that altered muscle stiffness varies depending on the muscle stiffness property under investigation. Sarcopenic subjects may potentially have an altered SWV under passive stretching. Muscle stiffness could also be a useful tool as a component in fall risk assessment as reduced muscle stiffness may compromise the delivery of tensile power in the muscle-tendon unit. Therefore, longitudinal studies of long follow-up durations should assess muscle SWE relationship with temporal changes in falls frequency and risk as well as muscle mass. The methodology should also incorporate postural (e.g. soleus) and phasic (e.g. vastus lateralis) muscles. Such research will generate valuable data on SWE ability to monitor the effects of ageing.

Research into the application of elastography in IIM is relatively more developed compared to the other investigated subjects. This thesis provided the evidence foundation to support further research in IIM. There is abundant room for further progress to establish the diagnostic role of muscle SWE. Prospective cohort studies need to recruit suspected and treatment naïve IIM patients to determine SWE diagnostic performance. The role of SWE in IIM would be most influential for monitoring disease activity. The study in Chapter 5 has cross-sectionally analysed only one aspect of disease activity (serum creatine kinase). More advanced tools to record disease activity could be applied such as the myositis disease activity assessment tool developed by the International Myositis Assessment & Clinical Studies group [600]. Such measures are not limited to muscle enzyme levels or strength testing; they capture a multitude of disease activity aspects including extra muscular manifestations.

Further work need to determine if muscle stiffness alteration patterns vary between IIM subtypes. This has been demonstrated using MRI [519]. Furthermore, future studies should consider investigating SWE construct validity against conventional B-mode and Doppler imaging. This may provide a composite of useful ultrasonographic bed-side methods to evaluate IIM. In the context of the OMERACT filter, multiple questions remain unanswered at present including discrimination sensitivity in clinical trials and the optimum SWV cut-off points.

The promising results in Chapter 6 warrants further research on a larger sample size. To detect a 15% difference in the vastus lateralis SWV after 3 months with 90% power and 0.05 alpha level, a future study should aim to recruit a minimum of 63 GCA patients. Longer follow-up durations are recommended to monitor the myopathic changes that may take as long as a year [351]. Changes in muscle stiffness under passive stretching might arise after such durations.

The principal clinical aim in CIM is to detect early myopathic signs prior to their manifestation. Hence, muscle strength testing must be included in the methodology to test if SWE alterations arise prior to consequent muscle weakness. Histological correlation, though less feasible, can provide valuable results and assess the construct validity of muscle SWE. The content validity can also be evaluated by assessing active muscle elasticity (i.e. elasticity under voluntary contraction). This recommendation applies also to future studies on ageing and myositis.

Despite the negative results in Chapter 7 on RA patients, the considerable observed muscle weakness calls for further research to understand the underlying mechanisms and develop assessment methods that can identify patients at risk of disability. Nevertheless, SWE may have a role for assessing joint synovium in RA subjects. If synovitis in joints of patients with inflammatory arthritides show unique alterations in stiffness, it may have a role in differential diagnosis and assessment of treatment response.

On a wider musculoskeletal level, SWE has promising and growing future perspectives. However, several areas remain under investigated such SWE assessment of ligaments and cartilages. Elastography is expected to be most

clinically useful in cases where no changes are evident on conventional B-mode and Doppler imaging.

8.5 Conclusions

SWE is a quantitative method for assessing soft tissue stiffness with various applications that have already transformed the management of several pathologies. However, the field of muscle SWE has been relatively under-investigated. Alteration in muscle stiffness was hypothesised to exist as a result of ageing, myositis, corticosteroid use and joint inflammation. The initial work undertaken in this thesis identified various SWE acquisition aspects that could affect the measurements variability and recommended the best techniques to improve muscle SWE reliability. The techniques were later experimented on a wide age range of healthy volunteers and showed that muscle stiffness decreased significantly in older age groups suggesting a potential use in sarcopenia assessment. The observed muscle stiffness declines in IIM and after corticosteroid treatment are the two most important and promising findings in this thesis. The results inform prospective adequately powered clinical trials.

To summarise, the work in this PhD thesis has improved the understanding of muscle SWE reliability and explored potential applications on established and suspected muscle diseases. This thesis provides an evidence base to allow SWE to be considered an objective and non-invasive assessment tool of muscle diseases. SWE is expected to be a useful complementary imaging tool in the clinical investigation of multiple musculoskeletal conditions. The future research agenda in muscle SWE needs to validate the myositis and corticosteroid findings in addition to further exploring the impact of ageing on muscle stiffness.

References

1. McLeod, M., et al., *Live strong and prosper: the importance of skeletal muscle strength for healthy ageing.* Biogerontology, 2016. **17**(3): p. 497-510.
2. Bernatsky, S., et al., *Healthcare costs of inflammatory myopathies.* The Journal of rheumatology, 2011. **38**(5): p. 885-888.
3. UK, A. *Healthy Ageing Evidence Review*. 2011 [cited 2018 03/2018]; Available from: https://www.ageuk.org.uk/globalassets/age-uk/documents/reports-and-publications/reports-and-briefings/health--wellbeing/rb_april11_evidence_review_healthy_ageing.pdf.
4. Cardy, C.M. and T. Potter, *The predictive value of creatine kinase, EMG and MRI in diagnosing muscle disease.* Rheumatology, 2007. **46**(10): p. 1617-1618.
5. Correa-de-Araujo, R., et al., *The Need for Standardized Assessment of Muscle Quality in Skeletal Muscle Function Deficit and Other Aging-Related Muscle Dysfunctions: A Symposium Report.* Frontiers in Physiology, 2017. **8**(87).
6. Ferrara, R. and L. Mansi, *Fundamentals of Medical Imaging (2nd edition).* European Journal of Nuclear Medicine and Molecular Imaging, 2011. **38**(2): p. 50, 91, 116, 145.
7. Dietrich, C.F., et al., *EFSUMB Guidelines and Recommendations on the Clinical Use of Liver Ultrasound Elastography, Update 2017 (Long Version).* Ultraschall Med, 2017.
8. Cosgrove, D., et al., *WFUMB Guidelines and Recommendations on the Clinical Use of Ultrasound Elastography: Part 4. Thyroid.* Ultrasound Med Biol, 2017. **43**(1): p. 4-26.
9. Yasuda, K., T. Anazawa, and S.i. Ishiwata, *Microscopic analysis of the elastic properties of nebulin in skeletal myofibrils.* Biophysical journal, 1995. **68**(2): p. 598-608.
10. OpenStax, *Anatomy & Physiology*. 2013: OpenStax CNX.
11. Stefan, G. and K. Karsten, *Spontaneous waves in muscle fibres.* New Journal of Physics, 2007. **9**(11): p. 417.
12. Huxley, A.F. and R. Niedergerke, *Structural changes in muscle during contraction: interference microscopy of living muscle fibres.* Nature, 1954. **173**(4412): p. 971.
13. Laing, N.G., *The sarcomere and skeletal muscle disease*. Vol. 642. 2009: Springer Science & Business Media.
14. Laing, N.G. and K.J. Nowak, *When contractile proteins go bad: the sarcomere and skeletal muscle disease.* BioEssays, 2005. **27**(8): p. 809-822.
15. Lacomis, D., D.W. Zochodne, and S.J. Bird, *Critical illness myopathy.* Muscle & nerve, 2000. **23**(12): p. 1785-1788.
16. Massa, R., et al., *Loss and renewal of thick myofilaments in glucocorticoid-treated rat soleus after denervation and reinnervation.* Muscle & nerve, 1992. **15**(11): p. 1290-1298.
17. Morfey, C.L., *Dictionary of Acoustics*. 2000: Academic Press. 430.
18. Newman, P.G. and G.S. Rozycki, *The History Of Ultrasound.* Surgical Clinics of North America, 1998. **78**(2): p. 179-195.

19. White, D.N., *Neurosonology pioneers.* Ultrasound in Medicine & Biology, 1988. **14**(7): p. 541-561.
20. Blitz, J. and G. Simpson, *Ultrasonic methods of non-destructive testing*. Vol. 2. 1995: Springer Science & Business Media.
21. Ensminger, D. and F.B. Stulen, *Ultrasonics: data, equations and their practical uses*. 2008: CRC press.
22. Leksell, L., *Echo-encephalography. I. Detection of intracranial complications following head injury.* Acta Chirurgica Scandinavica, 1956. **110**(4): p. 301.
23. NHS.England. *Statistics » Diagnostic Imaging Dataset 2017-18 Data*. 2018 12/01/2019]; Available from: https://www.england.nhs.uk/statistics/statistical-work-areas/diagnostic-imaging-dataset/diagnostic-imaging-dataset-2017-18-data/.
24. Sidhu, P.S., *Multiparametric Ultrasound (MPUS) Imaging: Terminology Describing the Many Aspects of Ultrasonography.* Ultraschall in Med, 2015. **36**(04): p. 315-317.
25. Tanter, M. and M. Fink, *Ultrafast imaging in biomedical ultrasound.* IEEE Transactions on Ultrasonics, Ferroelectrics, and Frequency Control, 2014. **61**(1): p. 102-119.
26. Jacobson, J.A., *Musculoskeletal Ultrasound: Focused Impact on MRI.* American Journal of Roentgenology, 2009. **193**(3): p. 619-627.
27. Naredo, E., et al., *Current state of musculoskeletal ultrasound training and implementation in Europe: results of a survey of experts and scientific societies.* Rheumatology, 2010. **49**(12): p. 2438-2443.
28. Wakefield, R.J., et al., *The value of sonography in the detection of bone erosions in patients with rheumatoid arthritis: a comparison with conventional radiography.* Arthritis & Rheumatology, 2000. **43**(12): p. 2762-2770.
29. Wakefield, R.J., et al., *Should oligoarthritis be reclassified? Ultrasound reveals a high prevalence of subclinical disease.* Ann Rheum Dis, 2004. **63**(4): p. 382-5.
30. Ozgocmen, S., et al., *Clinical evaluation and power Doppler sonography in rheumatoid arthritis: evidence for ongoing synovial inflammation in clinical remission.* South Med J, 2008. **101**(3): p. 240-5.
31. Balint, P.V., et al., *Ultrasonography of entheseal insertions in the lower limb in spondyloarthropathy.* Ann Rheum Dis, 2002. **61**(10): p. 905-10.
32. D'Agostino, M.A., et al., *How to diagnose spondyloarthritis early? Accuracy of peripheral enthesitis detection by power Doppler ultrasonography.* Annals of the Rheumatic Diseases, 2011. **70**(8): p. 1433-1440.
33. Naredo, E., et al., *Ultrasound-detected musculoskeletal urate crystal deposition: which joints and what findings should be assessed for diagnosing gout?* Ann Rheum Dis, 2014. **73**(8): p. 1522-8.
34. Ottaviani, S., T. Bardin, and P. Richette, *Usefulness of ultrasonography for gout.* Joint Bone Spine, 2012. **79**(5): p. 441-5.
35. Luqmani, R., et al., *The Role of Ultrasound Compared to Biopsy of Temporal Arteries in the Diagnosis and Treatment of Giant Cell Arteritis (TABUL): a diagnostic accuracy and cost-effectiveness study.* Health Technol Assess, 2016. **20**(90): p. 1-238.

36. Iagnocco, A., et al., *Ultrasound evaluation of hand, wrist and foot joint synovitis in systemic lupus erythematosus.* Rheumatology (Oxford), 2014. **53**(3): p. 465-72.
37. Kang, T., P. Emery, and R.J. Wakefield, *A brief history of ultrasound in rheumatology: where we are now.* Clin Exp Rheumatol, 2014. **32**(1 Suppl 80): p. S7-11.
38. Aletaha, D., et al., *2010 Rheumatoid arthritis classification criteria: An American College of Rheumatology/European League Against Rheumatism collaborative initiative.* Arthritis & Rheumatism, 2010. **62**(9): p. 2569-2581.
39. Morii, T., et al., *Differential diagnosis between benign and malignant soft tissue tumors utilizing ultrasound parameters.* Journal of Medical Ultrasonics, 2017.
40. Hotfiel, T., et al., *Contrast-Enhanced Ultrasound as a New Investigative Tool in Diagnostic Imaging of Muscle Injuries-A Pilot Study Evaluating Conventional Ultrasound, CEUS, and Findings in MRI.* Clinical Journal of Sport Medicine, 2017.
41. Klauser, A., et al., *Contrast enhanced gray-scale sonography in assessment of joint vascularity in rheumatoid arthritis: results from the IACUS study group.* European radiology, 2005. **15**(12): p. 2404-2410.
42. Klauser, A.S., et al., *Detection of vascularity in wrist tenosynovitis: power doppler ultrasound compared with contrast-enhanced grey-scale ultrasound.* Arthritis research & therapy, 2010. **12**(6): p. R209.
43. Schueller-Weidekamm, C., et al., *Power Doppler sonography and pulse-inversion harmonic imaging in evaluation of rheumatoid arthritis synovitis.* American Journal of Roentgenology, 2007. **188**(2): p. 504-508.
44. Ghalioungui, P., *Magic and Medical Science in Ancient Egypt.* 1963.
45. Walker, H.K., *The origins of the history and physical examination.* 1990.
46. Crawford, P. and J.A. Crop, *Evaluation of scrotal masses.* Am Fam Physician, 2014. **89**(9): p. 723-7.
47. Garra, B.S., et al., *Elastography of breast lesions: initial clinical results.* Radiology, 1997. **202**(1): p. 79-86.
48. Yamakoshi, Y., J. Sato, and T. Sato, *Ultrasonic imaging of internal vibration of soft tissue under forced vibration.* IEEE transactions on ultrasonics, ferroelectrics, and frequency control, 1990. **37**(2): p. 45-53.
49. Eisensher, A., et al., *La palpation échographique rythméeechosismographie.* J. Radiol, 1983. **64**: p. 255-61.
50. Ophir, J., et al., *Elastography: a quantitative method for imaging the elasticity of biological tissues.* Ultrasonic imaging, 1991. **13**(2): p. 111-134.
51. Cespedes, I., et al., *Elastography: elasticity imaging using ultrasound with application to muscle and breast in vivo.* Ultrasonic imaging, 1993. **15**(2): p. 73-88.
52. Krouskop, T.A., et al., *Elastic moduli of breast and prostate tissues under compression.* Ultrasonic imaging, 1998. **20**(4): p. 260-274.
53. Mahendran, M., *The modulus of elasticity of steel-is it 200 GPa?* 1996.
54. Wells, P.N. and H.D. Liang, *Medical ultrasound: imaging of soft tissue strain and elasticity.* J R Soc Interface, 2011. **8**(64): p. 1521-49.
55. Coombes, B., et al., *Quantifying tendon elasticity in healthy and diseased tendon using shearwave elastography: A systematic review.* Journal of Science and Medicine in Sport, 2017. **20**: p. e114.

56. Budiansky, B., *On the elastic moduli of some heterogeneous materials.* Journal of the Mechanics and Physics of Solids, 1965. **13**(4): p. 223-227.
57. Sanada, M., et al., *Clinical evaluation of sonoelasticity measurement in liver using ultrasonic imaging of internal forced low-frequency vibration.* Ultrasound in medicine & biology, 2000. **26**(9): p. 1455-1460.
58. Urban, M.W., et al., *Discrepancies in Reporting Tissue Material Properties.* Journal of Ultrasound in Medicine, 2013. **32**(5): p. 886-888.
59. Capurro, M. and F. Barberis, *Evaluating the mechanical properties of biomaterials.* Biomaterials for Bone Regeneration: Novel Techniques and Applications, 2014: p. 270.
60. Hoskins, P.R., K. Martin, and A. Thrush, *Diagnostic ultrasound: physics and equipment*, ed. n. edition. 2010: Cambridge University Press. 196-216.
61. Clevert, D., M. D'Onofrio, and E. Quaia, *Atlas of Elastosonography*. Clinical Applications with Imaging Correlations. 2016: Springer.
62. Cosgrove, D., et al., *EFSUMB guidelines and recommendations on the clinical use of ultrasound elastography. Part 2: Clinical applications.* Ultraschall in der Medizin-European Journal of Ultrasound, 2013. **34**(03): p. 238-253.
63. Ferraioli, G., et al., *WFUMB guidelines and recommendations for clinical use of ultrasound elastography: Part 3: liver.* Ultrasound Med Biol, 2015. **41**(5): p. 1161-1179.
64. Barr, R.G. and Z. Zhang, *Effects of precompression on elasticity imaging of the breast: development of a clinically useful semiquantitative method of precompression assessment.* J Ultrasound Med, 2012. **31**(6): p. 895-902.
65. Gilbertson, M.W. and B.W. Anthony, *Force and Position Control System for Freehand Ultrasound.* IEEE Transactions on Robotics, 2015. **31**(4): p. 835-849.
66. Friedrich-Rust, M., et al., *Real-time tissue elastography versus FibroScan for noninvasive assessment of liver fibrosis in chronic liver disease.* Ultraschall Med, 2009. **30**(5): p. 478-84.
67. Ferraioli, G., et al., *Performance of real-time strain elastography, transient elastography, and aspartate-to-platelet ratio index in the assessment of fibrosis in chronic hepatitis C.* AJR Am J Roentgenol, 2012. **199**(1): p. 19-25.
68. Gulizia, R., G. Ferraioli, and C. Filice, *Open Questions in the Assessment of Liver Fibrosis Using Real-Time Elastography.* American Journal of Roentgenology, 2008. **190**(6): p. W370-W371.
69. Kiessel, L.M., T. Hall, and J. Jiang. *P4F-7 Integration of a Pressure Sensing Array Into Ultrasound Elastography*. in *2007 IEEE Ultrasonics Symposium Proceedings*. 2007.
70. Itoh, A., et al., *Breast disease: clinical application of US elastography for diagnosis.* Radiology, 2006. **239**(2): p. 341-50.
71. Wang, H., et al., *Comparison of strain ratio with elastography score system in differentiating malignant from benign thyroid nodules.* Clin Imaging, 2013. **37**(1): p. 50-5.
72. Zhi, H., et al., *Ultrasonic elastography in breast cancer diagnosis: strain ratio vs 5-point scale.* Acad Radiol, 2010. **17**(10): p. 1227-33.

73. Zhang, Y., et al., *Differentiation of prostate cancer from benign lesions using strain index of transrectal real-time tissue elastography.* Eur J Radiol, 2012. **81**(5): p. 857-62.
74. Wang, H., et al., *Comparison of strain ratio with elastography score system in differentiating malignant from benign thyroid nodules.* Clinical imaging, 2013. **37**(1): p. 50-55.
75. Barr, R.G., et al., *WFUMB guidelines and recommendations for clinical use of ultrasound elastography: Part 2: breast.* Ultrasound Med Biol, 2015. **41**(5): p. 1148-1160.
76. Cosgrove, D., et al., *WFUMB Guidelines and Recommendations on the Clinical Use of Ultrasound Elastography: Part 4. Thyroid.* Ultrasound in Medicine & Biology, 2017. **43**(1): p. 4-26.
77. Niitsu, M., et al., *Muscle hardness measurement by using ultrasound elastography: a feasibility study.* Acta Radiol, 2011. **52**(1): p. 99-105.
78. Ariji, Y., et al., *Use of sonographic elastography of the masseter muscles for optimizing massage pressure: a preliminary study.* J Oral Rehabil, 2009. **36**(9): p. 627-35.
79. Yanagisawa, O., et al., *Evaluation of human muscle hardness after dynamic exercise with ultrasound real-time tissue elastography: a feasibility study.* Clin Radiol, 2011. **66**(9): p. 815-9.
80. Akagi, R., et al., *Relationships between muscle size and hardness of the medial gastrocnemius at different ankle joint angles in young men.* Acta Radiol, 2012. **53**(3): p. 307-11.
81. Berko, N.S., et al., *Ultrasound elastography in children: establishing the normal range of muscle elasticity.* Pediatr Radiol, 2014. **44**(2): p. 158-63.
82. Chino, K., et al., *Reliability and validity of quantifying absolute muscle hardness using ultrasound elastography.* PLoS One, 2012. **7**(9): p. e45764.
83. Botar-Jid, C., et al., *The contribution of ultrasonography and sonoelastography in assessment of myositis.* Med Ultrason, 2010. **12**(2): p. 120-6.
84. Berko, N.S., et al., *Efficacy of ultrasound elastography in detecting active myositis in children: can it replace MRI?* Pediatr Radiol, 2015. **45**(10): p. 1522-8.
85. Illomei, G., et al., *Muscle elastography: a new imaging technique for multiple sclerosis spasticity measurement.* Neurol Sci, 2017. **38**(3): p. 433-439.
86. Yasar, E., et al., *Assessment of forearm muscle spasticity with sonoelastography in patients with stroke.* Br J Radiol, 2016. **89**(1068): p. 20160603.
87. Brune, J.N., *Tectonic stress and the spectra of seismic shear waves from earthquakes.* Journal of Geophysical Research, 1970. **75**(26): p. 4997-5009.
88. Levinson, S.F., M. Shinagawa, and T. Sato, *Sonoelastic determination of human skeletal muscle elasticity.* Journal of Biomechanics, 1995. **28**(10): p. 1145-1154.
89. Catheline, S., et al., *Diffraction field of a low frequency vibrator in soft tissues using transient elastography.* IEEE Transactions on Ultrasonics, Ferroelectrics, and Frequency Control, 1999. **46**(4): p. 1013-1019.

90. Palmeri, M.L., et al., *Noninvasive evaluation of hepatic fibrosis using acoustic radiation force-based shear stiffness in patients with nonalcoholic fatty liver disease.* J Hepatol, 2011. **55**(3): p. 666-672.
91. Sun, C.-Y., et al., *Virtual touch tissue imaging and quantification (VTIQ) in the evaluation of thyroid nodules: the associated factors leading to misdiagnosis.* Scientific Reports, 2017. **7**: p. 41958.
92. Bercoff, J., M. Tanter, and M. Fink, *Supersonic shear imaging: a new technique for soft tissue elasticity mapping.* IEEE Trans Ultrason Ferroelectr Freq Control, 2004. **51**(4): p. 396-409.
93. Gerber, L., et al., *Assessment of liver fibrosis with 2-D shear wave elastography in comparison to transient elastography and acoustic radiation force impulse imaging in patients with chronic liver disease.* Ultrasound Med Biol, 2015. **41**(9): p. 2350-9.
94. Woo, H., et al., *Comparison of the Reliability of Acoustic Radiation Force Impulse Imaging and Supersonic Shear Imaging in Measurement of Liver Stiffness.* Radiology, 2015. **277**(3): p. 881-6.
95. Leung, V.Y., et al., *Quantitative elastography of liver fibrosis and spleen stiffness in chronic hepatitis B carriers: comparison of shear-wave elastography and transient elastography with liver biopsy correlation.* Radiology, 2013. **269**(3): p. 910-8.
96. Kim, H.J., et al., *Quantitative comparison of transient elastography (TE), shear wave elastography (SWE) and liver biopsy results of patients with chronic liver disease.* J Phys Ther Sci, 2015. **27**(8): p. 2465-8.
97. Tozaki, M., et al., *Shear wave velocity measurements for differential diagnosis of solid breast masses: a comparison between virtual touch quantification and virtual touch IQ.* Ultrasound Med Biol, 2013. **39**(12): p. 2233-45.
98. Zeng, J., et al., *Comparison of 2-D Shear Wave Elastography and Transient Elastography for Assessing Liver Fibrosis in Chronic Hepatitis B.* Ultrasound Med Biol, 2017. **43**(8): p. 1563-1570.
99. Paul, S.B., et al., *Assessment of liver fibrosis in chronic hepatitis: comparison of shear wave elastography and transient elastography.* Abdom Radiol (NY), 2017. **42**(12): p. 2864-2873.
100. Elkrief, L., et al., *Prospective comparison of spleen and liver stiffness by using shear-wave and transient elastography for detection of portal hypertension in cirrhosis.* Radiology, 2015. **275**(2): p. 589-98.
101. Chung, J.H., et al., *The usefulness of transient elastography, acoustic-radiation-force impulse elastography, and real-time elastography for the evaluation of liver fibrosis.* Clin Mol Hepatol, 2013. **19**(2): p. 156-64.
102. Webb, M., et al., *Assessment of Liver and Spleen Stiffness in Patients With Myelofibrosis Using FibroScan and Shear Wave Elastography.* Ultrasound Q, 2015. **31**(3): p. 166-9.
103. Friedrich-Rust, M., et al., *Point Shear Wave Elastography by Acoustic Radiation Force Impulse Quantification in Comparison to Transient Elastography for the Noninvasive Assessment of Liver Fibrosis in Chronic Hepatitis C: A Prospective International Multicenter Study.* Ultraschall Med, 2015. **36**(3): p. 239-47.
104. Wu, T., et al., *Comparison of Two-Dimensional Shear Wave Elastography and Real-Time Tissue Elastography for Assessing Liver Fibrosis in Chronic Hepatitis B.* Dig Dis, 2016. **34**(6): p. 640-649.

105. Poynard, T., et al., *Real-Time Shear Wave versus Transient Elastography for Predicting Fibrosis: Applicability, and Impact of Inflammation and Steatosis. A Non-Invasive Comparison.* PLoS One, 2016. **11**(10): p. e0163276.
106. Fang, C., et al., *Reproducibility of 2-Dimensional Shear Wave Elastography Assessment of the Liver: A Direct Comparison With Point Shear Wave Elastography in Healthy Volunteers.* J Ultrasound Med, 2017. **36**(8): p. 1563-1569.
107. Ferraioli, G., et al., *Accuracy of real-time shear wave elastography for assessing liver fibrosis in chronic hepatitis C: A pilot study.* Hepatology, 2012. **56**(6): p. 2125-2133.
108. Cassinotto, C., et al., *Non-invasive assessment of liver fibrosis with impulse elastography: comparison of Supersonic Shear Imaging with ARFI and FibroScan(R).* J Hepatol, 2014. **61**(3): p. 550-7.
109. Yoneda, M., et al., *Supersonic Shear Imaging and Transient Elastography With the XL Probe Accurately Detect Fibrosis in Overweight or Obese Patients With Chronic Liver Disease.* Clin Gastroenterol Hepatol, 2015. **13**(8): p. 1502-9.e5.
110. Chen, Y.P., et al., *Comparison of Virtual Touch Tissue Quantification and Virtual Touch Tissue Imaging Quantification for diagnosis of solid breast tumors of different sizes.* Clin Hemorheol Microcirc, 2016. **64**(2): p. 235-244.
111. Ren, W.W., et al., *Two-dimensional shear wave elastography of breast lesions: Comparison of two different systems.* Clin Hemorheol Microcirc, 2017. **66**(1): p. 37-46.
112. Marcon, J., et al., *Shear wave elastography of the testes in a healthy study collective - Differences in standard values between ARFI and VTIQ techniques.* Clin Hemorheol Microcirc, 2016. **64**(4): p. 721-728.
113. Brum, J., et al., *Application of 1-D transient elastography for the shear modulus assessment of thin-layered soft tissue: comparison with supersonic shear imaging technique.* IEEE Trans Ultrason Ferroelectr Freq Control, 2012. **59**(4): p. 703-14.
114. Franchi-Abella, S., C. Elie, and J.M. Correas, *Performances and Limitations of Several Ultrasound-Based Elastography Techniques: A Phantom Study.* Ultrasound Med Biol, 2017. **43**(10): p. 2402-2415.
115. Ariji, Y., et al., *Shear-wave sonoelastography for assessing masseter muscle hardness in comparison with strain sonoelastography: study with phantoms and healthy volunteers.* Dentomaxillofac Radiol, 2016. **45**(2): p. 20150251.
116. Dillman, J.R., et al., *Superficial ultrasound shear wave speed measurements in soft and hard elasticity phantoms: repeatability and reproducibility using two ultrasound systems.* Pediatr Radiol, 2015. **45**(3): p. 376-85.
117. Mulabecirovic, A., et al., *In Vitro Comparison of Five Different Elastography Systems for Clinical Applications, Using Strain and Shear Wave Technology.* Ultrasound Med Biol, 2016. **42**(11): p. 2572-2588.
118. Leong, H.-T., et al., *Quantitative estimation of muscle shear elastic modulus of the upper trapezius with supersonic shear imaging during arm positioning.* PloS one, 2013. **8**(6): p. e67199.

119. Kim, J.R., et al., *The diagnostic performance of shear-wave elastography for liver fibrosis in children and adolescents: A systematic review and diagnostic meta-analysis.* Eur Radiol, 2017.
120. Yang, Z., et al., *Assessment of Diffuse Thyroid Disease by Strain Ratio in Ultrasound Elastography.* Ultrasound Med Biol, 2015. **41**(11): p. 2884-9.
121. Hu, X., Y. Liu, and L. Qian, *Diagnostic potential of real-time elastography (RTE) and shear wave elastography (SWE) to differentiate benign and malignant thyroid nodules: A systematic review and meta-analysis.* Medicine (Baltimore), 2017. **96**(43): p. e8282.
122. Tian, W., et al., *Comparing the Diagnostic Accuracy of RTE and SWE in Differentiating Malignant Thyroid Nodules from Benign Ones: a Meta-Analysis.* Cell Physiol Biochem, 2016. **39**(6): p. 2451-2463.
123. Carlsen, J.F., et al., *A comparative study of strain and shear-wave elastography in an elasticity phantom.* AJR Am J Roentgenol, 2015. **204**(3): p. W236-42.
124. Barr, R.G. and Z. Zhang, *Shear-wave elastography of the breast: value of a quality measure and comparison with strain elastography.* Radiology, 2015. **275**(1): p. 45-53.
125. Seo, M., et al., *Comparison and Combination of Strain and Shear Wave Elastography of Breast Masses for Differentiation of Benign and Malignant Lesions by Quantitative Assessment: Preliminary Study.* J Ultrasound Med, 2017.
126. Zhang, F., et al., *Comparison of Acoustic Radiation Force Impulse Imaging and Strain Elastography in Differentiating Malignant From Benign Thyroid Nodules.* J Ultrasound Med, 2017. **36**(12): p. 2533-2543.
127. Chang, J.M., et al., *Comparison of shear-wave and strain ultrasound elastography in the differentiation of benign and malignant breast lesions.* AJR Am J Roentgenol, 2013. **201**(2): p. W347-56.
128. Youk, J.H., et al., *Comparison of strain and shear wave elastography for the differentiation of benign from malignant breast lesions, combined with B-mode ultrasonography: qualitative and quantitative assessments.* Ultrasound Med Biol, 2014. **40**(10): p. 2336-44.
129. Ma, Y., et al., *Comparison of strain and shear-wave ultrasounic elastography in predicting the pathological response to neoadjuvant chemotherapy in breast cancers.* Eur Radiol, 2017. **27**(6): p. 2282-2291.
130. Gennisson, J.L., et al., *Ultrasound elastography: principles and techniques.* Diagn Interv Imaging, 2013. **94**(5): p. 487-95.
131. Sebag, F., et al., *Shear wave elastography: a new ultrasound imaging mode for the differential diagnosis of benign and malignant thyroid nodules.* The Journal of Clinical Endocrinology & Metabolism, 2010. **95**(12): p. 5281-5288.
132. Garra, B.S., *Elastography: current status, future prospects, and making it work for you.* Ultrasound Q, 2011. **27**(3): p. 177-86.
133. Barr, R.G., et al., *WFUMB Guidelines and Recommendations on the Clinical Use of Ultrasound Elastography: Part 5. Prostate.* Ultrasound Med Biol, 2017. **43**(1): p. 27-48.
134. De Zordo, T., et al., *Real-time sonoelastography of lateral epicondylitis: comparison of findings between patients and healthy volunteers.* AJR Am J Roentgenol, 2009. **193**(1): p. 180-5.

135. Barr, R.G., *Sonographic breast elastography: a primer.* J Ultrasound Med, 2012. **31**(5): p. 773-83.
136. Lin, C.Y., et al., *An Artifact in Supersonic Shear Wave Elastography.* Ultrasound Med Biol, 2017. **43**(2): p. 517-530.
137. America, R.S.o.N. *Quantitative Imaging Biomarkers Alliance (QIBA)*. 2017 [cited 2017 02/12/2017]; Available from: https://www.rsna.org/QIBA/.
138. Gennisson, J.-L., et al., *Viscoelastic and anisotropic mechanical properties of in vivo muscle tissue assessed by supersonic shear imaging.* Ultrasound Med Biol, 2010. **36**(5): p. 789-801.
139. Royer, D., et al., *On the elasticity of transverse isotropic soft tissues (L).* The Journal of the Acoustical Society of America, 2011. **129**(5): p. 2757-2760.
140. Caenen, A., et al., *A versatile and experimentally validated finite element model to assess the accuracy of shear wave elastography in a bounded viscoelastic medium.* IEEE Trans Ultrason Ferroelectr Freq Control, 2015. **62**(3): p. 439-50.
141. Kudo, M., et al., *JSUM ultrasound elastography practice guidelines: liver.* J Med Ultrason (2001), 2013. **40**(4): p. 325-57.
142. Sporea, I., et al., *Romanian national guidelines and practical recommendations on liver elastography.* Med Ultrason, 2014. **16**(2): p. 123-38.
143. Jiang, T., et al., *Diagnostic Accuracy of 2D-Shear Wave Elastography for Liver Fibrosis Severity: A Meta-Analysis.* PLoS One, 2016. **11**(6): p. e0157219.
144. Liu, H., et al., *Acoustic Radiation Force Impulse Elastography for the Non-Invasive Evaluation of Hepatic Fibrosis in Non-Alcoholic Fatty Liver Disease Patients: A Systematic Review & Meta-Analysis.* PLoS One, 2015. **10**(7): p. e0127782.
145. Tsochatzis, E.A., et al., *Elastography for the diagnosis of severity of fibrosis in chronic liver disease: a meta-analysis of diagnostic accuracy.* J Hepatol, 2011. **54**(4): p. 650-9.
146. Bota, S., et al., *Meta-analysis: ARFI elastography versus transient elastography for the evaluation of liver fibrosis.* Liver Int, 2013. **33**(8): p. 1138-47.
147. Njei, B., et al., *Use of transient elastography in patients with HIV-HCV coinfection: A systematic review and meta-analysis.* J Gastroenterol Hepatol, 2016. **31**(10): p. 1684-1693.
148. Friedrich-Rust, M., et al., *Performance of Acoustic Radiation Force Impulse imaging for the staging of liver fibrosis: a pooled meta-analysis.* J Viral Hepat, 2012. **19**(2): p. e212-9.
149. Chon, Y.E., et al., *Performance of transient elastography for the staging of liver fibrosis in patients with chronic hepatitis B: a meta-analysis.* PLoS One, 2012. **7**(9): p. e44930.
150. Nierhoff, J., et al., *The efficiency of acoustic radiation force impulse imaging for the staging of liver fibrosis: a meta-analysis.* Eur Radiol, 2013. **23**(11): p. 3040-53.
151. Li, Y., et al., *Systematic review with meta-analysis: the diagnostic accuracy of transient elastography for the staging of liver fibrosis in patients with chronic hepatitis B.* Aliment Pharmacol Ther, 2016. **43**(4): p. 458-69.

152. Li, C., et al., *Diagnostic Accuracy of Real-Time Shear Wave Elastography for Staging of Liver Fibrosis: A Meta-Analysis.* Med Sci Monit, 2016. **22**: p. 1349-59.
153. Feng, J.C., et al., *Diagnostic Accuracy of SuperSonic Shear Imaging for Staging of Liver Fibrosis: A Meta-analysis.* J Ultrasound Med, 2016. **35**(2): p. 329-39.
154. NICE. *Cirrhosis in over 16s: assessment and management | Guidance and guidelines | NICE*. 2016 [cited 2017 04/12/2017]; Available from: https://www.nice.org.uk/guidance/ng50.
155. NICE. *Virtual Touch Quantification to diagnose and monitor liver fibrosis in chronic hepatitis B and C | Guidance and guidelines | NICE*. 2015 04/12/2017]; Available from: https://www.nice.org.uk/guidance/mtg27.
156. Ying, L., et al., *Clinical utility of acoustic radiation force impulse imaging for identification of malignant liver lesions: a meta-analysis.* European Radiology, 2012. **22**(12): p. 2798-2805.
157. Ma, X., et al., *Elastography for the differentiation of benign and malignant liver lesions: a meta-analysis.* Tumor Biology, 2014. **35**(5): p. 4489-4497.
158. Jiao, Y., et al., *Shear wave elastography imaging for detecting malignant lesions of the liver: a systematic review and pooled meta-analysis.* Med Ultrason, 2017. **19**(1): p. 16-22.
159. Yu, H. and S.R. Wilson, *Differentiation of benign from malignant liver masses with Acoustic Radiation Force Impulse technique.* Ultrasound Q, 2011. **27**(4): p. 217-23.
160. Park, H., et al., *Characterization of focal liver masses using acoustic radiation force impulse elastography.* World Journal of Gastroenterology : WJG, 2013. **19**(2): p. 219-226.
161. Saarenmaa, I., et al., *The effect of age and density of the breast on the sensitivity of breast cancer diagnostic by mammography and ultasonography.* Breast Cancer Res Treat, 2001. **67**(2): p. 117-23.
162. Athanasiou, A., et al., *Breast lesions: quantitative elastography with supersonic shear imaging--preliminary results.* Radiology, 2010. **256**(1): p. 297-303.
163. Berg, W.A., et al., *Shear-wave Elastography Improves the Specificity of Breast US: The BE1 Multinational Study of 939 Masses.* Radiology, 2012. **262**(2): p. 435-449.
164. Chen, L., et al., *Diagnostic performances of shear-wave elastography for identification of malignant breast lesions: a meta-analysis.* Jpn J Radiol, 2014. **32**(10): p. 592-9.
165. Cosgrove, D.O., et al., *Shear wave elastography for breast masses is highly reproducible.* Eur Radiol, 2012. **22**(5): p. 1023-32.
166. NICE. *Aixplorer ShearWave Elastography for ultrasound imaging and assessing suspicious breast lesions | Guidance and guidelines | NICE*. 2014 8/12/2017]; Available from: https://www.nice.org.uk/advice/mib15/chapter/Summary.
167. Yoon, J.H., et al., *Shear-wave elastography in the diagnosis of solid breast masses: what leads to false-negative or false-positive results?* Eur Radiol, 2013. **23**(9): p. 2432-40.
168. Tanter, M., et al., *Quantitative Assessment of Breast Lesion Viscoelasticity: Initial Clinical Results Using Supersonic Shear Imaging.* Ultrasound in Medicine & Biology, 2008. **34**(9): p. 1373-1386.

169. Barr, R.G. *The Role of Sonoelastography in Breast Lesions*. in *Seminars in Ultrasound, CT and MRI*. 2017. Elsevier.
170. Brito, J.P., et al., *The accuracy of thyroid nodule ultrasound to predict thyroid cancer: systematic review and meta-analysis.* J Clin Endocrinol Metab, 2014. **99**(4): p. 1253-63.
171. Zhan, J., et al., *Acoustic radiation force impulse imaging (ARFI) for differentiation of benign and malignant thyroid nodules—A meta-analysis.* European Journal of Radiology, 2015. **84**(11): p. 2181-2186.
172. Dong, F.J., et al., *Acoustic Radiation Force Impulse imaging for detecting thyroid nodules: a systematic review and pooled meta-analysis.* Med Ultrason, 2015. **17**(2): p. 192-9.
173. Lin, P., et al., *Diagnostic performance of shear wave elastography in the identification of malignant thyroid nodules: a meta-analysis.* European Radiology, 2014. **24**(11): p. 2729-2738.
174. Liu, B.-J., et al., *Quantitative Shear Wave Velocity Measurement on Acoustic Radiation Force Impulse Elastography for Differential Diagnosis between Benign and Malignant Thyroid Nodules: A Meta-analysis.* Ultrasound in Medicine & Biology, 2015. **41**(12): p. 3035-3043.
175. Zhang, B., et al., *Shear wave elastography for differentiation of benign and malignant thyroid nodules: a meta-analysis.* J Ultrasound Med, 2013. **32**(12): p. 2163-9.
176. Nattabi, H.A., et al., *Is Diagnostic Performance of Quantitative 2D-Shear Wave Elastography Optimal for Clinical Classification of Benign and Malignant Thyroid Nodules?: A Systematic Review and Meta-analysis.* Acad Radiol, 2017.
177. Phipps, S., et al., *Measurement of tissue mechanical characteristics to distinguish between benign and malignant prostatic disease.* Urology, 2005. **66**(2): p. 447-50.
178. Sang, L., et al., *Accuracy of shear wave elastography for the diagnosis of prostate cancer: A meta-analysis.* Scientific Reports, 2017. **7**: p. 1949.
179. Alan, B., et al., *Role of Acoustic Radiation Force Impulse (ARFI) Elastography in Determination of Severity of Benign Prostate Hyperplasia.* Medical Science Monitor : International Medical Journal of Experimental and Clinical Research, 2016. **22**: p. 4523-4528.
180. Correas, J.M., et al., *Update on ultrasound elastography: Miscellanea. Prostate, testicle, musculo-skeletal.* European Journal of Radiology, 2013. **82**(11): p. 1904-1912.
181. Zhang, Z.J. and S.N. Fu, *Shear Elastic Modulus on Patellar Tendon Captured from Supersonic Shear Imaging: Correlation with Tangent Traction Modulus Computed from Material Testing System and Test-Retest Reliability.* PLoS One, 2013. **8**(6): p. e68216.
182. Aubry, S., et al., *Biomechanical properties of the calcaneal tendon in vivo assessed by transient shear wave elastography.* Skeletal Radiol, 2013. **42**(8): p. 1143-50.
183. Chen, X.M., et al., *Shear wave elastographic characterization of normal and torn achilles tendons: a pilot study.* J Ultrasound Med, 2013. **32**(3): p. 449-55.
184. Aubry, S., et al., *[Transient elastography of calcaneal tendon: preliminary results and future prospects].* J Radiol, 2011. **92**(5): p. 421-7.
185. Dirrichs, T., et al., *Shear Wave Elastography (SWE) for the Evaluation of Patients with Tendinopathies.* Acad Radiol, 2016. **23**(10): p. 1204-13.

186. Arda, K., et al., *Quantitative assessment of normal soft-tissue elasticity using shear-wave ultrasound elastography.* AJR Am J Roentgenol, 2011. **197**(3): p. 532-6.
187. Aubry, S., et al., *Viscoelasticity in Achilles tendonopathy: quantitative assessment by using real-time shear-wave elastography.* Radiology, 2015. **274**(3): p. 821-9.
188. Fu, S., et al., *Elastic Characteristics of the Normal Achilles Tendon Assessed by Virtual Touch Imaging Quantification Shear Wave Elastography.* J Ultrasound Med, 2016. **35**(9): p. 1881-7.
189. Quack, V., et al., *Shear wave elastography (SWE) of healthy Achilles tendons: A comparison between professional athletes and the non-athletic general population*, in *ORS 2017 Annual Meeting*, OSR, Editor. 2017, OSR.
190. Slane, L.C., et al., *Quantitative ultrasound mapping of regional variations in shear wave speeds of the aging Achilles tendon.* Eur Radiol, 2017. **27**(2): p. 474-482.
191. Weinreb, J.H., et al., *Tendon structure, disease, and imaging.* Muscles Ligaments Tendons J, 2014. **4**(1): p. 66-73.
192. Peers, K.H.E., P.P.M. Brys, and R.J.J. Lysens, *Correlation between power Doppler ultrasonography and clinical severity in Achilles tendinopathy.* International Orthopaedics, 2003. **27**(3): p. 180-183.
193. Ooi, C.C., et al., *Diagnostic performance of axial-strain sonoelastography in confirming clinically diagnosed Achilles tendinopathy: comparison with B-mode ultrasound and color Doppler imaging.* Ultrasound Med Biol, 2015. **41**(1): p. 15-25.
194. Zhang, L.N., et al., *Evaluation of Elastic Stiffness in Healing Achilles Tendon After Surgical Repair of a Tendon Rupture Using In Vivo Ultrasound Shear Wave Elastography.* Med Sci Monit, 2016. **22**: p. 1186-91.
195. Drakonaki, E.E., G.M. Allen, and D.J. Wilson, *Real-time ultrasound elastography of the normal Achilles tendon: reproducibility and pattern description.* Clinical Radiology, 2009. **64**(12): p. 1196-1202.
196. Krouskop, T., D. Dougherty, and F. Vinson, *A pulsed Doppler ultrasonic system for making noninvasive measurements of the mechanical properties of soft tissue.* J Rehabil Res Dev, 1987. **24**(2): p. 1-8.
197. Levinson, S.F., *Ultrasound propagation in anisotropic soft tissues: the application of linear elastic theory.* Journal of biomechanics, 1987. **20**(3): p. 251-260.
198. Akagi, R. and S. Kusama, *Comparison Between Neck and Shoulder Stiffness Determined by Shear Wave Ultrasound Elastography and a Muscle Hardness Meter.* Ultrasound Med Biol, 2015. **41**(8): p. 2266-71.
199. Kelly, J.P., et al., *Characterization of tissue stiffness of the infraspinatus, erector spinae, and gastrocnemius muscle using ultrasound shear wave elastography and superficial mechanical deformation.* J Electromyogr Kinesiol, 2018. **38**: p. 73-80.
200. Chuang, L.-l., C.-y. Wu, and K.-c. Lin, *Reliability, validity, and responsiveness of myotonometric measurement of muscle tone, elasticity, and stiffness in patients with stroke.* Arch Phys Med Rehab, 2012. **93**(3): p. 532-540.

201. Korhonen, R., et al., *Can mechanical myotonometry or electromyography be used for the prediction of intramuscular pressure?* Physiol Meas, 2005. **26**(6): p. 951.
202. Lacourpaille, L., et al., *Supersonic shear imaging provides a reliable measurement of resting muscle shear elastic modulus.* Physiol Meas, 2012. **33**(3): p. N19.
203. Yoshitake, Y., et al., *Muscle shear modulus measured with ultrasound shear-wave elastography across a wide range of contraction intensity.* Muscle & nerve, 2014. **50**(1): p. 103-113.
204. Kot, B.C.W., et al., *Elastic modulus of muscle and tendon with shear wave ultrasound elastography: variations with different technical settings.* PloS one, 2012. **7**(8): p. e44348.
205. Botanlioglu, H., et al., *Shear wave elastography properties of vastus lateralis and vastus medialis obliquus muscles in normal subjects and female patients with patellofemoral pain syndrome.* Skeletal Radiol, 2013. **42**(5): p. 659-66.
206. Dubois, G., et al., *Reliable Protocol for Shear Wave Elastography of Lower Limb Muscles at Rest and During Passive Stretching.* Ultrasound in medicine & biology, 2015. **41**(9): p. 2284-2291.
207. Wang, C.Z., et al., *Age and Sex Effects on the Active Stiffness of Vastus Intermedius under Isometric Contraction.* Biomed Res Int, 2017. **2017**: p. 9469548.
208. Akagi, R., Y. Yamashita, and Y. Ueyasu, *Age-Related Differences in Muscle Shear Moduli in the Lower Extremity.* Ultrasound Med Biol, 2015. **41**(11): p. 2906-12.
209. Tas, S., et al., *Shear Wave Elastography Is a Reliable and Repeatable Method for Measuring the Elastic Modulus of the Rectus Femoris Muscle and Patellar Tendon.* J Ultrasound Med, 2017. **36**(3): p. 565-570.
210. Morales-Artacho, A.J., L. Lacourpaille, and G. Guilhem, *Effects of warm-up on hamstring muscles stiffness: Cycling vs foam rolling.* Scand J Med Sci Sports, 2017. **27**(12): p. 1959-1969.
211. Eriksson Crommert, M., et al., *Massage induces an immediate, albeit short-term, reduction in muscle stiffness.* Scandinavian journal of medicine & science in sports, 2015. **25**(5).
212. Cortez, C.D., et al., *Ultrasound shear wave velocity in skeletal muscle: A reproducibility study.* Diagn Interv Imag, 2016. **97**(1): p. 71-79.
213. Leung, W.K.C., K.L. Chu, and C. Lai, *Sonographic evaluation of the immediate effects of eccentric heel drop exercise on Achilles tendon and gastrocnemius muscle stiffness using shear wave elastography.* PeerJ, 2017. **5**: p. e3592.
214. Nakamura, M., et al., *Acute effects of static stretching on the shear elastic moduli of the medial and lateral gastrocnemius muscles in young and elderly women.* Musculoskelet Sci Pract, 2017. **32**: p. 98-103.
215. Chino, K. and H. Takashi, *Association of Gastrocnemius Muscle Stiffness With Passive Ankle Joint Stiffness and Sex-Related Difference in the Joint Stiffness.* J Appl Biomech, 2017: p. 1-21.
216. Yoshida, K., et al., *Application of shear wave elastography for the gastrocnemius medial head to tennis leg.* Clinical Anatomy, 2017. **30**(1): p. 114-119.
217. Ohya, S., et al., *The effect of a running task on muscle shear elastic modulus of posterior lower leg.* J Foot Ankle Res, 2017. **10**: p. 56.

218. Kusano, K., et al., *Acute effect and time course of extension and internal rotation stretching of the shoulder on infraspinatus muscle hardness.* J Shoulder Elbow Surg, 2017. **26**(10): p. 1782-1788.
219. Itoigawa, Y., et al., *Feasibility assessment of shear wave elastography to rotator cuff muscle.* Clinical anatomy, 2015. **28**(2): p. 213-218.
220. Badea, I., et al., *Quantitative assessment of the masseter muscle's elasticity using Acoustic Radiation Force Impulse.* Medical ultrasonography, 2014. **16**(2): p. 89.
221. Creze, M., et al., *Feasibility assessment of shear wave elastography to lumbar back muscles: A Radioanatomic Study.* Clin Anat, 2017. **30**(6): p. 774-780.
222. Heizelmann, A., et al., *Measurements of the trapezius and erector spinae muscles using virtual touch imaging quantification ultrasound-Elastography: a cross section study.* BMC Musculoskelet Disord, 2017. **18**(1): p. 370.
223. Hirayama, K., R. Akagi, and H. Takahashi, *Reliability of ultrasound elastography for the quantification of transversus abdominis elasticity.* Acta radiologica open, 2015. **4**(9): p. 2058460115603420.
224. Hirayama, K., et al., *TRANSVERSUS ABDOMINIS ELASTICITY DURING VARIOUS EXERCISES: A SHEAR WAVE ULTRASOUND ELASTOGRAPHY STUDY.* Int J Sports Phys Ther, 2017. **12**(4): p. 601-606.
225. Moreau, B., et al., *Non-invasive assessment of human multifidus muscle stiffness using ultrasound shear wave elastography: A feasibility study.* Proceedings of the Institution of Mechanical Engineers, Part H: Journal of Engineering in Medicine, 2016. **230**(8): p. 809-814.
226. Coombes, B.K., et al., *Heterogeneity of passive elastic properties within the quadriceps femoris muscle-tendon unit.* Eur J Appl Physiol, 2018. **118**(1): p. 213-221.
227. Le Sant, G., et al., *Stiffness mapping of lower leg muscles during passive dorsiflexion.* J Anat, 2017. **230**(5): p. 639-650.
228. Miyamoto, N., K. Hirata, and H. Kanehisa, *Effects of hamstring stretching on passive muscle stiffness vary between hip flexion and knee extension maneuvers.* Scand J Med Sci Sports, 2017. **27**(1): p. 99-106.
229. Brandenburg, J.E., et al., *Feasibility and reliability of quantifying passive muscle stiffness in young children by using shear wave ultrasound elastography.* J Ultrasound Med, 2015. **34**(4): p. 663-70.
230. Le Sant, G., et al., *Elastography Study of Hamstring Behaviors during Passive Stretching.* PLoS One, 2015. **10**(9): p. e0139272.
231. Umehara, J., et al., *Effect of hip and knee position on tensor fasciae latae elongation during stretching: An ultrasonic shear wave elastography study.* Clin Biomech (Bristol, Avon), 2015. **30**(10): p. 1056-9.
232. Nordez, A. and F. Hug, *Muscle shear elastic modulus measured using supersonic shear imaging is highly related to muscle activity level.* J Appl Physiol (1985), 2010. **108**(5): p. 1389-94.
233. Sasaki, K., S. Toyama, and N. Ishii, *Length-force characteristics of in vivo human muscle reflected by supersonic shear imaging.* J Appl Physiol (1985), 2014. **117**(2): p. 153-62.
234. Bouillard, K., A. Nordez, and F. Hug, *Estimation of individual muscle force using elastography.* PLoS One, 2011. **6**(12): p. e29261.

235. Shinohara, M., et al., *Real-time visualization of muscle stiffness distribution with ultrasound shear wave imaging during muscle contraction.* Muscle Nerve, 2010. **42**(3): p. 438-441.
236. Erdemir, A., et al., *Model-based estimation of muscle forces exerted during movements.* Clin Biomech (Bristol, Avon), 2007. **22**(2): p. 131-54.
237. Baumer, T.G., et al., *Shear wave elastography of the supraspinatus muscle and tendon: Repeatability and preliminary findings.* J Biomech, 2017. **53**: p. 201-204.
238. Koo, T.K., et al., *Quantifying the passive stretching response of human tibialis anterior muscle using shear wave elastography.* Clinical Biomechanics, 2014. **29**(1): p. 33-39.
239. Miyamoto, N., et al., *Validity of measurement of shear modulus by ultrasound shear wave elastography in human pennate muscle.* PLOS ONE, 2015. **10**(4): p. e0124311.
240. Rosskopf, A.B., et al., *Quantitative Shear-Wave US Elastography of the Supraspinatus Muscle: Reliability of the Method and Relation to Tendon Integrity and Muscle Quality.* Radiology, 2015. **278**(2): p. 465-474.
241. Akagi, R., et al., *A Six-Week Resistance Training Program Does Not Change Shear Modulus of the Triceps Brachii.* J Appl Biomech, 2016. **32**(4): p. 373-8.
242. Chen, J., et al., *Ultrasound shear wave elastography in the assessment of passive biceps brachii muscle stiffness: influences of sex and elbow position.* Clin Imaging, 2017. **45**: p. 26-29.
243. Castera, L., et al., *Pitfalls of liver stiffness measurement: a 5-year prospective study of 13,369 examinations.* Hepatology, 2010. **51**(3): p. 828-35.
244. Cortez, C.D., et al., *Ultrasound shear wave velocity in skeletal muscle: a reproducibility study.* Diagnostic and interventional imaging, 2015.
245. Toennies, K.D., *Digital Image Acquisition*, in *Guide to Medical Image Analysis*. 2017, Springer. p. 23-94.
246. Eby, S.F., et al., *Validation of shear wave elastography in skeletal muscle.* J Biomech, 2013. **46**(14): p. 2381-7.
247. Ewertsen, C., et al., *Evaluation of healthy muscle tissue by strain and shear wave elastography-Dependency on depth and ROI position in relation to underlying bone.* Ultrasonics, 2016.
248. Akagi, R. and H. Takahashi, *Acute effect of static stretching on hardness of the gastrocnemius muscle.* Med Sci Sport Exer, 2013. **45**(7): p. 1348-1354.
249. Kuo, W.-H., et al., *Neck muscle stiffness quantified by sonoelastography is correlated with body mass index and chronic neck pain symptoms.* Ultrasound in medicine & biology, 2013. **39**(8): p. 1356-1361.
250. Ateş, F., et al., *Muscle shear elastic modulus is linearly related to muscle torque over the entire range of isometric contraction intensity.* J Electromyog Kines, 2015. **25**(4): p. 703-708.
251. Chino, K. and H. Takahashi, *Measurement of gastrocnemius muscle elasticity by shear wave elastography: association with passive ankle joint stiffness and sex differences.* European journal of applied physiology, 2016. **116**(4): p. 823-830.
252. Bortolotto, C., et al., *Influence of subjects' characteristics and technical variables on muscle stiffness measured by shear wave elastosonography.* J Ultrasound, 2017. **20**(2): p. 139-146.

253. Youk, J.H., et al., *Performance of shear-wave elastography for breast masses using different region-of-interest (ROI) settings.* Acta Radiologica, 2017. **0**(0): p. 0284185117735562.
254. Schellhaas, B., et al., *Two-dimensional shear-wave elastography: a new method comparable to acoustic radiation force impulse imaging?* Eur J Gastroenterol Hepatol, 2017. **29**(6): p. 723-729.
255. Huang, Z.P., et al., *Study of detection times for liver stiffness evaluation by shear wave elastography.* World J Gastroenterol, 2014. **20**(28): p. 9578-84.
256. Boursier, J., et al., *Learning curve and interobserver reproducibility evaluation of liver stiffness measurement by transient elastography.* Eur J Gastroenterol Hepatol, 2008. **20**(7): p. 693-701.
257. Choi, S.H., et al., *How many times should we repeat measuring liver stiffness using shear wave elastography?: 5-repetition versus 10-repetition protocols.* Ultrasonics, 2016. **72**: p. 158-64.
258. Carpenter, E.L., et al., *Skeletal Muscle in Healthy Subjects versus Those with GNE-Related Myopathy: Evaluation with Shear-Wave US--A Pilot Study.* Radiology, 2015. **277**(2): p. 546-54.
259. Lam, A.C., et al., *The influence of precompression on elasticity of thyroid nodules estimated by ultrasound shear wave elastography.* Eur Radiol, 2016. **26**(8): p. 2845-52.
260. Lindle, R.S., et al., *Age and gender comparisons of muscle strength in 654 women and men aged 20–93 yr.* Journal of Applied Physiology, 1997. **83**(5): p. 1581-1587.
261. Brown, M., *Skeletal muscle and bone: effect of sex steroids and aging.* Advances in Physiology Education, 2008. **32**(2): p. 120-126.
262. Wu, C.H., *Does sex influence biceps brachii muscle stiffness?* Clin Imaging, 2017.
263. Souron, R., et al., *Sex differences in active tibialis anterior stiffness evaluated using supersonic shear imaging.* Journal of biomechanics, 2016. **49**(14): p. 3534-3537.
264. Faulkner, J.A., et al., *Age-related changes in the structure and function of skeletal muscles.* Clinical and Experimental Pharmacology and Physiology, 2007. **34**(11): p. 1091-1096.
265. Altman, D.G. and P. Royston, *The cost of dichotomising continuous variables.* BMJ, 2006. **332**(7549): p. 1080.
266. Lacourpaille, L., et al., *Early detection of exercise-induced muscle damage using elastography.* European journal of applied physiology, 2017. **117**(10): p. 2047-2056.
267. Dahmane, R., et al., *Spatial fiber type distribution in normal human muscle Histochemical and tensiomyographical evaluation.* J Biomech, 2005. **38**(12): p. 2451-9.
268. Jakubowski, K.L., et al., *Passive material properties of stroke-impaired plantarflexor and dorsiflexor muscles.* Clin Biomech (Bristol, Avon), 2017. **49**: p. 48-55.
269. Mathevon, L., et al., *Two-dimensional and shear wave elastography ultrasound: A reliable method to analyse spastic muscles?* Muscle Nerve, 2018. **57**(2): p. 222-228.
270. Wu, C.-H., et al., *Evaluation of Post-Stroke Spastic Muscle Stiffness Using Shear Wave Ultrasound Elastography.* Ultrasound in Medicine & Biology, 2017. **43**(6): p. 1105-1111.

271. Bilgici, M.C., et al., *Quantitative assessment of muscular stiffness in children with cerebral palsy using acoustic radiation force impulse (ARFI) ultrasound elastography.* Journal of Medical Ultrasonics, 2017.
272. Brandenburg, J.E., et al., *Quantifying passive muscle stiffness in children with and without cerebral palsy using ultrasound shear wave elastography.* Dev Med Child Neurol, 2016. **58**(12): p. 1288-1294.
273. Ceyhan Bilgici, M., et al., *Quantitative assessment of muscle stiffness with acoustic radiation force impulse elastography after botulinum toxin A injection in children with cerebral palsy.* Journal of Medical Ultrasonics, 2018. **45**(1): p. 137-141.
274. Lee, S.S.M., et al., *Use of Shear Wave Ultrasound Elastography to Quantify Muscle Properties in Cerebral Palsy.* Clinical biomechanics (Bristol, Avon), 2016. **31**: p. 20-28.
275. Gilbert, F., et al., *Supraspinatus muscle elasticity measured with real time shear wave ultrasound elastography correlates with MRI spectroscopic measured amount of fatty degeneration.* BMC Musculoskeletal Disorders, 2017. **18**(1): p. 549.
276. Masaki, M., et al., *Association of low back pain with muscle stiffness and muscle mass of the lumbar back muscles, and sagittal spinal alignment in young and middle-aged medical workers.* Clinical Biomechanics, 2017. **49**: p. 128-133.
277. Lacourpaille, L., et al., *Non-invasive assessment of muscle stiffness in patients with duchenne muscular dystrophy.* Muscle & Nerve, 2015. **51**(2): p. 284-286.
278. Lacourpaille, L., et al., *Effects of Duchenne muscular dystrophy on muscle stiffness and response to electrically-induced muscle contraction: A 12-month follow-up.* Neuromuscular Disorders, 2017. **27**(3): p. 214-220.
279. Du, L.J., et al., *Ultrasound shear wave elastography in assessment of muscle stiffness in patients with Parkinson's disease: a primary observation.* Clin Imaging, 2016. **40**(6): p. 1075-1080.
280. Akiyama, K., et al., *Shear Modulus of the Lower Leg Muscles in Patients with Medial Tibial Stress Syndrome.* Ultrasound in Medicine & Biology, 2016. **42**(8): p. 1779-1783.
281. Saeki, J., et al., *Muscle stiffness of posterior lower leg in runners with a history of medial tibial stress syndrome.* Scandinavian Journal of Medicine & Science in Sports, 2018. **28**(1): p. 246-251.
282. Lacourpaille, L., et al., *Time‐course effect of exercise‐induced muscle damage on localized muscle mechanical properties assessed using elastography.* Acta Physiologica, 2014. **211**(1): p. 135-146.
283. Hotfiel, T., et al., *Application of Acoustic Radiation Force Impulse (ARFI) Elastography in Imaging of Delayed Onset Muscle Soreness (DOMS): A Comparative Analysis With 3T MRI.* J Sport Rehabil, 2018: p. 1-21.
284. Leong, H.T., F. Hug, and S.N. Fu, *Increased Upper Trapezius Muscle Stiffness in Overhead Athletes with Rotator Cuff Tendinopathy.* PLOS ONE, 2016. **11**(5): p. e0155187.
285. Zhang, Z.J., et al., *Increase in passive muscle tension of the quadriceps muscle heads in jumping athletes with patellar tendinopathy.* Scandinavian Journal of Medicine & Science in Sports, 2017. **27**(10): p. 1099-1104.

286. Burke, C.J., J.S. Babb, and R.S. Adler, *Shear wave elastography in the pronator quadratus muscle following distal radial fracture fixation: A feasibility study comparing the operated versus nonoperated sides.* Ultrasound, 2017. **25**(4): p. 222-228.
287. Kragstrup, T.W., M. Kjaer, and A.L. Mackey, *Structural, biochemical, cellular, and functional changes in skeletal muscle extracellular matrix with aging.* Scand J Med Sci Sports, 2011. **21**(6): p. 749-57.
288. Lexell, J., C.C. Taylor, and M. Sjöström, *What is the cause of the ageing atrophy?: Total number, size and proportion of different fiber types studied in whole vastus lateralis muscle from 15-to 83-year-old men.* Journal of the neurological sciences, 1988. **84**(2-3): p. 275-294.
289. Rodrigues, C.J. and A.J. Rodrigues Junior, *A comparative study of aging of the elastic fiber system of the diaphragm and the rectus abdominis muscles in rats.* Braz J Med Biol Res, 2000. **33**(12): p. 1449-54.
290. Delmonico, M.J., et al., *Longitudinal study of muscle strength, quality, and adipose tissue infiltration.* The American Journal of Clinical Nutrition, 2009. **90**(6): p. 1579-1585.
291. Organization, W.H., *World report on ageing and health*. 2015: World Health Organization.
292. Silva, A.M., et al., *Ethnicity-related skeletal muscle differences across the lifespan.* American Journal of Human Biology, 2010. **22**(1): p. 76-82.
293. Rosenberg, I.H., *Summary comments.* The American journal of clinical nutrition, 1989. **50**(5): p. 1231-1233.
294. Fielding, R.A., et al., *Sarcopenia: an undiagnosed condition in older adults. Current consensus definition: prevalence, etiology, and consequences. International working group on sarcopenia.* Journal of the American Medical Directors Association, 2011. **12**(4): p. 249-256.
295. Cruz-Jentoft, A.J., et al., *Sarcopenia: European consensus on definition and diagnosis Report of the European Working Group on Sarcopenia in Older People.* Age and ageing, 2010. **39**(4): p. 412–423.
296. Muscaritoli, M., et al., *Consensus definition of sarcopenia, cachexia and pre-cachexia: joint document elaborated by Special Interest Groups (SIG)"cachexia-anorexia in chronic wasting diseases" and "nutrition in geriatrics".* Clinical nutrition, 2010. **29**(2): p. 154-159.
297. Chen, X., G. Mao, and S.X. Leng, *Frailty syndrome: an overview.* Clin Interv Aging, 2014. **9**(433): p. e41.
298. von Haehling, S., J.E. Morley, and S.D. Anker, *An overview of sarcopenia: facts and numbers on prevalence and clinical impact.* Journal of cachexia, sarcopenia and muscle, 2010. **1**(2): p. 129-133.
299. Landi, F., et al., *Sarcopenia as a risk factor for falls in elderly individuals: results from the ilSIRENTE study.* Clinical nutrition, 2012. **31**(5): p. 652-658.
300. Kim, H., et al., *Long-term effects of exercise and amino acid supplementation on muscle mass, physical function and falls in community-dwelling elderly Japanese sarcopenic women: A 4-year follow-up study.* Geriatrics & gerontology international, 2016. **16**(2): p. 175-181.
301. Chang, S.F. and P.L. Lin, *Systematic Literature Review and Meta-Analysis of the Association of Sarcopenia With Mortality.* Worldviews on Evidence-Based Nursing, 2016.

302. Janssen, I., et al., *The healthcare costs of sarcopenia in the United States.* Journal of the American Geriatrics Society, 2004. **52**(1): p. 80-85.
303. Kalinkovich, A. and G. Livshits, *Sarcopenia – The search for emerging biomarkers.* Ageing Research Reviews, 2015. **22**: p. 58-71.
304. Clark, B.C. and T.M. Manini, *Sarcopenia =/= dynapenia.* J Gerontol A Biol Sci Med Sci, 2008. **63**(8): p. 829-34.
305. McGregor, R.A., D. Cameron-Smith, and S.D. Poppitt, *It is not just muscle mass: a review of muscle quality, composition and metabolism during ageing as determinants of muscle function and mobility in later life.* Longev Healthspan, 2014. **3**(1): p. 9.
306. Clark, B.C. and T.M. Manini, *What is dynapenia?* Nutrition, 2012. **28**(5): p. 495-503.
307. Manini, T.M. and B.C. Clark, *Dynapenia and aging: an update.* J Gerontol A Biol Sci Med Sci, 2012. **67**(1): p. 28-40.
308. Lieber, R.L. and J. Friden, *Clinical significance of skeletal muscle architecture.* Clin Orthop Relat Res, 2001(383): p. 140-51.
309. Zoico, E., et al., *Myosteatosis and myofibrosis: relationship with aging, inflammation and insulin resistance.* Archives of gerontology and geriatrics, 2013. **57**(3): p. 411-416.
310. Artaza-Artabe, I., et al., *The relationship between nutrition and frailty: Effects of protein intake, nutritional supplementation, vitamin D and exercise on muscle metabolism in the elderly. A systematic review.* Maturitas, 2016. **93**: p. 89-99.
311. Morley, J.E., et al., *Sarcopenia with limited mobility: an international consensus.* Journal of the American Medical Directors Association, 2011. **12**(6): p. 403-409.
312. Lourenço, R.A., et al., *Performance of the European Working Group on Sarcopenia in Older People algorithm in screening older adults for muscle mass assessment.* Age and ageing, 2015. **44**(2): p. 334-338.
313. Urano, T. and S. Inoue, *Recent genetic discoveries in osteoporosis, sarcopenia and obesity [Review].* Endocrine journal, 2015. **62**(6): p. 475-484.
314. Yoshida, D., et al., *Using two different algorithms to determine the prevalence of sarcopenia.* Geriatr Gerontol Int, 2014. **14 Suppl 1**: p. 46-51.
315. Miller, F.W., *Classification of Idiopathic Inflammatory Myopathies*, in *The Inflammatory Myopathies*. 2009, Springer. p. 15-28.
316. Sultan, S., et al., *Outcome in patients with idiopathic inflammatory myositis: morbidity and mortality.* Rheumatology, 2002. **41**(1): p. 22-26.
317. Ponyi, A., et al., *Functional outcome and quality of life in adult patients with idiopathic inflammatory myositis.* Rheumatology, 2005. **44**(1): p. 83-88.
318. Bohan, A. and J.B. Peter, *Polymyositis and dermatomyositis.* New England Journal of Medicine, 1975. **292**(8): p. 403-407.
319. Dalakas, M.C., *Polymyositis, dermatomyositis, and inclusion-body myositis.* New England Journal of Medicine, 1991. **325**(21): p. 1487-1498.
320. Dalakas, M.C. and R. Hohlfeld, *Polymyositis and dermatomyositis.* The Lancet, 2003. **362**(9388): p. 971-982.

321. Hoogendijk, J.E., et al., *119th ENMC international workshop: trial design in adult idiopathic inflammatory myopathies, with the exception of inclusion body myositis, 10–12 October 2003, Naarden, The Netherlands.* Neuromuscular Disorders, 2004. **14**(5): p. 337-345.
322. Oddis, C.V., et al., *International consensus guidelines for trials of therapies in the idiopathic inflammatory myopathies.* Arthritis & Rheumatism, 2005. **52**(9): p. 2607-2615.
323. Lundberg, I.E., et al., *2017 European League Against Rheumatism/American College of Rheumatology classification criteria for adult and juvenile idiopathic inflammatory myopathies and their major subgroups.* Annals of the Rheumatic Diseases, 2017. **76**(12): p. 1955-1964.
324. Dubowitz, V., C.A. Sewry, and A. Oldfors, *Muscle biopsy: a practical approach*. 2013: Elsevier Health Sciences.
325. Patel, H., et al., *In epidemiological studies: Findings from the hertfordshire sarcopenia study (HSS).* The journal of nutrition, health & aging, 2011. **15**(1): p. 10-15.
326. Weber, M.-A., M. Krix, and S. Delorme, *Quantitative evaluation of muscle perfusion with CEUS and with MR.* European radiology, 2007. **17**(10): p. 2663-2674.
327. Vlekkert, J., et al., *Combining MRI and muscle biopsy improves diagnostic accuracy in subacute‐onset idiopathic inflammatory myopathy.* Muscle & nerve, 2015. **51**(2): p. 253-258.
328. Adler, R.S. and G. Garofalo, *Ultrasound in the evaluation of the inflammatory myopathies*, in *The Inflammatory Myopathies*. 2009, Springer. p. 147-164.
329. Kieseier, B.C., et al., *Expression of specific matrix metalloproteinases in inflammatory myopathies.* Brain, 2001. **124**(2): p. 341-351.
330. Ancuţa, C., et al., *Immunohistochemical study of skeletal muscle in rheumatoid myositis.* Romanian Journal of Morphology and Embryology, 2009. **50**(2009): p. 223-227.
331. Ancuta, C., et al., *Rheumatoid myositis, myth or reality? A clinical, imaging and histological study.* Romanian journal of morphology and embryology= Revue roumaine de morphologie et embryologie, 2014. **55**(3): p. 781.
332. TRAUT, E.F. and K.M. CAMPIONE, *Histopathology of muscle in rheumatoid arthritis and other diseases.* AMA archives of internal medicine, 1952. **89**(5): p. 724-735.
333. Yates, D., *Muscular changes in rheumatoid arthritis.* Annals of the rheumatic diseases, 1963. **22**(5): p. 342.
334. Edstrom, L. and R. Nordemar, *Differential changes in type I and type II muscle fibres in rheumatoid arthritis: a biopsy study.* Scandinavian journal of rheumatology, 1974. **3**(3): p. 155-160.
335. Wróblewski, R. and R. Nordemar, *Ultrastructural and histochemical studies of muscle in rheumatoid arthritis.* Scandinavian journal of rheumatology, 1975. **4**(4): p. 197-204.
336. Magyar, é., et al., *Muscle changes in rheumatoid arthritis.* Virchows Archiv, 1977. **373**(3): p. 267-278.
337. Halla, J.T., et al., *Rheumatoid myositis.* Arthritis & Rheumatism, 1984. **27**(7): p. 737-743.

338. Miró, Ó., et al. *Muscle involvement in rheumatoid arthritis: clinicopathological study of 21 symptomatic cases*. in *Seminars in arthritis and rheumatism*. 1996. Elsevier.
339. De Palma, L., et al., *Muscle involvement in rheumatoid arthritis: an ultrastructural study.* Ultrastructural pathology, 2000. **24**(3): p. 151-156.
340. Agrawal, V., et al., *Muscle involvement in rheumatoid arthritis: clinical and histological characteristics and review of literature.* J Indian Rheumatol Assoc, 2003. **11**(4): p. 98-103.
341. Steiner, G. and J. Chason, *Differential diagnosis of rheumatoid arthritis by biopsy of muscle.* American journal of clinical pathology, 1948. **18**(12): p. 931-939.
342. Haslock, D., V. Wright, and D. Harriman, *Neuromuscular disorders in rheumatoid arthritis.* QJM, 1970. **39**(3): p. 335-358.
343. Pecori Giraldi, F., M. Moro, and F. Cavagnini, *Study Group on the Hypothalamo–Pituitary–Adrenal Axis of the Italian Society of Endocrinology. Gender-related differences in the presentation and course of Cushing's disease.* J Clin Endocrinol Metab, 2003. **88**(4): p. 1554-8.
344. Alshekhlee, A., H.J. Kaminski, and R.L. Ruff, *Neuromuscular manifestations of endocrine disorders.* Neurologic clinics, 2002. **20**(1): p. 35-58.
345. Walsh, L., et al., *Adverse effects of oral corticosteroids in relation to dose in patients with lung disease.* Thorax, 2001. **56**(4): p. 279-284.
346. Hanson, P., et al., *Acute corticosteroid myopathy in intensive care patients.* Muscle & nerve, 1997. **20**(11): p. 1371-1380.
347. Van Balkom, R., et al., *Corticosteroid-induced myopathy of the respiratory muscles.* The Netherlands journal of medicine, 1994. **45**(3): p. 114-122.
348. Fardet, L., et al., *Corticosteroid-induced adverse events in adults.* Drug safety, 2007. **30**(10): p. 861-881.
349. Yates, D.A., *Steroid myopathy.* Rheumatol Phys Med, 1971. **11**(1): p. 28-33.
350. Kumar, S., *Steroid-induced myopathy following a single oral dose of prednisolone.* Neurology India, 2003. **51**(4): p. 554.
351. Betters, J.L., et al., *Nitric oxide reverses prednisolone-induced inactivation of muscle satellite cells.* Muscle & nerve, 2008. **37**(2): p. 203-209.
352. Dasgupta, B., et al., *BSR and BHPR guidelines for the management of giant cell arteritis.* Rheumatology, 2010.
353. Wilson, J.C., et al. *Serious adverse effects associated with glucocorticoid therapy in patients with giant cell arteritis (GCA): A nested case–control analysis*. in *Seminars in Arthritis and Rheumatism*. 2016. Elsevier.
354. Wilson, J.C., et al. *Incidence of outcomes potentially associated with corticosteroid therapy in patients with giant cell arteritis*. in *Seminars in Arthritis and Rheumatism*. 2016. Elsevier.
355. Broder, M.S., et al. *Corticosteroid-related adverse events in patients with giant cell arteritis: A claims-based analysis*. in *Seminars in Arthritis and Rheumatism*. 2016. Elsevier.

356. Askari, A., P.J. Vignos, and R.W. Moskowitz, *Steroid myopathy in connective tissue disease.* The American journal of medicine, 1976. **61**(4): p. 485-492.
357. Amato, A.A. and D. Dumitru, *Electrodiagnostic medicine.* 2002.
358. Schakman, O., et al., *Glucocorticoid-induced skeletal muscle atrophy.* The international journal of biochemistry & cell biology, 2013. **45**(10): p. 2163-2172.
359. Kesikburun, S., et al., *Assessment of spasticity with sonoelastography following stroke: a feasibility study.* PM&R, 2015. **7**(12): p. 1254-1260.
360. Zhang, Z., et al., *Increase in passive muscle tension of the quadriceps muscle heads in jumping athletes with patellar tendinopathy.* Scandinavian Journal of Medicine & Science in Sports, 2016.
361. Baker, J.F., et al., *Deficits in muscle mass, muscle density, and modified associations with fat in rheumatoid arthritis.* Arthritis care & research, 2014. **66**(11): p. 1612-1618.
362. Beenakker, K.G., et al., *Patterns of muscle strength loss with age in the general population and patients with a chronic inflammatory state.* Ageing research reviews, 2010. **9**(4): p. 431-436.
363. Ekblom, B., et al., *Physical performance in patients with rheumatoid arthritis.* Scandinavian journal of rheumatology, 1974. **3**(3): p. 121-125.
364. Burmester, G., et al., *Rheumatoid Arthritis: pathogenesis and clinical features.* EULAR textbook on Rheumatic Diseases. BMJ group, London, 2012: p. 206-231.
365. Curtis, A. and H. Pollard, *Felty's syndrome; its several features, including tissue changes, compared with other forms of rheumatoid arthritis.* Annals of Internal Medicine, 1940. **13**(12): p. 2265-2284.
366. Steiner, G., et al., *Lesions of skeletal muscles in rheumatoid arthritis: nodular polymyositis.* The American journal of pathology, 1946. **22**(1): p. 103.
367. Nakajima, A., et al., *High frequencies and co-existing of myositis-specific autoantibodies in patients with idiopathic inflammatory myopathies overlapped to rheumatoid arthritis.* Rheumatology international, 2012. **32**(7): p. 2057-2061.
368. Freund, H.A., et al., *Nodular polymyositis in rheumatoid arthritis.* Science, 1945. **101**(2617): p. 202-203.
369. Clawson, B., J. Noble, and N. Lufkin, *Nodular inflammatory and degenerative lesions of muscles from 450 autopsies.* Archives of pathology, 1947. **43**(6): p. 579.
370. Morrison, L., et al., *THE NEUROMUSCULAR SYSTEM IN RHEUMATOID ARTHRITS ELECTROMYOGRAPHIC AND HISTOLOGIC OBSERVATIONS.* The American journal of the medical sciences, 1947. **214**(1): p. 33-49.
371. Sokoloff, L., S. Wilens, and J. Bunim, *Arteritis of striated muscle in rheumatoid arthritis.* The American journal of pathology, 1951. **27**(1): p. 157.
372. Rubin, M. and A. Klein, *The differential diagnosis of inflammatory myopathy*, in *The Inflammatory Myopathies*. 2009, Springer. p. 231-251.
373. Martin, N., C.K. Li, and L.R. Wedderburn, *Juvenile dermatomyositis: new insights and new treatment strategies.* Therapeutic advances in musculoskeletal disease, 2011: p. 1759720X11424460.

374. Kennis, E., et al., *Longitudinal impact of aging on muscle quality in middle-aged men.* Age (Dordr), 2014. **36**(4): p. 9689.
375. Takai, Y., et al., *Sit-to-stand test to evaluate knee extensor muscle size and strength in the elderly: a novel approach.* Journal of physiological anthropology, 2009. **28**(3): p. 123-128.
376. Barbat-Artigas, S., et al., *How to assess functional status: A new muscle quality index.* The journal of nutrition, health & aging, 2012. **16**(1): p. 67-77.
377. Amato, A.A. and R.H. Brown, *Muscular Dystrophies and Other Muscle Diseases*, in *Harrison's Principles of Internal Medicine, 19e*, D. Kasper, et al., Editors. 2015, McGraw-Hill Education: New York, NY. p. 462.
378. Miller, F.W., et al., *Proposed preliminary core set measures for disease outcome assessment in adult and juvenile idiopathic inflammatory myopathies.* Rheumatology (Oxford), 2001. **40**(11): p. 1262-73.
379. Hirano, M., et al., *Acute quadriplegic myopathy.* A complication of treatment with steroids, nondepolarizing blocking agents, or both, 1992. **42**(11): p. 2082-2082.
380. Minetto, M.A., et al., *Muscle fiber conduction slowing and decreased levels of circulating muscle proteins after short-term dexamethasone administration in healthy subjects.* J Clin Endocrinol Metab, 2010. **95**(4): p. 1663-71.
381. Mathiowetz, V., et al., *Reliability and validity of grip and pinch strength evaluations.* The Journal of hand surgery, 1984. **9**(2): p. 222-226.
382. Bohannon, R.W., *Dynamometer measurements of hand-grip strength predict multiple outcomes.* Perceptual and motor skills, 2001. **93**(2): p. 323-328.
383. Wind, A.E., et al., *Is grip strength a predictor for total muscle strength in healthy children, adolescents, and young adults?* European journal of pediatrics, 2010. **169**(3): p. 281-287.
384. Bohannon, R.W., *Hand-Grip Dynamometry Predicts Future Outcomes in Aging Adults.* Journal of geriatric physical therapy, 2008. **31**(1): p. 3-10.
385. Cooper, R., D. Kuh, and R. Hardy, *Objectively measured physical capability levels and mortality: systematic review and meta-analysis.* Bmj, 2010. **341**: p. c4467.
386. Fees, E., *Grip Strength (2nd ed).* Chicago: American Society of Hand Therapists, 1992.
387. Alvares, J.B.d.A.R., et al., *Inter-machine reliability of the Biodex and Cybex isokinetic dynamometers for knee flexor/extensor isometric, concentric and eccentric tests.* Physical Therapy in Sport, 2015. **16**(1): p. 59-65.
388. Maffiuletti, N.A., et al., *Reliability of knee extension and flexion measurements using the Con-Trex isokinetic dynamometer.* Clinical physiology and functional imaging, 2007. **27**(6): p. 346-353.
389. Delitto, A., *Isokinetic dynamometry.* Muscle & nerve, 1990. **13**(S1).
390. Bohannon, R.W., et al., *Grip and knee extension muscle strength reflect a common construct among adults.* Muscle & nerve, 2012. **46**(4): p. 555-558.
391. Porter, M.M., A.A. Vandervoort, and J.F. Kramer, *Eccentric peak torque of the plantar and dorsiflexors is maintained in older women.* The Journals of Gerontology Series A: Biological Sciences and Medical Sciences, 1997. **52**(2): p. B125-B131.

392. Vandervoort, A.A., *Aging of the human neuromuscular system.* Muscle & Nerve, 2002. **25**(1): p. 17-25.
393. Häkkinen, A., et al., *Muscle strength, pain, and disease activity explain individual subdimensions of the Health Assessment Questionnaire disability index, especially in women with rheumatoid arthritis.* Annals of the rheumatic diseases, 2006. **65**(1): p. 30-34.
394. Fridén, C., et al., *Higher pain sensitivity and lower muscle strength in postmenonpausal women with early rheumatoid arthritis compared with age-matched healthy women–a pilot study.* Disability and rehabilitation, 2013. **35**(16): p. 1350-1356.
395. Meireles, S., et al., *Isokinetic evaluation of the knee in patients with rheumatoid arthritis.* Joint Bone Spine, 2002. **69**(6): p. 566-573.
396. Schiottz-Christensen, B., et al., *Use of isokinetic muscle strength as a measure of severity of rheumatoid arthritis: a comparison of this assessment method for RA with other assessment methods for the disease.* Clinical rheumatology, 2001. **20**(6): p. 423-427.
397. Neri, R., et al., *Functional and isokinetic assessment of muscle strength in patients with idiopathic inflammatory myopathies.* Autoimmunity, 2006. **39**(3): p. 255-259.
398. Stoll, T., et al., *Muscle strength assessment in polymyositis and dermatomyositis evaluation of the reliability and clinical use of a new, quantitative, easily applicable method.* J Rheumatol, 1995. **22**(3): p. 473-7.
399. Guralnik, J.M., et al., *A short physical performance battery assessing lower extremity function: association with self-reported disability and prediction of mortality and nursing home admission.* Journal of gerontology, 1994. **49**(2): p. M85-M94.
400. Böhler, C., et al., *Rheumatoid arthritis and falls: the influence of disease activity.* Rheumatology, 2012: p. kes198.
401. Luoto, S., et al., *Impaired postural control is associated with worse scores on the health assessment questionnaire disability index among women with rheumatoid arthritis.* Journal of rehabilitation medicine, 2011. **43**(10): p. 900-905.
402. Studenski, S., et al., *Gait speed and survival in older adults.* Jama, 2011. **305**(1): p. 50-58.
403. Guralnik, J.M., et al., *Lower extremity function and subsequent disability consistency across studies, predictive models, and value of gait speed alone compared with the short physical performance battery.* The Journals of Gerontology Series A: Biological Sciences and Medical Sciences, 2000. **55**(4): p. M221-M231.
404. Shin, S., et al., *Lower extremity muscle quality and gait variability in older adults.* Age Ageing, 2012. **41**(5): p. 595-9.
405. Jones, C.J., R.E. Rikli, and W.C. Beam, *A 30-s chair-stand test as a measure of lower body strength in community-residing older adults.* Research quarterly for exercise and sport, 1999. **70**(2): p. 113-119.
406. Agarwal, S. and P.D.W. Kiely, *Two simple, reliable and valid tests of proximal muscle function, and their application to the management of idiopathic inflammatory myositis.* Rheumatology, 2006. **45**(7): p. 874-879.
407. Carlson, H.L., *Electromyography*, in *The Inflammatory Myopathies*, L.J. Kagen, Editor. 2009, Humana Press: Totowa, NJ. p. 111-125.

408. Neuromuscular, A.A.o. and E. Medicine, *Proper performance and interpretation of electrodiagnostic studies.* Muscle & nerve, 2006. **33**(3): p. 436.
409. Clark, D.J., et al., *Impaired voluntary neuromuscular activation limits muscle power in mobility-limited older adults.* J Gerontol A Biol Sci Med Sci, 2010. **65**(5): p. 495-502.
410. Kanda, F., et al., *Steroid myopathy: pathogenesis and effects of growth hormone and insulin-like growth factor-I administration.* Hormone Research in Paediatrics, 2001. **56**(Suppl. 1): p. 24-28.
411. O'Rourke, K.S., *Myopathies, Polymyalgia Rheumatica, and Giant Cell Arteritis*, in *Hazzard's Geriatric Medicine and Gerontology, 7e*, J.B. Halter, et al., Editors. 2017, McGraw-Hill Education: New York, NY. p. 120.
412. Baker, J.F., et al., *Are men at greater risk of lean mass deficits in rheumatoid arthritis?* Arthritis care & research, 2015. **67**(1): p. 112-119.
413. Huang, Z.-g., et al., *An efficacy analysis of whole-body magnetic resonance imaging in the diagnosis and follow-up of polymyositis and dermatomyositis.* PLOS ONE, 2017. **12**(7): p. e0181069.
414. Guimaraes, J.B., et al., *Sporadic Inclusion Body Myositis: MRI Findings and Correlation With Clinical and Functional Parameters.* AJR Am J Roentgenol, 2017. **209**(6): p. 1340-1347.
415. Malattia, C., et al., *Whole-body MRI in the assessment of disease activity in juvenile dermatomyositis.* Ann Rheum Dis, 2014. **73**(6): p. 1083-90.
416. Zong, M., et al., *Anakinra treatment in patients with refractory inflammatory myopathies and possible predictive response biomarkers: a mechanistic study with 12 months follow-up.* Ann Rheum Dis, 2014. **73**(5): p. 913-20.
417. Sanner, H., et al., *Long-term muscular outcome and predisposing and prognostic factors in juvenile dermatomyositis: A case-control study.* Arthritis Care Res (Hoboken), 2010. **62**(8): p. 1103-11.
418. Lovitt, S., et al., *MRI in myopathy.* Neurol Clin, 2004. **22**(3): p. 509-38, v.
419. Janssen, I., et al., *Skeletal muscle mass and distribution in 468 men and women aged 18-88 yr.* J Appl Physiol (1985), 2000. **89**(1): p. 81-8.
420. Yoon, M.A., et al., *Multiparametric MR Imaging of Age-related Changes in Healthy Thigh Muscles.* Radiology, 2018. **287**(1): p. 235-246.
421. McCullough, M.B., et al., *Evaluation of Muscles Affected by Myositis Using Magnetic Resonance Elastography.* Muscle & nerve, 2011. **43**(4): p. 585-590.
422. Reimers, C.D., et al., *Muscular ultrasound in idiopathic inflammatory myopathies of adults.* Journal of the Neurological Sciences, 1993. **116**(1): p. 82-92.
423. Heckmatt, J.Z., N. Pier, and V. Dubowitz, *Real-time ultrasound imaging of muscles.* Muscle & Nerve, 1988. **11**(1): p. 56-65.
424. Campbell, S.E., R. Adler, and C.M. Sofka, *Ultrasound of muscle abnormalities.* Ultrasound quarterly, 2005. **21**(2): p. 87-94.
425. Noto, Y., et al., *Contrasting echogenicity in flexor digitorum profundus-flexor carpi ulnaris: a diagnostic ultrasound pattern in sporadic inclusion body myositis.* Muscle Nerve, 2014. **49**(5): p. 745-8.
426. Weber, M.A., et al., *Contrast-enhanced ultrasound in dermatomyositis-and polymyositis.* J Neurol, 2006. **253**(12): p. 1625-32.

427. Rech, A., et al., *Echo intensity is negatively associated with functional capacity in older women.* Age, 2014. **36**(5): p. 9708.
428. Men, Y., et al., *The size and strength of the quadriceps muscles of old.* Clinical Physiology, 1985. **5**(2): p. 145-154.
429. Thom, J.M., et al., *Influence of muscle architecture on the torque and power-velocity characteristics of young and elderly men.* Eur J Appl Physiol, 2007. **100**(5): p. 613-9.
430. Reeves, N.D., C.N. Maganaris, and M.V. Narici, *Ultrasonographic assessment of human skeletal muscle size.* European Journal of Applied Physiology, 2004. **91**(1): p. 116-118.
431. English, C., L. Fisher, and K. Thoirs, *Reliability of real-time ultrasound for measuring skeletal muscle size in human limbs in vivo: a systematic review.* Clin Rehabil, 2012. **26**(10): p. 934-44.
432. Hernaez, R., *Reliability and agreement studies: a guide for clinical investigators.* Gut, 2015. **64**(7): p. 1018-27.
433. Shin, H.J., et al., *Comparison of shear wave velocities on ultrasound elastography between different machines, transducers, and acquisition depths: a phantom study.* Eur Radiol, 2016. **26**(10): p. 3361-7.
434. Song, P., et al. *Shear wave elastography on the GE LOGIQ E9 with Comb-push Ultrasound Shear Elastography (CUSE) and time aligned sequential tracking (TAST)*. in *Ultrasonics Symposium (IUS), 2014 IEEE International*. 2014. IEEE.
435. Bland, J.M. and D.G. Altman, *Statistics Notes: Measurement error proportional to the mean.* BMJ, 1996. **313**(7049): p. 106.
436. Landis, J.R. and G.G. Koch, *The measurement of observer agreement for categorical data.* Biometrics, 1977: p. 159-174.
437. Bland, J.M. and D.G. Altman, *Measuring agreement in method comparison studies.* Stat Methods Med Res, 1999. **8**(2): p. 135-160.
438. Song, P., et al., *Two-dimensional shear-wave elastography on conventional ultrasound scanners with time-aligned sequential tracking (TAST) and comb-push ultrasound shear elastography (CUSE).* IEEE T Ultrason Ferr, 2015. **62**(2): p. 290-302.
439. Velotta, J., et al. *Relationship between leg dominance tests and type of task*. in *ISBS-Conference Proceedings Archive*. 2011.
440. Charlton, C., Rasbash, J., Browne, W.J., Healy, M. and Cameron, B, *MLwiN Version 3.00.* Centre for Multilevel Modelling, University of Bristol., 2017.
441. Lacourpaille, L., et al., *Supersonic shear imaging provides a reliable measurement of resting muscle shear elastic modulus.* Physiol Meas, 2012. **33**(3): p. N19-28.
442. Lapole, T., et al., *Contracting biceps brachii elastic properties can be reliably characterized using supersonic shear imaging.* European journal of applied physiology, 2015. **115**(3): p. 497-505.
443. Méndez, J. and A. Keys, *Density and composition of mammalian muscle.* Metabolism-Clinical and Experimental, 1960. **9**(2): p. 184-188.
444. Martin, A.D., et al., *Adipose tissue density, estimated adipose lipid fraction and whole body adiposity in male cadavers.* Int J Obes Relat Metab Disord, 1994. **18**(2): p. 79-83.
445. Youk, J.H., et al., *Shear-wave elastography for breast masses: local shear wave speed (m/sec) versus Young modulus (kPa).* Ultrasonography, 2013. **33**(1): p. 34-39.

446. Goertz, R.S., et al., *An abdominal and thyroid status with Acoustic Radiation Force Impulse Elastometry--a feasibility study: Acoustic Radiation Force Impulse Elastometry of human organs.* Eur J Radiol, 2011. **80**(3): p. e226-30.
447. Greening, J. and A. Dilley, *Posture-induced changes in peripheral nerve stiffness measured by ultrasound shear-wave elastography.* Muscle & nerve, 2016.
448. Publications, U.N., *World Population Ageing, 2017 Highlights*. 2017: UN.
449. Manini, T.M., et al., *Knee extension strength cutpoints for maintaining mobility.* Journal of the American Geriatrics Society, 2007. **55**(3): p. 451-457.
450. Fukagawa, N.K., et al., *Strength is a major factor in balance, gait, and the occurrence of falls.* The Journals of Gerontology Series A: Biological Sciences and Medical Sciences, 1995. **50**(Special_Issue): p. 64-67.
451. Tinetti, M.E. and C. Kumar, *The patient who falls: "It's always a trade-off".* Jama, 2010. **303**(3): p. 258-66.
452. Boyé, N.D., et al., *The impact of falls in the elderly.* Trauma, 2013. **15**(1): p. 29-35.
453. Greenlund, L.J.S. and K.S. Nair, *Sarcopenia—consequences, mechanisms, and potential therapies.* Mechanisms of Ageing and Development, 2003. **124**(3): p. 287-299.
454. Kohrt, W.M. and J.O. Holloszy, *Loss of skeletal muscle mass with aging: effect on glucose tolerance.* J Gerontol A Biol Sci Med Sci, 1995. **50 Spec No**: p. 68-72.
455. Kragstrup, T.W., M. Kjaer, and A. Mackey, *Structural, biochemical, cellular, and functional changes in skeletal muscle extracellular matrix with aging.* Scandinavian journal of medicine & science in sports, 2011. **21**(6): p. 749-757.
456. Hsiao, M.-Y., et al., *Reduced Patellar Tendon Elasticity with Aging: In Vivo Assessment by Shear Wave Elastography.* Ultrasound in Medicine & Biology, 2015. **41**(11): p. 2899-2905.
457. Stenroth, L., et al., *Age-related differences in Achilles tendon properties and triceps surae muscle architecture in vivo.* Journal of Applied Physiology, 2012. **113**(10): p. 1537-1544.
458. Gao, Y., et al., *Age-related changes in the mechanical properties of the epimysium in skeletal muscles of rats.* Journal of biomechanics, 2008. **41**(2): p. 465-469.
459. Gosselin, L.E., et al., *Effect of exercise training on passive stiffness in locomotor skeletal muscle: role of extracellular matrix.* Journal of applied physiology, 1998. **85**(3): p. 1011-1016.
460. Fragala, M.S., A.M. Kenny, and G.A. Kuchel, *Muscle quality in aging: a multi-dimensional approach to muscle functioning with applications for treatment.* Sports Med, 2015. **45**(5): p. 641-58.
461. Metter, E.J., et al., *Muscle quality and age: cross-sectional and longitudinal comparisons.* Journals of Gerontology Series A: Biomedical Sciences and Medical Sciences, 1999. **54**(5): p. B207-B218.
462. Dodds, R.M., et al., *Grip strength across the life course: normative data from twelve British studies.* PloS one, 2014. **9**(12): p. e113637.
463. Lindle, R.S., et al., *Age and gender comparisons of muscle strength in 654 women and men aged 20-93 yr.* J Appl Physiol (1985), 1997. **83**(5): p. 1581-7.

464. Mitchell, W., et al., *Sarcopenia, Dynapenia, and the Impact of Advancing Age on Human Skeletal Muscle Size and Strength; a Quantitative Review.* Frontiers in Physiology, 2012. **3**(260).
465. Faul, F., et al., *Statistical power analyses using G* Power 3.1: Tests for correlation and regression analyses.* Behavior research methods, 2009. **41**(4): p. 1149-1160.
466. Barbour, K.E., et al., *Vital Signs: Prevalence of Doctor-Diagnosed Arthritis and Arthritis-Attributable Activity Limitation-United States, 2013-2015.* MMWR. Morbidity and mortality weekly report, 2017. **66**(9): p. 246-253.
467. Heaven, A., et al., *Keeping it credible in cohort multiple Randomised Controlled Trials: the Community Ageing Research 75+ (CARE 75+) study model of patient and public involvement and engagement.* Research Involvement and Engagement, 2016. **2**: p. 30.
468. Hubbard, R.E., et al., *Frailty, financial resources and subjective well-being in later life.* Archives of Gerontology and Geriatrics, 2014. **58**(3): p. 364-369.
469. Wall, J.C., et al., *The Timed Get-up-and-Go test revisited: measurement of the component tasks.* Journal of rehabilitation research and development, 2000. **37**(1): p. 109.
470. Botolfsen, P., et al., *Reliability and concurrent validity of the Expanded Timed Up-and-Go test in older people with impaired mobility.* Physiother Res Int, 2008. **13**(2): p. 94-106.
471. Buchner, D.M., et al., *Evidence for a non-linear relationship between leg strength and gait speed.* Age Ageing, 1996. **25**(5): p. 386-91.
472. Studenski, S., et al., *Physical performance measures in the clinical setting.* J Am Geriatr Soc, 2003. **51**(3): p. 314-22.
473. Maggio, M., et al., *Instrumental and non-instrumental evaluation of 4-meter walking speed in older individuals.* PloS one, 2016. **11**(4): p. e0153583.
474. Lauretani, F., et al., *Age-associated changes in skeletal muscles and their effect on mobility: an operational diagnosis of sarcopenia.* Journal of applied physiology, 2003. **95**(5): p. 1851-1860.
475. Telenius, E.W., K. Engedal, and A. Bergland, *Inter-rater reliability of the Berg Balance Scale, 30 s chair stand test and 6 m walking test, and construct validity of the Berg Balance Scale in nursing home residents with mild-to-moderate dementia.* BMJ open, 2015. **5**(9): p. e008321.
476. El Mhandi, L. and F. Bethoux, *Isokinetic testing in patients with neuromuscular diseases: a focused review.* Am J Phys Med Rehabil, 2013. **92**(2): p. 163-78.
477. Payton, C. and R. Bartlett, *Biomechanical evaluation of movement in sport and exercise: the British Association of Sport and Exercise Sciences guide*. 2nd ed. 2017: Routledge.
478. Frontera, W.R., et al., *Aging of skeletal muscle: a 12-yr longitudinal study.* Journal of applied physiology, 2000. **88**(4): p. 1321-1326.
479. Poulin, M.J., et al., *Eccentric and concentric torques of knee and elbow extension in young and older men.* Canadian journal of sport sciences = Journal canadien des sciences du sport, 1992. **17**(1): p. 3-7.
480. Goodpaster, B.H., et al., *Attenuation of skeletal muscle and strength in the elderly: The Health ABC Study.* Journal of applied physiology, 2001. **90**(6): p. 2157-2165.

481. Ferri, A., et al., *Strength and power changes of the human plantar flexors and knee extensors in response to resistance training in old age.* Acta Physiologica, 2003. **177**(1): p. 69-78.
482. J., S.J., et al., *Quadriceps weakness, patella alta, and structural features of patellofemoral osteoarthritis.* Arthritis Care & Research, 2011. **63**(10): p. 1391-1397.
483. Mijnarends, D.M., et al., *Validity and reliability of tools to measure muscle mass, strength, and physical performance in community-dwelling older people: a systematic review.* Journal of the American Medical Directors Association, 2013. **14**(3): p. 170-178.
484. Khalil, S.F., M.S. Mohktar, and F. Ibrahim, *The theory and fundamentals of bioimpedance analysis in clinical status monitoring and diagnosis of diseases.* Sensors, 2014. **14**(6): p. 10895-10928.
485. B.V., T.E. *Body Composition Analyzer DC-430MA III Manual*. DC4307601(1)-1604FA 2016 [cited 2017 5/5/2017]; Available from: https://tanita.eu/media/wysiwyg/manuals/medical-approved-body-composition-monitors/dc-430ma-instruction-manual-gb.pdf.
486. Janssen, I., et al., *Skeletal muscle cutpoints associated with elevated physical disability risk in older men and women.* American journal of epidemiology, 2004. **159**(4): p. 413-421.
487. Masanés, F., et al., *Cut-off points for muscle mass—not grip strength or gait speed—determine variations in sarcopenia prevalence.* The journal of nutrition, health & aging, 2017. **21**(7): p. 825-829.
488. Pallant, J., *SPSS survival manual*. 2013: McGraw-Hill Education (UK).
489. Bowers, D., *Medical statistics from scratch: an introduction for health professionals*. Second Edition ed. 2014: John Wiley & Sons.
490. Starodubtseva, M.N., *Mechanical properties of cells and ageing.* Ageing research reviews, 2011. **10**(1): p. 16-25.
491. Domire, Z.J., et al., *Feasibility of using magnetic resonance elastography to study the effect of aging on shear modulus of skeletal muscle.* Journal of applied biomechanics, 2009. **25**(1): p. 93-97.
492. Ochala, J., et al., *Single Skeletal Muscle Fiber Elastic and Contractile Characteristics in Young and Older Men.* The Journals of Gerontology Series A: Biological Sciences and Medical Sciences, 2007. **62**(4): p. 375-381.
493. Ditroilo, M., et al., *Assessment of musculo-articular and muscle stiffness in young and older men.* Muscle & nerve, 2012. **46**(4): p. 559-565.
494. Lacraz, G., et al., *Increased Stiffness in Aged Skeletal Muscle Impairs Muscle Progenitor Cell Proliferative Activity.* PLoS One, 2015. **10**(8): p. e0136217.
495. Eby, S.F., et al., *Shear wave elastography of passive skeletal muscle stiffness: Influences of sex and age throughout adulthood.* Clinical Biomechanics, 2015. **30**(1): p. 22-27.
496. Debernard, L., et al., *Analysis of thigh muscle stiffness from childhood to adulthood using magnetic resonance elastography (MRE) technique.* Clinical Biomechanics, 2011. **26**(8): p. 836-840.
497. Costa, P.B., et al., *Acute effects of passive stretching on the electromechanical delay and evoked twitch properties.* European Journal of Applied Physiology, 2009. **108**(2): p. 301.
498. Meyer, A., et al., *Incidence and prevalence of inflammatory myopathies: a systematic review.* Rheumatology, 2015. **54**(1): p. 50-63.

499. Lampa, J., et al., *MRI guided muscle biopsy confirmed polymyositis diagnosis in a patient with interstitial lung disease.* Annals of the rheumatic diseases, 2001. **60**(4): p. 423-426.
500. Van De Vlekkert, J., et al., *Combining MRI and muscle biopsy improves diagnostic accuracy in subacute-onset idiopathic inflammatory myopathy.* Muscle & nerve, 2015. **51**(2): p. 253-258.
501. Wisdom, K.M., S.L. Delp, and E. Kuhl, *Use it or lose it: multiscale skeletal muscle adaptation to mechanical stimuli.* Biomechanics and Modeling in Mechanobiology, 2015. **14**(2): p. 195-215.
502. Kagen, L.J., *The inflammatory myopathies*. 2009: Springer.
503. Song, Y., et al., *Strain sonoelastography of inflammatory myopathies: comparison with clinical examination, magnetic resonance imaging and pathologic findings.* Brit J Radiol, 2016. **89**(1065): p. 20160283.
504. Lewallen, S. and P. Courtright, *Epidemiology in Practice: Case-Control Studies.* Community Eye Health, 1998. **11**(28): p. 57-58.
505. Julious, S.A., *Sample size of 12 per group rule of thumb for a pilot study.* Pharmaceutical Statistics, 2005. **4**(4): p. 287-291.
506. Lancaster, G.A., S. Dodd, and P.R. Williamson, *Design and analysis of pilot studies: recommendations for good practice.* Journal of evaluation in clinical practice, 2004. **10**(2): p. 307-312.
507. Oddis, C.V., et al., *Rituximab in the treatment of refractory adult and juvenile dermatomyositis and adult polymyositis: A randomized, placebo-phase trial.* Arthritis & Rheumatism, 2013. **65**(2): p. 314-324.
508. Rothman, K.J., S. Greenland, and T.L. Lash, *Modern epidemiology.* 2008: p. 171-172.
509. Pearce, N., *Analysis of matched case-control studies.* BMJ, 2016. **352**.
510. Pinal-Fernandez, I., et al., *Thigh muscle MRI in immune-mediated necrotising myopathy: extensive oedema, early muscle damage and role of anti-SRP autoantibodies as a marker of severity.* Ann Rheum Dis, 2017. **76**(4): p. 681-687.
511. Cox, F.M., et al., *Magnetic resonance imaging of skeletal muscles in sporadic inclusion body myositis.* Rheumatology, 2011. **50**(6): p. 1153-1161.
512. Hosmer Jr, D.W., S. Lemeshow, and R.X. Sturdivant, *Applied logistic regression*. Third edition ed. Vol. 398. 2013: John Wiley & Sons.
513. Bland, M., *An introduction to medical statistics*. Fourth edition ed. 2015: Oxford University Press (UK).
514. Sheskin, D.J., *Handbook of parametric and nonparametric statistical procedures*. Fourth edition ed. 2003: CRC Press.
515. Sultan, S.M. and D.A. Isenberg, *Re-classifying myositis.* Rheumatology, 2010. **49**(5): p. 831-833.
516. Krivickas, L.S., et al., *Preservation of in vitro muscle fiber function in dermatomyositis and inclusion body myositis: a single fiber study.* Neuromuscular Disorders, 2005. **15**(5): p. 349-354.
517. De Bleecker, J.L., et al., *Differential expression of chemokines in inflammatory myopathies.* Neurology, 2002. **58**(12): p. 1779-85.
518. Bachasson, D., et al., *Muscle Shear Wave Elastography in Inclusion Body Myositis: Feasibility, Reliability and Relationships with Muscle Impairments.* Ultrasound in Medicine & Biology, 2018. **44**(7): p. 1423-1432.

519. Maurer, B. and U.A. Walker, *Role of MRI in diagnosis and management of idiopathic inflammatory myopathies.* Curr Rheumatol Rep, 2015. **17**(11): p. 67.
520. Zheng, Y., et al., *Magnetic resonance imaging changes of thigh muscles in myopathy with antibodies to signal recognition particle.* Rheumatology (Oxford), 2015. **54**(6): p. 1017-24.
521. Mahajan, A. and V.R. Tandon, *Corticosteroids in rheumatology: Friends or foes.* Journal, Indian Academy of Clinical Medicine, 2005. **6**(4): p. 275-280.
522. Fardet, L., I. Petersen, and I. Nazareth, *Description of oral glucocorticoid prescriptions in general population.* La Revue de medecine interne, 2011. **32**(10): p. 594-599.
523. Overman, R.A., J.Y. Yeh, and C.L. Deal, *Prevalence of oral glucocorticoid usage in the United States: a general population perspective.* Arthritis Care Res, 2013. **65**(2): p. 294-8.
524. Manson, S.C., et al., *The cumulative burden of oral corticosteroid side effects and the economic implications of steroid use.* Respiratory Medicine, 2009. **103**(7): p. 975-994.
525. Bodine, S.C. and J.D. Furlow, *Glucocorticoids and Skeletal Muscle*, in *Glucocorticoid Signaling: From Molecules to Mice to Man*, J.-C. Wang and C. Harris, Editors. 2015, Springer New York: New York, NY. p. 145-176.
526. Sartor, O., et al., *Effect of prednisone on prostate-specific antigen in patients with hormone-refractory prostate cancer.* Urology, 1998. **52**(2): p. 252-256.
527. Levine, A., et al., *Evaluation of oral budesonide for treatment of mild and moderate exacerbations of Crohn's disease in children.* The Journal of pediatrics, 2002. **140**(1): p. 75-80.
528. Decramer, M., et al., *Corticosteroids contribute to muscle weakness in chronic airflow obstruction.* American journal of respiratory and critical care medicine, 1994. **150**(1): p. 11-16.
529. Nawata, T., et al., *Change in muscle volume after steroid therapy in patients with myositis assessed using cross-sectional computed tomography.* BMC Musculoskelet Disord, 2018. **19**(1): p. 93.
530. Silver, E.M. and W. Ochoa, *Glucocorticoid-Induced Myopathy in a Patient with Systemic Lupus Erythematosus (SLE): A Case Report and Review of the Literature.* American Journal of Case Reports, 2018. **19**: p. 277-283.
531. Decramer, M. and K.J. Stas, *Corticosteroid-induced myopathy involving respiratory muscles in patients with chronic obstructive pulmonary disease or asthma.* American Review of Respiratory Disease, 1992. **146**: p. 800-800.
532. Bowyer, S.L., M.P. LaMothe, and J.R. Hollister, *Steroid myopathy: incidence and detection in a population with asthma.* J Allergy Clin Immunol, 1985. **76**(2 Pt 1): p. 234-42.
533. Byers, R., A. Bergman, and M. Joseph, *Steroid myopathy: report of five cases occurring during treatment of rheumatic fever.* Pediatrics, 1962. **29**(1): p. 26-36.
534. Yates, D., *Steroid myopathy.* Rheumatology, 1971. **11**(1): p. 28-33.

535. KOSTYO, J.L. and A.F. REDMOND, *Role of protein synthesis in the inhibitory action of adrenal steroid hormones on amino acid transport by muscle.* Endocrinology, 1966. **79**(3): p. 531-540.
536. Hasselgren, P.O., *Glucocorticoids and muscle catabolism.* Curr Opin Clin Nutr Metab Care, 1999. **2**(3): p. 201-5.
537. Dekhuijzen, P.N., et al., *Corticosteroid treatment and nutritional deprivation cause a different pattern of atrophy in rat diaphragm.* J Appl Physiol (1985), 1995. **78**(2): p. 629-37.
538. Schakman, O., H. Gilson, and J.P. Thissen, *Mechanisms of glucocorticoid-induced myopathy.* J Endocrinol, 2008. **197**(1): p. 1-10.
539. Guis, S., J.P. Mattei, and F. Liote, *Drug-induced and toxic myopathies.* Best Pract Res Clin Rheumatol, 2003. **17**(6): p. 877-907.
540. Levin, O.S., et al., *Steroid myopathy in patients with chronic respiratory diseases.* J Neurol Sci, 2014. **338**(1-2): p. 96-101.
541. Wilson, J.C., et al., *Incidence of outcomes potentially associated with corticosteroid therapy in patients with giant cell arteritis.* Semin Arthritis Rheum, 2017. **46**(5): p. 650-656.
542. Broder, M.S., et al., *Corticosteroid-related adverse events in patients with giant cell arteritis: A claims-based analysis.* Semin Arthritis Rheum, 2016. **46**(2): p. 246-52.
543. Wilson, J.C., et al., *Serious adverse effects associated with glucocorticoid therapy in patients with giant cell arteritis (GCA): A nested case-control analysis.* Semin Arthritis Rheum, 2017. **46**(6): p. 819-827.
544. Proven, A., et al., *Glucocorticoid therapy in giant cell arteritis: duration and adverse outcomes.* Arthritis Rheum, 2003. **49**(5): p. 703-8.
545. Mandel, S., *Steroid myopathy.* Postgraduate Medicine, 1982. **72**(5): p. 207-215.
546. Minetto, M., et al., *Steroid myopathy: some unresolved issues.* Journal of endocrinological investigation, 2011. **34**(5): p. 370-375.
547. Minetto, M.A., et al., *Diagnostic work-up in steroid myopathy.* Endocrine, 2018. **60**(2): p. 219-223.
548. Alev, K., et al., *Glucocorticoid-Induced Changes in Rat Skeletal Muscle Biomechanical and Viscoelastic Properties: Aspects of Aging.* J Manipulative Physiol Ther, 2018. **41**(1): p. 19-24.
549. Hunder, G.G., et al., *The American College of Rheumatology 1990 criteria for the classification of giant cell arteritis.* Arthritis Rheum, 1990. **33**(8): p. 1122-8.
550. West, B.T., *Analyzing Longitudinal Data With the Linear Mixed Models Procedure in SPSS.* Evaluation & the Health Professions, 2009. **32**(3): p. 207-228.
551. Suresh, E. and S. Wimalaratna, *Proximal myopathy: diagnostic approach and initial management.* Postgrad Med J, 2013. **89**(1054): p. 470-7.
552. Minetto, M.A., et al., *Diagnostic evaluation in steroid-induced myopathy: case report suggesting clinical utility of quantitative muscle ultrasonography.* Endocr Res, 2018: p. 1-11.
553. Hoes, J., et al., *Adverse events of low-to-medium-dose oral glucocorticoids in inflammatory diseases: a meta-analysis.* Annals of the rheumatic diseases, 2008.
554. Srinivasan, R., et al., *Fiber type composition and maximum shortening velocity of muscles crossing the human shoulder.* Clinical Anatomy: The

Official Journal of the American Association of Clinical Anatomists and the British Association of Clinical Anatomists, 2007. **20**(2): p. 144-149.
555. Garrett Jr, W., J. Califf, and F. Bassett, *Histochemical correlates of hamstring injuries.* The American journal of sports medicine, 1984. **12**(2): p. 98-103.
556. LaPier, T.K., *Glucocorticoid-induced muscle atrophy. The role of exercise in treatment and prevention.* J Cardiopulm Rehabil, 1997. **17**(2): p. 76-84.
557. Barton, B. and J. Peat, *Medical statistics: a guide to SPSS, data analysis and critical appraisal*. 2014: John Wiley & Sons.
558. *Introducing Multilevel Modeling*. 1998: London.
559. Cojocaru, M., et al., *Extra-articular Manifestations in Rheumatoid Arthritis.* Mædica, 2010. **5**(4): p. 286-291.
560. Turesson, C., et al., *Extra-articular disease manifestations in rheumatoid arthritis: incidence trends and risk factors over 46 years.* Ann Rheum Dis, 2003. **62**(8): p. 722-7.
561. Schlaeger, J.M., et al., *Treatment-Seeking Behaviors of Persons With Rheumatoid Arthritis.* J Holist Nurs, 2018. **36**(2): p. 179-191.
562. Yamada, T., et al., *Muscle Weakness in Rheumatoid Arthritis: The Role of Ca(2+) and Free Radical Signaling.* EBioMedicine, 2017. **23**: p. 12-19.
563. Masuko, K., *Rheumatoid cachexia revisited: a metabolic co-morbidity in rheumatoid arthritis.* Front Nutr, 2014. **1**: p. 20.
564. Kramer, H.R., et al., *Muscle Density in Rheumatoid Arthritis: Associations with Disease Features and Functional Outcomes.* Arthritis and rheumatism, 2012. **64**(8): p. 2438-2450.
565. Browne, R.H., *On the use of a pilot sample for sample size determination.* Stat Med, 1995. **14**(17): p. 1933-40.
566. Fransen, J. and P.L. van Riel, *The Disease Activity Score and the EULAR response criteria.* Rheum Dis Clin North Am, 2009. **35**(4): p. 745-57, vii-viii.
567. Fransen, J., M. Creemers, and P. Van Riel, *Remission in rheumatoid arthritis: agreement of the disease activity score (DAS28) with the ARA preliminary remission criteria.* Rheumatology, 2004. **43**(10): p. 1252-1255.
568. Aletaha, D., et al., *Remission and active disease in rheumatoid arthritis: Defining criteria for disease activity states.* Arthritis & Rheumatism, 2005. **52**(9): p. 2625-2636.
569. Felson, D.T., et al., *American College of Rheumatology/European League Against Rheumatism provisional definition of remission in rheumatoid arthritis for clinical trials.* Arthritis & Rheumatism, 2011. **63**(3): p. 573-586.
570. Yamada, T., et al., *Nitrosative modifications of the Ca2+ release complex and actin underlie arthritis-induced muscle weakness.* Annals of the Rheumatic Diseases, 2015. **74**(10): p. 1907-1914.
571. Targowski, T., *Sarcopaenia and rheumatoid arthritis.* Reumatologia, 2017. **55**(2): p. 84-87.
572. Helliwell, P.S. and S. Jackson, *Relationship between weakness and muscle wasting in rheumatoid arthritis.* Annals of the Rheumatic Diseases, 1994. **53**(11): p. 726-728.
573. Fraser, A., et al., *Predicting 'normal' grip strength for rheumatoid arthritis patients.* Rheumatology, 1999. **38**(6): p. 521-528.

574. Lemmey, A.B., et al., *Tight control of disease activity fails to improve body composition or physical function in rheumatoid arthritis patients.* Rheumatology, 2016. **55**(10): p. 1736-1745.
575. Madsen, O.R. and C. Egsmose, *Associations of isokinetic knee extensor and flexor strength with steroid use and walking ability in women with rheumatoid arthritis.* Clin Rheumatol, 2001. **20**(3): p. 207-12.
576. Stanmore, E.K., *Recommendations for assessing and preventing falls in adults of all ages with rheumatoid arthritis.* British Journal of Community Nursing, 2015. **20**(11): p. 529-533.
577. Iversen, G.R., et al., *Analysis of variance*. 1987: Sage.
578. McQueen, F., et al., *Magnetic resonance imaging evidence of tendinopathy in early rheumatoid arthritis predicts tendon rupture at six years.* Arthritis Rheum, 2005. **52**(3): p. 744-51.
579. Boers, M., et al., *Developing Core Outcome Measurement Sets for Clinical Trials: OMERACT Filter 2.0.* Journal of Clinical Epidemiology, 2014. **67**(7): p. 745-753.
580. Jeon, M., K. Youn, and S. Yang, *Reliability and quantification of gastrocnemius elasticity at relaxing and at submaximal contracted condition.* Med Ultrason, 2018. **20**(3): p. 342-347.
581. Aslan, A., et al., *Shear Wave and Strain Elastographic Features of the Brachial Plexus in Healthy Adults: Reliability of the Findings-a Pilot Study.* J Ultrasound Med, 2018. **37**(10): p. 2353-2362.
582. Mendes, B., et al., *Hamstring stiffness pattern during contraction in healthy individuals: analysis by ultrasound-based shear wave elastography.* Eur J Appl Physiol, 2018. **118**(11): p. 2403-2415.
583. Liu, J., et al., *Non-invasive Quantitative Assessment of Muscle Force Based on Ultrasonic Shear Wave Elastography.* Ultrasound in Medicine & Biology, 2018. **[In Press]**.
584. Ewertsen, C., et al., *Reference values for shear wave elastography of neck and shoulder muscles in healthy individuals.* Ultrasound international open, 2018. **4**(01): p. E23-E29.
585. Rominger, M.B., et al., *Influencing Factors of 2D Shear Wave Elastography of the Muscle - An Ex Vivo Animal Study.* Ultrasound Int Open, 2018. **4**(2): p. E54-e60.
586. Byenfeldt, M., A. Elvin, and P. Fransson, *Influence of Probe Pressure on Ultrasound-Based Shear Wave Elastography of the Liver Using Comb-Push 2-D Technology.* Ultrasound Med Biol, 2018. **[In Press]**.
587. Maslarska, M., et al., *Shear Wave Elastography of Peripheral Muscle Weakness in Patients with Chronic Congestive Heart Failure.* Ultrasound Med Biol, 2018. **44**(12): p. 2531-2539.
588. Sanabria, S.J., et al., *Speed of sound ultrasound: a pilot study on a novel technique to identify sarcopenia in seniors.* European Radiology, 2019. **29**(1): p. 3-12.
589. Narici, M., M. Franchi, and C. Maganaris, *Muscle structural assembly and functional consequences.* Journal of Experimental Biology, 2016. **219**(2): p. 276-284.
590. Purslow, P.P., *Muscle fascia and force transmission.* J Bodyw Mov Ther, 2010. **14**(4): p. 411-7.
591. Taş, S., F. Korkusuz, and Z. Erden, *Neck Muscle Stiffness in Participants With and Without Chronic Neck Pain: A Shear-Wave*

Elastography Study. Journal of Manipulative and Physiological Therapeutics, 2018. **41**(7): p. 580-588.
592. Takashima, M., et al., *Quantitative evaluation of masseter muscle stiffness in patients with temporomandibular disorders using shear wave elastography.* J Prosthodont Res, 2017. **61**(4): p. 432-438.
593. Kimura, K., et al., *Quantitative analysis of the relation between soft tissue stiffness palpated from the body surface and tissue hemodynamics in the human forearm.* Physiol Meas, 2007. **28**(12): p. 1495-505.
594. Vigotsky, A.D., E.J. Rouse, and S.S. Lee. *In vivo relationship between joint stiffness, joint-based estimates of muscle stiffness, and shear-wave velocity*. in *2018 40th Annual International Conference of the IEEE Engineering in Medicine and Biology Society (EMBC)*. 2018. IEEE.
595. Gonzalez, E.A., S.E. Romero, and B. Castaneda, *Real Time Crawling Wave Sonoelastography for human muscle characterization: Initial results.* IEEE Transactions on Ultrasonics, Ferroelectrics, and Frequency Control, 2018: p. 1-1.
596. Ferraioli, G., et al., *Evaluation of Inter-System Variability in Liver Stiffness Measurements.* Ultraschall in der Medizin-European Journal of Ultrasound, 2018.
597. Hudert, C.A., et al., *US Time-Harmonic Elastography: Detection of Liver Fibrosis in Adolescents with Extreme Obesity with Nonalcoholic Fatty Liver Disease.* Radiology, 2018. **288**(1): p. 99-106.
598. Yin, L., et al., *Three-Dimensional Shear Wave Elastography of Skeletal Muscle: Preliminary Study.* J Ultrasound Med, 2018. **37**(8): p. 2053-2062.
599. Perkisas, S., et al., *Application of ultrasound for muscle assessment in sarcopenia: towards standardized measurements.* European Geriatric Medicine, 2018. **9**(6): p. 739-757.
600. Sultan, S.M., et al., *Reliability and validity of the myositis disease activity assessment tool.* Arthritis Rheum, 2008. **58**(11): p. 3593-9.